

AD-A225 717

DTIC FILE COPY

The Jet Propulsion Laboratory, Faculty of Aerospace, Technion-IIT

**Novel, Post-Stall, Thrust-Vectored F-15 RPVs:
Laboratory and Flight Tests**

Program Manager : Douglas Bowers

1ST-Year Report

Principal Investigator: Benjamin Gal-Or

April 24, 1990

DTIC
ELECTE
AUG 20 1990

E

D

DISTRIBUTION STATEMENT A

Approved for public release;
Distribution Unlimited

90 08 17 120

Unclassified
SECURITY CLASSIFICATION OF THIS PAGE

REPORT DOCUMENTATION PAGE				Form Approved OMB No. 0704-0188	
1a. REPORT SECURITY CLASSIFICATION Unclassified			1b. RESTRICTIVE MARKINGS		
2a. SECURITY CLASSIFICATION AUTHORITY			3. DISTRIBUTION/AVAILABILITY OF REPORT Approved for public release :		
2b. DECLASSIFICATION/DOWNGRADING SCHEDULE			Distribution unlimited		
4. PERFORMING ORGANIZATION REPORT NUMBER(S) Technion Res. No. 160-0559 (Gal-Or, B.)			5. MONITORING ORGANIZATION REPORT NUMBER(S) Purch. Reg. No. FY 1456-8905052		
6a. NAME OF PERFORMING ORGANIZATION Technion - Israel Institute of Technology		6b. OFFICE SYMBOL (if applicable) F		7a. NAME OF MONITORING ORGANIZATION European Office of Aerospace Research and Development	
6c. ADDRESS (City, State, and ZIP Code) Gal-Or, Faculty of Aerospace Eng. Technion City, Haifa, 32000, Israel			7b. ADDRESS (City, State, and ZIP Code) Box 14 FPO New York 09510-0200		
8a. NAME OF FUNDING/SPONSORING ORGANIZATION Wright Research and Development Center		8b. OFFICE SYMBOL (if applicable) FIMM		9. PROCUREMENT INSTRUMENT IDENTIFICATION NUMBER FY1456-8905052; AFOSR-89-0445	
8c. ADDRESS (City, State, and ZIP Code) Wright-Patterson AFB, OH 45433-6523			10. SOURCE OF FUNDING NUMBERS		
			PROGRAM ELEMENT NO.	PROJECT NO.	TASK NO.
			WORK UNIT ACCESSION NO.		
11. TITLE (Include Security Classification) Agile, Thrust-Vectored F-15 HPVs: Laboratory and Flight Tests [High-Alpha Inlets, Thrust-Vectoring Nozzles]					
12. PERSONAL AUTHOR(S) Prof. Benjamin Gal-Or, Head, Jet Propulsion Lab, TIT					
13a. TYPE OF REPORT Annual		13b. TIME COVERED FROM 89/4/1 TO 90/3/31		14. DATE OF REPORT (Year, Month, Day) April 24, 1990	
15. PAGE COUNT					
16. SUPPLEMENTARY NOTATION The USAF [Flight-Dynamics Lab/WPAFB] project at the JPL of the Technion					
17. COSATI CODES			18. SUBJECT TERMS (Continue on reverse if necessary and identify by block number)		
FIELD	GROUP	SUB-GROUP	Key Words : Thrust Vectoring, Vektored Propulsion, Post-Stall Inlets/Vectoring Nozzles, Upgrading F-15		
19. ABSTRACT (Continue on reverse if necessary and identify by block number)					
<p>Presenting the major problems confronting the development, tests and validation of Post-Stall (PST) Thrust-Vectored Fighters (TVF), this project is based on the development of an integrated laboratory-flight testing methodology of PST-F-15-TVF/HPVs, including the tests of new types of yaw-pitch and roll-yaw-pitch thrust-vectoring nozzles and high-alpha, PST inlets.</p>					
20. DISTRIBUTION/AVAILABILITY OF ABSTRACT <input type="checkbox"/> UNCLASSIFIED/UNLIMITED <input checked="" type="checkbox"/> SAME AS RPT. <input checked="" type="checkbox"/> DTIC USERS			21. ABSTRACT SECURITY CLASSIFICATION		
22a. NAME OF RESPONSIBLE INDIVIDUAL Douglas L. Bowers			22b. TELEPHONE (Include Area Code) (513)-255-6208		22c. OFFICE SYMBOL WRDC/FIMM

DD Form 1473, JUN 86

BENJAMIN GAL-OR
ISRAEL INSTITUTE OF TECHNOLOGY
TECHNION CITY
HAIFA, ISRAEL

TURBO ... LABORATORY
TECHNION ...

Unclassified
HAIFA, ISRAEL

REPORT OF INVENTIONS AND SUBCONTRACTS (Pursuant to "Patent Rights" Contract Clause) (See Instructions on Reverse Side.)										Form Approved GSA FPMR (41 CFR) 101-11.6 (Exempt from FAR, 101-11.6)	
1. NAME OF CONTRACTOR/SUBCONTRACTOR Gal-Or/Technion - IIT Haifa 32000, Israel		2. CONTRACT NUMBER AFOSR-89/0445		3. NAME OF GOVERNMENT PRIME CONTRACTOR AFOSR-WRC-WPAFB		4. CONTRACT NUMBER		5. TYPE OF REPORT (if any)		6. DATE OF REPORT (if any)	
3. ADDRESS (Include ZIP Code)		4. AWARD DATE (FY/MD/YY)		5. AWARD DATE (FY/MD/YY)		6. AWARD DATE (FY/MD/YY)		7. INTERIM		8. FINAL	
April 1, 89 - March 31, 1990		April 1, 89 - March 31, 1990		April 1, 89 - March 31, 1990		April 1, 89 - March 31, 1990		April 1, 89 - March 31, 1990		April 1, 89 - March 31, 1990	
SECTION I - SUBJECT INVENTIONS											
5. "SUBJECT INVENTIONS" REQUIRED TO BE REPORTED BY CONTRACTOR/SUBCONTRACTOR IF "None," so state											
6. NAME(S) OF INVENTION(S) Gal-Or, Benjamin		7. TITLE OF INVENTION(S) Yaw-Pitch and Roll-Yaw-Pitch Thrust-Vectoring, 2D-CD and 2D-C nozzles and P. 55.		8. DISCLOSURE NO. PATENT APPLICATION SERIAL NO. OR PATENT NO.		9. ELECTION TO FILE PATENT APPLICATIONS (1) United States (2) Foreign (3) Yes (4) No (5) Yes (6) No (7) Yes (8) No		10. CONFIRMATORY INSTRUMENT OR ASSIGNMENT FORWARDED TO CONTRACTING OFFICER (1) Yes (2) No		11. DATE OF REPORT (if any)	
12. NAME OF INVENTOR (Last, First, MI) Gal-Or, B.		13. NAME OF EMPLOYER Gal-Or, B.		14. ADDRESS OF EMPLOYER (Include ZIP Code)		15. ADDRESS OF EMPLOYER (Include ZIP Code)		16. ADDRESS OF EMPLOYER (Include ZIP Code)		17. ADDRESS OF EMPLOYER (Include ZIP Code)	
18. NAME OF INVENTOR (Last, First, MI) Gal-Or, B.		19. NAME OF EMPLOYER Gal-Or, B.		20. ADDRESS OF EMPLOYER (Include ZIP Code)		21. ADDRESS OF EMPLOYER (Include ZIP Code)		22. ADDRESS OF EMPLOYER (Include ZIP Code)		23. ADDRESS OF EMPLOYER (Include ZIP Code)	
SECTION II - SUBCONTRACTS (Containing a "Patent Rights" clause)											
6. SUBCONTRACTS AWARDED BY CONTRACTOR/SUBCONTRACTOR IF "None," so state											
7. NAME OF SUBCONTRACTOR(S)		8. ADDRESS (Include ZIP Code)		9. SUBCONTRACT NO(S)		10. NAME "PATENT RIGHTS" (1) Clause Number (2) Date (FY/MD/YY)		11. DESCRIPTION OF WORK TO BE PERFORMED UNDER SUBCONTRACT(S)		12. SUBCONTRACT DATES (FY/MD/YY) (1) Award (2) Estimated Completion	
General Policy at 50% to Inventor, 50% to Technion R & D Foundation Ltd.		Technion :									
SECTION III - CERTIFICATION											
7. CERTIFICATION OF REPORT BY CONTRACTOR/SUBCONTRACTOR											
8. NAME OF AUTHORIZED CONTRACTOR/SUBCONTRACTOR OFFICIAL (Last, First, MI) Y. Dvir, Technion R & D Fund.		9. SIGNATURE Y. Dvir		10. SIGNATURE B. Gal-Or		11. SIGNATURE B. Gal-Or		12. SIGNATURE B. Gal-Or		13. SIGNATURE B. Gal-Or	
14. TITLE Director		15. SIGNATURE Y. Dvir		16. SIGNATURE B. Gal-Or		17. SIGNATURE B. Gal-Or		18. SIGNATURE B. Gal-Or		19. SIGNATURE B. Gal-Or	
20. DATE April 1, 89		21. DATE April 1, 89		22. DATE April 1, 89		23. DATE April 1, 89		24. DATE April 1, 89		25. DATE April 1, 89	

The Jet Propulsion Laboratory, Faculty of Aerospace, Technion-IIT

Tel. (0)4-348-066; (0)4-292-807; (0)4-292-435

Fax : (0)4- 221-581

Novel, Post-Stall, Thrust-Vectored F-15 RPVs :

Laboratory and Flight Tests

Grant No. AFOSR-89-0445. Purchase Request No. FY1456-8905052.

Effective Starting Date: 01 April 89.

The USAF Program at the JPL, Aerospace, Technion-IIT

Program Manager : Douglas Bowers

1ST-Year Report

[April 1 1989 to March 31, 1990]

Approved For	
EARS 10001	
DMIC T-10	
U. S. AIR FORCE	
JPL Distribution	
By	
Distribution/	
Availability Codes	
Dist	Avail and/or Special
A-1	

Principal Investigator: Benjamin Gal-Or

Professor & head, the Jet Propulsion Laboratory, Faculty of Aerospace, TIIT.

Report Date : April 24, 1990



Abstract: This project aims at proof-of-concept/feasibility/validation studies of post-stall, supermaneuverable, **pitch-only, or yaw-pitch, or roll-yaw-pitch thrust-vector F-15 designs.**

For that purpose we employ a new integrated laboratory/flight-testing methodology to design, construct, flight-test and validate new yaw-pitch, or roll-yaw-pitch [1/7th-scale], thrust-vector F-15 models equipped with onboard computers which record conventional and/or **Post-Stall [PST] Thrust-Vectoring Maneuvers [TVM]**. Accordingly, post-flight analyses are intended to demonstrate/validate clear-cut advantages of vectored over conventional F-15 fighters.

This report summarizes the 1st-year efforts in this direction. During the past year the design, construction and **qualitative flight-testing demonstrations** of ["9-foot/17Kg/1st-generation"] yaw-pitch-vectored F-15 RPVs were completed. Also completed were the design, construction, calibration and preliminary flight tests of a light-weight, **onboard computer with sensors/instrumentation** that would later provide **quantitative post-flight analyses**. Additional work was completed in the design, construction and preliminary calibration runs of **subscale and fullscale PST F-15 inlets** (Cf. our latest calibration runs on p. 174-177).

Repeated flight tests of a yaw-pitch F-15 RPV have demonstrated **very poor thrust-vectored roll performance**. Hence, a **roll-yaw-pitch** wind-tunnel model and a thrust-vectored F-15 RPV have been designed and constructed. The geometry, dimensions and preliminary wind-tunnel test data for such a design are provided in Appendix A. If funded, such a 3rd-generation RPV is to be flight-tested with and without vertical stabilizers during the third year of the program.

The already-funded 2nd-year efforts are intended to demonstrate/validate a 2nd-generation set of light-weight **yaw-pitch** F-15 RPVs equipped with 2nd-generation computers/probes. These efforts will also include the development of new [vectorable] F-15 PST-Inlets and of new **Standard Agility Comparisons Maneuvers [SACM]** for PST-TVM, as well as [statistical] post-flight analyses. Additional flight tests are planned for **tailless** F-15 RPVs [with 50-, 75- and 100%-cut vertical stabilizers], and for Roll-Yaw-Pitch thrust-vectored F-15 RPVs **with and without vertical stabilizers** [during 1991].

A cost-sharing program in which we run jet-engine-tests with new yaw-pitch, or roll-yaw-pitch thrust-vectoring nozzles and modified F-15 inlets is conducted within this program. Another cost-sharing program is a similar F-16 program, financed by General Dynamics. A portion of this work is based on previous work financed by Teledyne and General Electric.

The research methodology employed throughout the project includes seven integrated phases. The main problems facing this new field of technology are described in the main text. Additional considerations, drawings and details are available in the Appendices and in our previous reports and **video cassettes**, as well as in our new book.

TABLE OF CONTENTS

Documentation pages	i
Abstract	iv
The 29 Participants-Contributors to this USAF Project	3
Notes	5
Projected Milestones in the USAF/JPL program	6
 Chapter I : OUTLINE	 7
Methodology	11
The 12 F-15 Baselines to be Flight Tested within the Framework of this Project	18
Minimum Instrumentation for flight testing the 12 F-15 Baselines	18
The Statistical Repeatability Required During Agility Comparisons of Baselines	19
Development of Three Complementary Test Methods for New "Vectorable" F-15 Inlets	20
Cost-Sharing Efforts For This Project	21a
Radio Interferences and Safety Considerations	21b
Time Tables/Milestones for 1990 - 1991	21b
Figures : Preliminary Calibration Flight Test Data Obtained from the Onboard Computer	33
Tailless, PST-RaNPAS, Roll-Yaw-Pitch, Thrust-Vectored, PST F-15 [Cf. App. A]....	40
 Chapter II: Our Methodology Vs. Different International Methodologies	 43
Different International Methodologies	43
Enhanced Pointing Capabilities	44
Technology Bottleneck	45
The Basic Definitions of Pure Vectored Aircraft (PVA)	45
Integrated Laboratory/Flight Tests Performed by this JPL	46
 Chapter III: Agility Comparisons Problems	 47
Missile/Aircraft Debated "Agility Metrics"	47
Supercontrollability	48
Specific "Agility Metrics" Problems in this Project	48
F-15 Baseline Comparisons	49
Ground and Low-Speed Handling	50

Chapter IV: ETV Vs. ITV [External vs Internal Thrust Vectoring]	51
Partially-Vectored Aircraft	51
By Products	52
IFPC [Integrated Flight Propulsion Control]	52
Chapter V: Tentative Concluding Remarks	53
REFERENCES	54
A Pictorial Sub-Report	55 - 71
Appendix A: Roll-Yaw-Pitch, PST-RaNPAS, F-15 Upgrading	72
The Major Problems	72
Design Objectives	72
Flow Considerations	74
Structural Considerations	74
Patentable Thrust-Vectoring Nozzles from this JPL	74A
Thrust Losses Tests	79A
Appendix B - Part 1: Introduction to High-Alpha Inlets [A Review]	80 - 103c
Concluding Remarks Extracted from Previously Published	
PST-Inlet Works	103a
Part 2: F-15 Inlet Test Rigs for PST Simulations	104
Part 3: Conceptual Inlet Configurations	108
Part 4: Preliminary Test Results [Ido & Roni]	116
Part 5: Inflight Maneuverability Benefits	151
Part 6: Preliminary DC and I²r Test Results for F-15 Inlet at	
Various AoA [Dr. Sherbaum & Dr. Rasputnis]	154
Part 7: Test Data By Improved, 360-deg-sweep F-15 Inlet	
Test Rig [Dr. Sherbaum & Dr. Rasputnis]	173
Our computerized new standard for plotting PST-Inlet Flow-Pressure	
Distortion Coefficients/Contours	174
Appendix C: How to Measure RPV's 3 Moments of Inertia: Calculations of Proper	
Springs/Balances, Frequency Vs. Error	178

The 29 Participants-Contributors to this USAF Project:

[PCSI is a Haifa-based computer company which has developed our special onboard computer. A number of the individuals listed below are part-time paid workers selected from the TIIT's aerospace community of students. Others are full-time or 1/2-time paid workers. A combined list of group members means unpaid work of students within their final, 2-semester "Design Project". Some of these students are mature pilots, or national/International champions in R/C model flying, or authorized military flyers of prop-RPVs.]

Amir Yogev [IDF authorized, "Day/Night/Operational" Military prop-RPV Flyer. Our 1st-rank Flyer of the vectored F-15 RPVs since March 1990].

Berkovitch Raphi [Lt. Colonel, IDF F-16 Pilot. Construction of elevator-less, Yaw-Pitch-Roll , Thrust-Vectored F-15 RPV to be flight tested during 1990/91]. **Cf. page 72.**

Cohen Zahi [Construction and stand-by flyer of the F-15 RPV till Feb. 1990]. **Cf. page 66**

Coslat Yaron [R/C model flyer. A stand-by flyer for the F-15 RPV since March 1990]

Dekel Eli [F-15 subscale and fullscale inlet/nozzle work, 2nd and 3rd-generation F-15 RPV construction]

Friedman Frez [Our 1st-rank Flyer of the F-15 RPV till March 1990. Construction and calibration of the 1st-generation vectored F-15 RPV]. **Cf. page 66.**

Gafni R. [Construction of elevator-less Yaw-Pitch-Roll Thrust-Vectored F-15 RPV to be flight tested during 1990/91].

Gal-Or Benjamin [Principal Investigator of this project. Head, JPL. Professor, Faculty of Aerospace Engineering. Video-camera operator during flight tests.].

Greenberg Israel [Israel's Champion for flying R/C models - since 87. 2nd-Position in the 88 European Cup].

Igal Harel [Construction, calibration and laboratory engine tests of F-15 RPV and Forces/Moments Metrics].

Ido Fenygsein and Yaron Sade [Construction and preliminary tests of F-15 Inlet Subscale Rig]
Cf. Appendix B -Part 4.

Meshaich Eli [F-15 subscale and fullscale inlet work, 2nd and 3rd-generation F-15 RPV construction].

Oren Yoav and Rami Aristozan [pure-vector, 4th-generation, elevator-less F-15 wind-tunnel models construction & tests & analysis]. Cf. page 796.

PCSI-Pesach Pascal and PCSI-Doron Rosenwasser [Design, construction and initial lab tests of 1st and 2nd-generation onboard computers and of the ground computer for flight tests]. Cf. pages 70, 71

Polansky Igal [Construction, calibration and laboratory engine tests of F-15 RPV and Forces/Moments Metrics].

Rasputnis, Dr. Alexander [Fullscale, F-15 vectoring nozzle calibrations & tests & computing procedures. Also Subscale & Fullscale F-15 "vectorable" inlet studies, calibrations & computing procedures]. Cf. pages 154-174.

Sapir Shaul [IDF 707 pilot. Design, construction, and lab tests of 4th-generation, elevator-less, yaw-pitch-roll F-15 RPV to be flight tested in 1990/91]. Cf. p. 72.

Sherbaum, Dr. Valery [Subscale & Fullscale F-15 "vectorable" inlet studies, calibrations & tests & computing procedures since Dec. 1989]. Cf. pages 62, 154-174.

Shlomo, Moshe and Igal [Design, construction, and lab tests of 4th-generation, elevator-less, yaw-pitch-roll F-15 RPV]

Spector, Ben-Zion [Construction, calibration and laboratory engine tests of F-15 RPV as well as construction and calibration of onboard computer-probes hardware]. Cf. p. 58.

Sofer Dan [Post-flight analysis and calibration of onboard computer-probes hardware].

Soreq Ilana [Typing, reporting, filing, budget monitoring, workers overtime-payment-procedures].

Tomi U [Typing, translating and figure positioning]

Vershavsky Dan [Post-flight analysis and calibration of onboard computer-probes hardware].

Vorovelchik Sara [Drawings, figure scaling, filing, and mechanical design].

Notes

The two **video-cassettes and the previous Progress Reports** submitted previously to the Program Manager form an integral part of this Report.

The following **Book reference** by the Principal Investigator was also submitted to the USAF. It is entitled as :

Vectored Propulsion, Supermaneuverability and Robot Aircraft

Foreword by Dr. G. Keith Richey,

Technical Director of the Wright Research and Development Center, Wright-Paterson Air Force Base.

This book has been published by Springer-Verlag, N.Y and Heidelberg, in 1990 .

[275 pages, with 189 Illustrations and 237 References],

This book may also be considered as part and parcel of this Report.

Chapter I

Outline

Presentation of The Main Problems

- Is thrust vectoring becoming the standard technology of fighter aircraft ? Indeed, how important it is to enhance maneuverability and controllability ?
- Are the roads to thrust vectoring (TV) also the roads to PST, and to low observability ?
- What are the fundamental concepts of "pure" and "partial" vectored aircraft ; or of "internal" and "external" TV ?
- What are the technology limits, and what is the state-of-the-art of TVM ?
- What is the lowest thrust-to-weight-ratio above which one can extract clear-cut advantages of vectored fighters over conventional ones? I.e., which of the existing fighters can be upgraded to become PST-vectored fighters?
- What are the most promising designs of PST-Stealth/vectored propulsion/vectored aircraft? Do we have the proper design philosophy to handle these problems? Are Soviet and Western TVM methodologies similar?

- Does yaw-pitch-roll TVM constitute a basic requirement for survivability and winning in the air combat arena? How can it contribute to the aircraft's STOL and agility characteristics?
- Can an efficient PST-inlet be developed? Can such inlets be installed on, and flight tested by PST-vectoring RPVs? Indeed, what should be the R&D tools for the evaluation of TVM?
- How should TVM and PST-fighter agility be defined? What are the measurable parameters, or "metrics", which define vectored aircraft agility?
- How can we identify maneuvers, missions, and flight regimes in which vectored aircraft demonstrate advantages over conventional ones? Can one express these advantages in terms of killing-ratios, or other measurable metrics?
- What should be the new flight/propulsion control rules for PST-vectoring aircraft? What are the new human factors involved with TVM? How an integrated cockpit/flight/propulsion control systems be designed for PST-TVM? On the basis of what experimental data bases?
- What specific new maneuvers, and what new pilot tactics are associated with "partial" and "pure" PST-TVM? Can one invent, test and verify such new maneuvers with the help of PST-vectoring RPV simulations? Is such a new methodology cost-effective? What are its inherent limitations?
- What are the expected g-loads, and other limitations, associated with PST-TVM?
- And, most important, how should vectorable engine nozzle and vectorable inlet geometric design, and aspect ratio (AR), be modified to meet a given set of new mission needs, such as low signatures, STOL-VTOL, air-to-air, or air-to-ground supermaneuverability and supercontrollability? In particular, what are the engine/nozzle/inlet efficiency variations and limitations associated with these new design trends?

A Few Preliminary Conclusions

The following preliminary conclusions have been extracted from the aforementioned book reference. Additional ones are presented in the next Chapters.

- The availability of PST vectored fighters, helmet-sight-aiming systems, all-aspect missiles and the new generation of EW systems, require reassessment of the optimal balance between aircraft agility and effectiveness, and the agility and effectiveness of missile/helmet-sight-aiming systems.

- Whatever is the aforementioned balance, high-performance fighter aircraft will gradually be based on improved thrust-vectored propulsion/maneuverability/controllability.

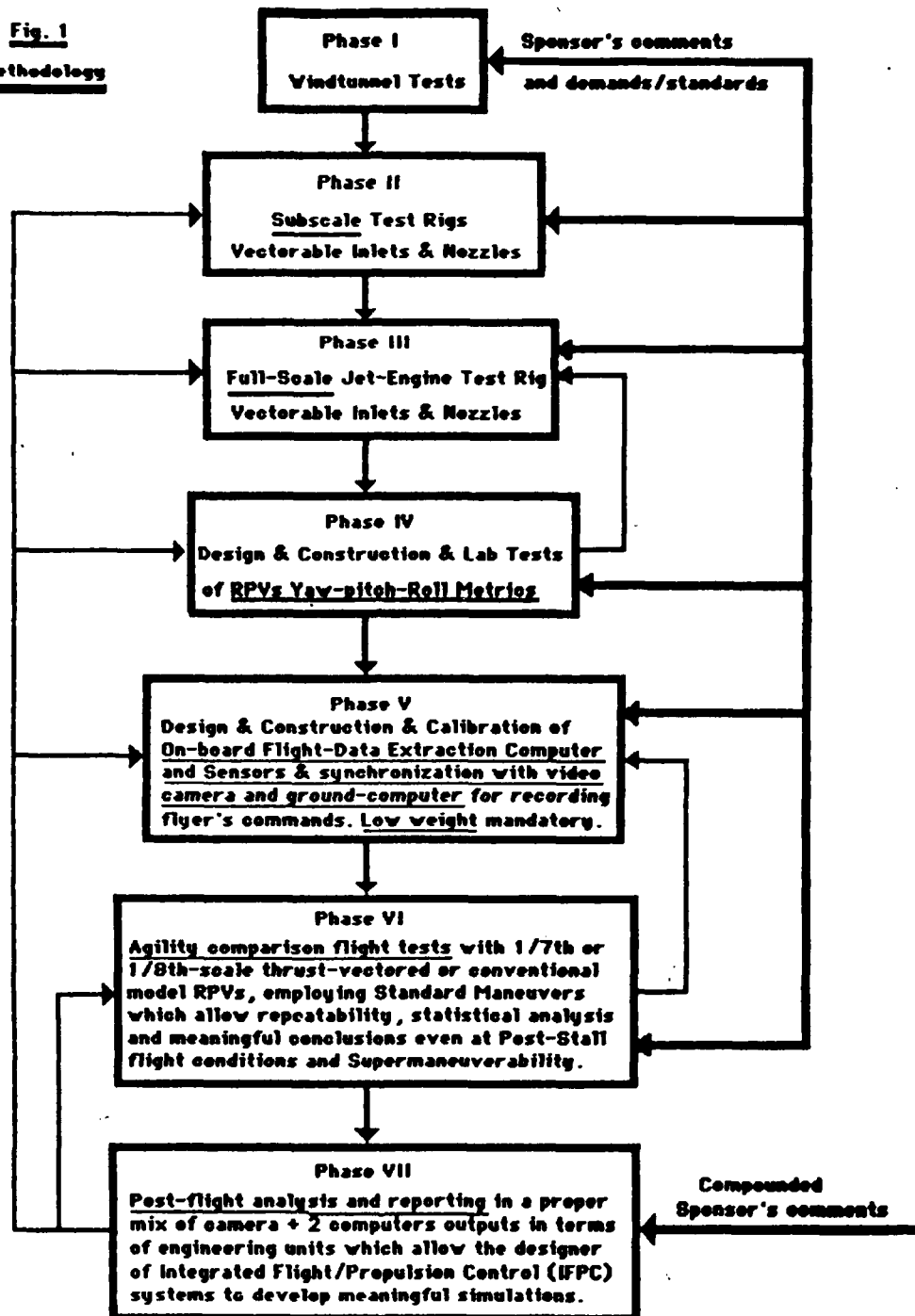
- New point-and-shoot weapons have reduced engagement times drastically, leaving aircraft with poor maneuverability and controllability at the mercy of those that can use their agility to point-and-shoot quickly during close-in combat.

- Since future fighter aircraft would be thrust-vectored, and since thrust-vectoring engines/nozzles/inlets would be used for enhanced maneuverability and controllability, as well as for brute-force propulsion, one must first define and test new propulsion concepts and new measurable "metrics", which would be employed in a realistic comparison of TVM with that of conventional ones.

- The ability to point the nose/weapon at the enemy quickly, while, simultaneously, computing and locking, so as to minimize the total length of delay times associated with secure locking and obtaining the shortest/optimal missile flight path/time from aircraft release point-attitude to the moving target, is key to offensive engagements. This requires aircraft conventional and PST-agility to be well-integrated with missile's high "g"/speed agility and initial vectoring conditions.

- Other conceptual and practical conclusions are available in this new reference. It also includes reviews of the various maneuvering and design methodologies and presentation of the main hardware design concepts. As stated in the Foreword by Dr. Richey, it is the first complete treatment to date of these complex subjects, and it addresses the key questions which are now the subject of active research and development programs in all major aerospace establishments.

* * *



Presentation of Our Integrated Test Methodology

The methodology developed by this laboratory and tested-validated by the 29 team members of this USAF project is schematically depicted in Figure 1. The figure is self-explanatory. However, additional details are provided below and in the Appendices.

Phases VI and VII are probably the most important ones. Hence we shall concentrate first on them.

To start with let us examine Fig. 2 which is also self-explanatory. To follow the various technical efforts required for the substantiation of these last two Phases one may first consult Figs. 3 and 4.

Agility comparisons, such as pitch rates & turn rates & roll rates at various conventional or thrust vectoring conditions are depicted schematically in Figs. 5 and 6.

On the other hand, in order to provide meaningful engineering results via Phase VII, one needs to first establish the powerplant "metrics" of the RPV during various combinations of yaw-pitch thrust vectoring at different throttle settings [Figs. 8 to 14]. Next one needs establish the relationships between "Effective" vs "Geometric" angles of the deflected jets [Figs. 15 and 16], during conventional thrust-vectoring maneuvers and during PST-TVM [Figs. 7 and 3].

It is the data reported in Figs. 15 and 16 that are of interest to the designer of **Integrated Flight Propulsion Control (IFPC)** systems and cockpits of future fighter aircraft. [For normalization purposes one may use the data presented in Fig. 17.]

Examples from the 1st-generation computer outputs are shown in Figs. 18 to 21. The data are for a prop model used as test-bed for the onboard computer. The computer itself was developed within the framework of this program. It was designed and produced by IPSI of Haifa. This computer was sampling 32 channels every 0.1 seconds while the IPSI-2nd-generation computer [which is now ready to fly] records 16 channels every 0.05 seconds [see below].

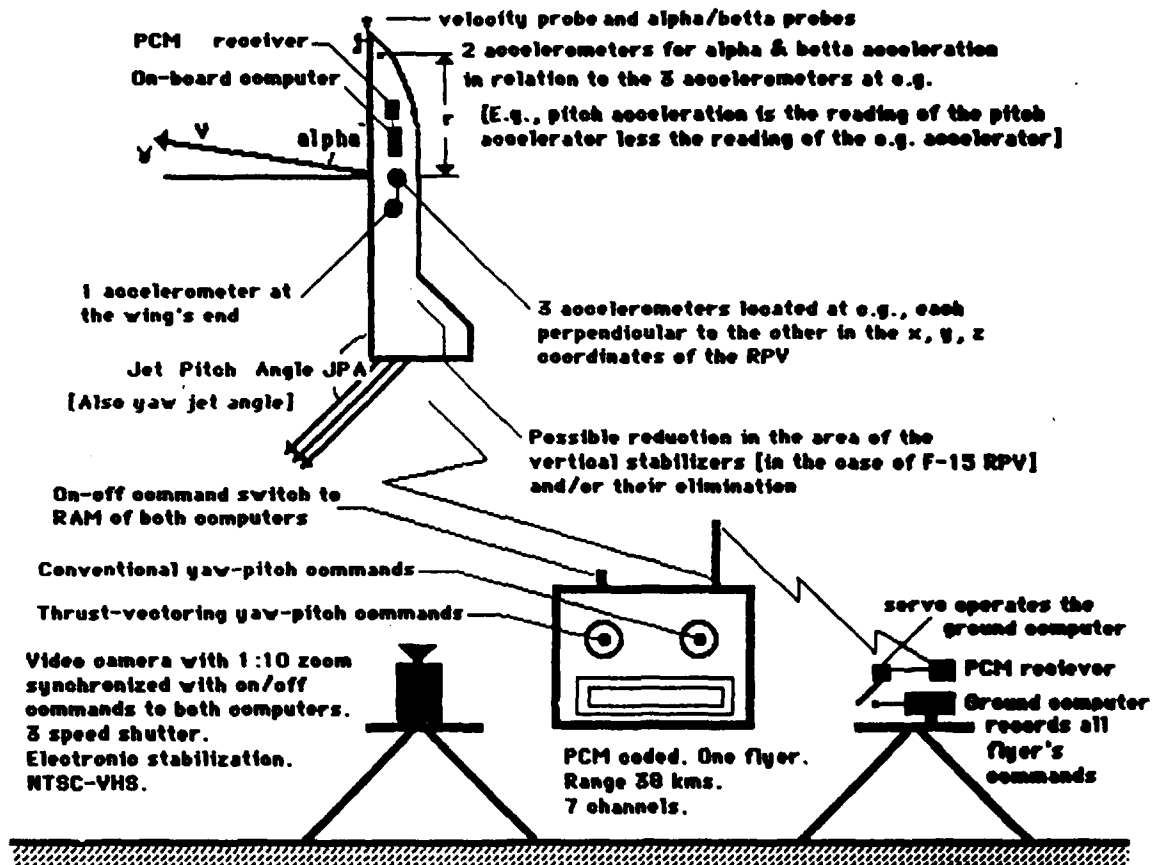
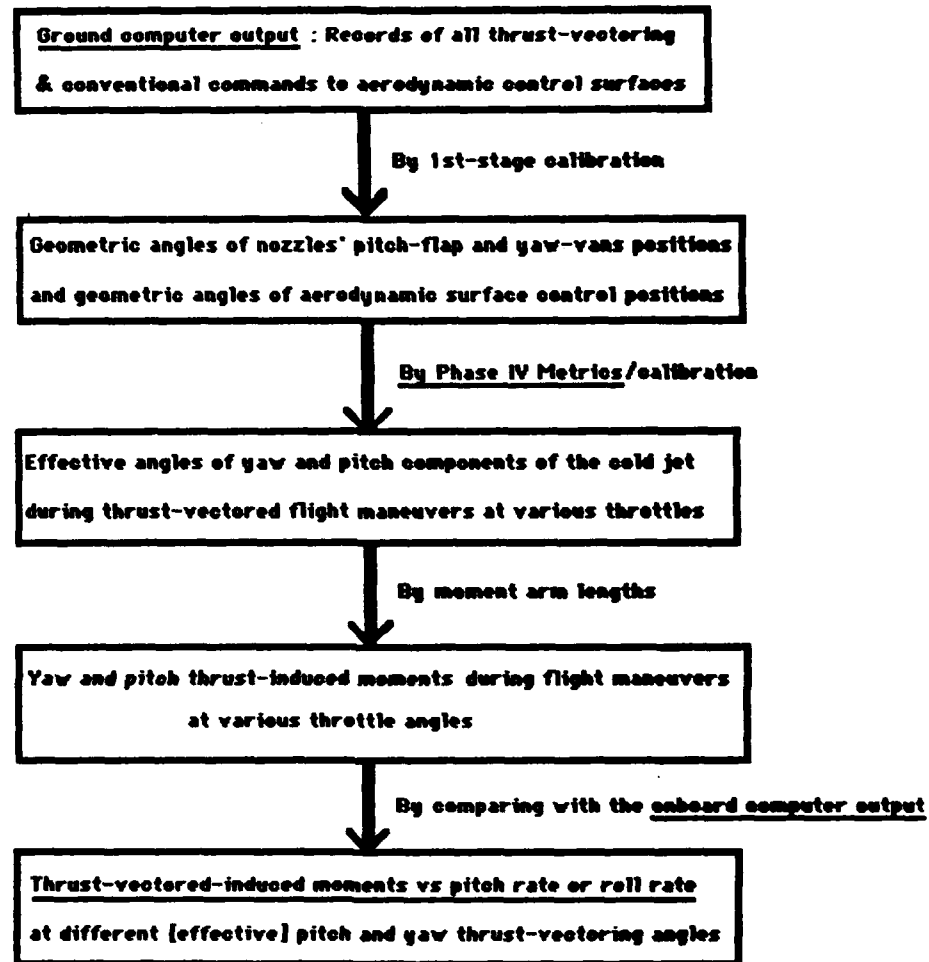


Fig. 2 : Computers/probes/camera/controls synchronization methodology as used during Phase VI of the program. RPV is shown during a Post-Stall maneuver. Conventional-Vectoring PCM R/C system for a single flyer, as shown here, has replaced earlier systems involving 2 flyers and, later, a single flyer with 2 separate R/C control systems. Thrust-vectoring joy-stick operates the yaw-pitch thrust-vectoring nozzle flaps/vanes in the same manner as the conventional joy-stick located on the right hand of the new, modified, control system.

Fig. 3 : Calibration Chart



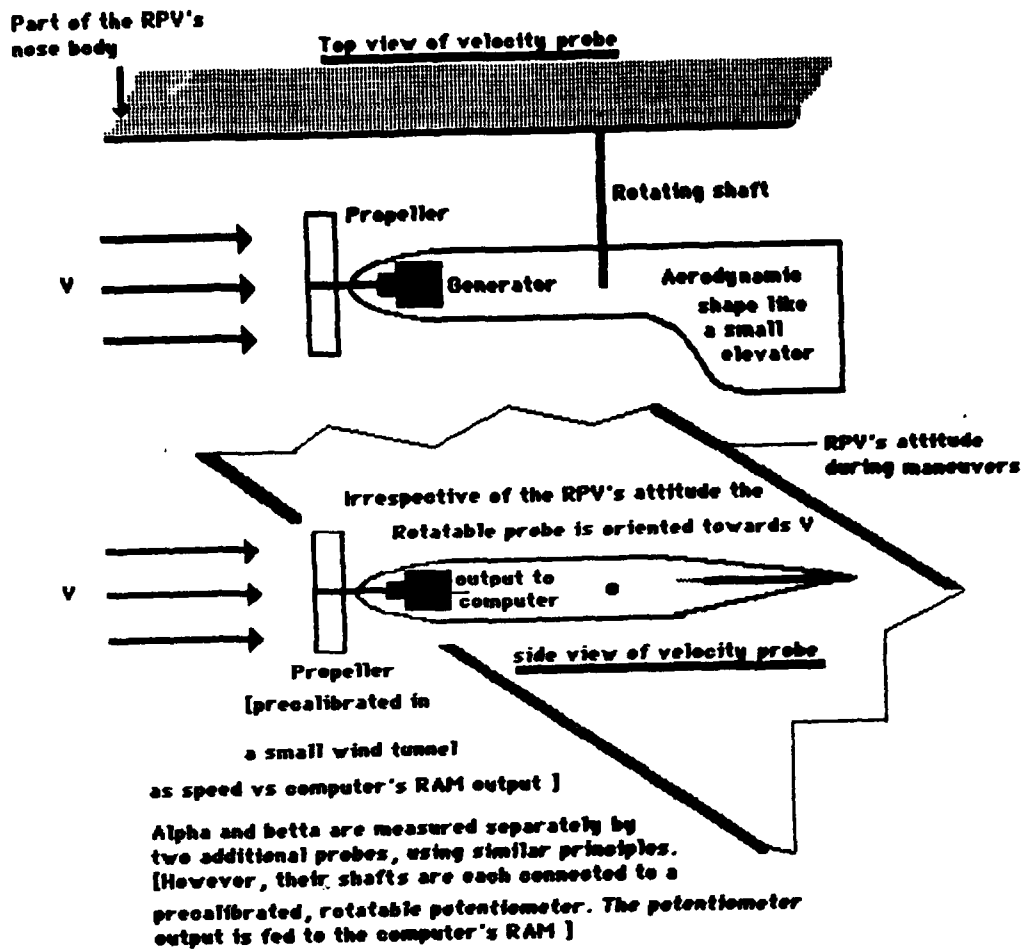


Fig. 4: The Velocity Probe

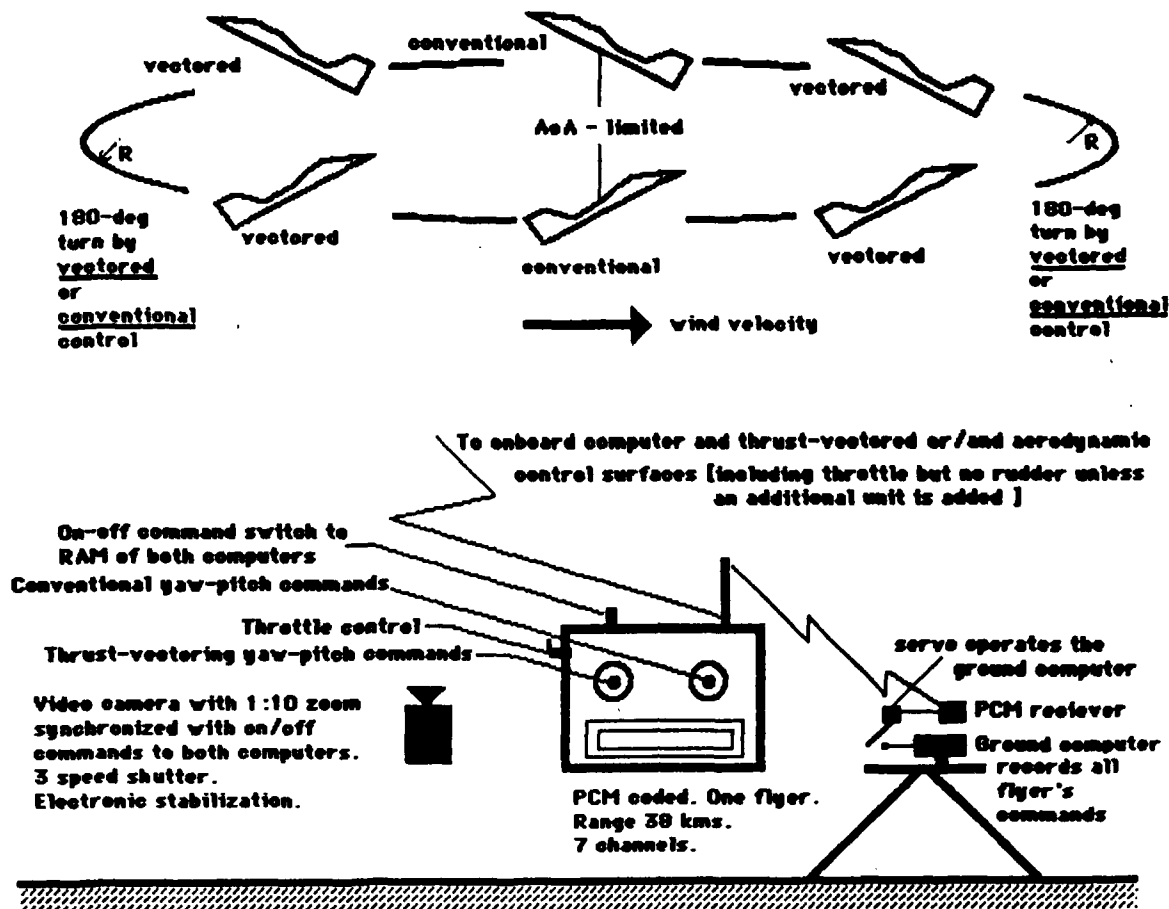


Fig. 5 : Pitch Rate & Turn Rate Tests at various speeds. Alternatively the flight tests may be conducted with only thrust-vectored control followed by only aerodynamic control and finally by both controls for maximum performance. However, conventional control may fail beyond a given AaA. Hence the comparison may be limited to pitch-rate tests up to that AaA.

Repeatability of the flight tests under similar conditions is required for statistical analysis and the generation of meaningful engineering results and conclusions.

Provided the video-camera is almost perpendicular to the flight path, its recordings [at high-shutter speeds] may be employed to verify pitch rate results obtainable from the computers].

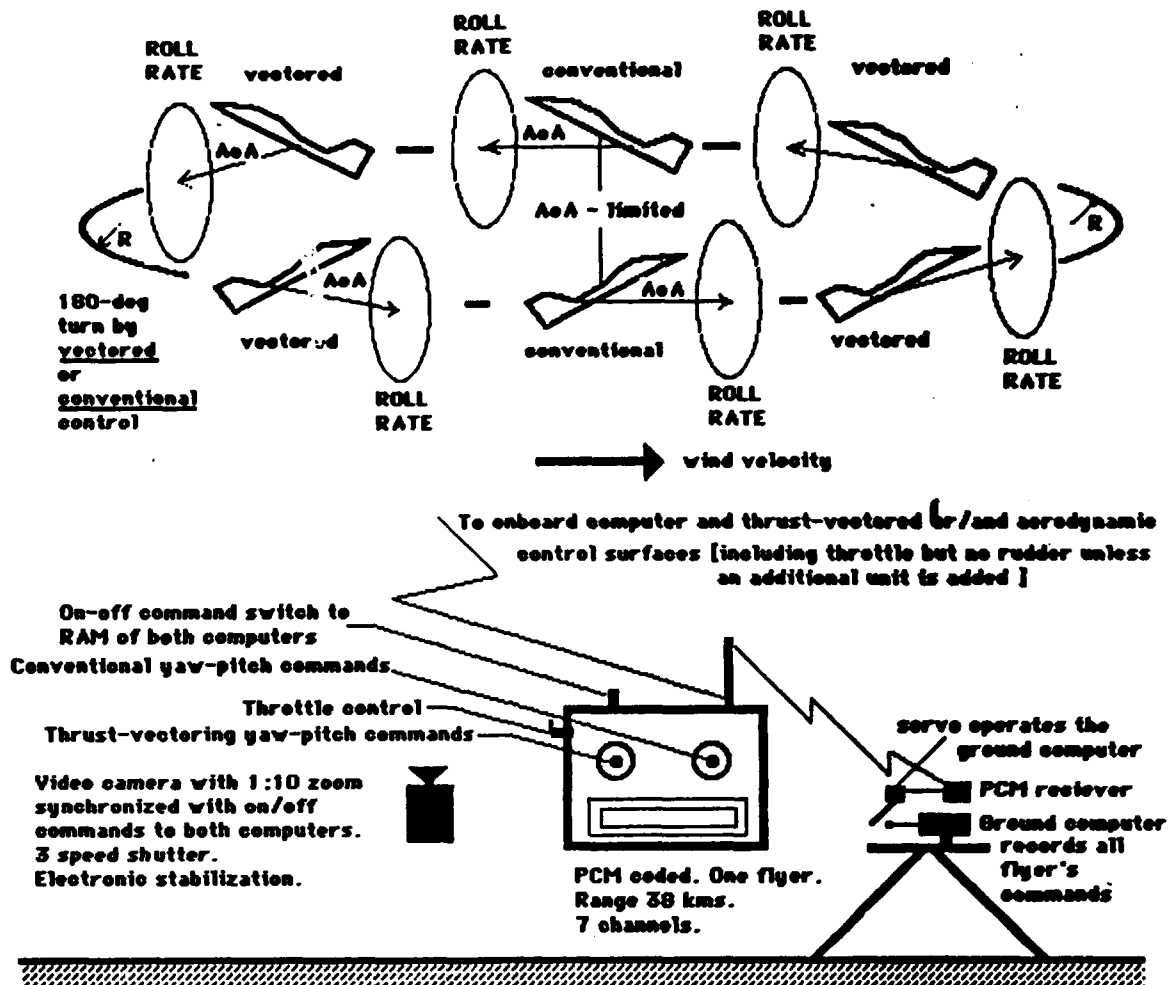


Fig. 6 : Thrust-vectored yaw and roll are strongly coupled in our flying RPV models. The introduction of PST/Vectored Technology requires reassessment of all maneuverability and controllability concepts, standards and technology limits.

Beyond a given AoA the roll rate of a conventional control system fails while that of a thrust-vectored system functions well. Hence, a major aim of the statistically repeated yaw-roll standard maneuvers to be worked out during the next-year flight-testing program is to establish the proper flight testing methodology-procedures-unit-operations which can provide the designer of a future IFPC system with meaningful flight-test data. The accelerometers outputs recorded on the onboard computer may be partially verified with the recordings of the video-camera [when the camera is placed almost perpendicular to the flight path]. Right and left roll directions should also be compared as well as the roll rate obtainable with both conventional and vectored controls.

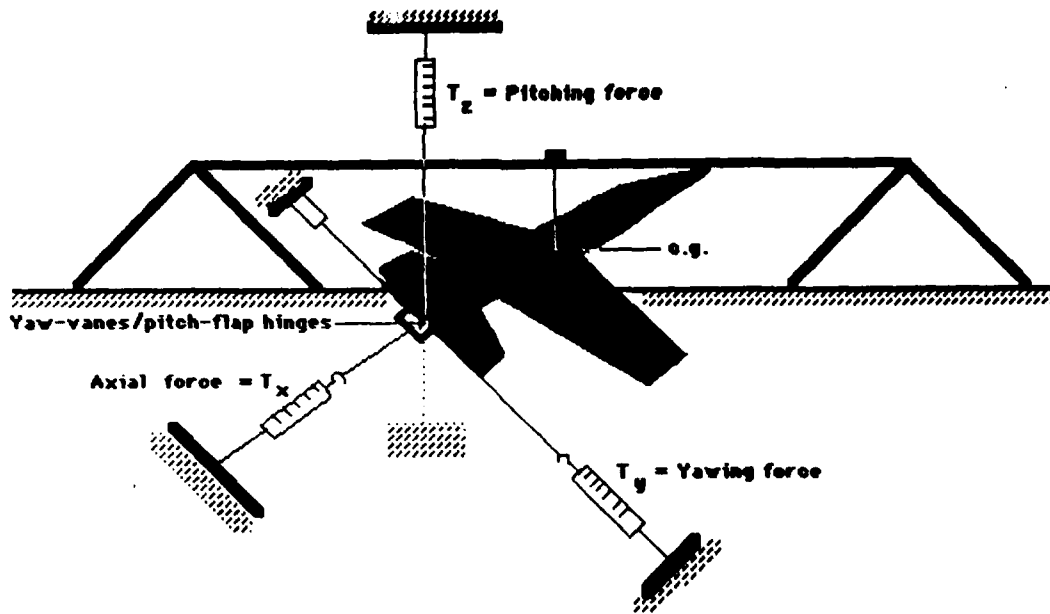


Fig. 7: RPV powerplant metrics are measured during Phase IV by this simple test rig. The most important results are those which compare GEOMETRIC with EFFECTIVE YAW and PITCH angles during thrust - vectoring. Each set of test results is obtained at a different throttle setting. Simultaneous yaw-pitch thrust vectoring is also evaluated experimentally by this test rig. The designer of WPC systems needs such data whenever he employs the flight test data, i.e., when, say, a command of 9 degrees yaw is made, the actual jet-yaw-angle may be higher or lower, depending on the particular thrust-vectoring nozzle used during the agility-comparing maneuvers.

Hence, what must be done during the last phase of this project is to re-express the commands recorded by the ground computer [the geometric angles of the yaw-vanes and pitch-flaps] in terms of the EFFECTIVE yaw-pitch angles of the jet(s). However, prior to that we must precalibrate the zero setting of the joy-stick with zero settings of the yaw and pitch geometric angles. It is only by going first through these stages that one can evaluate such parameters as the degree of coupling between yaw and roll for various vertical stabilizers, various speeds, various throttle settings, various maneuvers, etc. All initial maneuvers will be performed at constant FULL THROTTLE.

**Flight Testing of Simultaneous Yaw-Pitch, or Yaw-Pitch-Roll
Thrust-Vectored-Controlled F-15 RPVs**

The following 1/7th-scale F-15 RPV design versions are to be flight tested for agility comparisons:

- [**Baseline-1'**] unvectored F-15 RPV [with circular, axisymmetric, fixed nozzles];
- [**Baseline-2'**] unvectored, canard-configured, F-15 RPV [with circular, axisymmetric, fixed nozzles];
- [**Baseline-3'**] pitch-only, canard-configured, vectored F-15 RPV;
- [**Baseline-4'**] pitch-only, canardless, vectored F-15 RPV;
- [**Baseline-5'**] yaw-pitch, canard-configured, vectored F-15 RPV;
- [**Baseline-6'**] yaw-pitch, canardless, vectored F-15 RPV;
- [**Baseline-7'**] pitch-only, canard-configured, vectored F-15 RPV with one-half, or less, vertical stabilizers surface area;
- [**Baseline-8'**] pitch-only, canardless, vectored F-15 RPV with one-half, or less, vertical stabilizers surface area [Cf. Figs. 22 to 25];
- [**Baseline-9'**] yaw-pitch, canard-configured, vectored F-15 RPV with one-half, or less, vertical stabilizers surface area [Cf. Figs. 22 to 25];
- [**Baseline-10'**] yaw-pitch, canardless, vectored F-15 RPV with one-half, or less, vertical stabilizers surface area [Cf. Figs. 22 to 25];
- [**Baseline-11'**] yaw-pitch-roll, elevator-less/canardless, Pure Vectored F-15 RPV;
- [**Baseline-12'**] yaw-pitch-roll, elevator-less/canardless, without vertical stabilizers, Pure Vectored F-15 RPV [Cf. Figs. 22 to 25].

The Minimum Instrumentation Required

Every 0.05 sec., during conventional or PST-TVM, these RPVs must generate data-bases from:

- 6 onboard accelerometers,
- alpha probe,
- beta probe,
- velocity probe.

The RPV's responses to various flight/maneuvers are to be recorded by a video-camera and by an onboard computer. The flight commands are to be recorded by an additional ground computer [see Figure 2].

Requirements for Statistical Repeatability of the Flight Tests

The flight/maneuvers data are to be recorded by both computers every 0.05 seconds during "standard" maneuvers below and beyond the stall "limit". Each standard maneuver [SM] is to be repeated statistically so as to provide a reasonable basis for agility comparisons under statistically-similar maneuvering conditions. Similar weights (and, whenever feasible, also similar mass distributions), are to be maintained between the various "Baselines". This is not an easy task. In fact, it may become impossible with the canardless and the canard-configured F-15 RPVs.

Preliminary Computer-Accelerometers Calibration Tests

Preliminary flight-calibration data obtained every 0.1 seconds by the 1st-generation computer onboard of a prop-RPV are provided in figures 2 and 17 to 21. Originally we had gyros on board of the flying RPV. However, their current needs and weight have caused a penalty on agility. Consequently we had most recently switched to 6 accelerometers [3 are located at C.G., 2 in the nose, and one at wing tip - cf. Fig. 2]. These accelerometers weigh only 1/2 a gram each. However, each should be calibrated individually. Moreover, their different ranges of mv outputs require redesign of the amplifiers of the onboard computer.

The first computerized flight tests with the 2nd-generation computer/2nd-generation [light-weight] F-15 RPV are now planned for April 25, 1990 in Meggido Airfield (with Amir Yogeve as the flyer, Ben-Zion Spector, Dan Sofer and Dan Vershavsky as computer operators/calibrators/post-flight-analysts, Dekel Eli as the engine-ground operator and B. Gal-Or as video-camera operator/photographer/flight coordinator).

Previously the following attempts have been made with the 1st-generation [heavy-weight] F-15 RPV [without the onboard computer]:

Baseline-1 has been constructed and flight tested a few times till the summer of 1989.

Baseline-2 has been constructed and shortly took to the air on July 19 and on Aug. 8, 1989.

Baseline-4 pitch-only, canardless vectored F-15 RPV was flight tested on Aug. 26 and 27, 89.

Baseline-6 yaw-pitch, canardless, vectored F-15 RPV was flight tested on Aug. 26 and 27, 89.

The light-weight, 2nd-generation, vectored F-15 RPV with the 2nd-generation onboard computer was ready for flight tests in Meggido Airfield on March 27, 1990, with Amir Yogeve as the Flyer. However, engine starting problems have caused all our 3 starters to fail. Returning from abroad on April 18, the next attempt is scheduled for April 25.

Examples of Specific Flight Test Maneuvers with the Baselines
Defined in Page 18. [Initial tasks suitable for 2nd-Year Efforts]

The 2nd-year tasks depicted in Figs. 5 and 6 must be repeated for reasonable statistical post-flight analyses with each of the Baselines listed on page 18. The entire effort may take more than one year. To demonstrate the specific maneuvers required we list below examples of the maneuvers required.

1. Determine maximum nose-up/nose-down control with and without vectoring to determine **maximum pitch rates** for all baselines.
2. Determine maximum coordinated **roll rate** in 1-g flight at various throttle settings.
 - (a) Baselines 1, 2, 3, 4, 5, 6
 - (b) Baselines 1, 2, 3, 4, 5, 6 + reduced vertical stabilizers Baselines 7, 8, 9, 10.
 - (c) Baselines 1, 2, 3, 4, 5, 6 vs. Baselines 11, 12.
3. Determine maximum trimable/controllable AoA for various throttle settings. Configurations of interest:
 - (a) Basic F-15. [Baseline -1]
 - (b) F-15 with pitch vectoring. [Baseline -4]
 - (c) F-15 with pitch/yaw vectoring. [Baseline -6]
 - (d) F-15 with canard [Baseline -2 vs. Baselines -3 and -5]
4. Determine maximum **turn rates** in level flight for each Baseline
 - (a) Tail control only
 - (b) Pitch vectoring only
 - (c) Tail + vectoring
5. Takeoff distance with and without pitch vectoring for the various 12 baselines.
6. Departure resistance/recovery: Climb at steep angle until loss of control. Recover aircraft.
 - (a) Baselines 1, 2, 3, 4, 5, 6.
 - (b) Baselines 7, 8, 9, 10
 - (c) Baselines 11, 12
7. Attempt level/skidding turns with 5-10 degree heading change, with and without vectoring for all baselines.
8. Repeat the "Cobra" maneuver at different speeds, with all baselines.

**Preliminary Efforts to Develop Three Complementary Test Methods for
the Development of a New Family of "Vectorable" F-15 Inlets**

Three complementary test methods are employed here, **each with its pros and cons**. All combined, they are designed to provide **initial estimates** of the gross effects of high AoA [up to 90 degrees] on **Distortion Coefficients (DC) and Pressure Recovery (Pr)** at the downstream station of current F-15 inlets. Such gross effects, as deduced from the combined test results extractable from the three complementary methods, are to help initial conceptual and preliminary designs of **new ideas in "vectorable" inlets**. A few examples of such ideas are schematically shown in pages 108 to 115, while the three complementary test methods are described below:

1) - The [1/7th-scale] F-15 Inlet Subscale Test Rig

[Cf. Fig. 27, p. 42 and pages 57, 58, 67 - 70 and 105 ,174-177]

It should be stressed from the very beginning that this method cannot be used without the other two complementary methods, except for preliminary estimations based on a BASELINE [see below].

A REVIEW of the challenges and the multitude of complex problems involved in the development of such new Inlet concepts and of previous research efforts in this area is provided in **Appendix B - PART 1. Additional design and R&D&T treatments and considerations are available in our book.**

The major restricting reasons are scale effects and blowers/ducts restricted operating conditions.

However, we have used the **F-100 engine data and the increased mass-flow F-110 engine data** on the variations of the engine mass-flow rate **with Mach, altitude and throttle**, to calculate the **Reynolds numbers in station 2**, both in the subscale test rig and during low-speed-flight/minimum PLA [the domain of PST-TVM-RaNPAS of future fighters - cf. the next Chapters]. These comparisons show that **both Reynolds numbers are about the same [10^5 - 10^6]**. [Note also that we can increase the flow rate through the F-15 subscale inlet **by opening the butterfly valve of the "suction" blower to the maximum** - see Fig. 27, p. 41].

Nevertheless, a number of additional effects may still affect the accuracy and repeatability of this method, in particular the boundary-layer-theory deductions concerning the boundary-layers behavior in the actual and in the subscale inlets and the restricted blower-duct opening area vs. blowing speed considerations which cause increasing flow nonuniformities ahead of the inlet, especially at high incidence angles. These problems are resolved by combining the test results extracted from the subscale rig with those of the **FULL-SCALE TEST RIG** and by the use of deviations from the **TAKEOFF-BASELINE**, which is obtained with **ONLY THE SUCTION-BLOWER on** [Cf. p. 156 ,174].

It should be stressed that the TAKEOFF-FLOW-SIMULATION BASELINE [p. 156 and p. 163-4] is a basic one.

Deviations from this baseline are attributed to AoA-Induced distortions, Inlet Mach Number Effects and some blower/duct nonuniformities. [The blower/duct nonuniformities are eliminated in the TAKEOFF-FLOW-SIMULATION BASELINE and in the "Full-Scale Engine/Inlet Test Rig".]

A COMPUTER PROGRAM which automatically plots these deviations has been developed for this project [Cf. p. 174]. Its results are of a much greater degree of accuracy than the initial, preliminary maps provided now in Appendix B-Part 4.

Calibration and preliminary test results with the subscale F-15 inlet at various incidence angles and speeds are provided on pages 116 to 174 [Appendix B]. The [unvectored] inlet lowered ramp and external and internal dimensions used in these subscale studies [p. 105] are also those of the left-hand inlet installed on the first flying, 1/7th-scale F-15 RPV [Our PROTOTYPE No. 7]. Various vectorable devices [such as rotating inlet lips and rotating 'venecian' vans], are to be tested next for pressure recovery and distortion coefficients during 0 and 90 degrees incidence, i.e., for PST-TVM. So far the data indicate that a major distortion problem evolves beyond about 60 degrees incidence [cf. p. 117], thereby indicating the need for "vectorable" lips and/or vanes during PST maneuvers.

Figures such as the one shown on page 174 will now become our **standard inlet distortion maps**. Similar maps will be produced within the framework of the Full-Scale engine-Inlet tests described below.

It is mainly due to the boundary-layer behavior in this 1/7th subscale, that a clear-cut advantage is expected for up-scaling the 1/7th-scale inlet and installing it on an actual jet engine equipped with actual and expected new vectoring nozzles. Consequently, combined with the TAKEOFF BASELINE data [p. 156], this approach was adopted [see also "Full-scale Test Rig" below].

21 - THE "FULL-SCALE" ENGINE/F-15-INLET TEST RIG

[Cf. Figs. 7a, 7b p. 22a,22b, Fig. 26 p. 41 and pages 56, 57, 59, and Figs. B.2.2 to B.2.3 p. 106-107].

The needs to develop a complementary "Full-Scale Engine Test Rig" were enumerated above. This test rig is based on a Marbore-II turbo-jet engine. The full-scale F-15 Inlet [p. 56, 57, 106] is to be tested with this jet-engine during 1990-92 with a circular, or with a 2D yaw-pitch, or with a 2D yaw-pitch-roll thrust-vectoring nozzles [Cf. Fig. 26], as in the integrated thrust-vectorized propulsion systems which might be employed in future designs. This, in fact, is a cost-sharing effort.

Inlet-incidence at low subsonic conditions would be restricted [during full-scale tests] to 3 angles : 0 , 70 [as in the X-31A and in accordance with the preliminary results obtained with the subscale inlet], and finally at 90 degrees. These restrictions are due to cost, time and complex technical problems. Various vectorable devices [such as rotating inlet lips and rotating 'venecian' vans], are to be tested later in 91/92 for pressure recovery and distortion coefficients. At the present time we have started the instrumentation of the inlet. Zero incidence, calibration tests to establish BASELINES will begin around September or October 1990.

3] - Flight Testing of the 1/7th-scale F-15 Inlet During PST-TVM [Cf. p. 62-3]

The inlet lowered ramp and external and internal dimensions [p. 105] are those of the left-hand inlet installed on the first flying, 1/7th-scale F-15 RPV [Our PROTOTYPE No. 7]. It was instrumented with 19 internal pressure probes, as reported and depicted in our earlier figures, drawings, reports and video cassettes.

However, this method has so far been encountered with weight problems which directly affect agility. The problems originate from the anavailability of light-weight pressure transducers at the range of 0 to 0.15 PSI full-range. The need for 19 heavy-weight transducers has, so far, dictated their elimination from the 2nd-generation F-15 RPV. Consequently, the **2nd-generation F-15 RPV [PROTOTYPE 17]** weighs only 13.2 kg [without fuel] as compared with 16 kg [w/o fuel] of PROTOTYPE 7. In a cold-day this means **$T/W = 2 \times 5.5 / 13.2 = 0.83$** vs **$T/W = 2 \times 5.5 / 16 = 0.69$** for the 1st-generation F-15 RPV. These ratios are lower in hot weather and at the beginning of the flight test [which lasts about 8 minutes]. To increase these ratios, speed and safety, we have ordered now a new set of **25% higher power engines** [The O.S.-91VR-DF, which are new on the market and are now the highest-power ducted-fan engines available. These will replace our O.S.-77VR-DF.]. Hopefully these engines will considerably increase our T/W, speed and safety, starting from June 1990.

A Cost-Sharing Effort [For testing new types of nozzles and inlets]

This program includes a cost-sharing project to develop and test new families of thrust vectoring nozzles [Cf., e.g., p. 22d, Fig. 7d, pages 60, 65 and Figs. A-1 to A-6 in Appendix A] and PST Inlets [Cf., e.g., pages 56, 65, 108-115]. All these tests are performed with our "Full-Scale Engine Test Rig" [Cf. pages 41, 57, 59].

Another [minor] cost-sharing sub-program involves windtunnel tests of [yaw-pitch-roll, thrust-vectorred, canardless] F-15 models. Part of this effort has been completed now and the results be reported around September 1990. A few configurations which have been tested since 1986 are shown on p. 60. It was only the PVA prototype shown on top of the left group of models which has been scaled-up, constructed and flight tested on May 1987 [Cf. page 66]. A few variations of this configuration have been flight tested since.

The preliminary wind-tunnel tests include only Angle-of-Attack variations on the lift, drag and moment coefficients in the range of -10 to + 50 degrees in two low subsonic airspeeds : 16 and 32 m/sec. Higher velocity and AoA values are yet impossible to attain in our subsonic wind tunnel. The major purpose of these tests is to estimate expected AC changes due to the installation of integrated yaw-pitch-roll thrust-vectoring nozzles into the airframe of the 1/7th-scale RPV [Appendix A].

Interferences Affecting Flight Tests

During July and August 1989, in Ein Shemer Airfield, we have encountered strong radio interferences, causing considerable damages to the prototypes during a number of forced hard landings. To minimize such risks, we have moved the flight tests to the Dovrat airfield [near Mount TABOR].

However, the runway there is too steep and too narrow. Hence, we had moved our flight tests to Meggido airfield [where we also had encountered radio interference in the past.] Yet, to reduce the risk, involved, we have introduced Pre-Flight Safety Regulations which include **flying a prop model prior to the vectored RPV flights.**

Improved synchronization procedures for the video-camera-recording with the 'on-off' radio commands to the proper files of the onboard and the ground computers has also been introduced recently.

A PC-XT computer is to be taken to the airfield to reduce the risks of losing flight/maneuvering information before returning back to the laboratory [limited battery capacity]. Its use may also increase effectiveness. Following the flight tests, this PC-XT computer will be connected to the Lab PC-AT computers for extensive post-flight analysis and graphic displays.

A new video-camera, which fits with the American TV standard [NTSC], is now available in for flight tests and for recording the progress in the laboratory. [It replaces the private one of this investigator which fits only with the European PAL standard.] Unlike the previous one the new camera provides editing options and electronic image stabilization.

The Next Milestones/Time-Table

A schematic time-table estimation for the next stages is provided at the beginning of this Report.

Technical Report for the period April 1 1990 to March 31 1991 [10 copies, 1 Apr 89 - 31 Mar 91] will be delivered to the Science Officer (EOARD) on or before **30 May 91.**

Invention Report for the period April 1 1990 to March 31 1991 [3 copies, 1 Apr 89 - 31 Mar 91] will be delivered to the Science Officer (EOARD) on or before **30 May 91**.

Fiscal Report for the period April 1 1990 to March 31 1991 [2 copies, 1 Apr 89 - 31 Mar 91] will be delivered to the Contracting Officer (AFOSR/PKZ) on or before **30 May 91**.

This investigator is also expected to present (in late September, at WPAFB) **the 3rd video recordings of the efforts made from March 1990 to September 1990.**

The grantee will ship to the US Government/USAF/WPAFB/Flight-Dynamics-Laboratory, **on or before 30 May 91**, or **on or before 30 May 92**, the **VHS system [American TV standard]** purchased through Grant AFOSR-89-0445 ["Estimated Charge to grant Funds: \$1,700"], as well as any additional equipment/hardware/software that will be so-defined in the "ADDITIONAL PERIOD OF RESEARCH" documents for Grant AFOSR-89-0445 : Apr 1, 90 - Mar 31, 91 , or Apr 1, 91 - Mar 31, 92 in line with the contract documents and FAR Part 45.

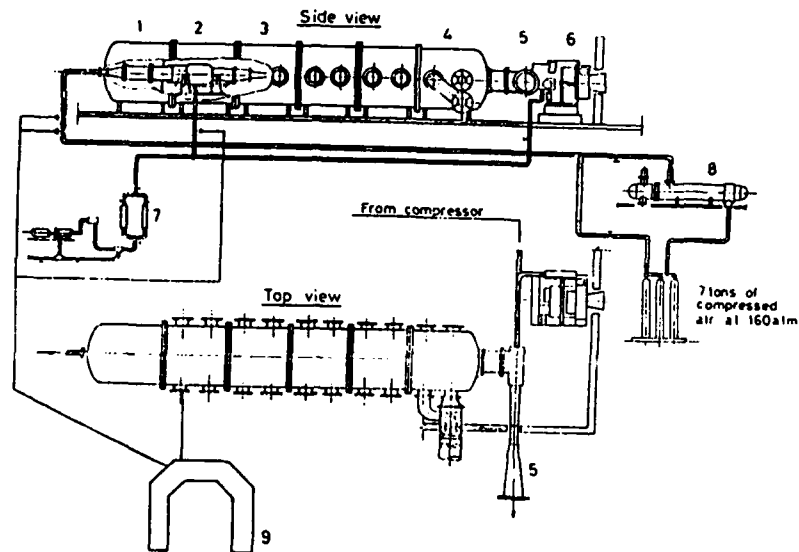


Fig. 7

The fullscale (altitude) engine test facility.

1,2,3, - Engine sector (Fig. 7a, p. 22a). 4,5,6, -Evacuation facilities. 7-fuel-supply systems. 8-7-ton S.S. heat exchanger for high-pressure/temperatures operating conditions, or for low-temperatures simulations. 9 - Control Room N.5 (cf. p.59).

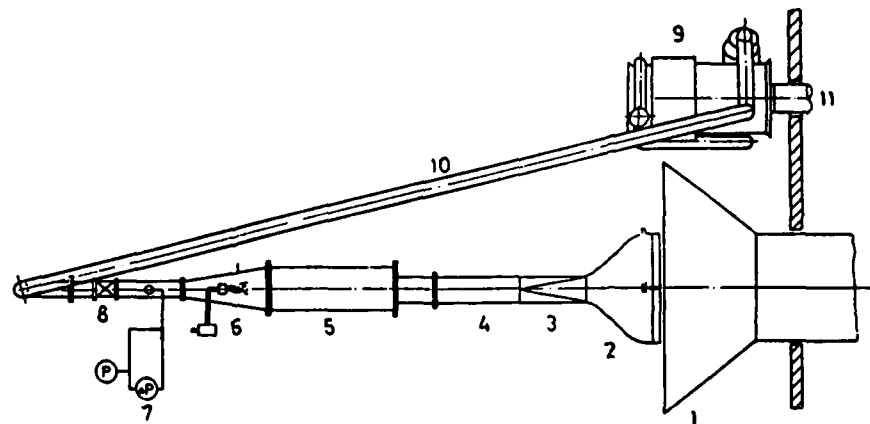


Fig. 7

The subscale vectoring nozzle test rig.

1-Exhaust system. 2-Roll-yaw-pitch thrust-vectoring nozzle. 3-4: Transition/cooling section. 5-T-56 combustor. 6-Fuel injector. 7-Flow monitoring. 8-Flow-control valve. 9-Gas turbine. 10-connecting pipe. 11-Gas turbine exhaust.

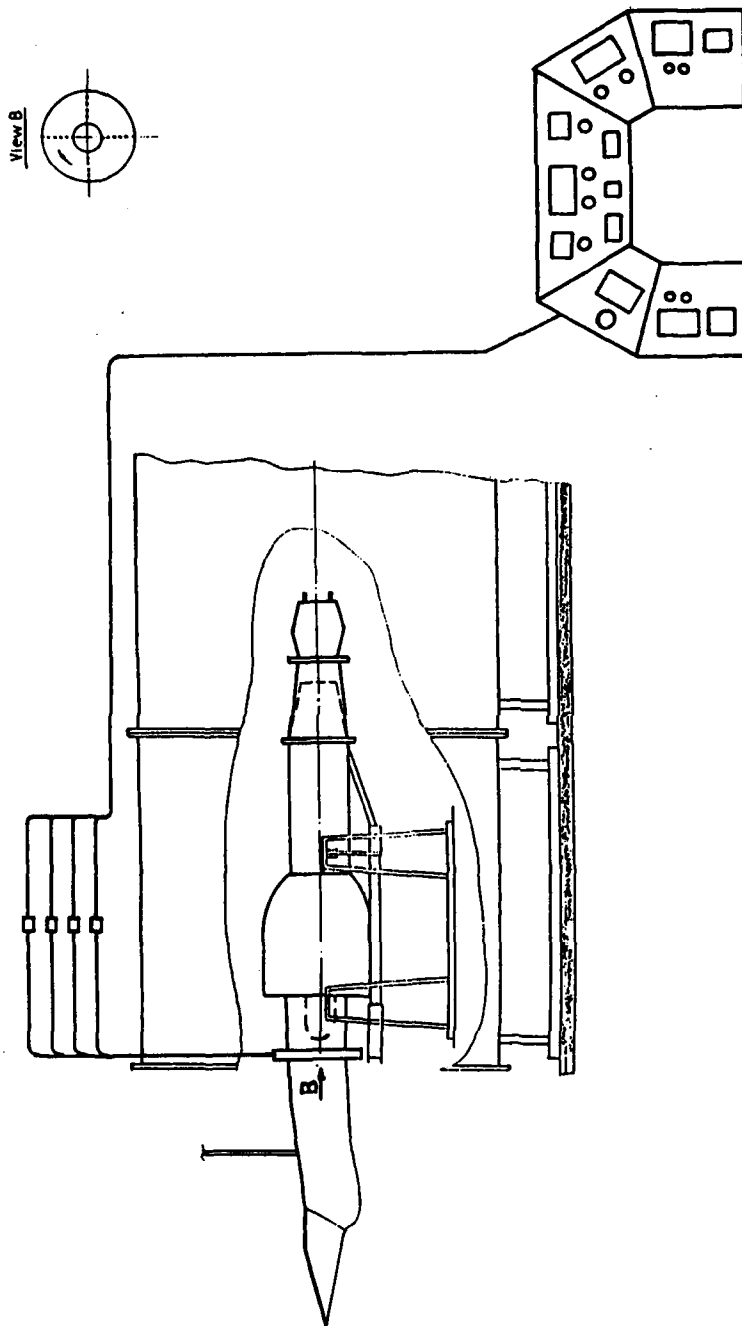


Fig. 7a: The "Full-Scale" Test Rig, cf. p. 22, 22b.
Inlet dimensions are provided in Fig. 7B, p. 22b.
See also pages 56 to 57 and the tentative
concluding remarks on pages 175-176.

Model B F-15 Inlet

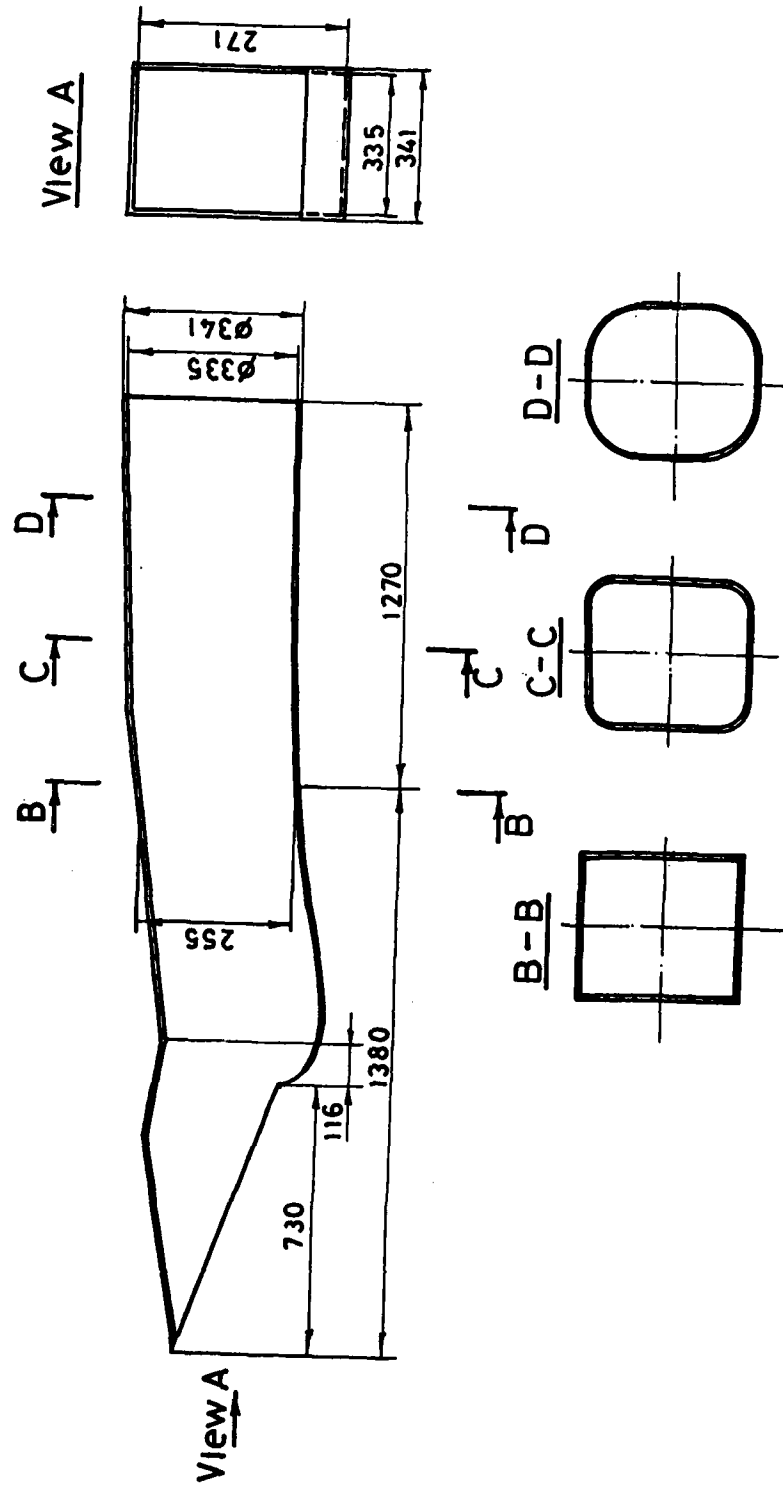
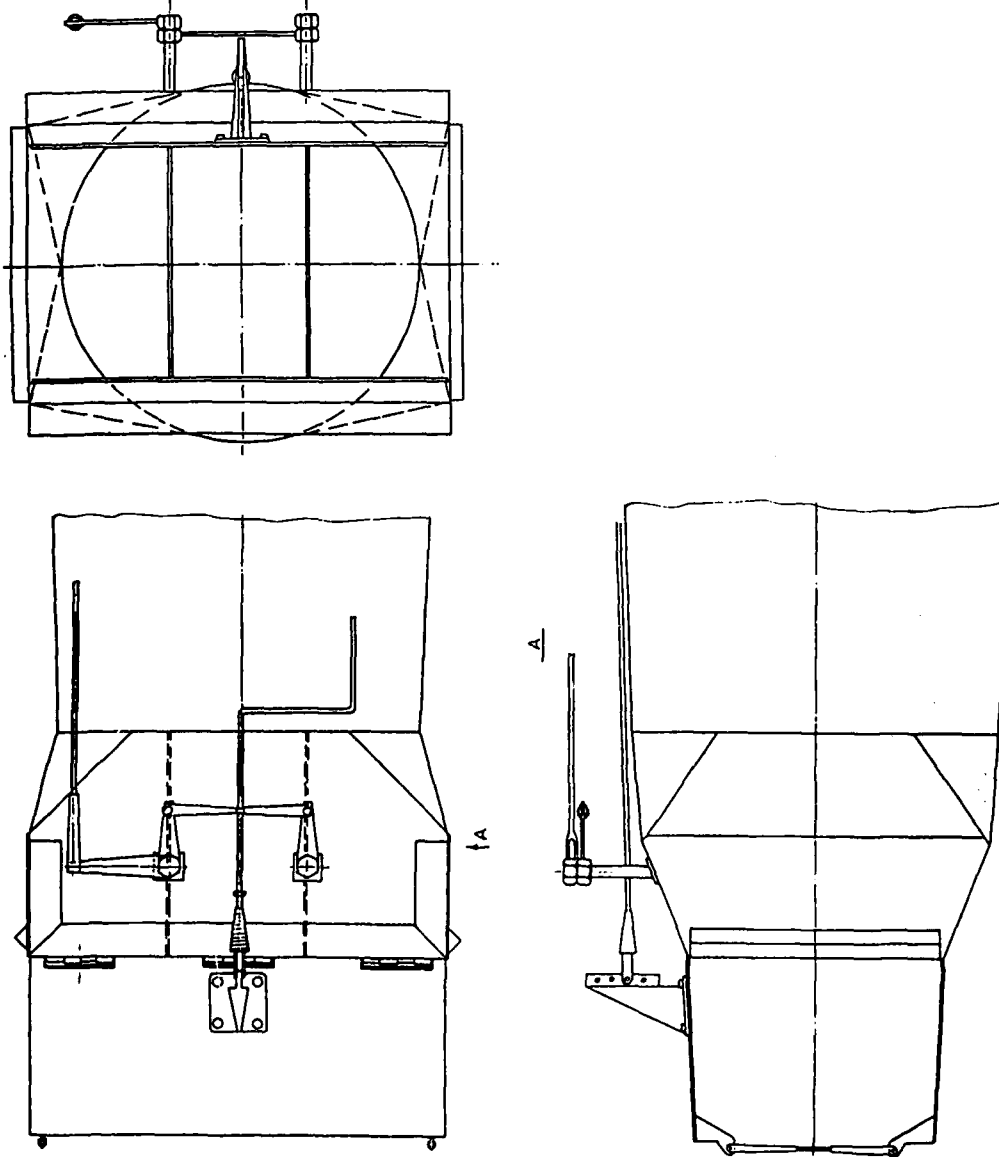


Fig. 7B : The "Full Scale" F-15 Inlet.
see also Fig. 7a, p.22a, the pictures on pages
56 and 57.

Fig. 7c : The Yaw-Pitch Nozzles which thrust-Vector the F-15RPVs.

Notes: To provide sufficient space to the rear-introduced starters, the yaw-vanes have been limited to two. The optimal number of yaw vanes is 4 with 2 additional side-doors (see pictures on pages 55 and 60 as well as Fig. 7d p.22d). Note also that the servos are "closed-loop ", namely, under aerodynamic/engine interactions during maneuvers they maintain the geometric deflection commanded by the flyer. See also Fig. 8 to 18 for calibration of these angles with jet-deflected angles. Also consult Fig.7 on p. 17.



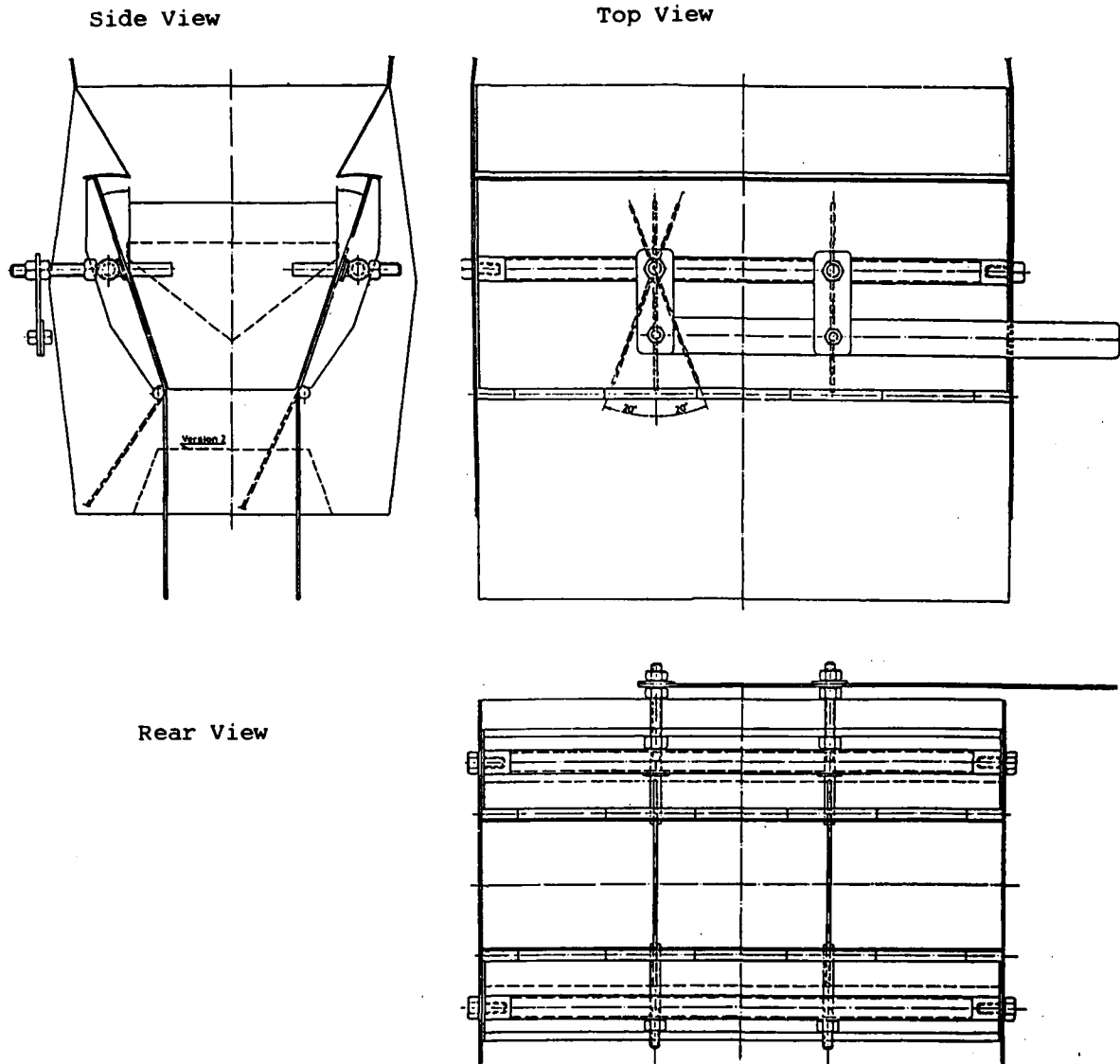


Fig. 7d : The First Proposed "Full-Scale" Yaw-Pitch Nozzle for the F-15 Fighter (Patentable), cf. p. 55

For more details see pictures on pages 55 and 60. Please note also that the new yaw vanes developed by this laboratory may have different shapes, space distribution, etc., to be further investigated during 1990/91. The design methodology of these new yaw-pitch and roll-yaw-pitch thrust-vectoring nozzles has been discussed in details in the author's new book (p.5).

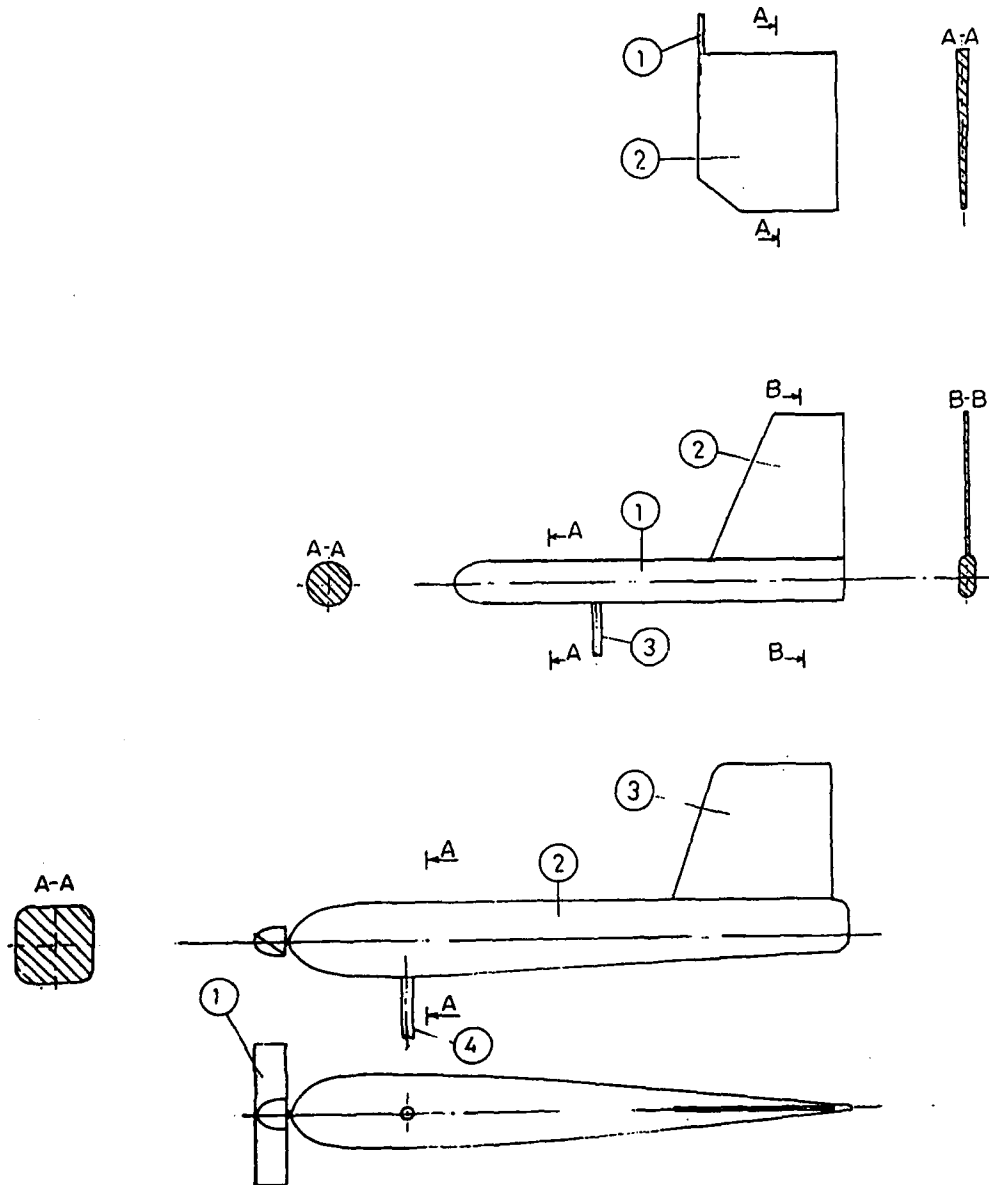
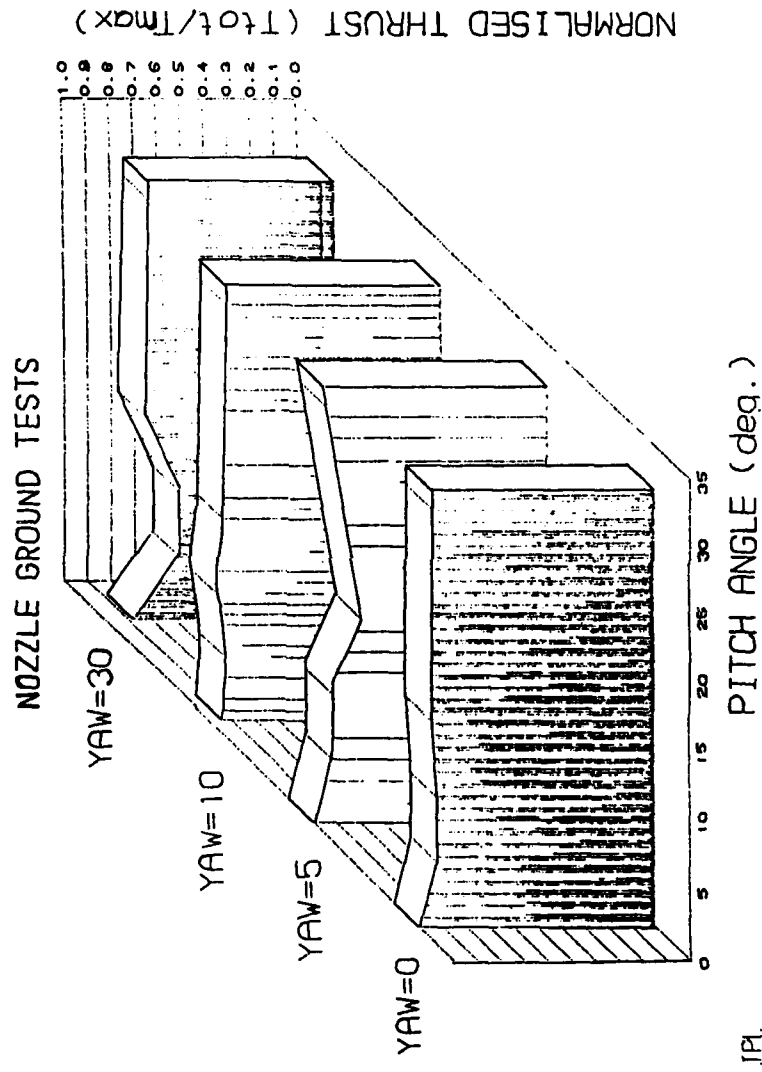


Fig. 7e : The beta probe (up), the alpha probe (center) and the velocity probe (see also Fig. 4).

Fig. 8 : YAW-PITCH THRUST-VECTORIZING RPV



IP1.

Fig. 9 : YAW-PITCH THRUST-VECTORING RPV

NOZZLE GROUND TESTS.

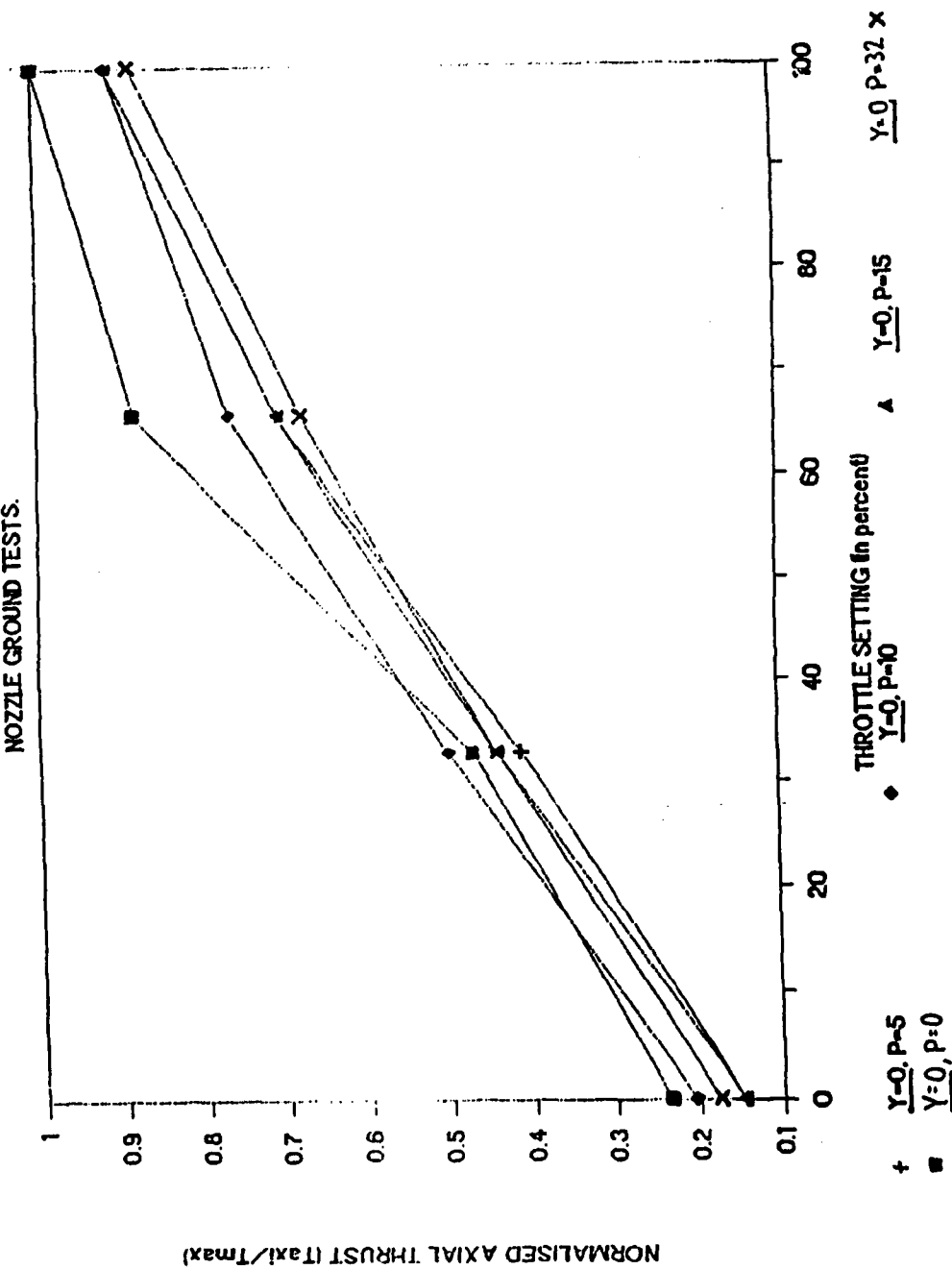


Fig. 10 : YAW-PITCH THRUST-VECTERING RPV
NOZZLE GROUND TESTS.

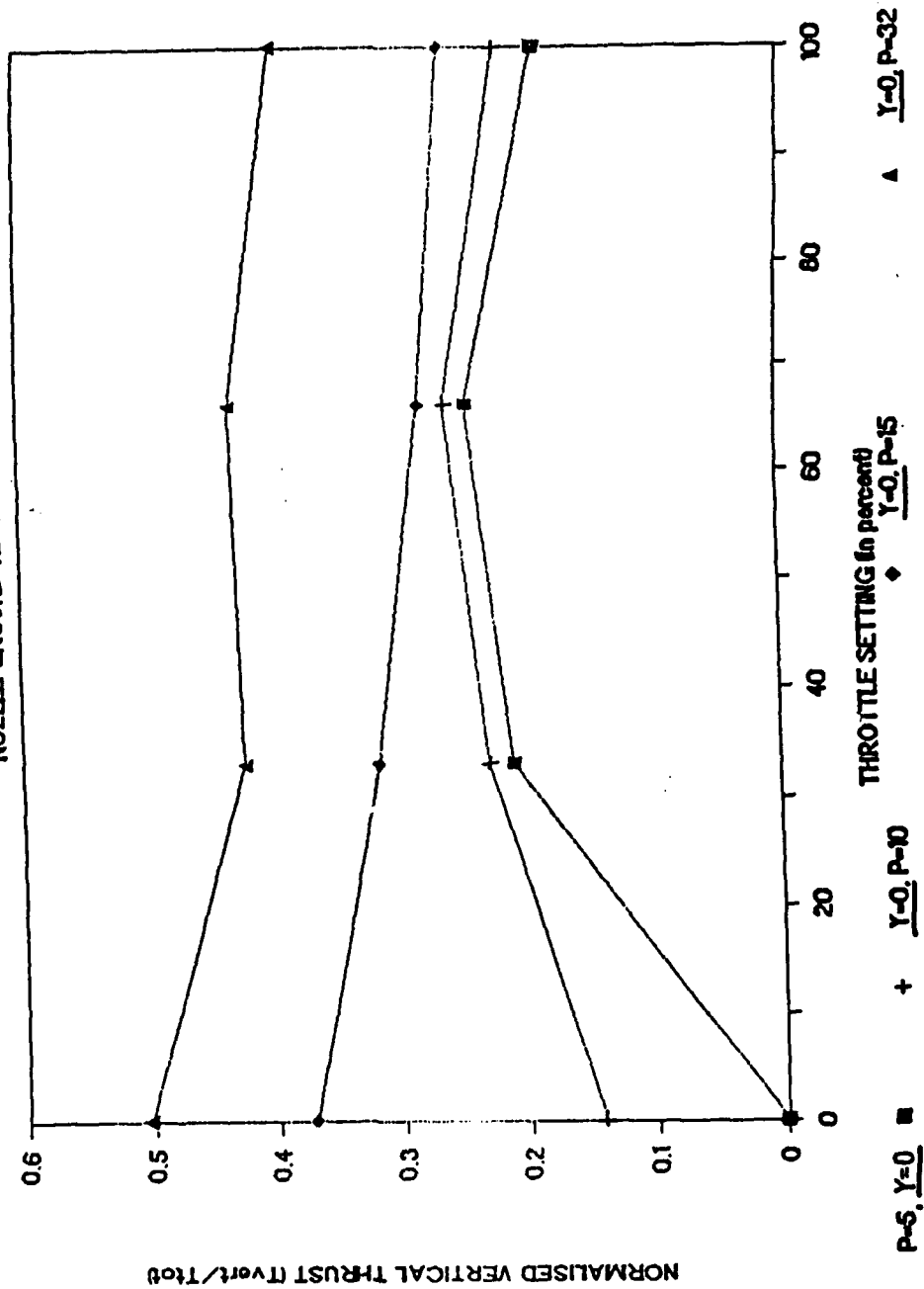


Fig. 11 : YAW-PITCH THRUST-VECTORING RPV

NOZZLE GROUND TESTS.

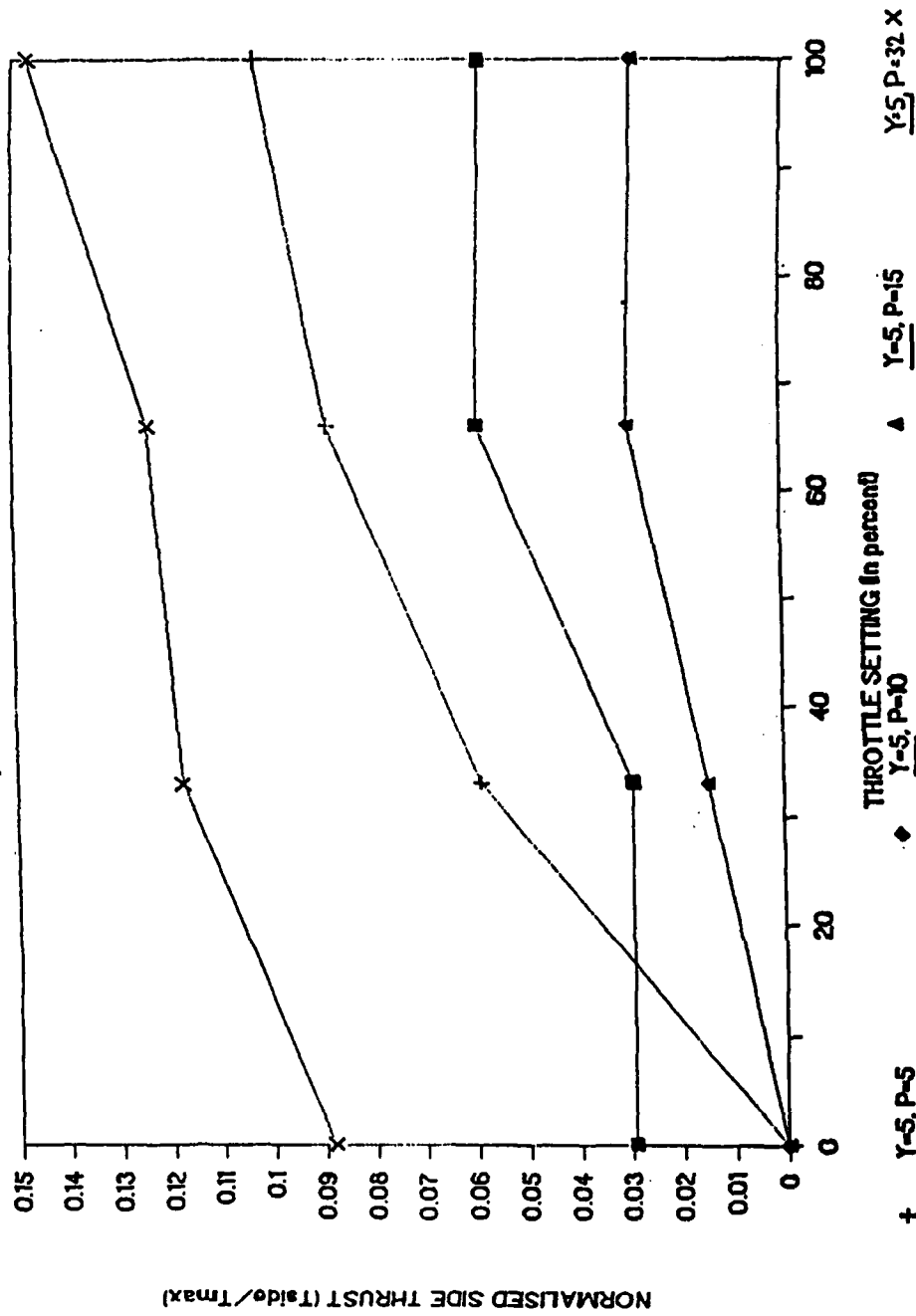


Fig. 12 : YAW-PITCH THRUST-VECTERING RPV

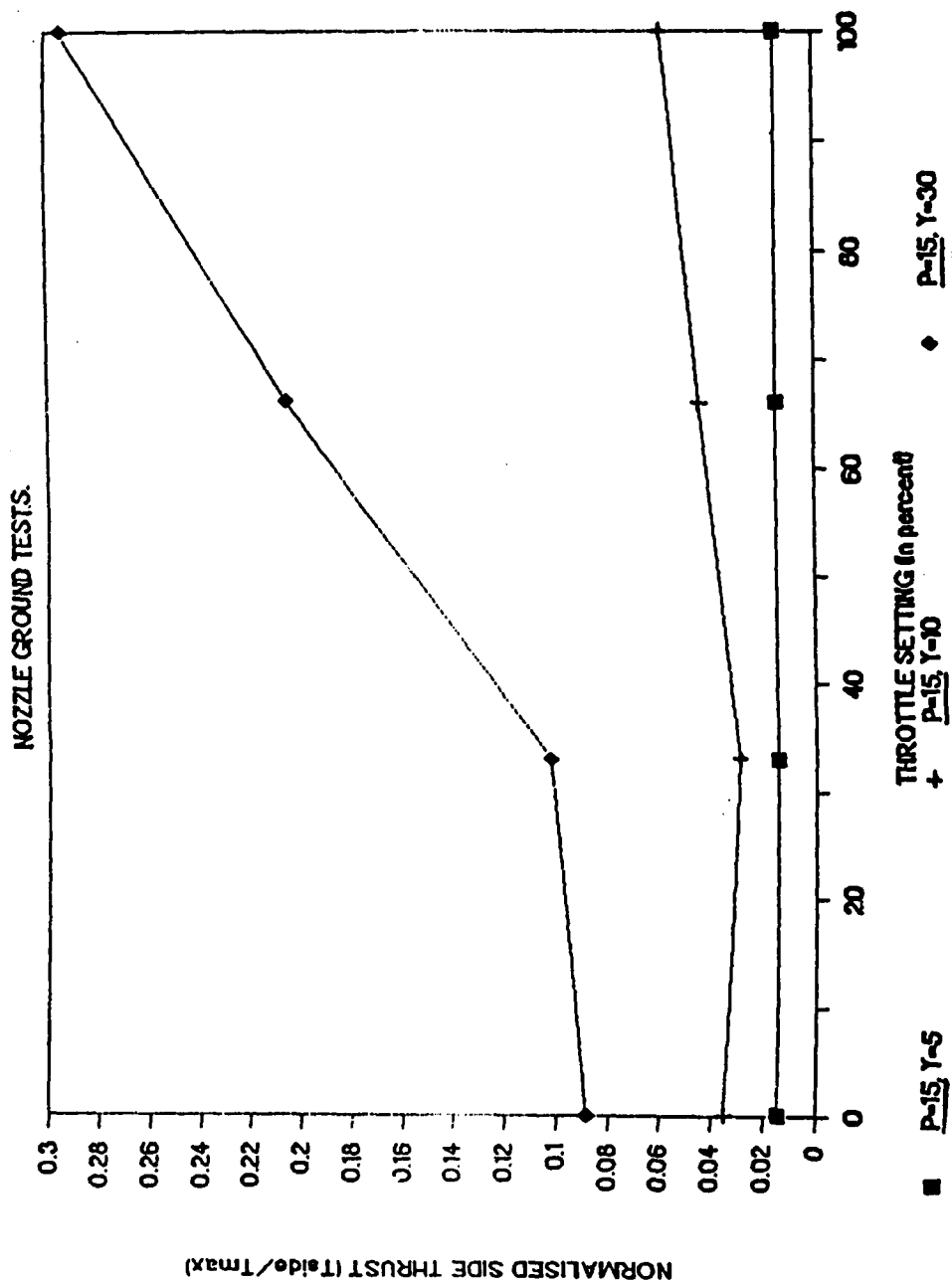


Fig. 13 : YAW-PITCH THRUST-VECTORING RPV

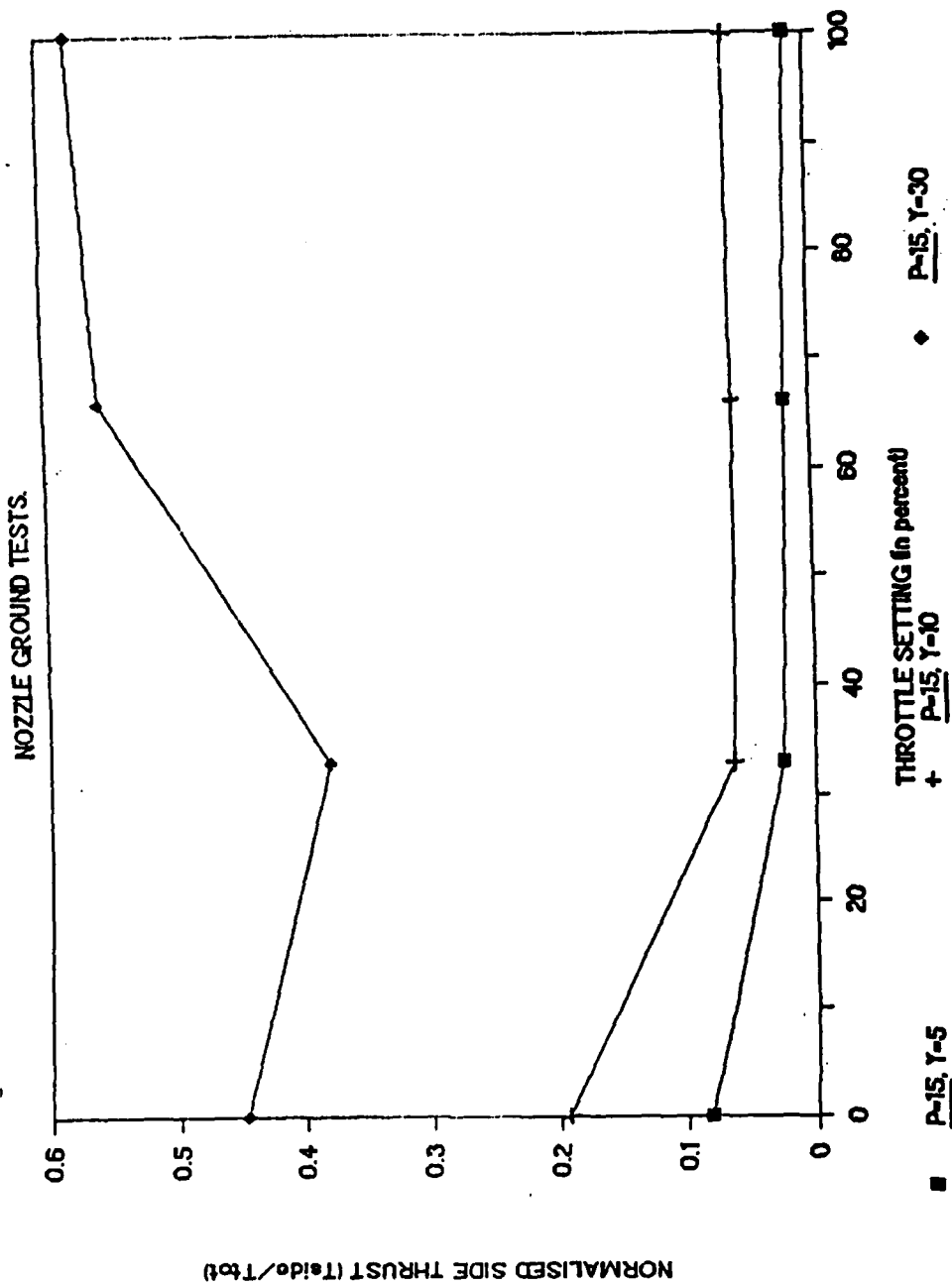


Fig. 14 : YAW-PITCH THRUST-VECTERING RPV

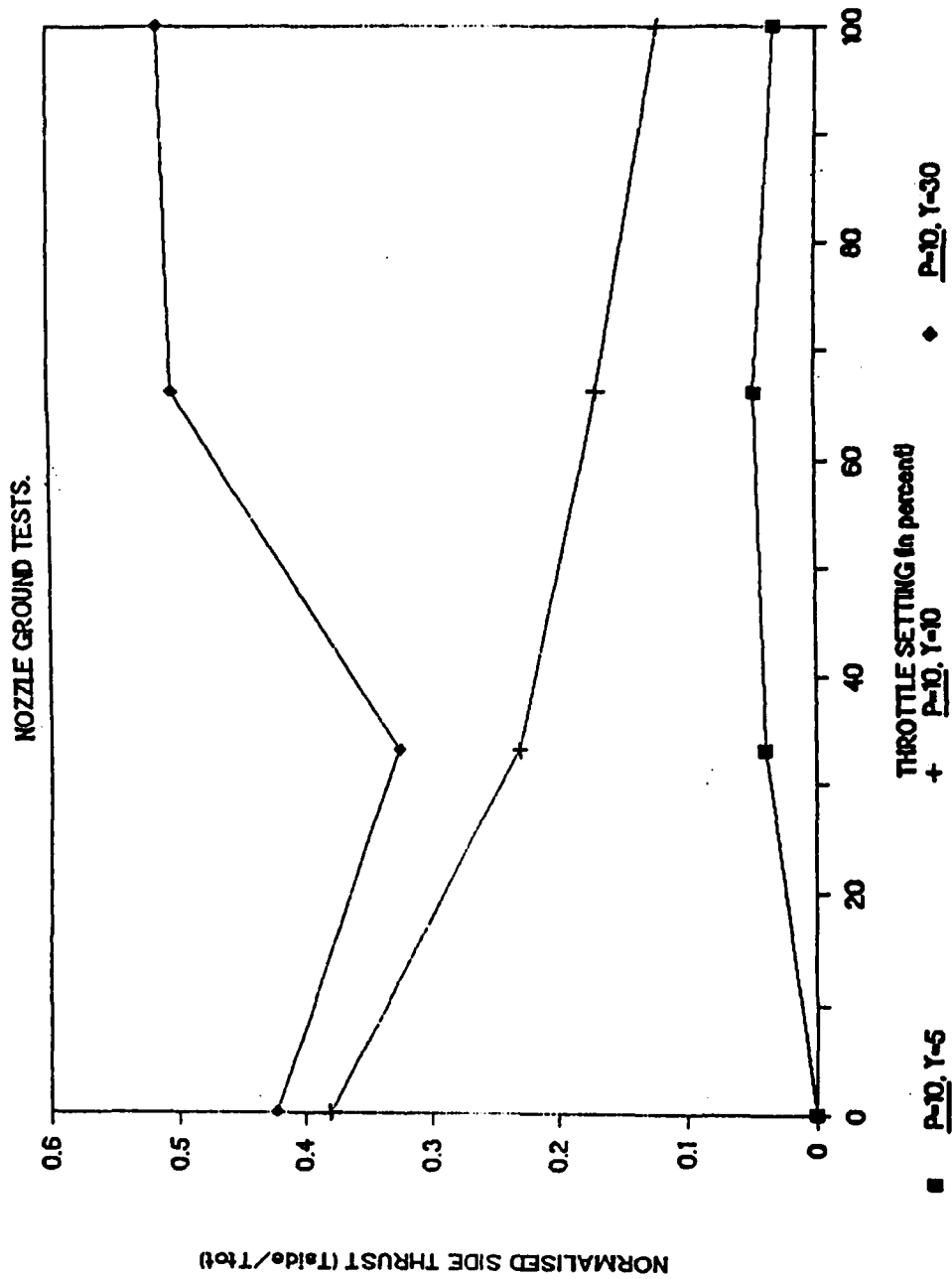


Fig. 15 : YAW-PITCH THRUST-VECTORING RPV

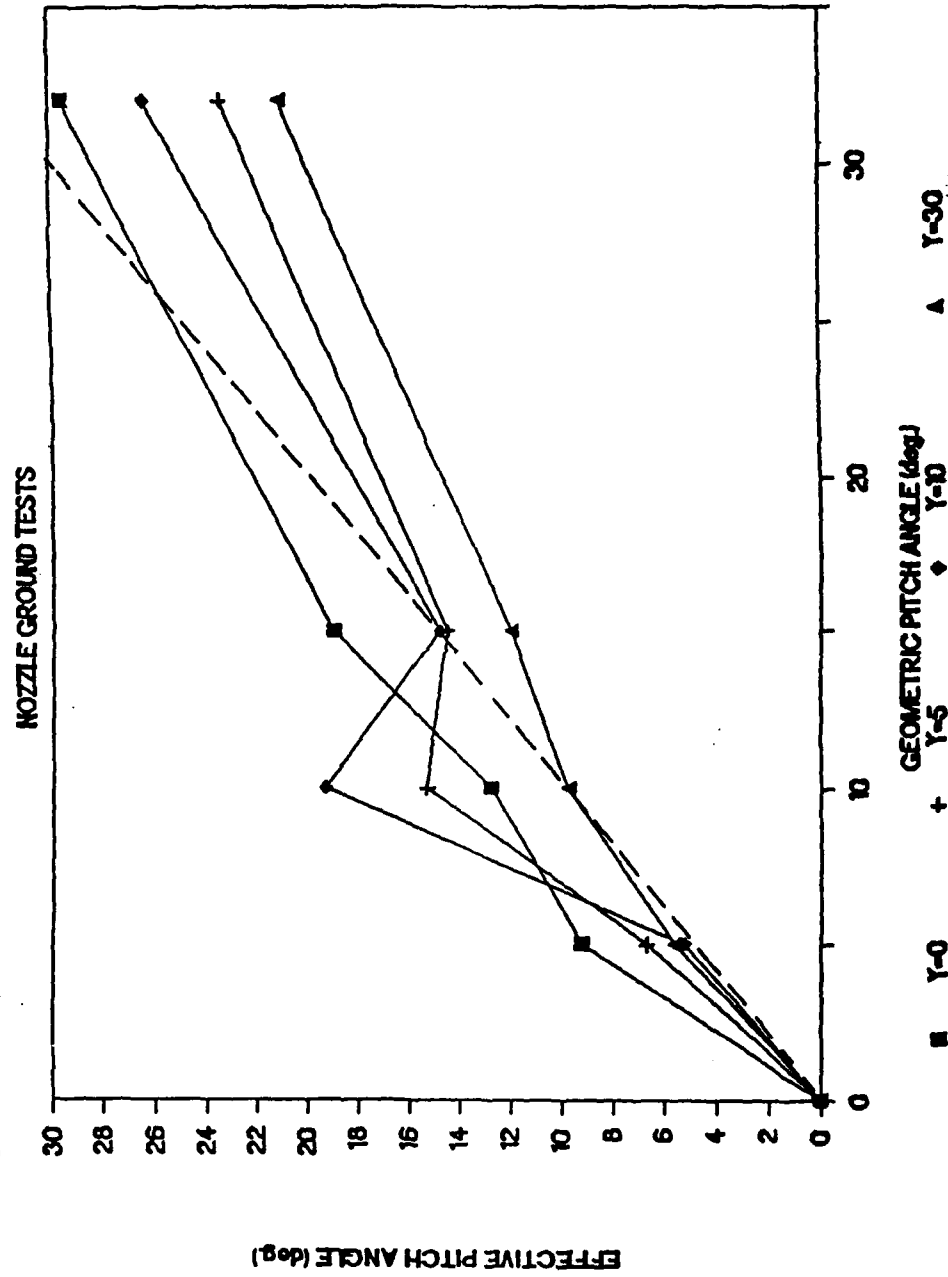


Fig. 16 : YAW-PITCH THRUST-VECTORING RPV
NOZZLE GROUND TESTS

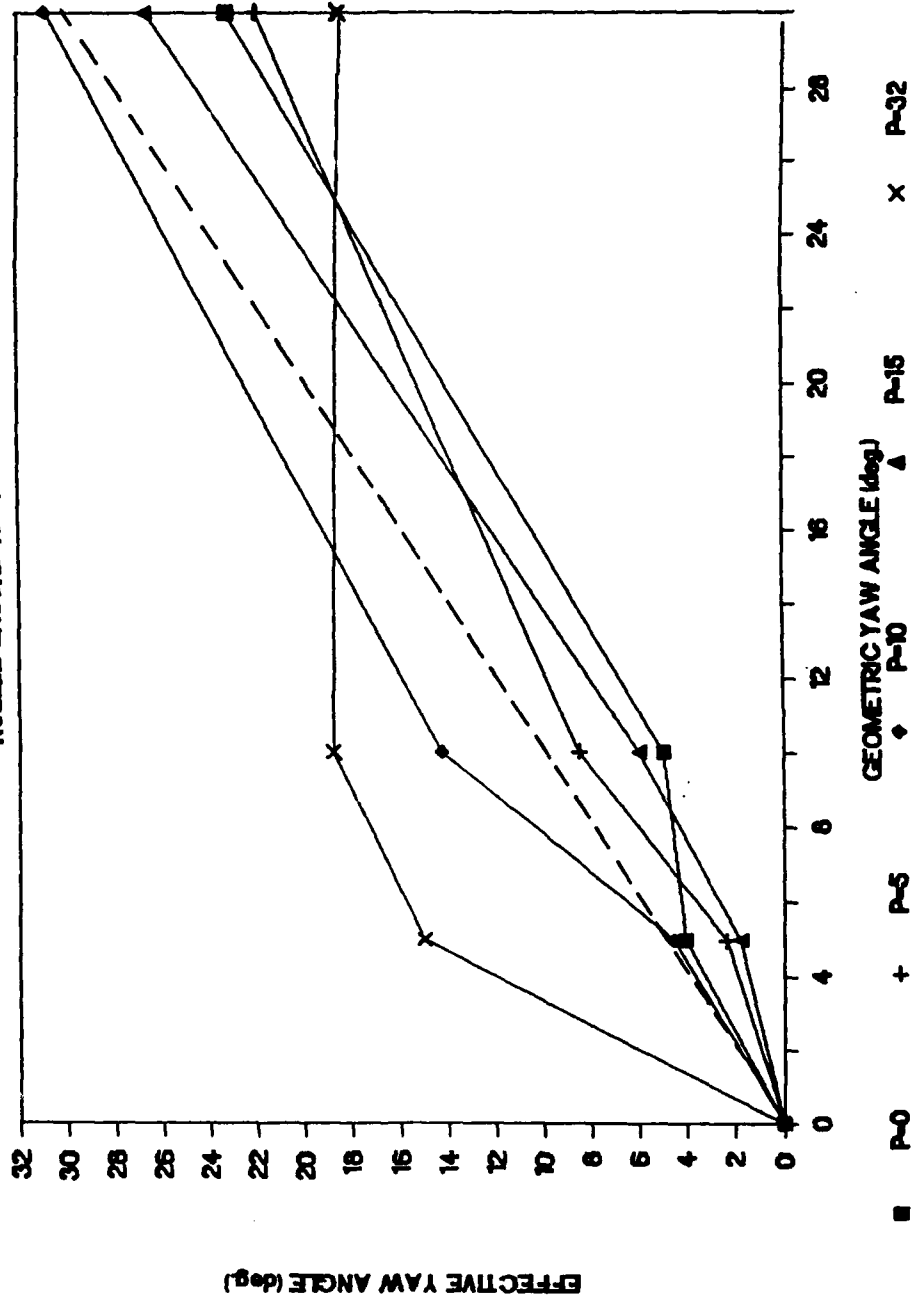
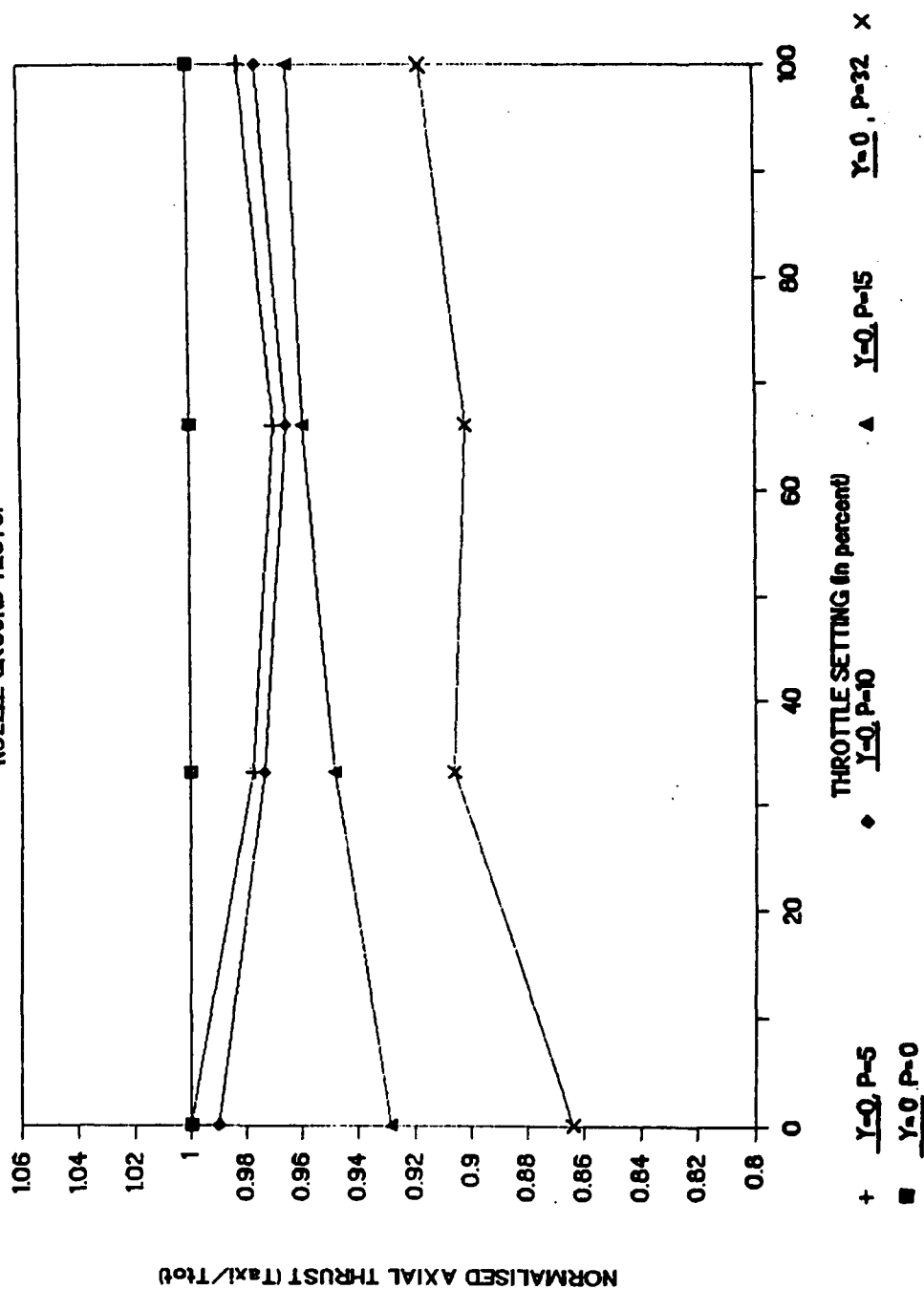
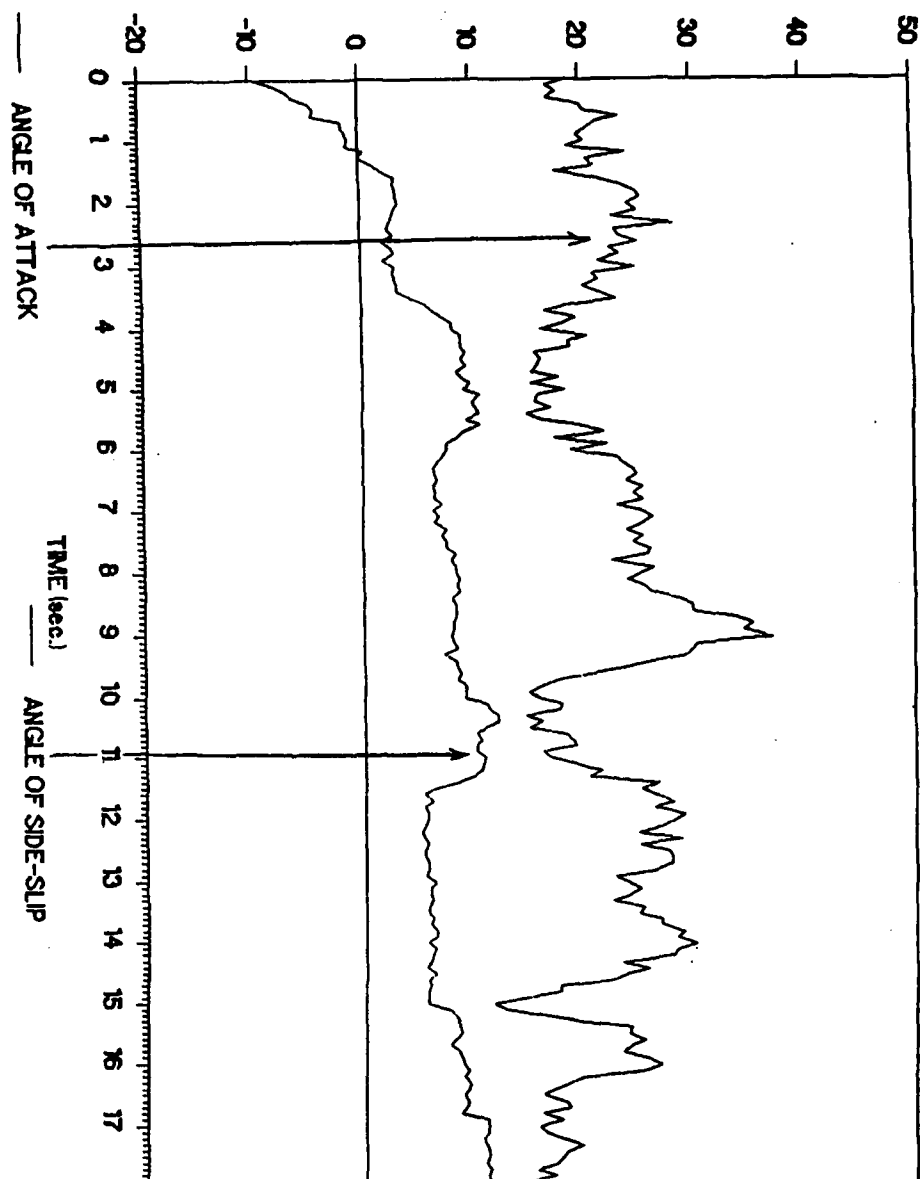


Fig. 17 : YAW-PITCH THRUST-VECTERING RPV
NOZZLE GROUND TESTS.





CONSECUTIVE STALLS.

Fig. 18 : ^cData-acquisition-system initial airworthiness trials:

During the above maneuver the RPV is flown on a stalled condition.

Note that: a) The α sensor shows quick response, but fluctuations are to be reduced.

b) The stall generates a right sideslip (positive angle).

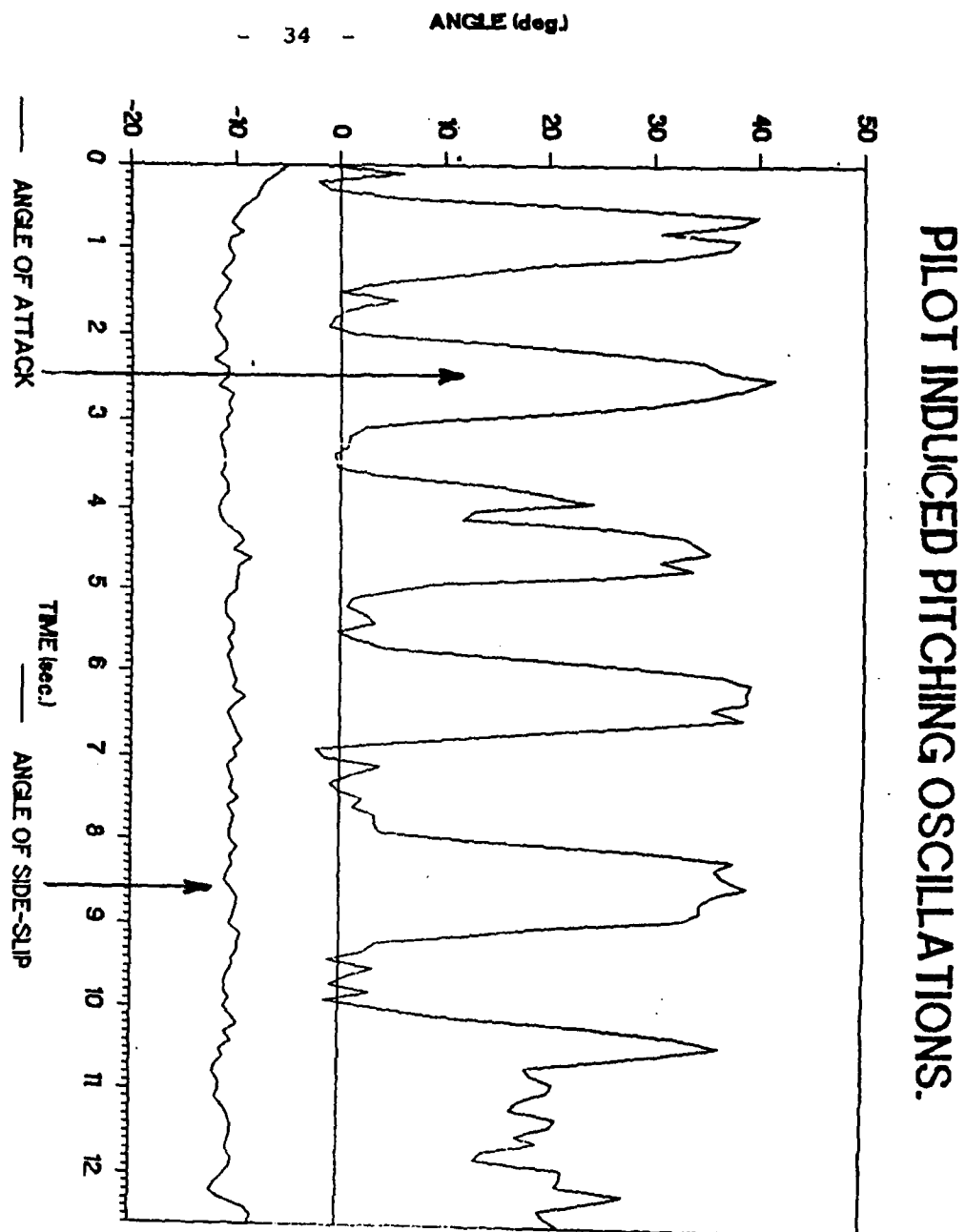


Fig. 19 : Data-aquisition-system initial air worthiness trials:

During the above maneuver the nose of the RPV is raised and lowered by the pilot. The α sensor shows a satisfactory time response. (Constant left sideslip due to out-of-trim RPV).

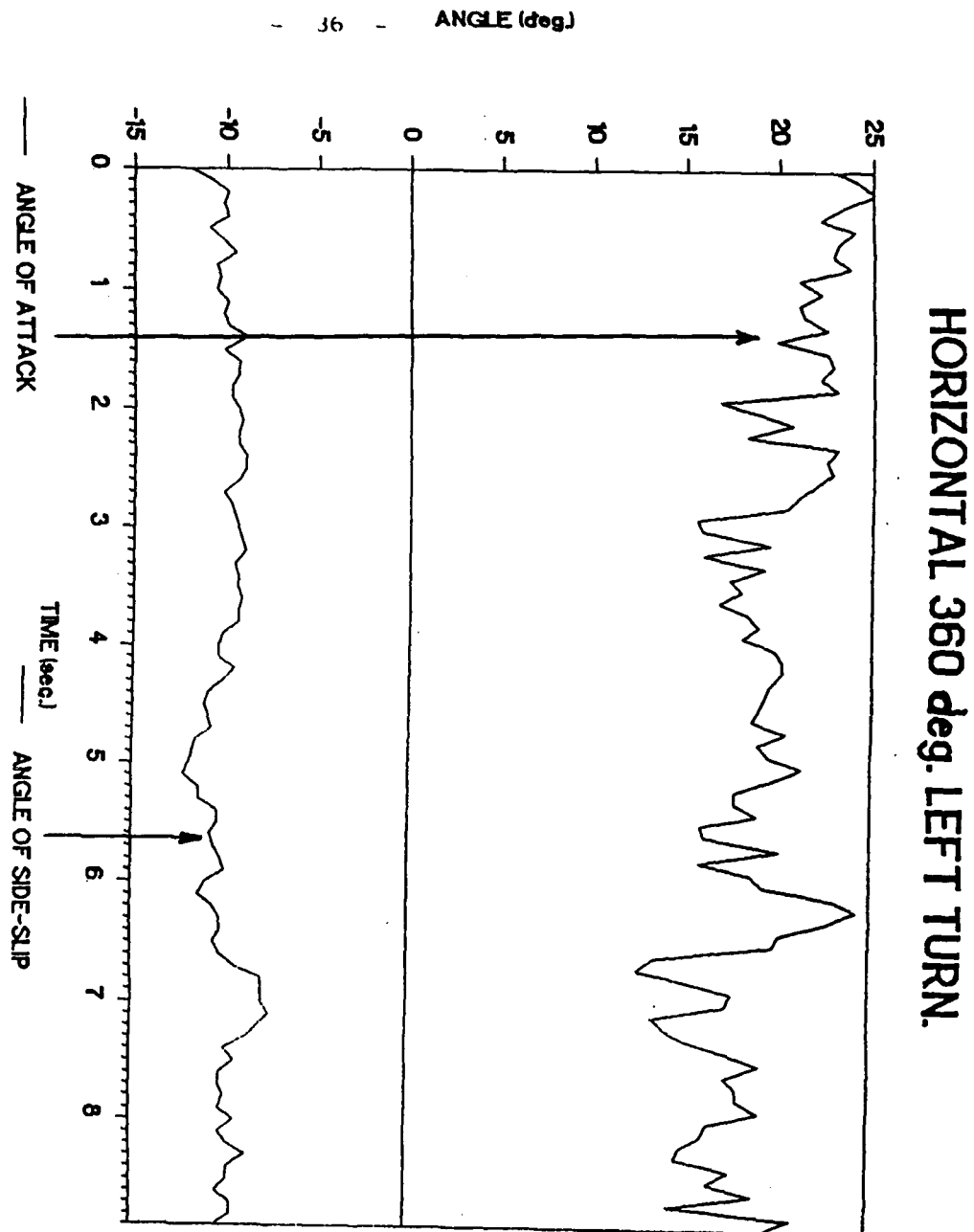
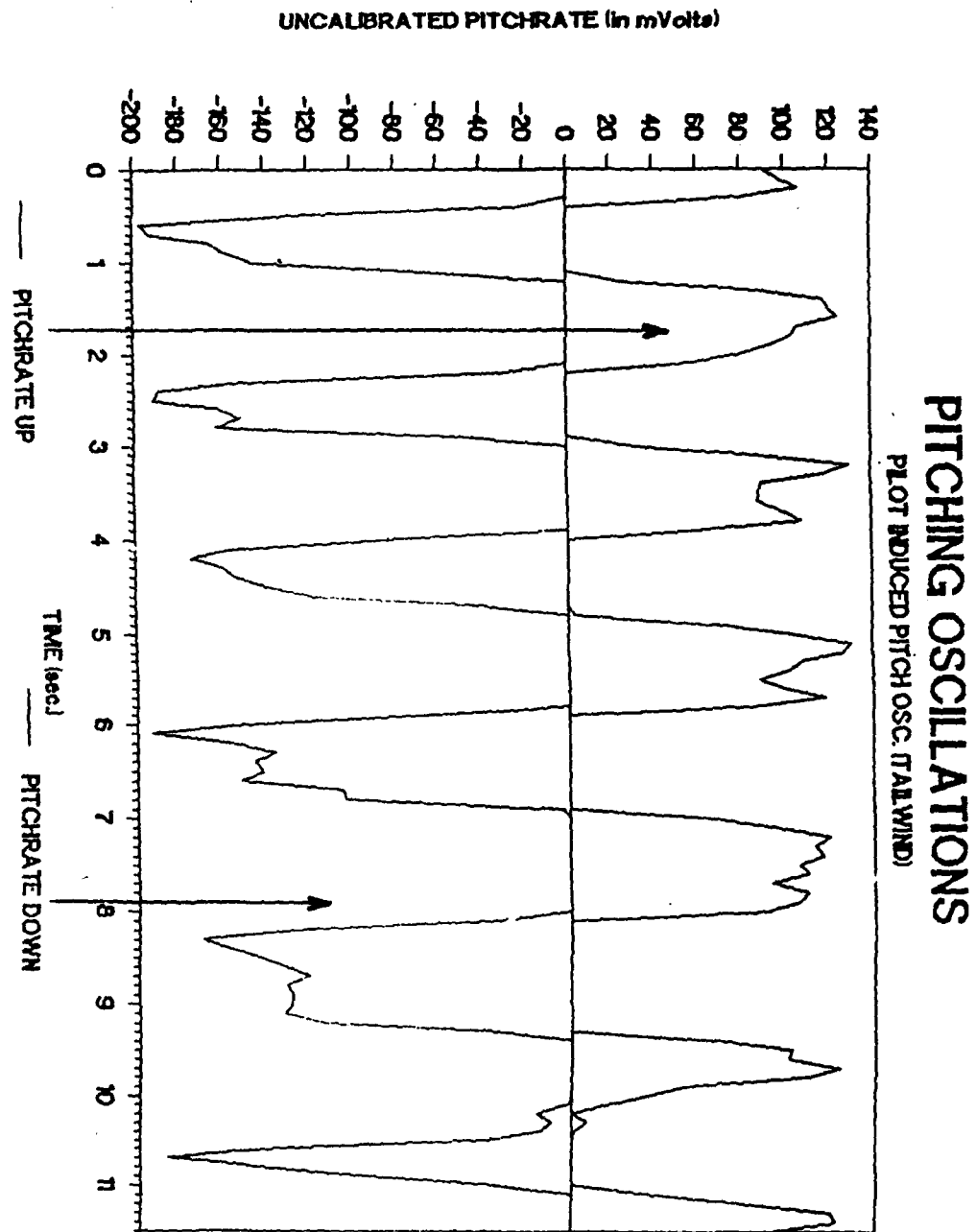


Fig. 21: ^c Data-acquisition-system initial airworthiness trials:

During the horizontal turn we observe:

- a) Fluctuations in side-slip angle, due to out-of-trim RPV and extremely bumpy weather.
- b) Fluctuations in α to be reduced through better sensor.
- c) General decrease in α during turn, in order to avoid stall/spin at low speed.



Fif. 20: ^cData-aquisition-system initial air worthiness trials:

During the above maneuver, the nose of the RPV is raised and lowered by the pilot, and pitch-rate is recorded. Note that pitch-up and pitch-down each requires a different channel, and the above test demonstrates the excellent ^bsynchronization between both channels.

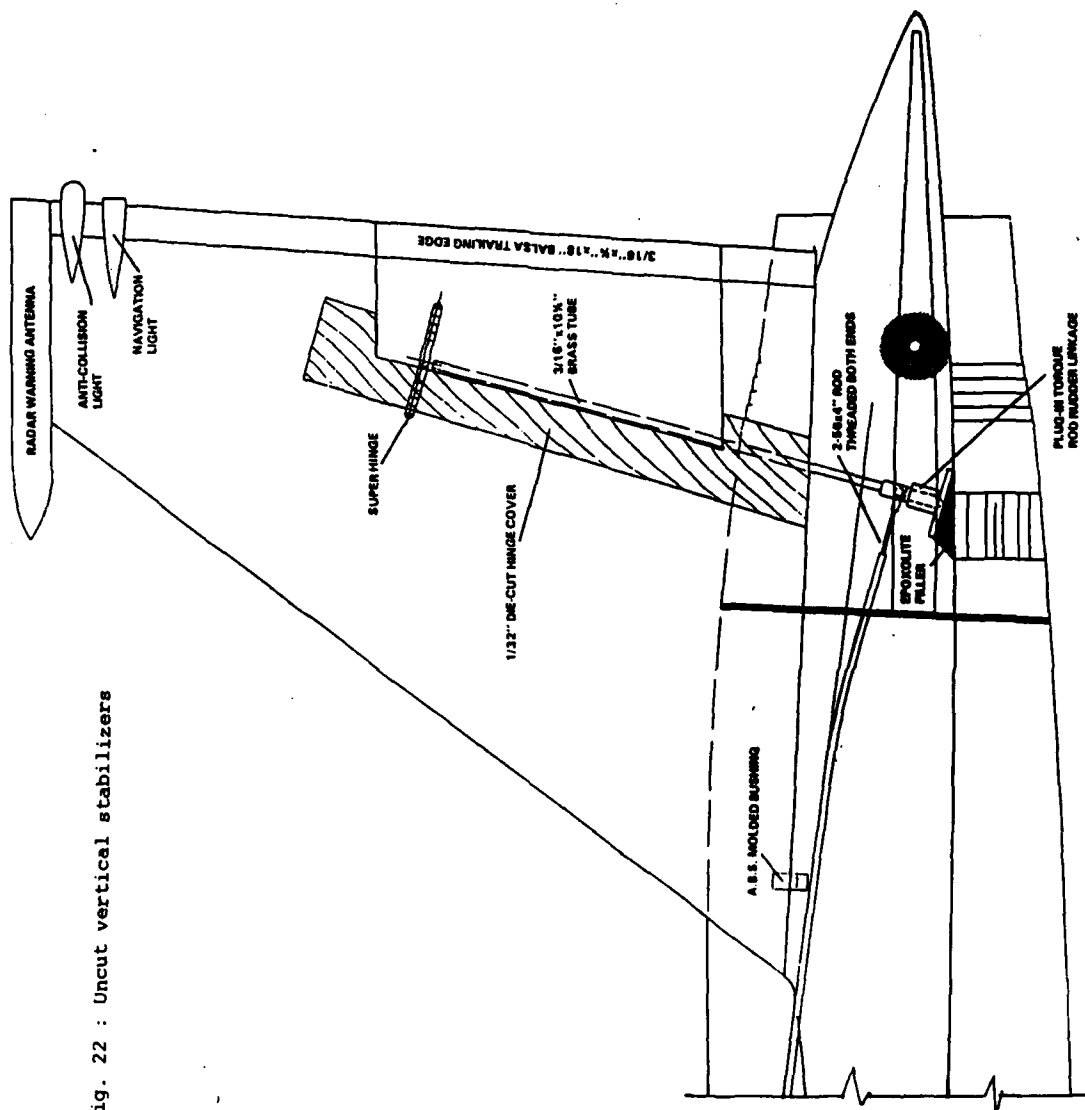


Fig. 22 : Uncut vertical stabilizers

Fig. 23 : About half-cut vertical stabilizers

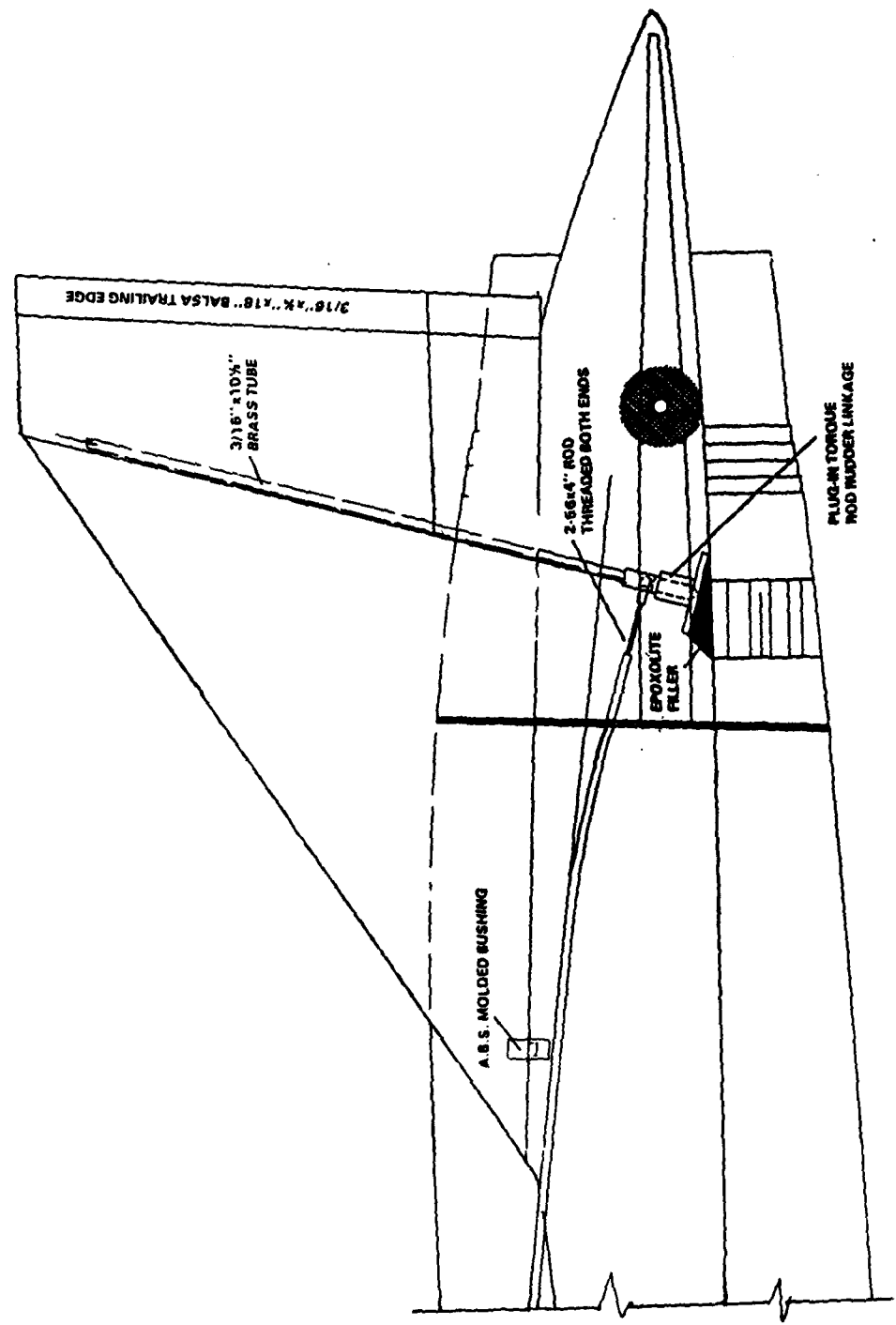


Fig. 24 : About 3/4 - cut vertical stabilizers

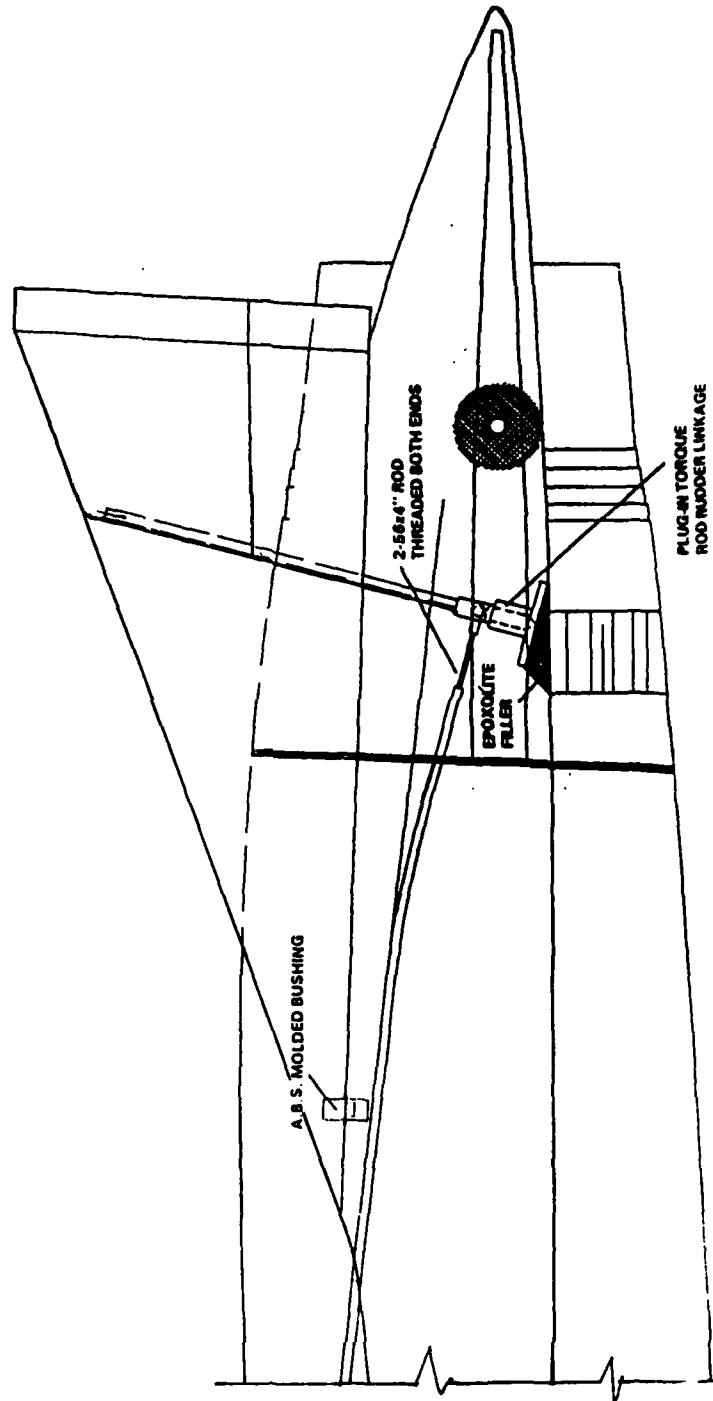
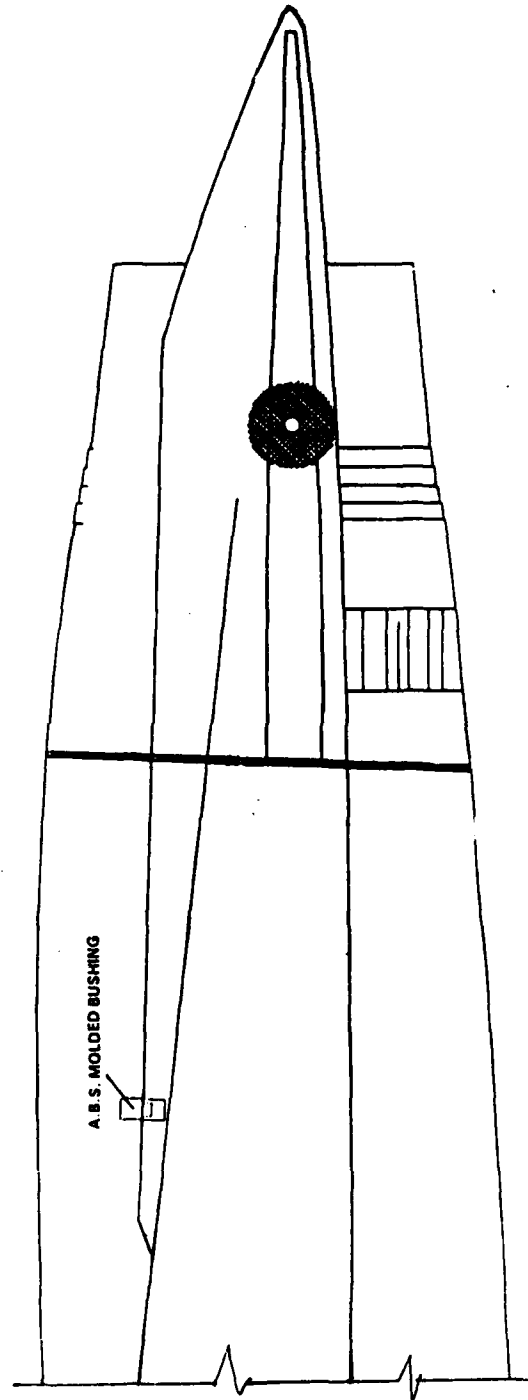


Fig. 25 : Tailless F-15 with no vertical stabilizers



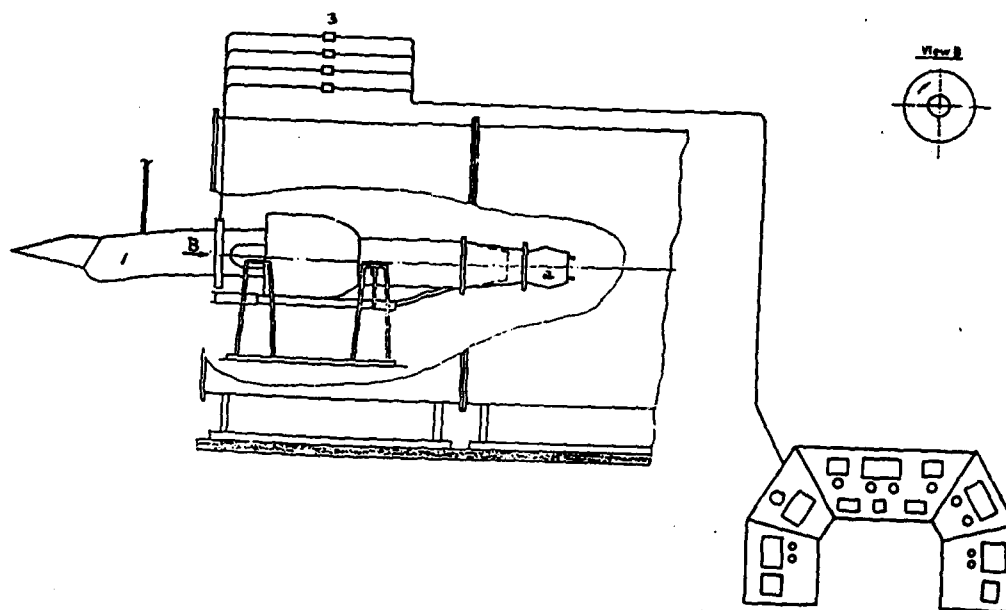


Fig. 26 :

Full-scale vectored F-15 inlet/nozzle test rig (cf. p. 22).

View B shows the distortion/pressure probes motion during various inlet incidence angle measurements.

1-Inlet, cf. p. 106.

2-Nozzle, cf. p. 22d.

3-Pressure transducers

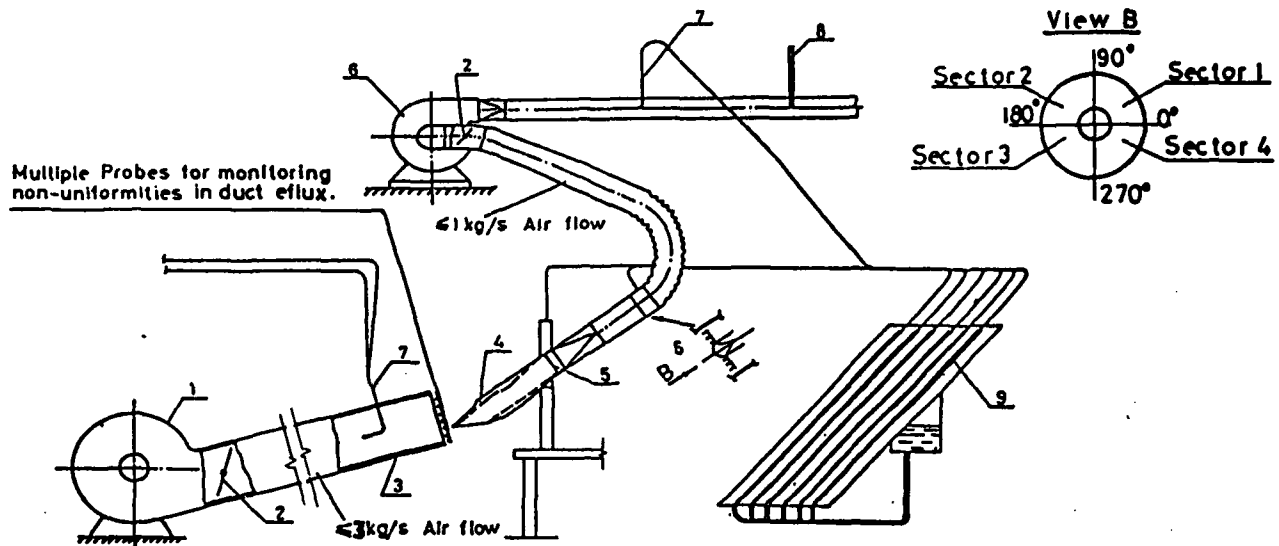


Fig. 27 : sub-scale test rig setup for F-15 inlet

View B is the most critical section.

The 4 sectors are marked.

1-blower, closed during "Takeoff-flow-simulations", while No. 6 is open. cf. p. 174-175.

2-Blower air mass flow control, calibrated for "1", "2" and "3", increasing flow positions. cf. p. 156.

3-Blowing duct. *Removed during "Takeoff Simulations".*

4-Sub-scale F-15 model (with and without variable lips, vanes etc.).

5-Front-section measurement section, as in the flying F-15 RPV.

5B-Compressor inlet station for distortion and Pr measurement .

6-Suction blower. "Takeoff Baseline" is produced with this blower only, cf. p. 174-175.

7-Pitot tube measurements.

8-Thermometer

9-Multiple-tube water manometer.

Chapter II

Our Methodology Vs

Different International Concepts of Thrust-Vectored, PST Fighter Aircraft

DIFFERENT INTERNATIONAL METHODOLOGIES

The fact that optimized TV methodologies have recently become the technology bottleneck for the development of superagile fighter aircraft is reflected by the accelerated efforts made recently in this field by governmental, industrial and academic bodies (Cf., e.g., Refs. 1 to 14).

Thus, we have most recently witnessed the flight tests of the thrust-vectored F-15 STOL Demonstrator. Around June 1990 we shall observe the flight tests of the thrust-vectored X-31A experimental airplane. The landing of a thrust-vectored, STOL version of the Su-27 (the 1014) on a carrier may soon be substantiated, according to public Soviet releases.

We have also witnessed recently the Central Institute of Aviation Motors in Moscow publishing computer simulations of yaw-pitch, thrust-vectored aircraft (2,14), as well as some similar French

(3), Israeli (1, 10) and Chinese (13) efforts. These efforts have, in part, been influenced by the early pioneering British technology of the Harrier, and by the works of Herbst (6) in West Germany. However, the main thrust in this field has long been the pioneering American programs [Cf., e.g., the contributions by Richey, Surber, and Berrier, Bowers, Laughrey, Hiley, Palcza (9, 1), Tamrat (4, 11), and Berrier and Mason (7, 8)].

There are also some instructive flight simulations of a thrust-vectoring version of the [now cancelled] X-29A (12).

A minor US program [GE, GD, Teledyne] is also conducted now at the JPL of the Technion to evaluate the pros and cons of simultaneous yaw-pitch or yaw-pitch-roll thrust vectoring (1). This program includes laboratory tests and flight testing of vectored F-16 RPVs equipped with various two-dimensional nozzles, ranging from 2 to 46.4 NAR. The TV-nozzles currently being tested include pitch-only, yaw-pitch, and simultaneous roll-yaw-pitch TV.

These design differences may be critical in the final assessment of fighter combat-effectiveness in the future. Hence, it is imperative, and timely, to experimentally compare the effectiveness of various thrust-vectoring methodologies.

Enhanced Pointing Capabilities

We assert that in future aerial combat, thrust-vectoring-induced pointing of the nose/weapon of the aircraft at the adversary will be required to win, since pointing first means having the first opportunity to shoot. Thrust vectoring may also become the standard technology to dramatically increase survivability (1, 4, 3, 4, 5, 6) as well as STOL characteristics (1). Moreover, a number of references (as reviewed in Ref. 1) stress the importance of TV to significantly decrease aircraft and efflux jet signatures.

However, as it stands now, this technology is still in its embryonic state. While the pitch-only [or the pitch/thrust-reversal] TV now appears to be maturing, the most critical technology of simultaneous yaw-pitch or yaw-pitch-roll TV is still far away from this stage. In light of the prolonged time inherently associated with the advancement and maturity of such an engineering field, one may expect its full exploitation only in the post-ATF era. Nevertheless, some of its proven elements may be gradually incorporated in such upgrading designs as those feasible now for the current F-15, F-18 and F-16, and perhaps also for other, older aircraft, having a thrust-to-weight-ratio above 0.6 - the value above which, according to Herbst (6), combat effectiveness of vectored fighters becomes significantly higher than that of conventional ones.

Technology Bottleneck

There is an inherent time-lag between the pace of evolution, and maturity, of advanced propulsion systems, and that of avionics. While the former shifts into a "new generation" every ten or twelve years, it may take the latter only four or six. This means that a premature selection of a TV engine, may later become the bottleneck in the evolution of high-performance aircraft. Hence, the designers of advanced (manned) airframe systems can test the integration of TV powerplants with advanced C³I systems, only during the last phase of the development/testing process of IFPC systems. However, the TV-coupling coefficients required for IFPC verification will not be available in time, unless simulated first by the integrated methodology proposed here.

The Basic Definitions

Vectored aircraft may be divided into those that are "pure" or "partial". In pure thrust vectoring the flight-control forces generated by the conventional, aerodynamic control surfaces of the aircraft, are replaced by the internal thrust forces of the jet engine(s). These multi-axis forces/moments may be simultaneously, or separately, oriented in all directions, i.e., in the yaw, pitch, roll, thrust-reversal, and forward thrust coordinates of the aircraft, so as to significantly enhance the aircraft flight control means both below and beyond the so-called "stall barrier".

Since engine forces (for post-stall-tailored inlets), are less dependent on the external-flow than the forces generated by the aerodynamic control surfaces, the flight-control forces of Pure Vectored Aircraft (PVA), remain highly effective even beyond the maximum-lift Angle-of-Attack (AoA), i.e., PVA are fully controllable even in the domain of Post Stall Technology (PST). (AoA may be splitted into conventional-AoA and PST-AoA. In our practice, AoA may be greater than 90 degrees.)

Therefore, thrust-vectored (TV) flight-control provides the highest payoffs at the weakest domains of conventional fighter aircraft (e.g., at PST-AoA, low (or zero) speeds, high altitude, high-rate spins, very-short runways, and during PST, Rapid-Nose-Pointing-and-Shooting (RaNPAS) maneuvers).

Consequently, subject to proper safety-vs-complexity reasonings, no rudders, ailerons, flaps, elevators, and flaperons, are required for the flight-control of PVAs, and even the vertical tail-stabilizers may become partially or fully redundant. Thus, by employing TV and Integrated Flight/Propulsion Control (IFPC), PVA need no conventional tail/vertical stabilizer(s), nor conventional aerodynamic control surfaces.

It should be further stressed that since the possibility of eliminating the vertical stabilizer can reduce the total aircraft drag in Pure or in Partial Sideslip Maneuvers (PSM), RaNPAS [Rapid-Nose-Pointing-and-Shooting] maneuvers combined with PSM may not degrade aircraft's energy/speed as much as a similar, high-drag, PST/RaNPAS maneuver.

Integrated laboratory/flight-testing Methodology.

Such concepts have been substantiated by this laboratory using a methodology of integrated laboratory/flight-testing. This resulted in the design, construction and laboratory testing of a family of yaw-pitch TV nozzles. The nozzles were tested on a small turbojet engine [Marbore IIC] to evaluate performance during yaw, pitch and yaw-pitch thrust vectoring runs.

The selected yaw-pitch TV nozzle was then scaled-down and installed and flight tested on-board of a 9ftx4ft, radio-controlled, thrust-vectorred F-15/RPV model .

The TV-nozzles have been integrated with the airframe-structure so as to provide low drag penalty. Simultaneous roll-yaw-pitch TV is provided by allowing yaw and pitch TV jet-angles to vary, during flights, in the range of ± 20 deg. However, all actual, high-performance maneuvers require less than 20 degrees deflection in the yaw-pitch coordinates.

On-board computers and video-camera recording are used to compare the agility of the vectored F-15 with that of the conventional F-15 RPV of comparable scale, with and without canards [as is the design of the F-15 STOL Demonstrator].

Flight control was initially conducted from the ground by two radio operators, one using conventional aerodynamic control surfaces, and the other only the TV nozzles. In later runs a new transmitter allows simultaneous TV and conventional control of the RPV from a single portable flight-control board.

The flight tests have been conducted in Ein-Shemmer and Megiddo Airfields since June 1989. The nose-pointing capability of the vectored F-15 RPV was significantly superior than that feasible with the conventional model having the same thrust-to-weight ratio .

Chapter III

Agility Comparison Problems

Missile/Aircraft Debated "Agility-Metrics"

Anticipating the introduction of vectored aircraft, McAtee (5), has, in 1987, defined fighter agility as composed of two complementary concepts : Maneuverability and controllability. PST maneuverability is then called "supermaneuverability", while PST controllability is named "supercontrollability. Thus, according to McAtee, the quality of fighter agility is the combination of three (measurable) tasks/abilities :

1) - The ability to "outpoint" the opponent (pointing at him before he points at you). This advantage must be such that the opponent does not have the opportunity to launch his weapon before he is destroyed. Otherwise, with current launch-and-leave weapons, mutual destruction would result. It is, therefore, the key ability to point at the enemy quickly to get the first shot (thereby reducing the sum-total of delay-times, including missile locking delays and path/time of flight). This ability is measurable in terms of Turn Rate vs. Bleed Rate of the aircraft/missile.

2) - The ability to continue maneuvering at high-turn rates over prolonged periods to retain the potential for performing defensive maneuvers, or make multiple kills when appropriate. I.e., to defend against attacks from other aircraft, or to accomplish multiple kills if the opportunity exists, an "agile" aircraft must be able to continue maneuvering at high-turn rates over prolonged periods. This key ability is measurable in terms of Residual Turn Rate vs. bleed rate of the aircraft .

3) - The ability to accelerate rapidly straight ahead, so as to leave a flight at will, to regain maneuvering speed when necessary, or to pursue a departing target when appropriate. This includes the ability to disengage, or escape from a battle without being destroyed in the process, as well as the acceleration necessary to "chase down" an enemy that is trying to escape. This key ability is measurable by acceleration vs. speed plots of the aircraft.

McAtee concludes that these three measurable tasks/abilities are crucial for success in modern close-in combat. Thus, the critical design features for modern fighters are those that enable the pilot to command very high maximum turn rates over prolonged periods and to perform a 1-g acceleration.

Supercontrollability

Good maneuverability must be integrated with effective controllability, i.e., the ability to change states rapidly (control power), and the ability to capture and hold a desired state with precision (handling qualities). Traditionally controllability was thought to be degraded at either of two conditions: High Mach number, or high AoA. However, the introduction of PST and vectored aircraft technology requires reassessment of the second condition. It also requires the introduction of new definitions, standards and MIL specs.

Pitch and yaw control requirements increase with AoA. For a given roll rate, as AoA increases, the requirements for pitch and yaw forces/moments (for non-thrust-vectoring aircraft), increase exponentially. At the same time, with conventional aerodynamic controls, the forces/moments available decrease as airspeed decreases. Thus, beyond a given limit, conventional control technology becomes obsolete. This technology limit is reached when the size and weight of the aerodynamic control surfaces needed to provide sufficient forces/moments become prohibitive. However, the introduction of PST and vectored aircraft technology (together denoted by McAtee as the new domain of "supercontrollability"), requires reassessment of all maneuverability and controllability concepts and requirements.

Thus, according to McAtee, new point-and-shoot weapons have reduced engagement times drastically, leaving aircraft with poor maneuverability and controllability at the mercy of those that can use their agility to kill quickly during close-in combat. Vectored PST maneuvers may thus be defined as supermaneuvers.

There are a few dozens candidate supermaneuvers, half of which may demonstrate a real combat promise (1). Ref. 1 provides a few examples for combat payoffs during the proper use, at the proper position/ timing, of yaw-pitch-roll thrust vectoring during "angles" and "energy" tactics. These tactics employ supermaneuvers well beyond the current flight envelopes of conventional fighter aircraft.

Specific Agility Comparison Problems in This Program

The main problems encountered in Phase VI [Chapter I, Fig. 1] may be grouped into 3 categories:

1) - The development of a realistic, cost-effective method to measure and compare the agility of two different designs, say, a conventional vs. a vectored, or a semi-vectored vs. PVA. The problem, however, is, that the very definition of agility is still being debated (3, 4, 10).

2) - The development of a cost-effective hardware to measure and compare the performance of two different RPVs. For this purpose we have developed an on-board, light-weight, low-cost, "metry" computer, which records flight data on its RAM. Our new computer is based on an advanced PC "card" which has been considerably modified for this purpose and then combined with amplifiers and analog-to-digital converters and various calibrated sensors.

[Our first computer records 32 channels every 0.1 sec. for 180 seconds - the net time required for 'standard' recorded maneuvers. The overall duration of each flight-test takes about 10 minutes.]

Combined with proper video recordings, this methodology saves cost, time and efforts. [Our inputs to the computer RAM include: AoA, sideslip angle, 6 accelerometers, all nozzle/vectoring angles, all aerodynamic-control-surfaces positions, speed, etc.] Each data extraction set begins and ends by a radio command, at the beginning and at the end of each specially-planned, "Standard Comparison Maneuver" (SCM). Thus, each SCM-set is properly filed for later analyses in the laboratory.

3) - The aforementioned hardware cannot be applied without a proper software to feed, calibrate, file, transfer, and identify the data extracted.

F-15 Baseline Comparisons

How to evaluate and compare the agility of different fighter aircraft? Or, what to measure, during what kind of SCM, with what RPV, for what purpose, at what cost, under what similarity rules?

During flight-testing programs we compare the "agility" of a conventional F-15-RPV ("Baseline-1 RPV"), with that of a "canard-configured" F-15 ("Baseline-2 RPV"), with that of "pitch-only" vectored-F-15-RPV ("Baseline-3 RPV"), with that of "yaw-pitch" vectored-F-15-RPV ("Baseline-4 RPV"), with that of "simultaneous roll-yaw-pitch" vectored-F-15-RPV, etc.

However, these categories may be further divided into flight testing vectored RPVs with or without [full or partial] vertical stabilizers, rudders, leading edge devices, and also into other subcategories involving, say, fixed or movable conventional aerodynamic control surfaces.

Yaw-Jet Control During Ground or Low-Speed Handling

The yaw vanes provide excellent ground handling qualities. Thus, during taxiing, the flyer uses the yaw vanes frequently to turn the RPV, as required. Similar advantages are easily obtainable at takeoffs, or during landings, or PST, low-speed maneuverability, e.g., during cross-winds at low speeds, or during very high AoA flight (approach or low-speed, PST-maneuvers), when the rudder is totally ineffective, the flyer can use the highly effective yaw vanes to obtain directional control at any speed.

Prior to takeoff one must recheck the yaw-vane zero-angle with respect to the unvectorred jet axis. Even slight deviations from zero-angle setting cause large moments that affect takeoff direction control and, in addition, cause thrust losses. Similar checks must be conducted with the pitch flaps.

Furthermore, prior to takeoff, the flyer must determine and select linear or exponential yaw/pitch control sensitivity modes. Especially on a hot day, the thrust of the engines must be measured just prior to takeoff. [High air temperatures deteriorate the piston-engine power, the thrust efficiency of the ducted fan jet, and the lift on the wings.]

Yaw-Jet Vs. Rudders Controls

Due to the limited number of radio channels on our PCM transmitter [which has been modified by our laboratory to function both in the conventional and vectored control modes, and also as a radio on/off commands to the onboard and ground-based computers - cf. Fig. 2, p. 12], we had to add a separate transmitter just for the F-15 rudders.

Now, one does not have to use the F-15 rudders during takeoffs. The jet-yaw control is much more effective for that purpose and for ground handling maneuverability and control.

However, during landings, when the engines throttle is reduced to idle, the yaw thrust control is almost nil. Hence, during this stage one may need the extra moment of the F-15 rudders.

For that purpose we added another flyer who is equipped with a single [rudder] channel on a second transmitter, or have the main flyer hold a double-tray with both transmitters installed on it.

Engine-Out and Other Emergency Situations

During the flight tests of the thrust-vectoring F-15 RPVs, we had encountered with a few engine-out emergency situations. The throttle of the remaining engine was then reduced to half-power, and the yaw-jet thrust control was found effective to bring the RPV to the final approach attitude/altitude/speed. However, as explained in the previous paragraph, we had to use the rudders during the landing, due to the final reduction of the throttle to the idle position.

Standby RPVs and Onboard Computers

Unfortunately we had also encountered with other emergency situations, which had caused hard landings on the runway, or on nearby cotton fields, and, **also a few crashes . These crashes have twice ended-up with a total loss of the RPV together with its onboard computer. Such losses produce long delays in the program (up to 4 or 6 months) and also force us to constantly build/test/calibrate standby RPVs and onboard computers.**

Chapter IV

ETV Vs. ITV

[External Vs. Internal Thrust Vectoring]

ETV is considered now more as a demonstration method for flight-testing upgraded fighters with a required level of PST-RaNPAS TVM performance, and less as a design/production option. However, with diminishing budgets, some airforces may adopt this simple, low-cost method to upgrade low-performance fighters. In comparison with yaw-pitch, or roll-yaw-pitch ITV, which is considered as the only ultimate design/production option, ETV is based on a very simple, yet quite cost-effective thrust vectoring devices which require almost no change in engine hardware. It is based on post-nozzle-exit, external vanes/flaps/pedals.

Thus, ETV is accomplished by single, or multiaxis, post-nozzle-exit "vanes", or curved pedals, which provide yaw-pitch, or [twin-engine] yaw-pitch-roll controllability (by deflecting the free jet emerging from axisymmetric, or from unvectorized 2D nozzles). This methodology is characterized by the absence of (high-aspect-nozzle-ratio) supercirculation lift-gains; partial-dependence on the external-flow regimes, low-efficiency in jet-deflection, relatively high RCS/IR signatures (especially with circular nozzles), and longer over-all fighter lengths [Cf. the (DARPA-MBB-RI) X-31A].

Nevertheless, the ETV-X-31 experimental fighter airplane [which is due to start flight tests around June 1990], constitutes one of the most important and most promising test aircraft in the evolution of vectored aircraft. Motivated by Herbst's ideas (1) the X-31's expected demonstrations in the new PST-RaNPAS TVM domains would certainly become a most significant milestone in aviation history.

Another important contribution to ETV was recently made in NASA-Langley Research Center (1, 2) and by Northrop (15). In one of the most promising designs (1,2, 15), post-exit vanes were mounted on the side-walls of a nonaxisymmetric 2D-CD nozzle .

Partially Vectored Propulsion/Aircraft Systems

Partial Jetborne Flight (PJF) may be defined as a flight in which elevons, ailerons, flaps, canards, elevators, leading-edge devices, vertical stabilizers, rudders, etc., are still being used in conjunction with a thrust-vectoring system. Most of the TV-methodologies assessed below, may be classified as PJF, e.g., those associated with the ETV-X-31, the ETV-F-18, and the ITV-F-15 S/MDT programs. This means that maximal maneuverability and controllability levels obtainable with PVA are reduced, to a

degree, by external-flow effects on conventional, aerodynamic control surfaces, especially in the PS domain.

Another objective of our programs is, therefore, to discover the *bone fide* technology limits of vectored propulsion, using both laboratory and flight-testing methodologies. In the near future we may thus prove whether or not the flight/propulsion control during PJF is more or less safe/complicated than that feasible with PVA.

Other By-products of this program may also reflect on the following assertions:

1) - PJF with partially-vectored F-15 RPVs involves too many variables, most of which are redundant.

On one hand, leaving the multiple aerodynamic control surfaces operative, adds safety, in case of total ITV or ETV failure. On the other hand, the redundancy involved, in comparison with PVA, may decrease safety and increase complexity beyond actual needs.

2) - A reliable IFPC system for PJF may have to overcome the lack of proper definitions of the relevant variables involved. However, inspite of extensive NASA and industrial work in this field, there is yet no experimental Database for the proper range, limits, and coupling effects among these variables during actual propulsion/flight control. The main reason for this lacuna is the redundancy of conventional aerodynamic variables and the high-cost, time-consuming efforts to flight-test manned, thrust-vectored fighters.

Hence, it is here that a properly-designed, highly-integrated, laboratory/flight-testing methodology may be highly cost-effective in establishing the yet-unknown technology limits, and in supplying preliminary IFPC-databases within the next few years.

IFPC

Vectored propulsion design should be based on new propulsion/flight control laws such as:

- 1- New TV-engine control rules and standards, in particular new nozzle and new inlet rules.
- 2- New TV-flight-propulsion rules for PST/PSM/RaNPAS maneuvers.
- 3- New TV-flight-propulsion rules and standards for takeoff and landing. [E.g., turning the jets up first, and, then, following aircraft rotation, turning them down for extra lift by direct engine force and, in a few advanced designs, also by supercirculation (3)].
- 4- New Coupling Rules, e.g., Directional Thrust Vectoring (DTV) to aileron cross-feeds to correct DTV coupling into roll; Lateral-directional cross-feed paths to provide stability-axis rolls with high AoA; Longitudinal TV gains vs. the longitudinal system loop, etc.

Chapter V

Tentative Concluding Remarks

1 - The research methodology employed here has been described in the previous chapters. Additional considerations, drawings and details are available in our previous reports and video cassettes as well as in Ref. 1 [p. 54].

2 - Subject to remark No. 1 we list below the general and technical conclusions as tentative remarks. These remarks may be considered together as a single methodological entity. Their verification is the subject of next-year efforts, especially in terms of accuracy and repeatability.

3 - The feasibility of yaw-pitch thrust vectoring nozzles for the F-15 configuration [and one or two of its combat potentials], has been demonstrated in laboratory and in repeated RPV flight tests [so far without a canard].

4 - The cost-effectiveness of integrated laboratory/RPV-flight-tests has been demonstrated. However, many technical and methodological problems are yet to be resolved.

5 - F-15 fighter aircraft can be upgraded by transforming its engine nozzles into [axi or 2D] yaw-pitch thrust-vectoring nozzles. Additional gains in performance and reduced signatures are extractable from our newer roll-yaw-pitch, high-aspect-ratio nozzles [Appendix A].

6 - Good controllability and rapid nose turns are obtainable during conventional and PST maneuvers. [So far we have tested the F-15 up to about 80 - 90 degrees AoA].

7 - Excellent recoveries from spins have been demonstrated by the use of the yaw-pitch vectoring nozzles. [No recovery from these situations was apparently possible with conventional control surfaces.]

8 - We have also been able to demonstrate, in flight, the so-called **COBRA maneuver**. It was repeatedly demonstrated by means of our thrust-vectoring F-15 RPV. During these repeated maneuvers the AoA was continuously maintained at about 80 degrees. This attitude was maintained unchanged for a few seconds without a noticeable change in altitude. Then, at the end of the maneuver, the nose was very easily thrust-vectoring down with the help of the thrust vectoring nozzles. Rapid nose-pointing capabilities, to negative AoA or to positive AoA has been repeatedly demonstrated with PROTOTYPE No. 7 on Aug. 27 in Meggido airfield. **[Cf. the (Aug-Sept-Oct-89) video cassette No. 1, which is part and parcel of this report].**

9 - Due to debated agility concepts [p. 47], and as a result of specific difficulties associated with different Baselines [p. 18] using the same yaw-pitch, PST-TVM [Ref. 1], we plan to develop, during the next year of the program, **STANDARD-AGILITY-COMPARISON-MANEUVERS [SACM]**.

10 - Validation attempts of 9 will be conducted in July 1990, in the presence of the Project Manager and his associates, and will continue during 1990-92 as our **post-flight analyses become more realistic and reliable for fullscale conclusions.**

11 - As far as we can see no clear-cut advantages of vectored over conventional fighters, and of yaw-pitch TVM over pitch-only-TVM, can be demonstrated without SACM and repeatable, statistically-verified, experimental data bases.

Furthermore, no IFPC system may apparently be designed to be useful without SACM and such experimental data bases. The present methodology provides an effective, low-cost, and relatively rapid solution to some of these fundamental problems.

12 - Excellent ground-taxiing control, and very good low-speed, high-AoA-handling, have been demonstrated by the use of two yaw vanes for thrust control. The yaw vanes must be coupled to and coordinated with pitch-thrust-vectoring-flaps flight-control commands. Four or six yaw-vanes-doors [p. 55] may, however, become the best choice for future yaw-pitch thrust-vectoring nozzles, as evaluated now by means of our [cost-sharing], full-scale engine test rigs [p. 21a].

13 - A low-degree of yaw and pitch control sensitivity is sufficient for all TVM. Very powerful moments are generated by geometric/effective deflections of less than 10 degrees [Cf. Figs. 8 to 17 on p. 23 to 32].

14 - STOL advantages have not yet been demonstrated. Its evaluation is postponed till we install the 25%-more-powerful-engines on our light-weight, 2nd-generation F-15 RPV [see below].

15 - The yaw thrust-control is especially useful during takeoffs and landings at high crosswind speeds. However, if the mechanical control of a single yaw-vane is lost, the free vibrating yaw-vane in the efflux jet stream can cause catastrophic results during takeoff, as had been twice encountered during our past flight tests.

16 - Three complementary test methods have been developed for high-alpha F-15 inlet feasibility studies. Each method has its pros and cons. All combined, they are designed to provide initial estimates of the gross effects of high AoA (up to about 90 degrees) on Distortion Coefficients (DC) and Pressure Recovery (Pr) at the "compressor's-face-station" of current F-15 inlets. Such gross effects, as deduced from the combined test results extractable from the three complementary methods, are to help initial, conceptual/preliminary designs of new ideas for "vectorable" inlets. A few examples of such unorthodox ideas are schematically shown in pages 108 to 115, while the three complementary test methods are described in Chapter I : Outline.

17 - The preliminary subscale-test-data indicate that a considerable deterioration of F-15 inlet performance is to be expected beyond about 60 degrees incidence. This phenomenon dictates the introduction of variable inlet lips/vanes, as will be investigated during the next phases of this program.

18 - The data presented on p. 174 can be used as a **Standard** for generating DC and Pr maps of deviations from **Takeoff-Baselines** (p. 156) due to high-incidence-inlet-angles. This approach is incorporated now in our new computer programs for plotting PST-inlet performance.

19 - The search for optimal [vectorable] inlet lips and/or variable inlet vanes for PST F-15 inlets will become a central goal of the 2nd-year inlet work. However, so far the last method described on p. 21a, i.e., flight tests of PST-inlets onboard an F-15 [1/7th-scale] RPV, has encountered weight/agility penalty problems. These problems may be resolved by the development of low-weight scanning valves or low-weight pressure transducers in the range 0.0 - 0.15 psi full-range.

20 - Further studies are required to demonstrate [TV-controlled] F-15 RPV flights with partial or no vertical stabilizers, and/or with canards, and/or with advanced, yaw-pitch-roll thrust-vectoring nozzles [with NAR in the range of 50], replacing the entire tail section of the F-15 RPV [Appendix A].

21 - The 2nd-generation F-15 RPV [PROTOTYPE 17] weighs only 13.2 kg [without fuel] as compared with 16 kg [w/o fuel] of PROTOTYPE 7. In a cold-day this means $T/W = 2 \times 5.5 / 13.2 = 0.83$ vs $T/W = 2 \times 5.5 / 16 = 0.69$ for the 1st-generation F-15 RPV. These ratios are lower in hot weather and at

the beginning of the flight test [which lasts about 8 minutes]. To increase these ratios, as well as speed and safety, we have ordered now a new set of 25%-higher-power-engines [The O.S.-91VR-DF, which are new on the market and are now the highest-power ducted-fan engines available. These new engines will replace our currently flying O.S.-77VR-DF.]. The new engines are therefore expected to considerably increase our T/W, speed and safety. They would arrive to the JPL around June 1990.

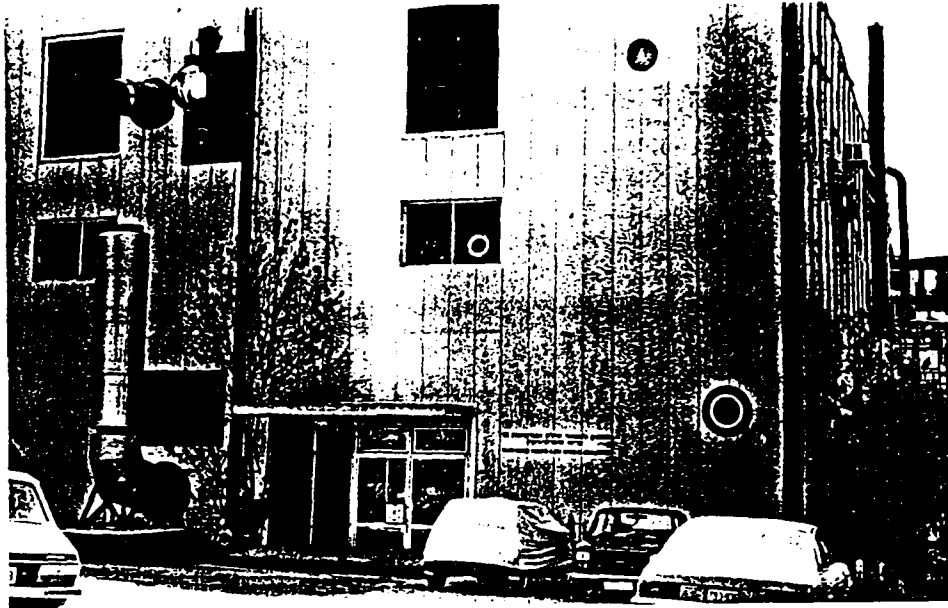
22 - Extensive reviews of previous works have been completed.

These reviews are available in Appendix B - Part 1, as well as in our new book. They cover the following areas:

- New thrust vectoring nozzles for partially-vectorized fighters.
- New thrust vectoring nozzles for pure-vectorized fighters.
- New inlet designs for PST fighters [Appendix B-PART 1 in this report].
- New PST-TVM-RaNPAS methodologies during aircombat.
- Propulsion technology limits beyond the year 2000 [Appendix B in the book].
- The definitions of Agility, supermaneuverability and supercontrollability [Also available in Chapter III, p. 47, of this report].
- Different International methodologies [Also available in Chapter II, p.43, in this report].

REFERENCES

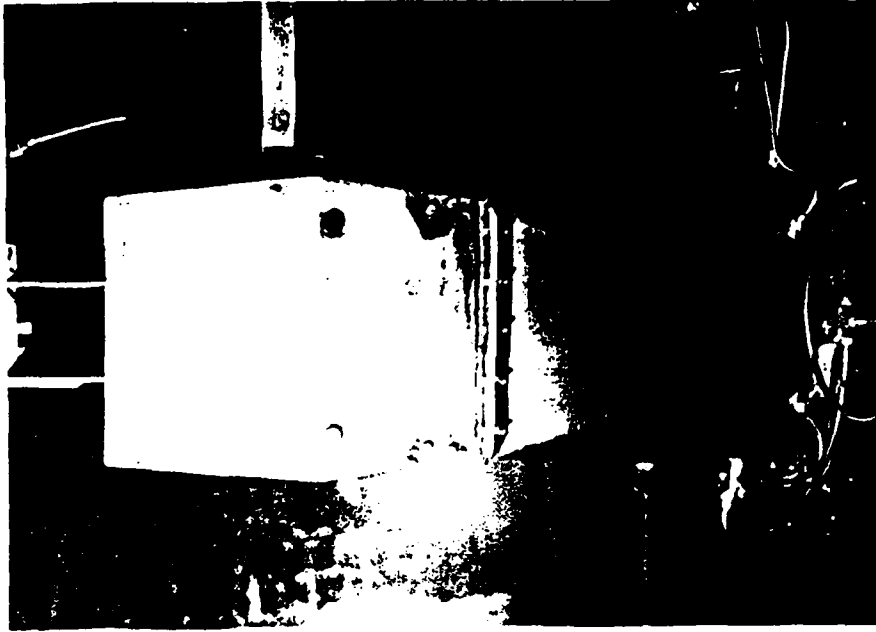
1. Gal-Or, B., Vectored Propulsion, Supermaneuverability and Robot Aircraft, Springer-Verlag, New York-Heidelberg, 1990. 276p., 235 refs., 145 figures. Also J. of Propulsion, In press.
2. Yugov, O. K., Selyvanov, O. D., Karasev, V. N., and Pokoteelo, P. L., "Methods of Integrated Aircraft Propulsion Control Program Definition", AIAA Paper 88-3268, Aug. 1988.
3. Costes, P., "Thrust Vectoring and Post-Stall Capability in Air Combat", AIAA Paper 88-4160-CP, Aug. 1988.
4. Tamrat, B. F., "Fighter Aircraft Agility Assessment Concepts and their Implication on Future Agile Fighter Design", AIAA Paper 88-4400, Aug. 1988.
5. McAtee, T. P., "Agility - Its Nature and Need in the 1990s", Society of Experimental Test Pilots Symposium, Sept. 1987.
6. Herbst, W. B., "Thrust Vectoring - Why and How ?" ISABE-87-7061. "Supermaneuverability", MBB/FEI/S/PUB/120, (7.10.1983); AGARD, FMP Conference on fighter maneuverability, Florence, 1981.
7. Mason, M. L. and Berrier, B. L., "Static Performance of Nonaxisymmetric Nozzles With Yaw Thrust-Vectoring", NASA Tech. Paper 2813, May 1988.
8. Berrier, B. L. and Mason, M. L., "Static Performance of an Axisymmetric Nozzle With Post-Exit Vanes for Multiaxis Thrust Vectoring", NASA Tech. Paper, 2800, May 1988.
9. Richey, G. K., Surber, L. E., and Berrier, B. L.; "Airframe-Propulsion Integration for Fighter Aircraft", AIAA Paper 83-0084, Aug. 1983.
10. Gal-Or, B., "The Principles of Vectored Propulsion", International J. of Turbo and Jet-Engines, Vol. 6, Oct. 1989, pp. 1- 15.
11. Tamrat, B. F. and Antani, D.L. , "Static Test Results of an Externally Mounted Thrust Vectoring Vane Concept ", AIAA Paper 88-3221, Aug. 1988.
12. Klafin, J.F., "Integrated Thrust Vectoring On The X-29A", AIAA Paper 88-4499, Dec. 1988.
13. Miao, J. J., Lin, S. A., Chou, J. H. , Wei , C. Y. , and Lin, C. K. "An Experimental Study of Flow in a Circular-Rectangular Transition Duct", AIAA Paper 88-3029, Dec. 1988.
14. Pavlenko, V. F., Powerplants with In-Flight Thrust Vector Deflection, Moscow, Izdatel'stvo Mashinostroenie, 1987. 200p., 37 refs. In Russian.



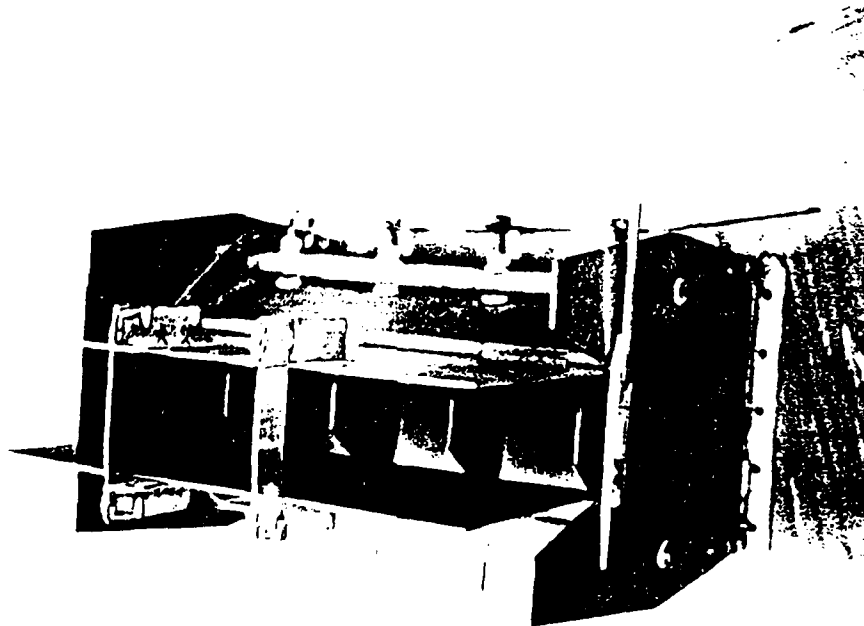
The front side of the Tark-Recu Turbo & Jet Engine Building



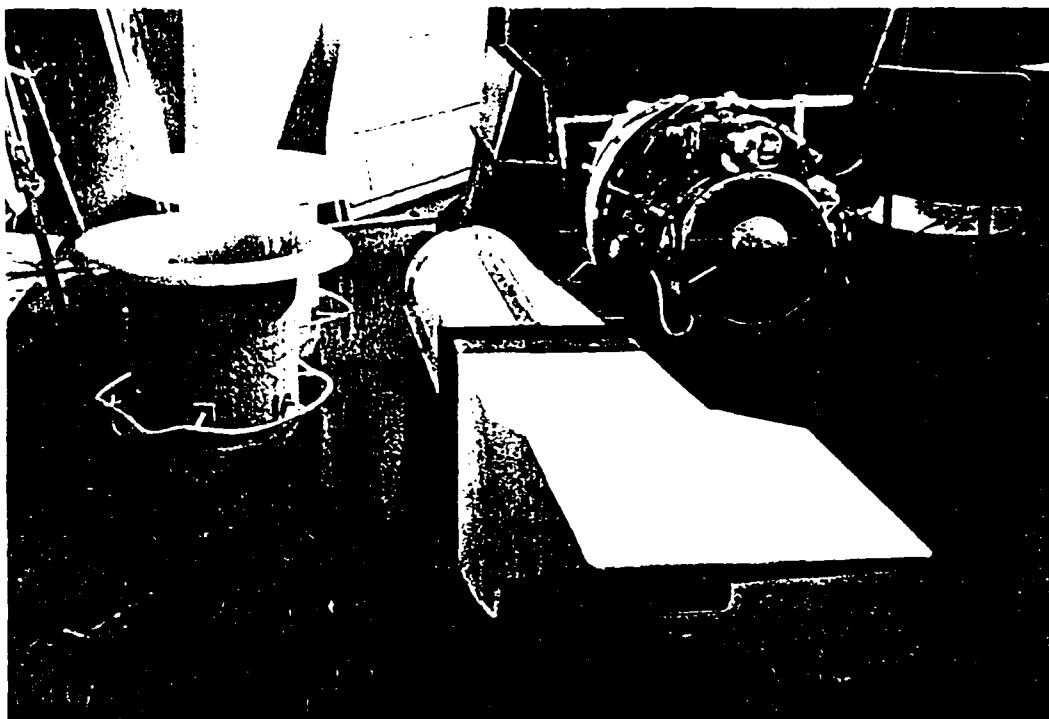
The rear side of the same building



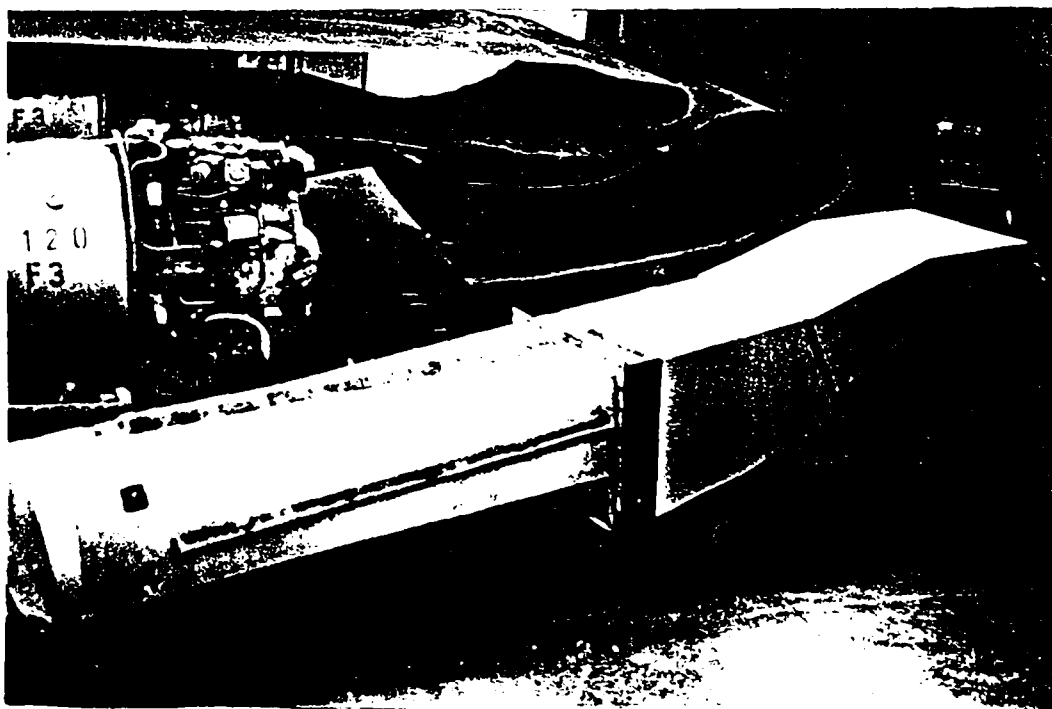
The type of recommended yaw-pitch, 2D-CD, vectoring nozzle for the yaw-pitch vectored F-15 fighter (see below). The nozzle is shown inside the engine altitude test rig. cf. Fig. 26. p. 41, Fig. 7d. p. 22d and p.60.



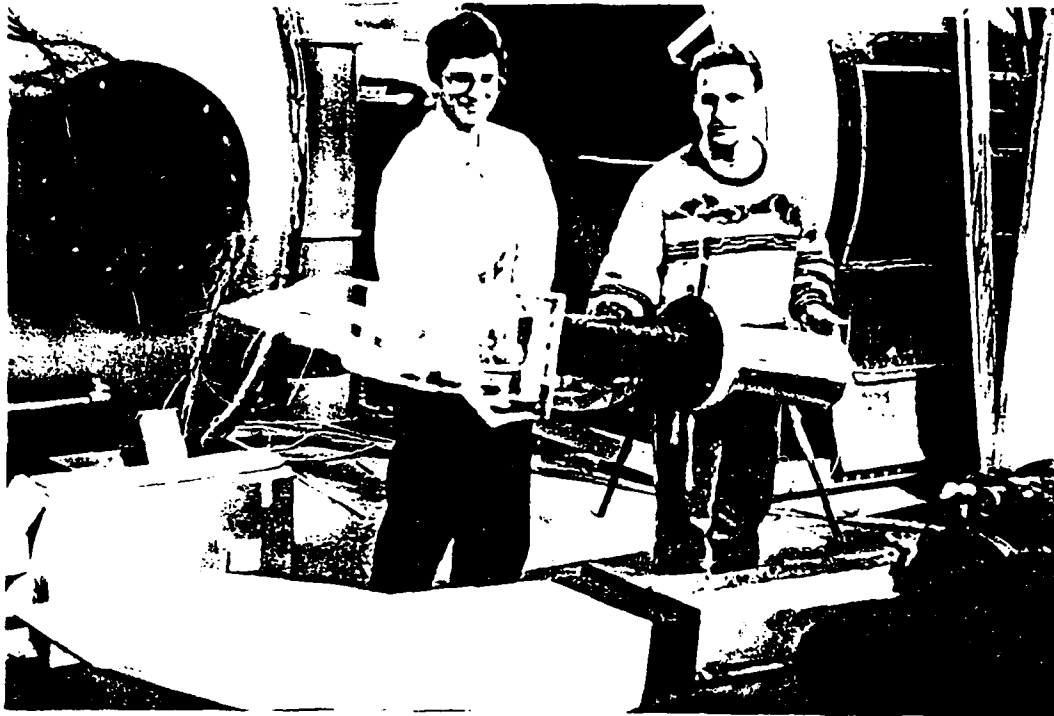
The yaw vanes/doors and the pitch flaps of the nozzle recommended by this laboratory for the next yaw-pitch vectored F-15 USAF feasibility studies. The USAF may issue a PATENT on this new concept/design! please instruct us ! cf. Fig. 7d, p.22d for dimensions, and p. 60 for a back view.



The "full-scale" F-15 inlet just before its installation on the Marboro jet engine. Shown also are the standard bellmouth inlets used for comparison tests. (see Appendix B). See Fig. B.2.2, p. 106 for dimensions and configuration.



The "full-scale" F-15 inlet prior to its installation on the Marboro jet engine. A low-signature inlet is shown in the background. See picture on page 57 (below) for the "miniature" full-scale system.



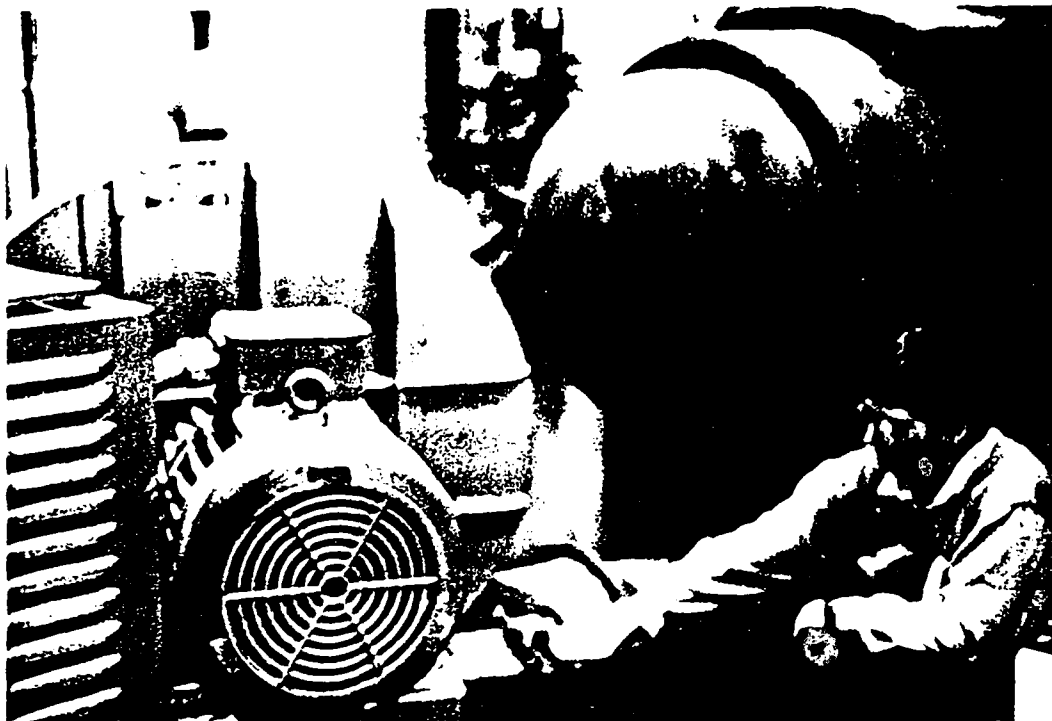
Roni and Ido with the "sub-scale" and "full-scale" F-15 inlets.

See Figs. B-2.1 and B-2.3, p.105, 106, for comparison of the relative dimensions.



The new high-aspect-ratio, low-signatures, roll-yaw-pitch nozzles designed, tested and validated by this JPL. Shown also are the F-15 and F-16 wind-tunnel models and the engine altitude test system.

The jet engine, with the installed F-15 inlet, is visible inside the altitude engine test facility.



Rena and one of the blowers of the sub-scale F-15 inlet system. Note: At the time, the air flow rate of this blower, the suction blower simulating takeoff flow through the inlet.

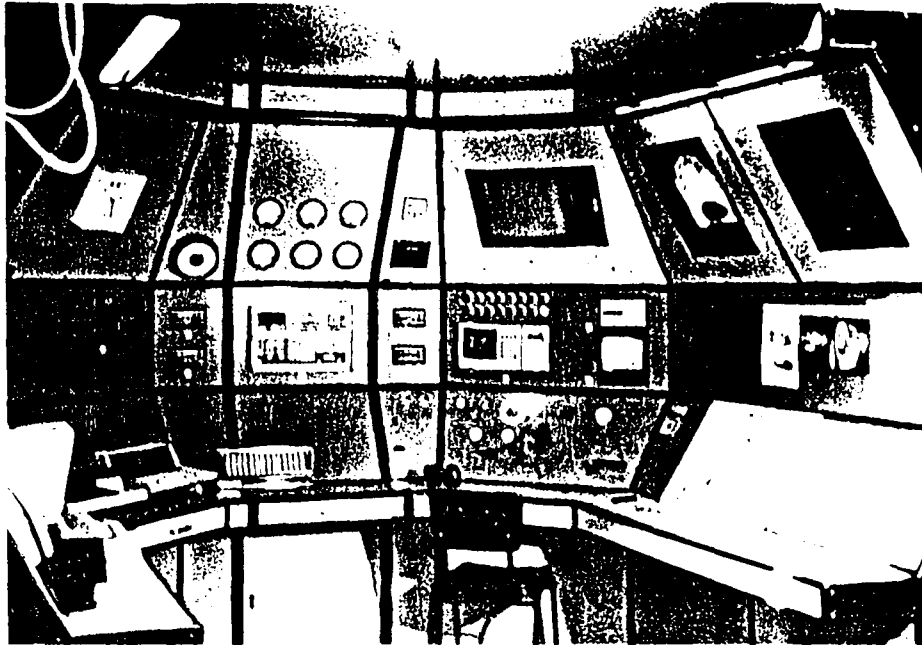


Rena-Ron Slicker and the left-hand nozzle of the newly-proposed yaw-pitch-roll, elevator-less vectored F-15 RFV of Appen, A).

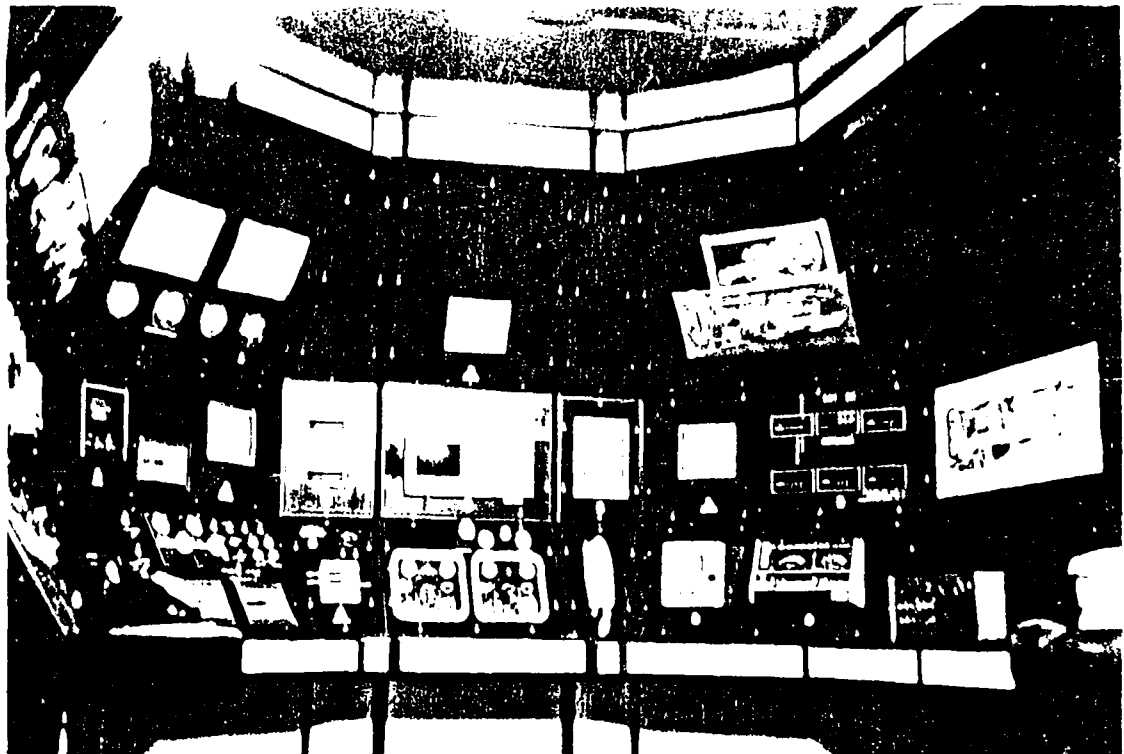
Most of this nozzle is inside the F-15 fuselage.

This new nozzle is air Patentable.

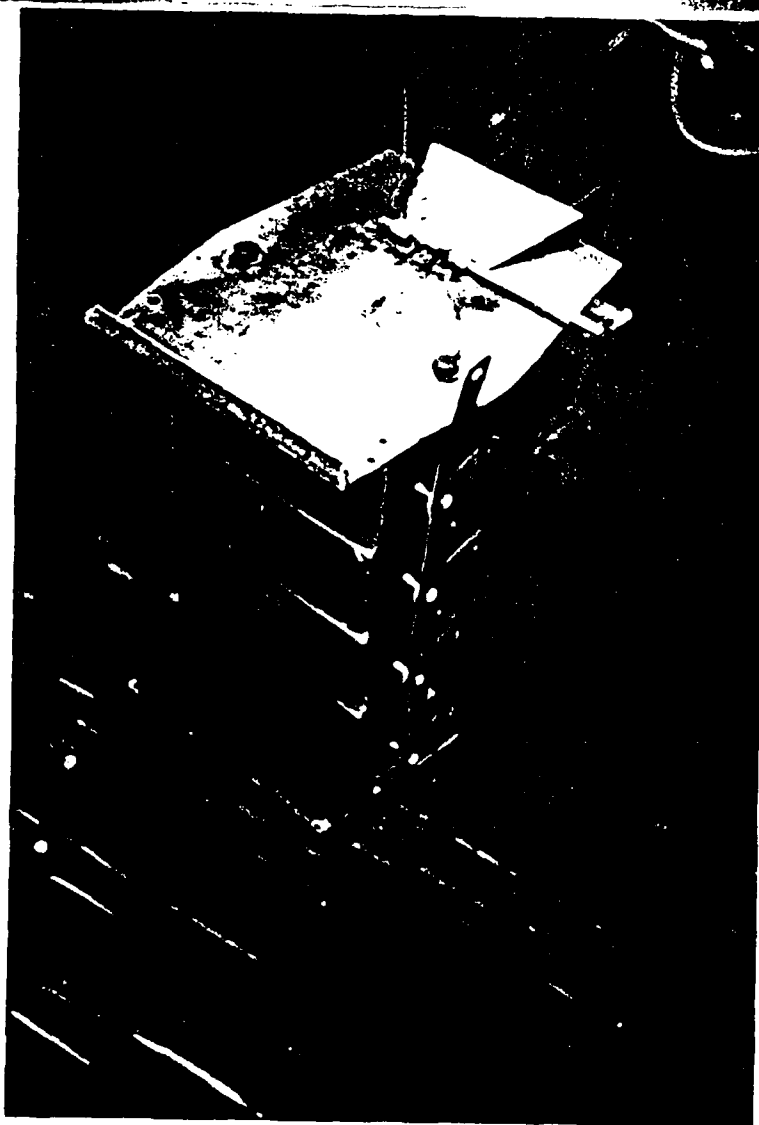
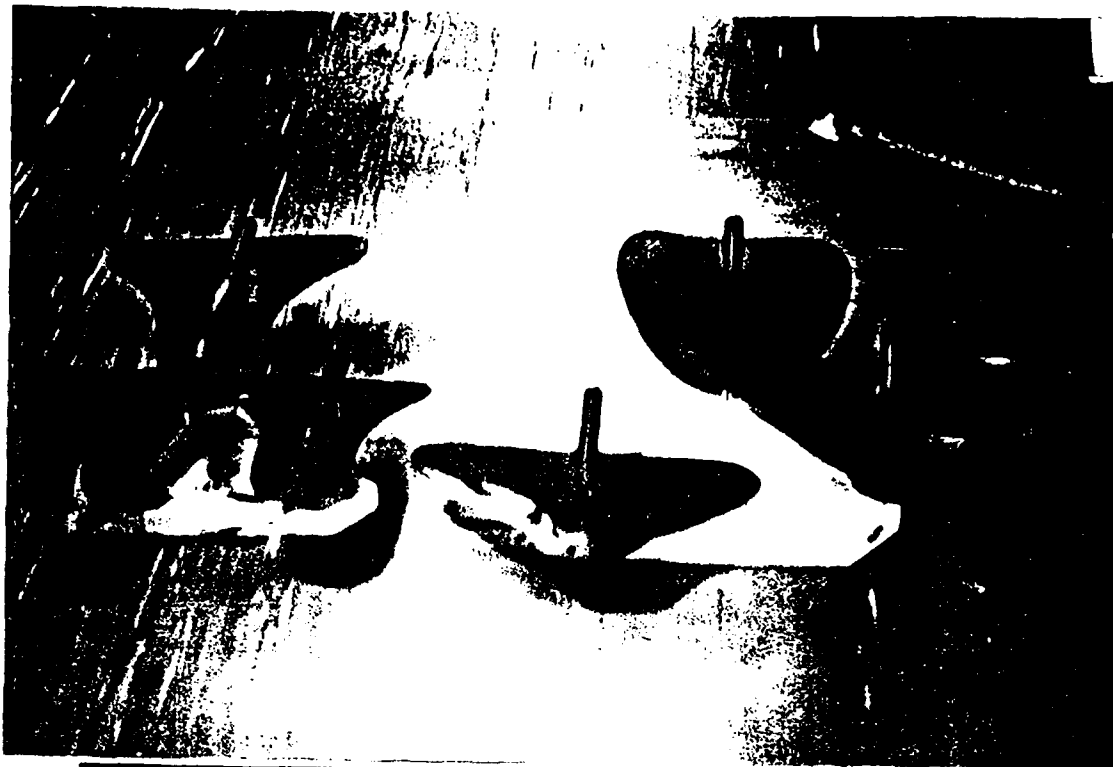
8 yaw vanes are installed inside the nozzle for jet deflections up to 15 or 30 degrees yaw. cf. Fig. A-1 p.75.



The "full-scale" altitude engine test rig is controlled from this control room (no.5), cf. Fig. 7a, p.22, Fig. 25, p.41 and p.57

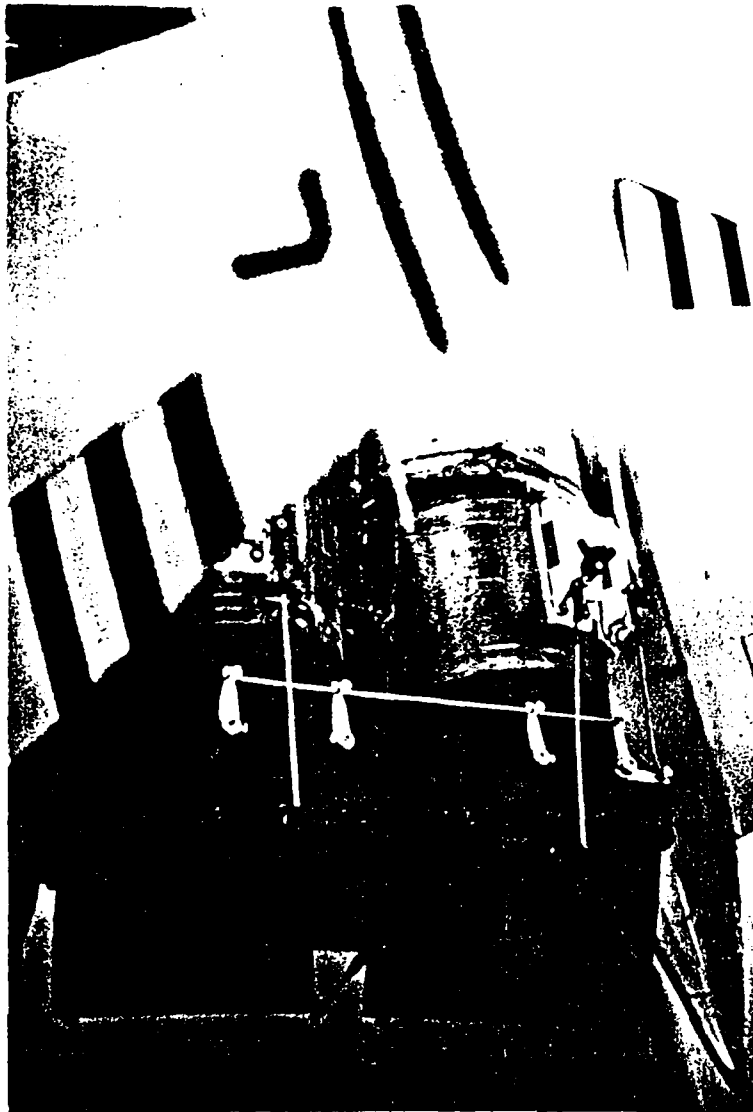


The "subscale" component test rig for initial feasibility studies of new types of nozzles and inlets are normally operated from this control room (no.4), cf. Fig. 27, p.42.



Various vectorable, low-signatures, wind-tunnel models are being tested since 1986. The model on top of the left group was scaled-up, and flight tested on May 1987 (see p.66).

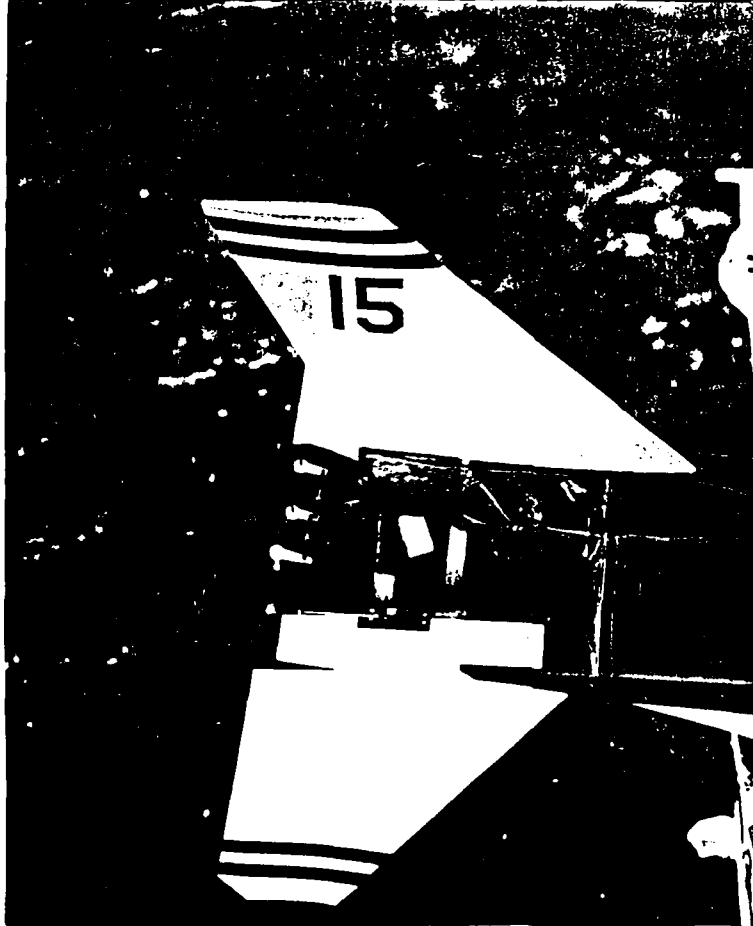
The PATENTABLE, new, 2D-CD yaw-pitch thrust vectoring nozzles developed, tested and validated by this laboratory. cf. Fig. 7d, p.22d, and p.55. This model has been developed within the cost-sharing program.



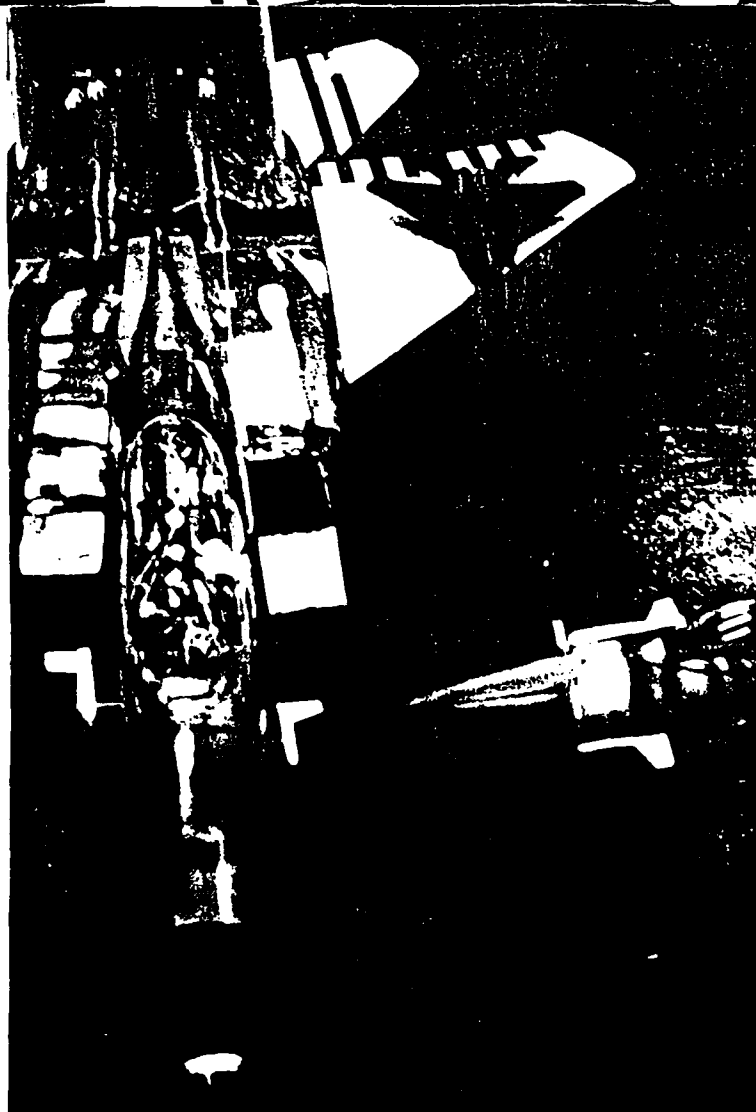
Down-scaling the nozzle shown in Fig. 7d, p.22d, we had to eliminate 2 yaw vanes to allow introduction of starter shaft from the rear end. See dimensions on p.22c, Fig. 7c.

Yaw-pitch forces-moments are measured from the hinges (Fig. 7 p.17).

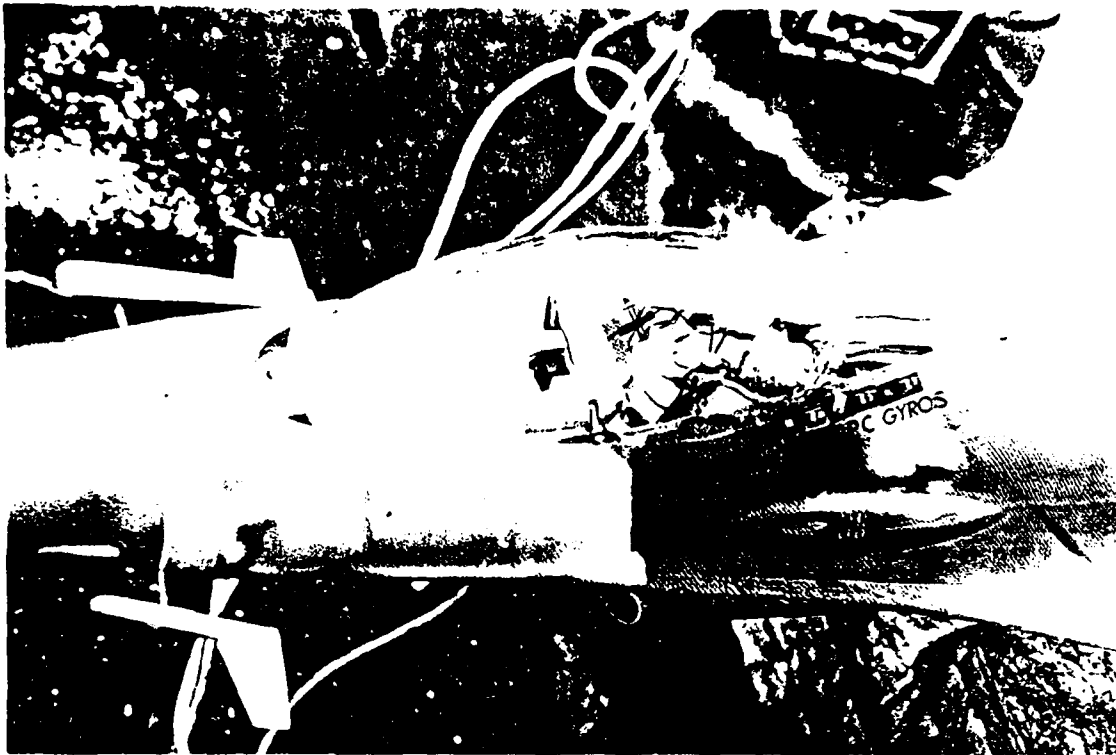
The current yaw-pitch thrust vectoring nozzles on the 1st-generation F-15 RPV cause minor drag changes, as evident from our early wind-tunnel test results.



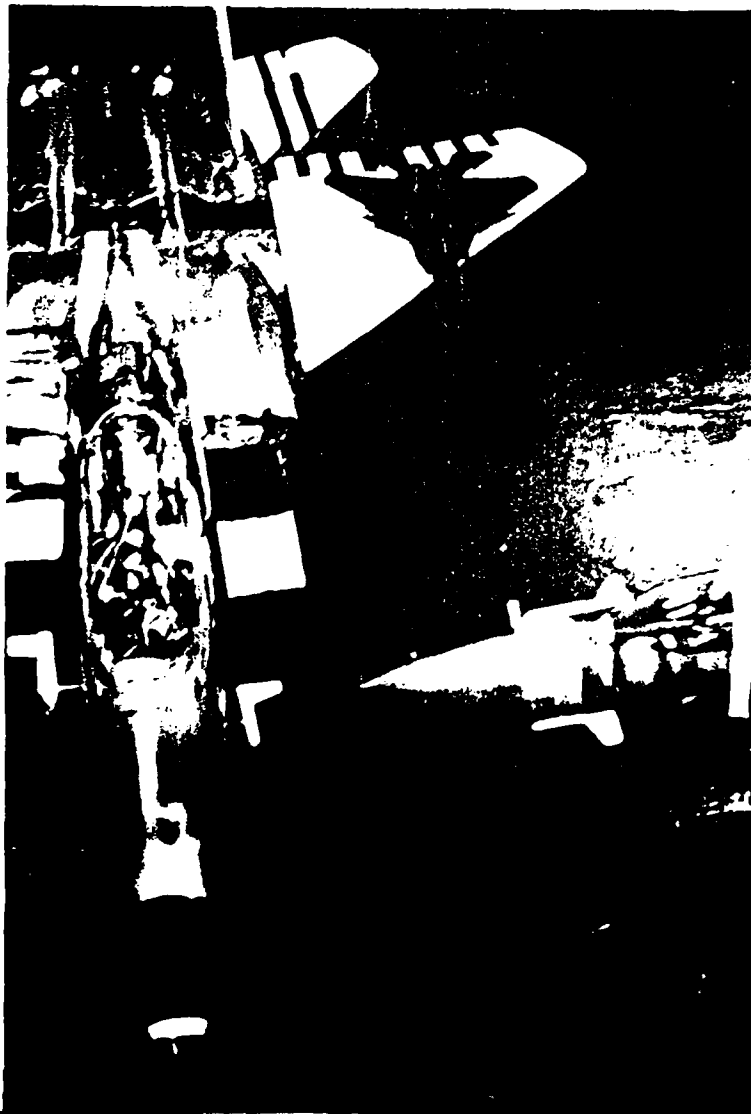
The current yaw-pitch thrust vectoring nozzle on the 2nd generation F-16 RPV. cf. Fig. 7c, p.22c.



Two views of the first-generation, vectored P-15 RPV (canardless). The left-hand inlet ramp is lowered to simulate operation at low speed. Nineteen pressure probes are installed inside this nozzle. However, as explained in page 11a, weight penalties have, so far, prevented DC and Pr tests during PST-flights. Seated is Dr. Valery Sherbaum, who had joined the JPL on Nov. 1, 1989.



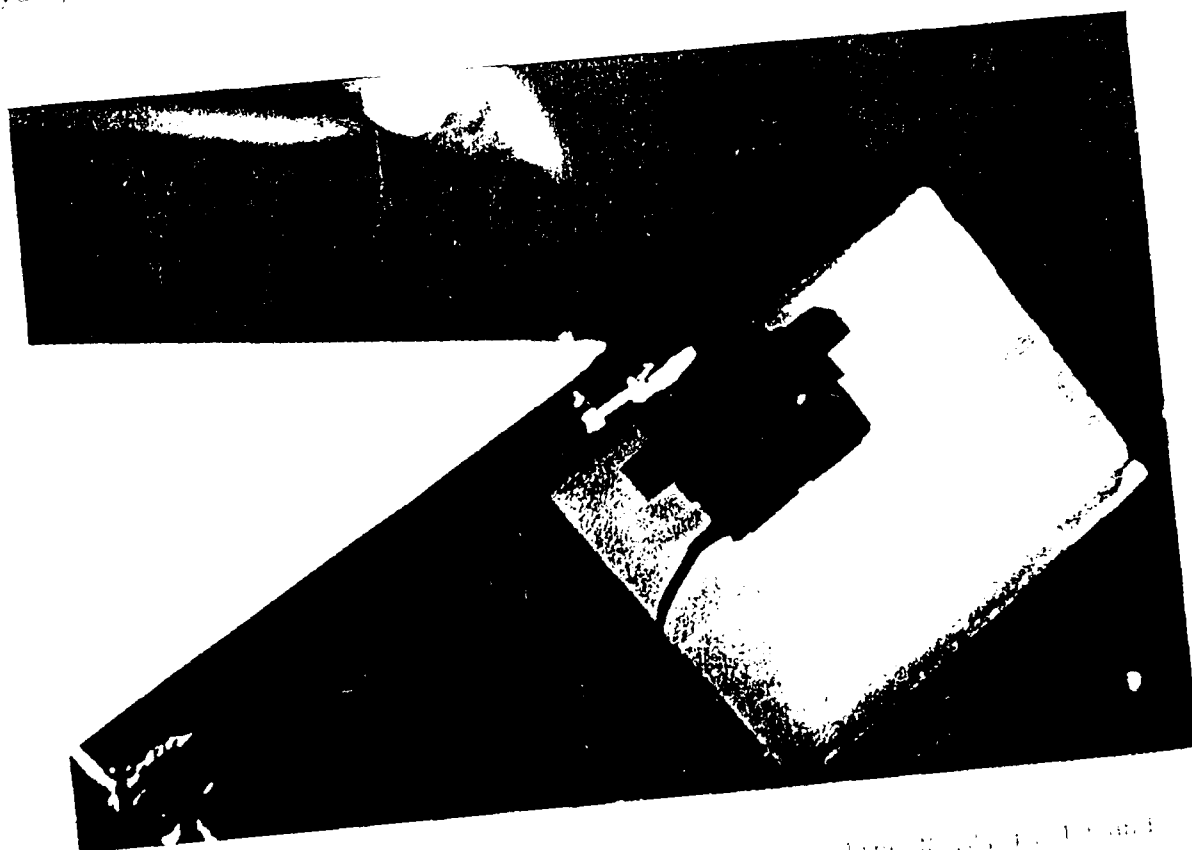
The velocity and alpha probes on the vectored F-16 RPV. Beta probe is below. See also p.22e and 14. The gyros have been replaced with accelerometers.



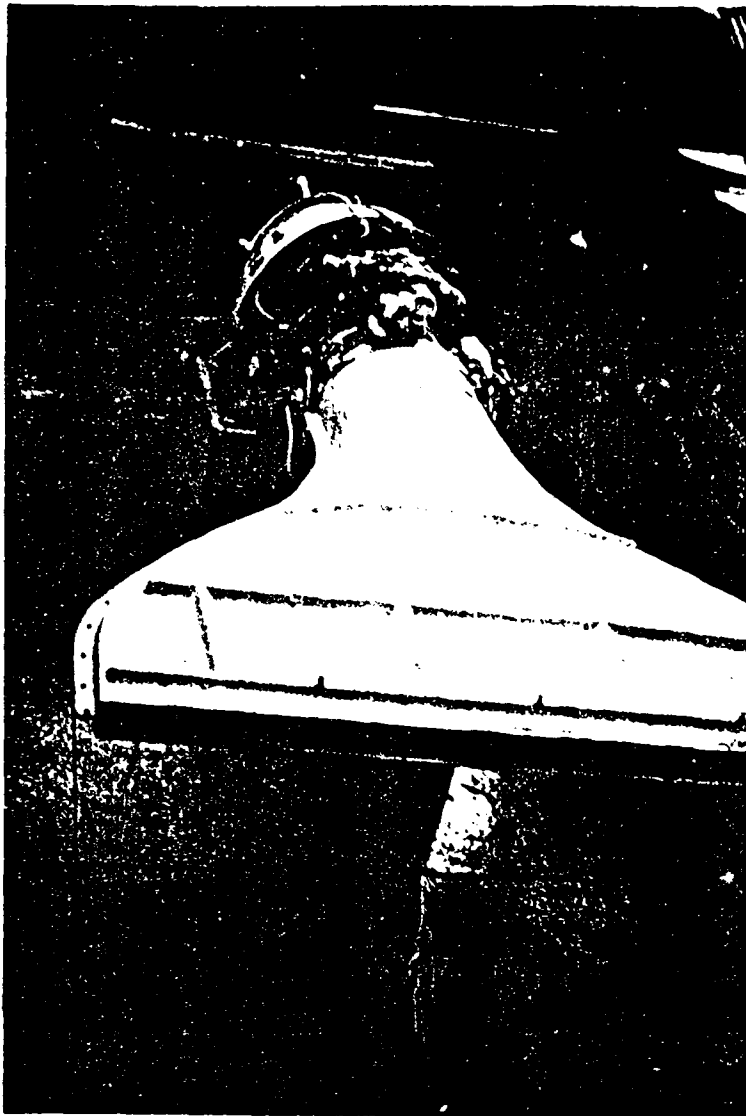
The velocity and alpha probes on the 1st-generation F-15 RPV. A wind-tunnel model of the vectored F-15 is shown on top of the vectored F-15 RPV. This wind tunnel model is modified now - see p. 64.



Oren and Morhe with newly proposed F-15 wind tunnel model (left) and our yaw-pitch vectored F-16 model. See Appendix A for details.

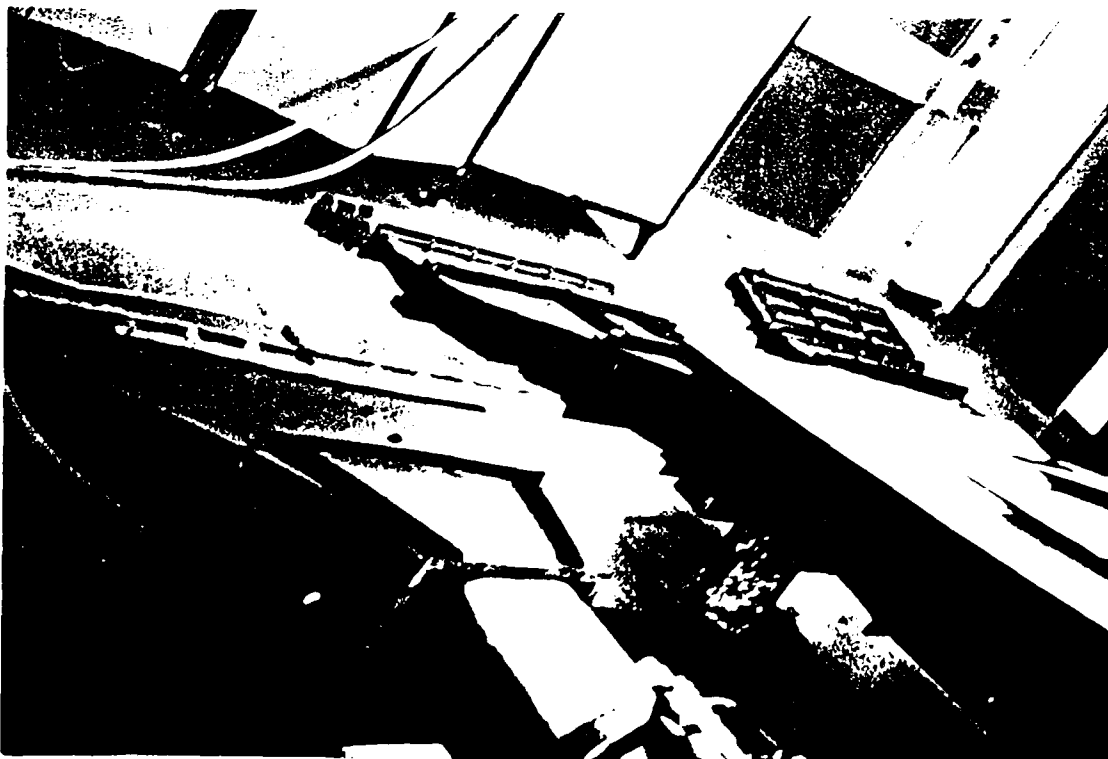


The F-15 inlet, canard and canard wing. See Appendix B for details. (Left) F-15 and (right) F-16.



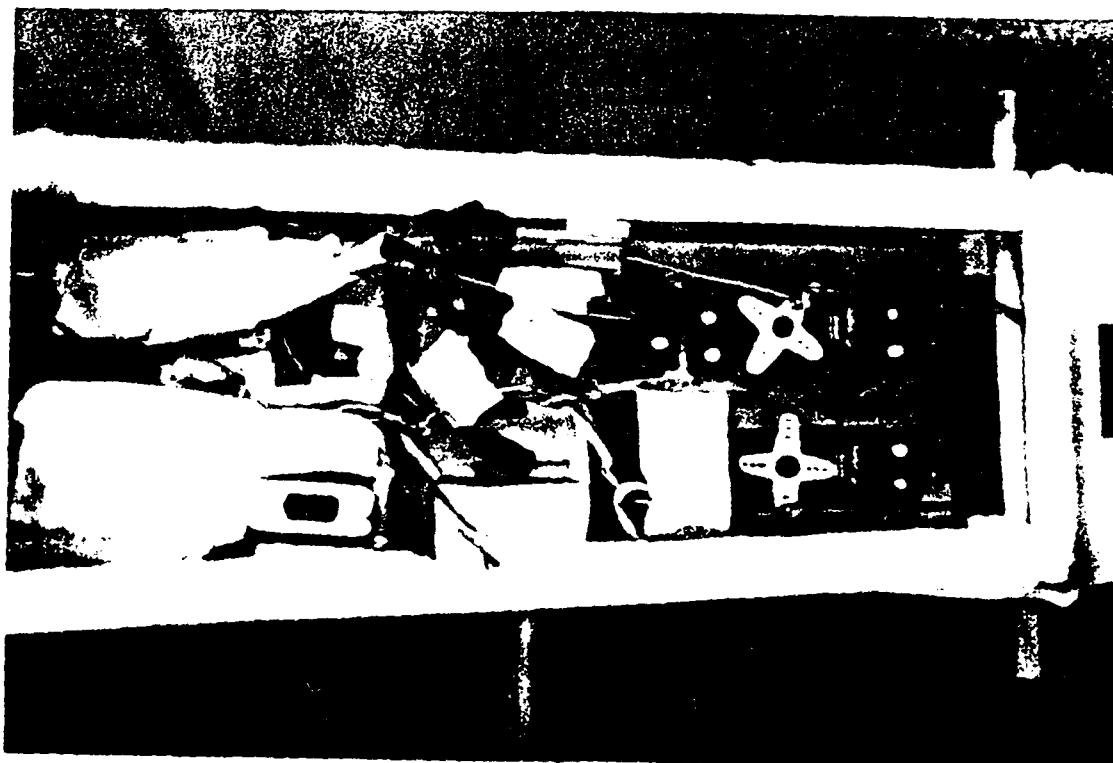
New, high-output ratio
inlets and engines are
under test in the
engine-altitude test
facility.

Highly efficient, low
split, roller-coated
vertical nozzle with
internal Al₂O₃ lining
KSR-16 engine is currently

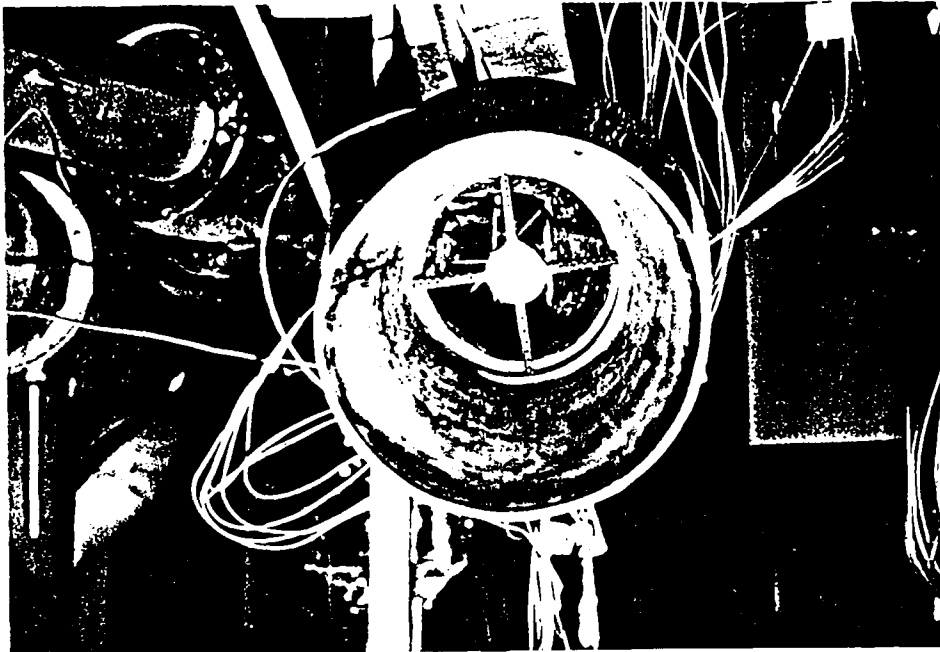




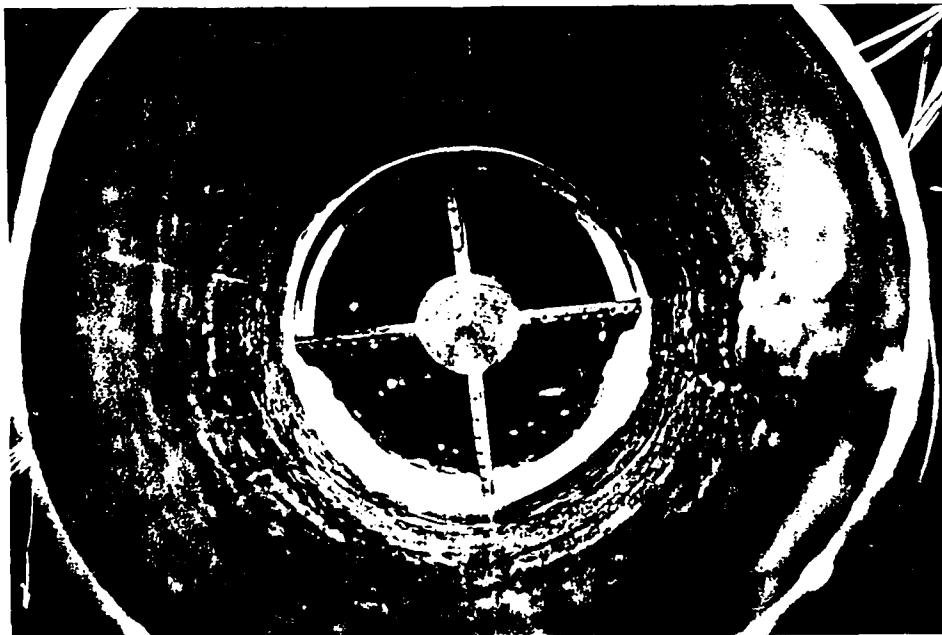
The Pure Vectored Aircraft (PVA) No. 1 shown here was first tested in May 1967. It has no rudders, no ailerons, no elevators, and no flaps. Its wing-tilt model is shown on top. Sitting from left: Lieut. Gen. William Miki, Surgeon, John Aiken.



The 1st generation PVA-1 computer prior to its first calibration flights and operations. It was built by the Air Force Research Office, Dayton, Ohio.



The rotatable pressure probes, at "Stations 2" of the "subscale" F-15 inlet, are used to evaluate Distortion Coefficients (DC) and pressure Recovery (Pr) during PST, and vectorable flight simulations (See Appendix B).

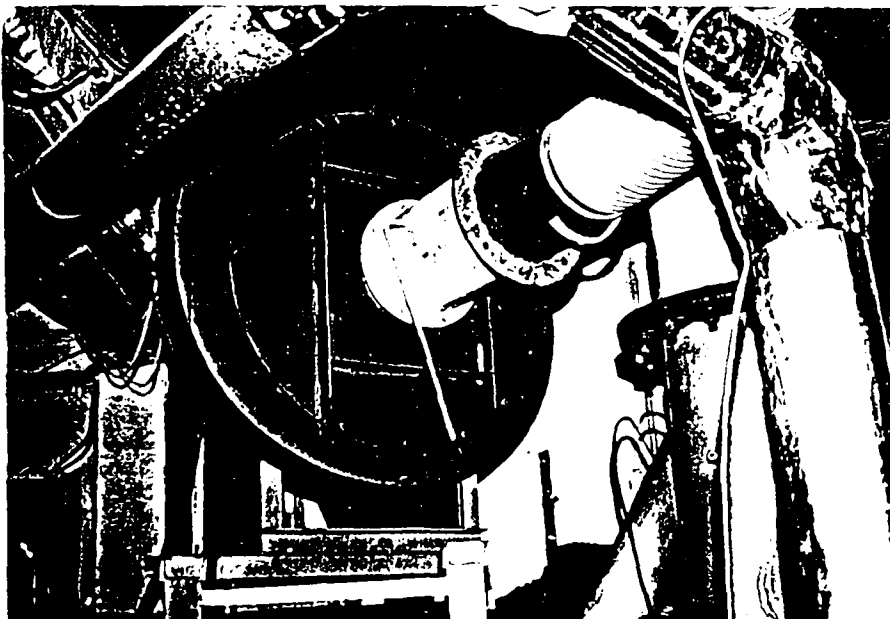


The 28 pressure probes are rotated up to 80 degrees for a "full-coverage" of the cross-sectional area at "engine-compressor-face".

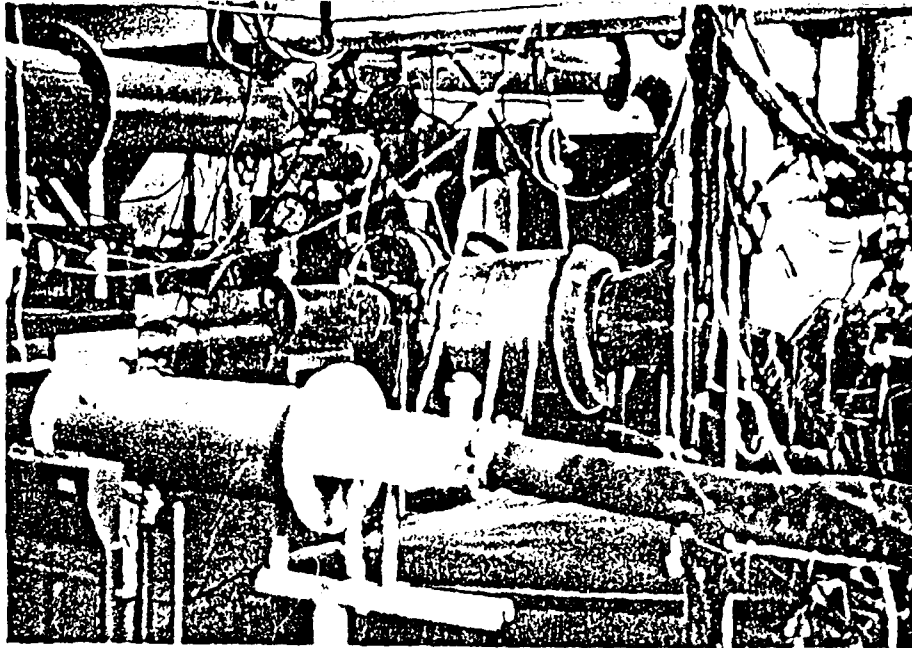


The "blowing fan" of the subscale F-10 inlet test rig.
See notes on pages P1-P1 and in Appendix B.

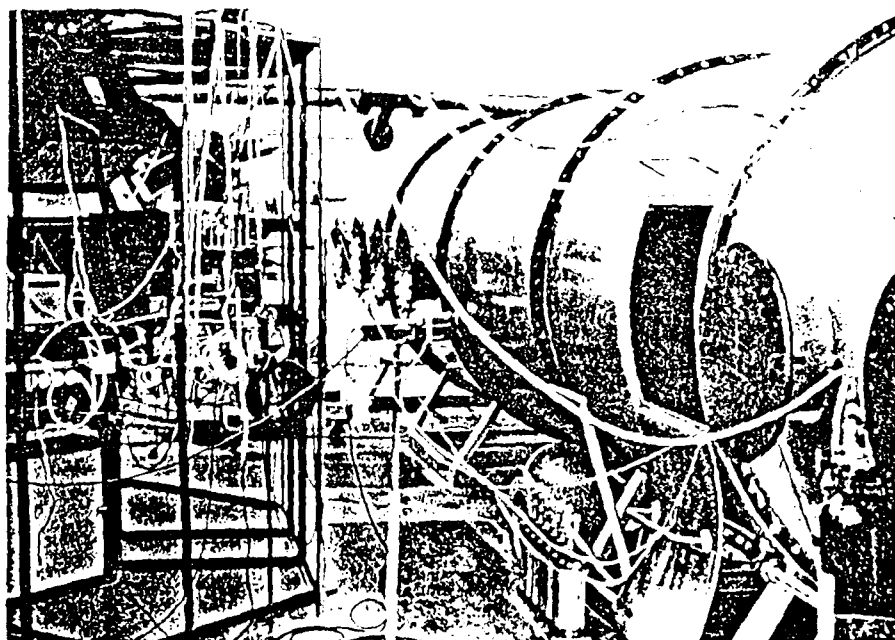
The "Takeoff Baseline Simulation" is obtained with only the
"suction blower" (cf. below) operating.



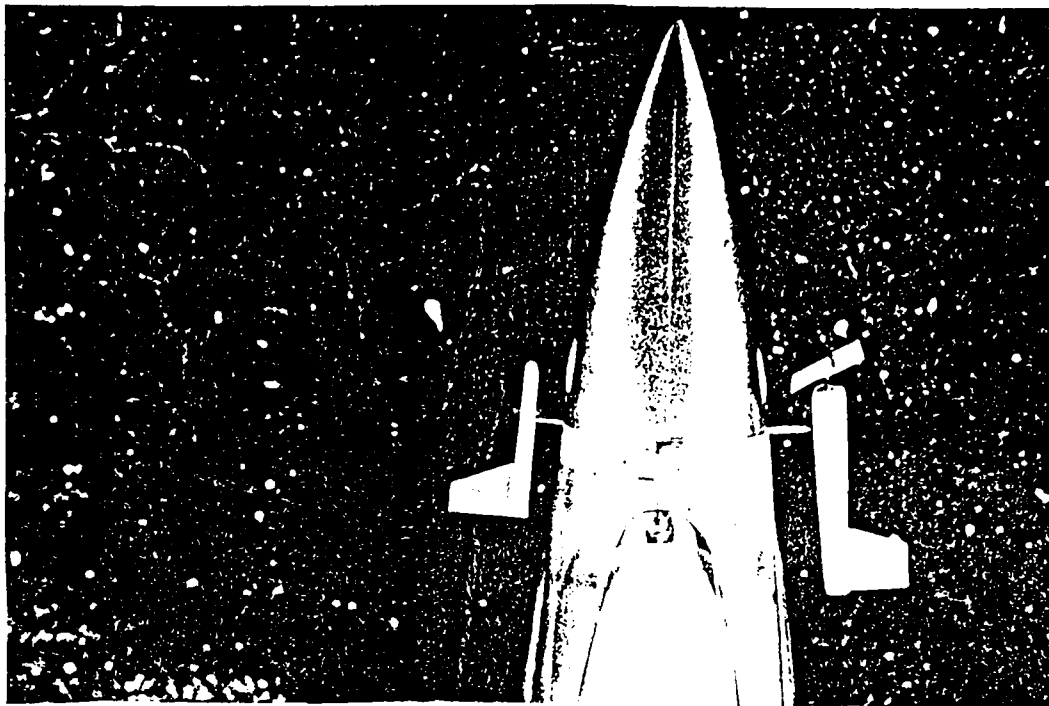
The "blowing fan" of the subscale F-10 inlet test rig is connected
various throttle-throttle positions. In the low Reynolds number conditions
of 10⁵ to 10⁶ conditions up to 10 degrees A. At the start of the simulation
inlet test with this fan simulator take it is well known at various
throttle positions, as marked on the lower part of the rig. $\sim 10^5$ to 10^6 .



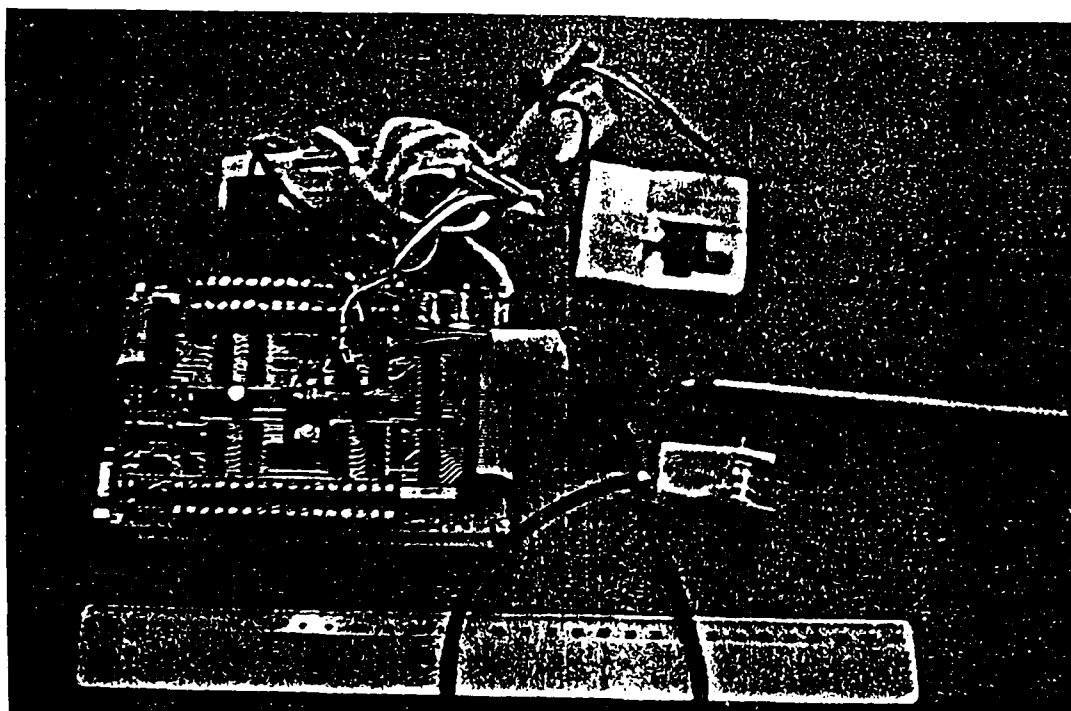
A view of the component-resonance test facility, Program 1, at the University of the Southwest, thrust vectoring nozzle test rig.



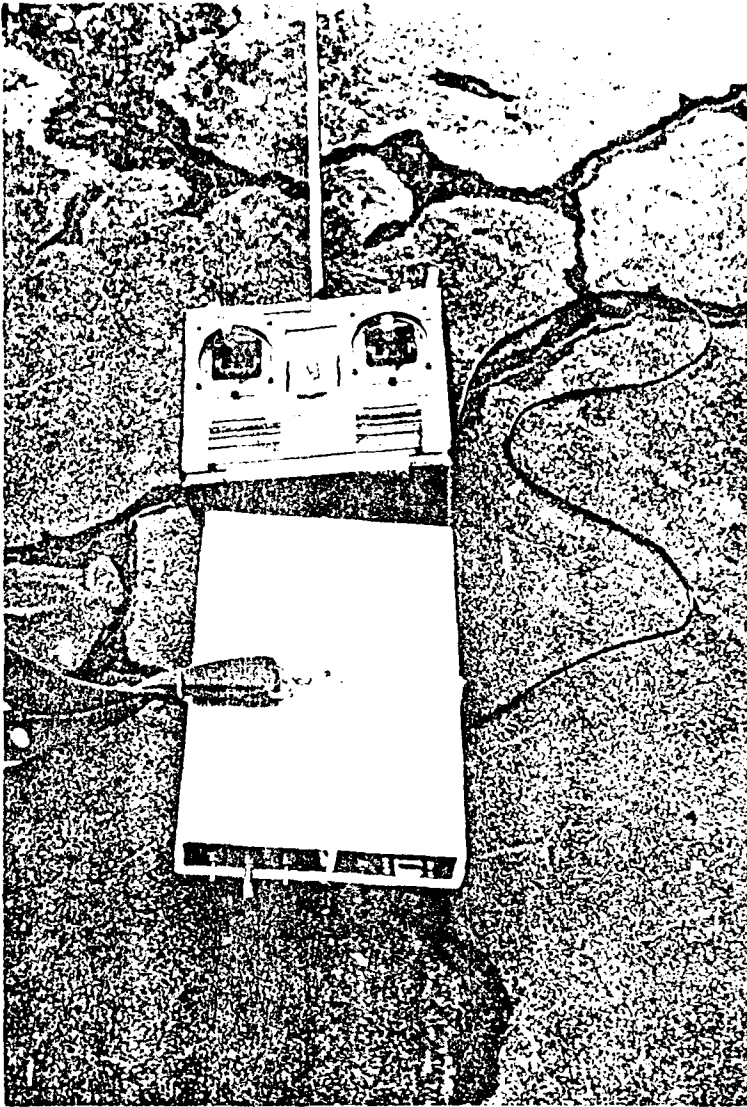
A view of the turbine engine test facility, Program 2, at the University of the Southwest, showing the turbine and compressor sections of the engine mounted on the test rig.



Examples of the modified AoA and improved velocity probes. The first probe is connected to a potentiometer, the second one to an electric motor. Outputs are connected to the computer shown below.



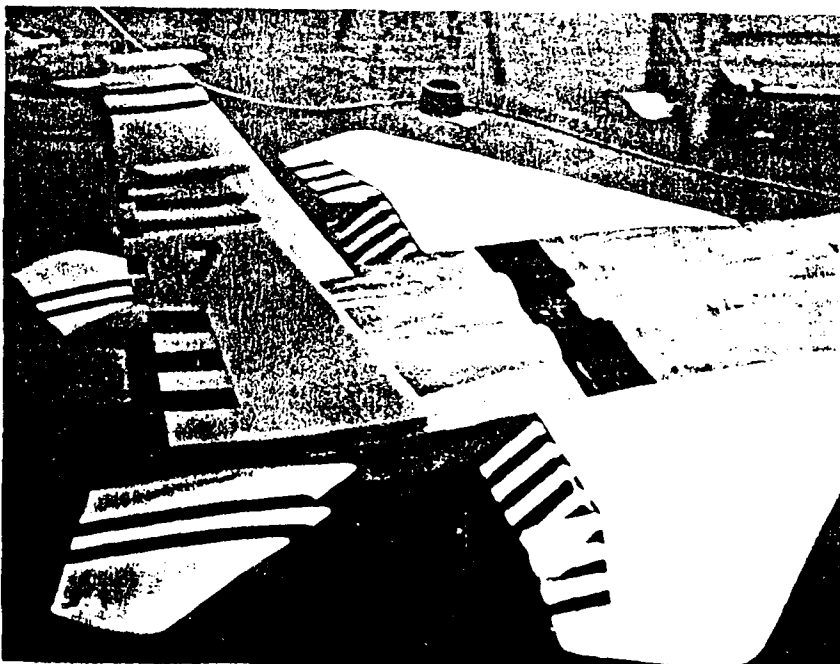
The 1st-generation onboard computer (cf. Fig.2,p. 12). It is switched to "on-off" by PCM command. The 2nd-generation computer is also connected to 6 accelerometers, sampling each channel 75 times per second.



The on-board computer is an absolute minimum, with conventional (main and stick) and vector (short-hand sticks) displays. The system cannot afford any more than a fixed-rate data base, or a vector-based data base, or a vector-based data base. (Data base, data base.)

Both the ground and the on-board computers were designed and manufactured according to specifications represented in the TCM project.

The Mission Management System (MMS) is a computerized system for the TCM project.



The MMS is a computerized system for the TCM project. It is a computerized system for the TCM project. It is a computerized system for the TCM project. It is a computerized system for the TCM project.

The MMS is a computerized system for the TCM project. It is a computerized system for the TCM project. It is a computerized system for the TCM project. It is a computerized system for the TCM project.

APPENDIX A

How can a Yaw-Pitch Vectored F-15 be Upgraded to Become Roll-Yaw-Pitch Vectored,
PST-RaNPAS F-15 Fighter ?

1. The Major Problems:

1.1 The main text, the figures, the pictures, the video cassettes and our previous Progress Reports describe our current efforts with low-AR, yaw-pitch, thrust-vectoring F-15 RPVs.

These efforts have clearly demonstrated the poor performance of roll thrust vectoring during flights.

To improve thrust-vectoring roll agility, one must increase the roll arm from aircraft longitudinal center-line to mid-nozzle, i.e., to increase the nozzles AR.

1.2 The aforementioned improvement may be combined with reduced RCS/IR signatures, provided the following design objectives are met.

2. Design Objectives for Stealth R-Y-P, PST-RaNPAS F-15 :

The new idea is quite simple:

Replace the current horizontal stabilizer/elevators with a high-AR Roll-Yaw-Pitch (R-Y-P) nozzle as shown in the drawings and pictures depicted in this Appendix.

Specific objectives, geometry considerations, etc. are enumerated below.

Much of this preliminary effort has been done by Raphi Berkovitch and Shaul Sapir, 2 Pilots-Engineers who, as students, have worked on these subjects during 2 semesters.

Listed below are their list of specific objectives.

3. Berkovitch and Sapir's Report to Gal-Or

3.1 Performance test of the nozzle with Pitch-Yaw and Roll capability (Subscale and "full-scale").

3.2 Relatively low weight.

3.3 External and internal Aerodynamic shape (horizontal stabilizer) so as to provide low drag (see Fig.3).

- 3.4 No deviation from the elevator's datum line and the fuselage line (Fig.4)
- 3.5 R.P.V. Control capability during no-engine approach (emergency landing) by aerodynamic forces created from the nozzle shape and the Pitch/Roll flaps.
- 3.6 Minimum airflow loss in the nozzle to obtain maximum thrust relative to the axisymmetric nozzle.
- 3.7 The flow cross-section along the nozzle (in the down-stream direction) is decreasing monotonously and its dimensions will be specified below.
- 3.8 Uniform mass flowrate through the exit cross section, i.e. evenly distributed mass flow rate through exit cross-section.
- 3.9 Thrust-roll capability by differential banking of the Pitch/Roll flaps.

4. Considerations for high-aspect-ratio exit-cross-section nozzle

- 4.1 Low "infra-Red" (IR) and RCS signatures as compared with the axisymmetric nozzle, with a similar thrust performance, can be accomplished by the heat dispersal across the nozzle width.
- 4.2 The new nozzle is relatively thin. This provides a reduced aerodynamic drag. The new nozzle also functions as a horizontal stabilizer.
- 4.3 The roll capability, by differential banking, of the Pitch/Roll flaps at the trailing edge (See Fig. 3) is improved.
- 4.4 The roll ability in a conventional airplane is poor at high-angle-of-attack as a result of the wing stall. But here the speed and the angle-of-attack do not have any effect on the roll moment, which exists even at very-low-speed.
- 4.5 The width of the flap gives the nozzle the quality of a horizontal stabilizer (the nozzle is similar to the elevator size. It also gives the possibility of using the flap for thrust vectoring and controlling the airplane during no-engine approach, as two elevators.
- 4.6 By using this kind of flap we discard the conventional elevator/conventional horizontal stabilizer.

5. Additional Geometry Considerations

- 5.1 The R.P.V.'s sizes and data are given in the Figures.
- 5.2 The engine requires Fan's cross-section area whose diameter is $\phi=160$ [mm].
- 5.3 The transition from circular-cross-section (engine's fan) to rectangular cross-section (nozzle inlet), to rectangular cross-section at exit, has been designed and constructed.

- 5.4 The size of the nozzle part which is inside the P.P.V.'s body is limited to the R.P.V.'s volume (Fig. 1, Fig. 4) and current external skin.
- 5.5 The size of the nozzle part which is outside the R.P.V. is similar to that of the elevator/horizontal stabilizer projection (Figs.1,4).
- 5.6 The engine start-up will be carried out through an "entrance duct" in the upper side of the nozzle, by a shaft 90° perpendicular to the Fan's axis.

6. Flow Considerations

- 6.1 The Fan's cross-sectional area A-A is $201 \text{ [cm}^2\text{]}$.
- 6.2 The exit cross-section area F-F, according to the engine producer (to obtain maximum thrust) is $A=113 \text{ [cm}^2\text{]}$.
- 6.3 The flow guiders divide the flow and create homogeneous flow across the nozzle exit cross-section.
- 6.4 The flow diversion is done through circular profiles and not through edge corners.
- 6.5 The nozzle's trailing edge has been constructed by means of a circular/triangle profile.
- 6.6 The cross-section area along the nozzle is decreasing monotonously to minimize flow energy losses inside the nozzle.
- 6.7 The depth of the flap was planned so as to achieve Pitch controllability by aerodynamic forces only in the case of engine shut-down (emergency landing).

7. Structural considerations

- 7.1 The nozzle skin is made of fiberglass coating on thin wood $0.6-0.8 \text{ [mm]}$.
- 7.2 Profiles are made of Balza 6 [mm] with a coating.
- 7.3 The fibre direction in the nozzle part was chosen so as to get maximum strength.
- 7.4 Along the triangle profile we provide an internal backing to avoid cross-section reduction near the trailing edge.
- 7.5 The internal surface of the nozzle is coated to protect the wood from moisture and oil.
- 7.6 The outersurface of the nozzle is coated with fiberglass for sealing and additional strength.

8. Nozzle Performance

8.1 The yaw force is created by 8 rotatable internal vanes located close to the exit cross-section. The vanes are connected to a single drive-control servo.

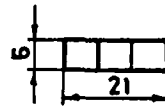
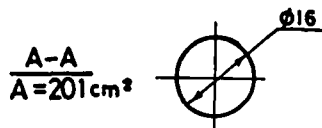
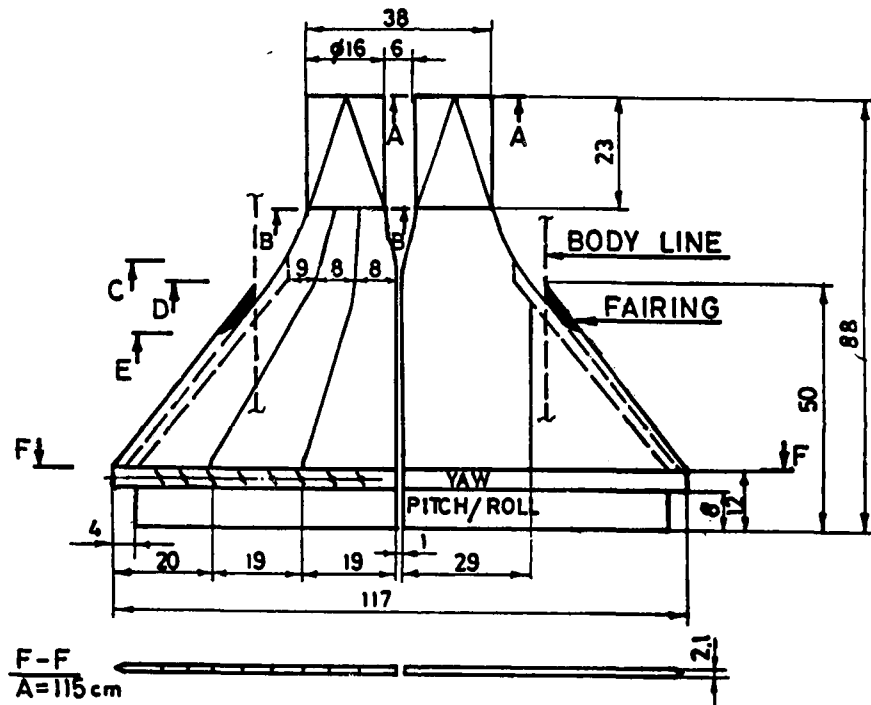
8.2 The pitch force is obtained by rotating the flaps.

8.3 Roll force is generated by opposite rotation of the flaps of the two nozzles.

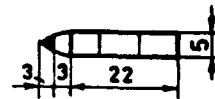
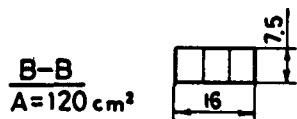
THIS NEW NOZZLE
IS ALSO
PATENTABLE.
USAF INSTRUCTIONS
AS TO PROTECTION OF
THIS PART OF
THE PROJECT BY
PATENTS ARE
REQUIRED.

Fig. A-1 : Proposed F-15 Yaw-Pitch-Roll
Thrust-Vectored 9-foot Model
NOW UNDERGOING LABORATORY TESTS

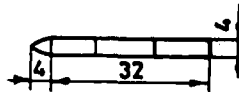
Dimensions - cm



C-C
 A=126 cm²

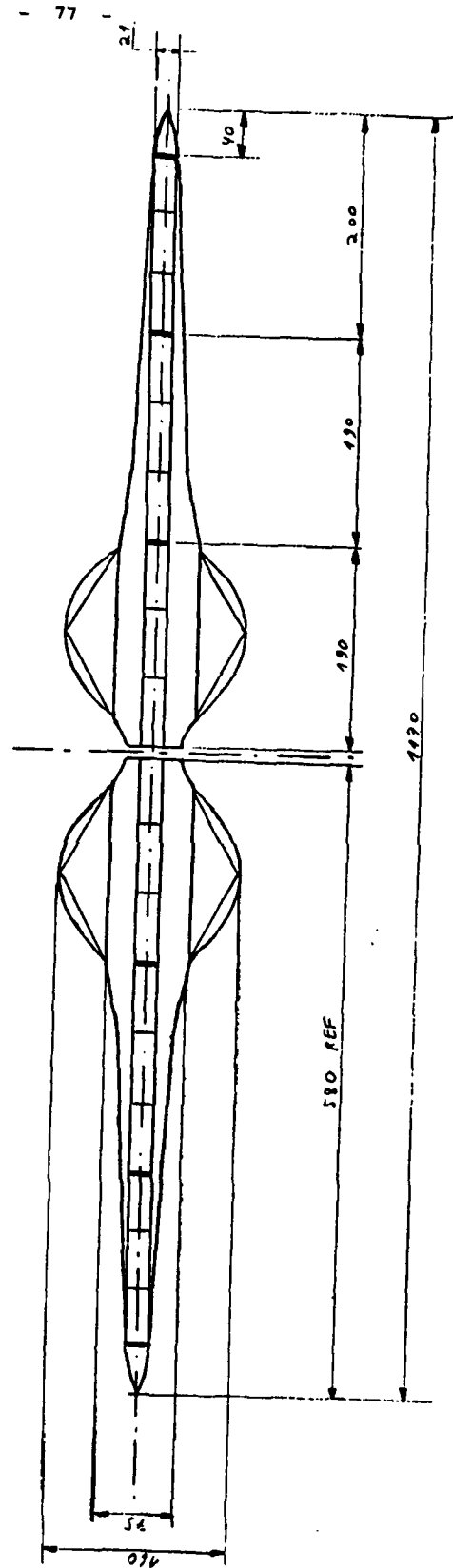


D-D
 A=12 cm²



E-E
 A=136 cm²

Fig. A-3 : Backview of Gal-Or's F-15 Yaw-Pitch-Roll RPV
1st updating Dec. 24, 89. Dimensions are in mm.



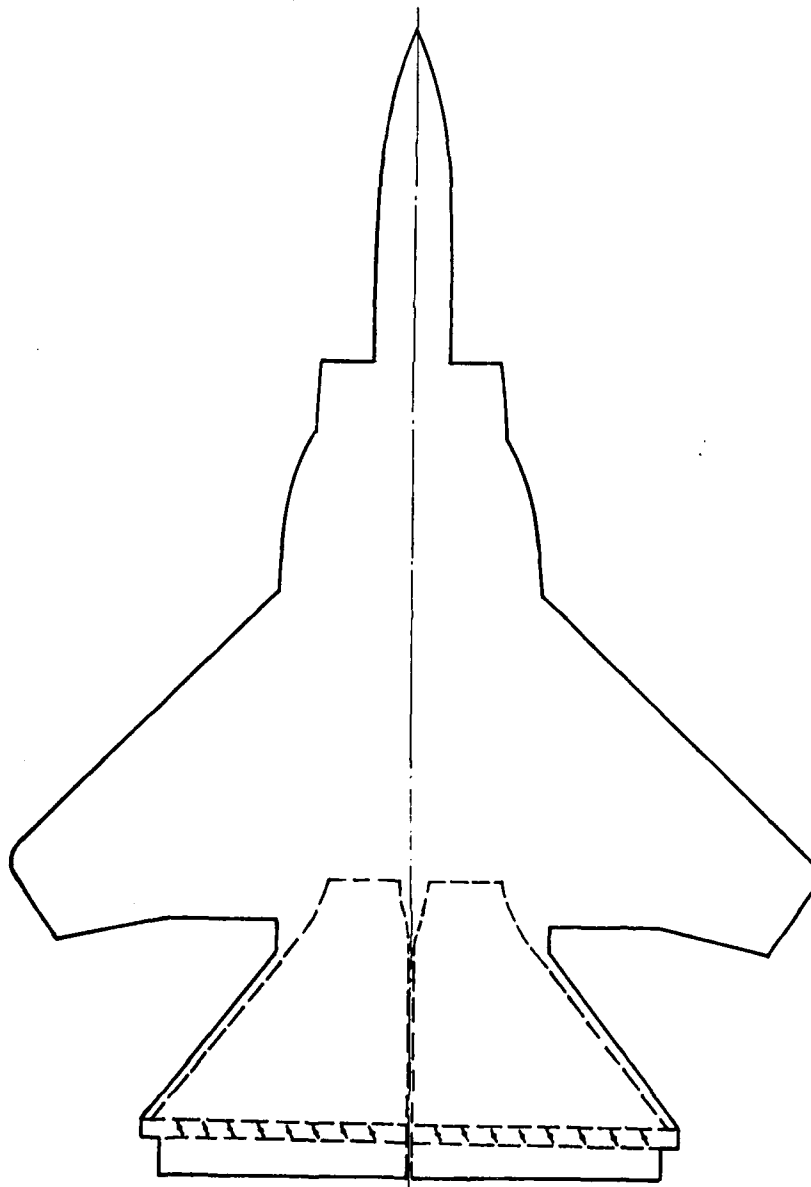
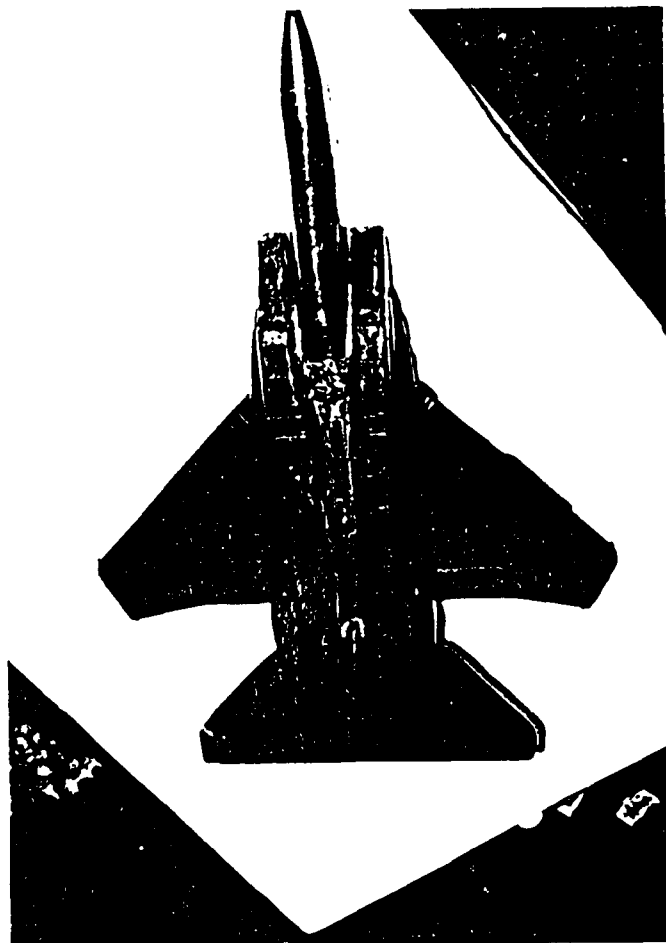
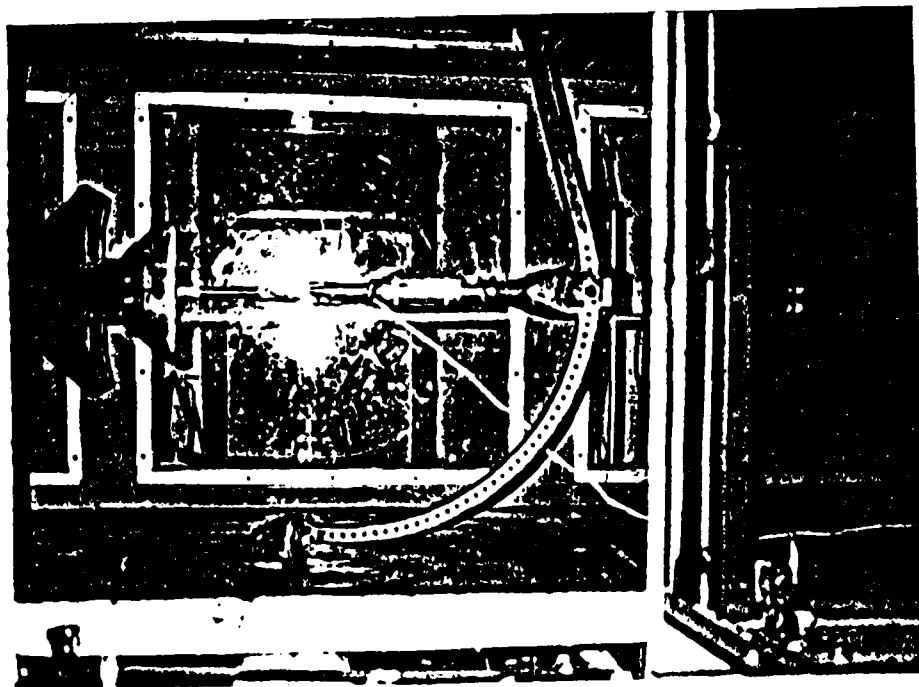


Fig. A-4 : Elevator-less, yaw-pitch-roll F-15 RPV.



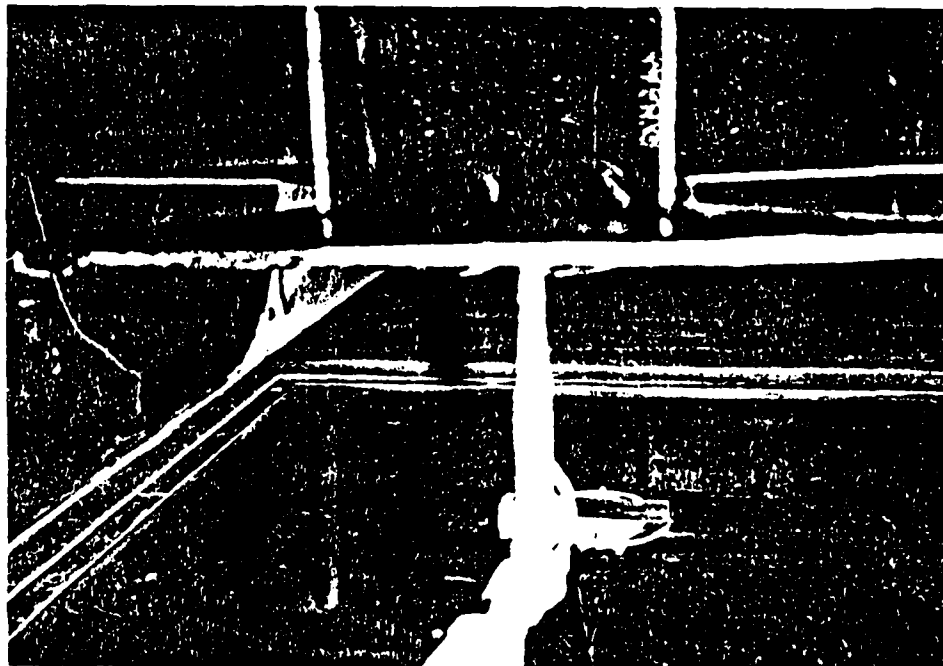
The Roll-Yaw-Pitch Thrust-Vectored F-15 model prior to wind-tunnel tests.



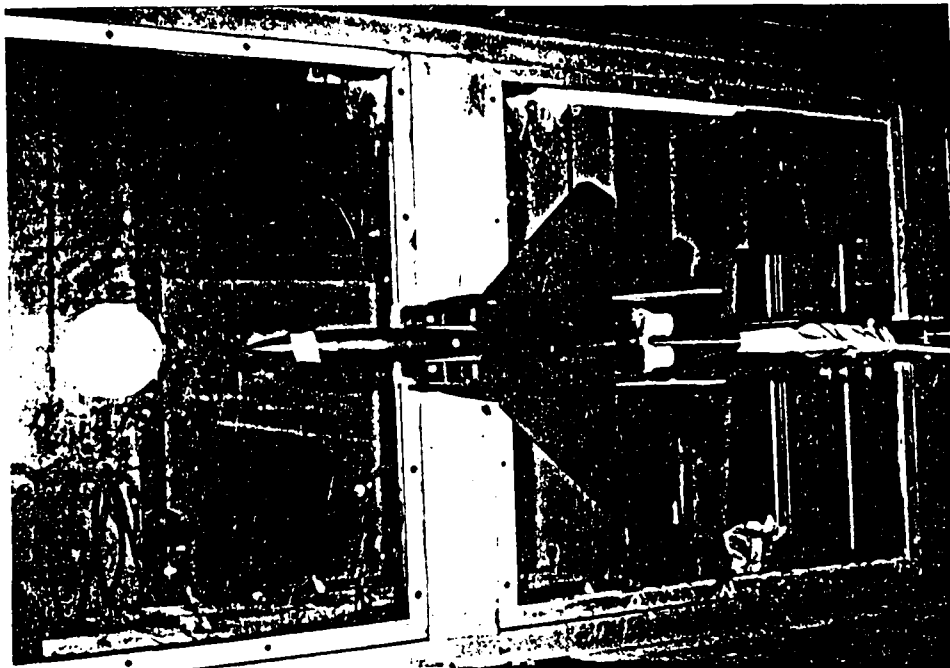
The Roll-Yaw-Pitch Model inside the subsonic wind-tunnel test chamber.



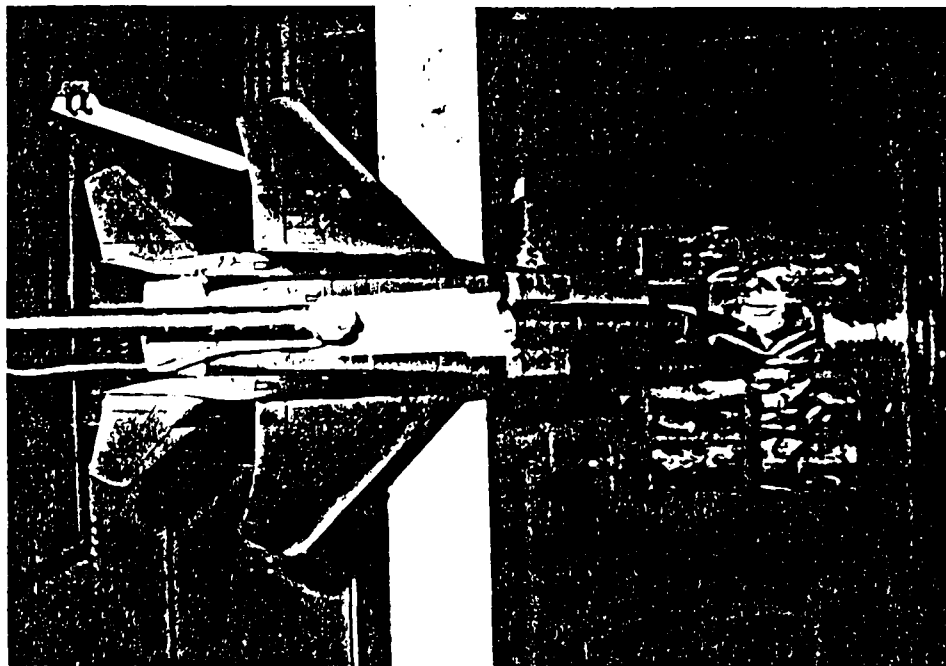
Rami Aristoraz and Yoav Oren with the Roll-Yaw-Pitch Thrust-Vectored F-15 model.



Side view of the R-Y-P model inside the wind tunnel. Note the change from circular engine cross-section ^{to} high-aspect-ratio rectangular.

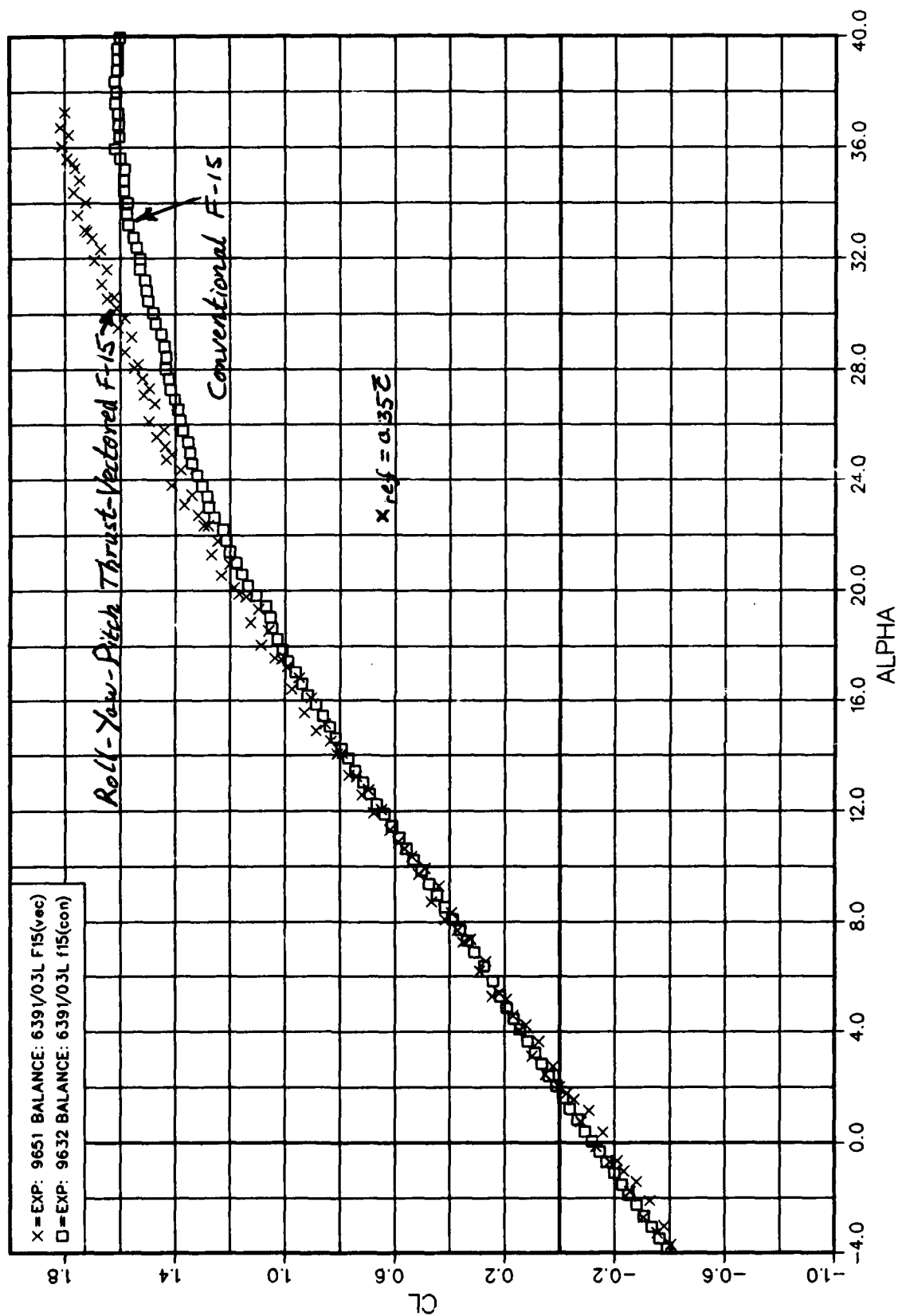


The conventional F-15 model inside the subsonic wind tunnel test chamber.



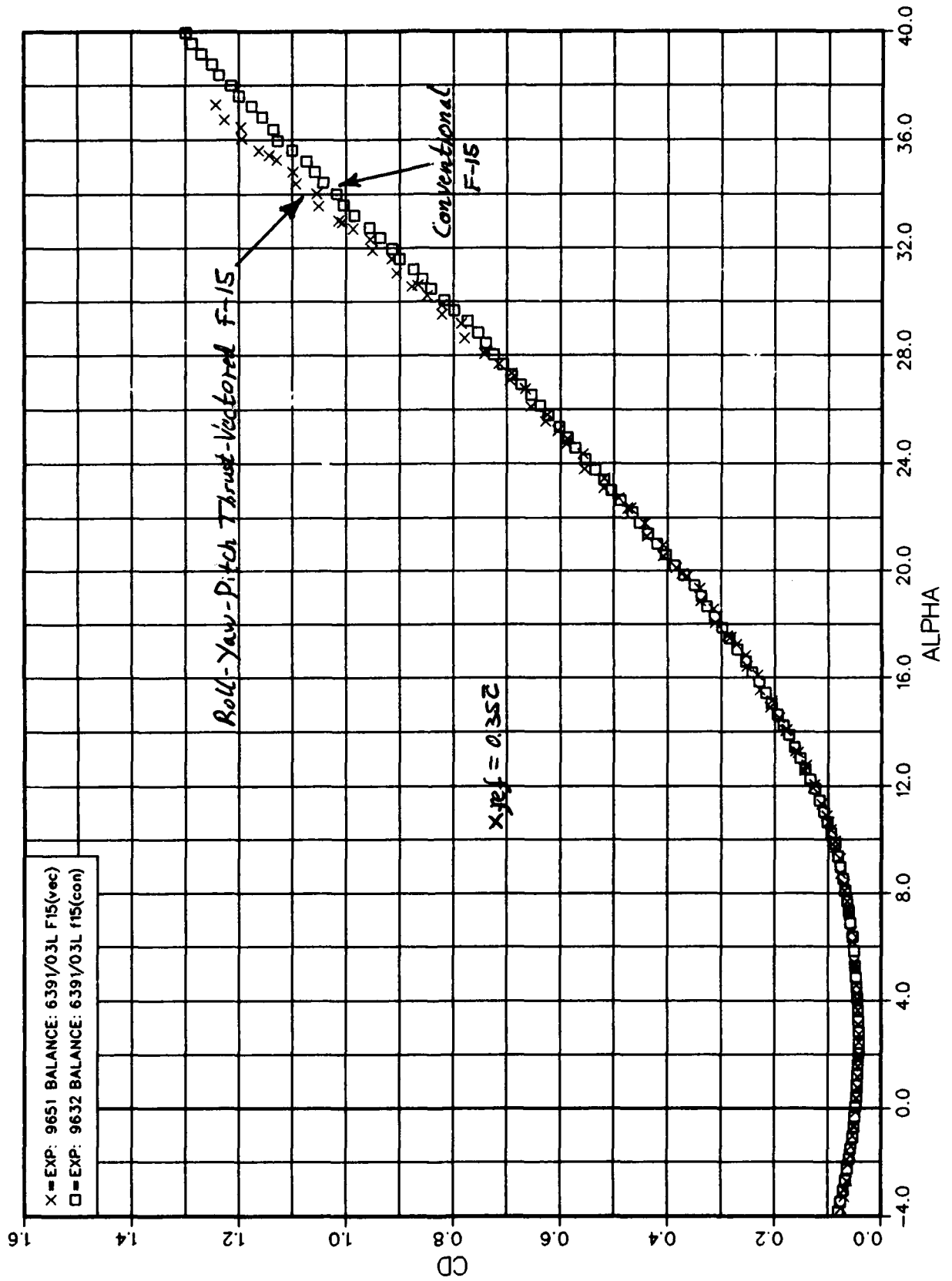
Technion, Wind Tunnel Laboratory

$x_{ref} = 35\% \bar{c}$



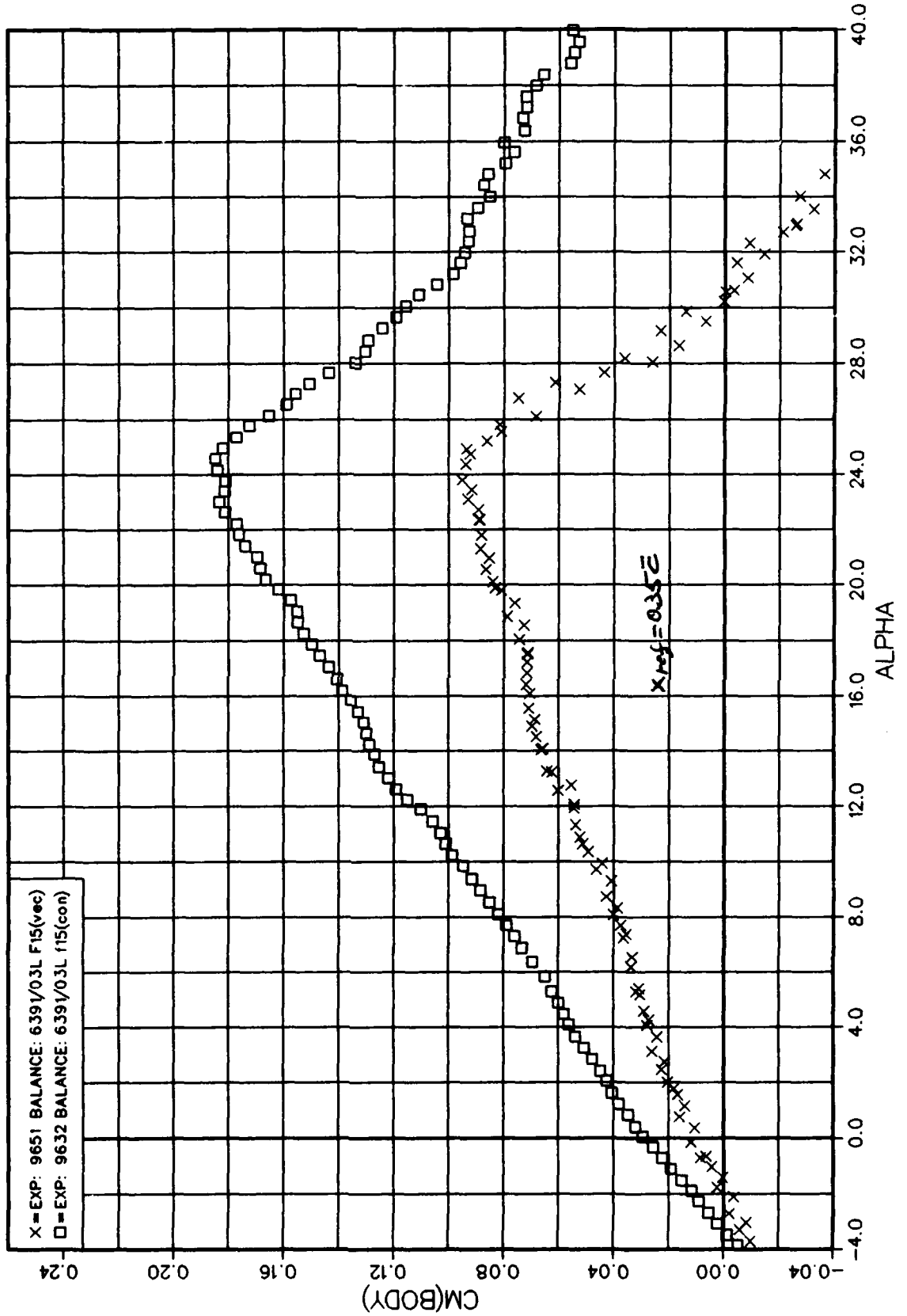
Technion, Wind Tunnel Laboratory

$X_{ref} = 35\% \bar{c}$

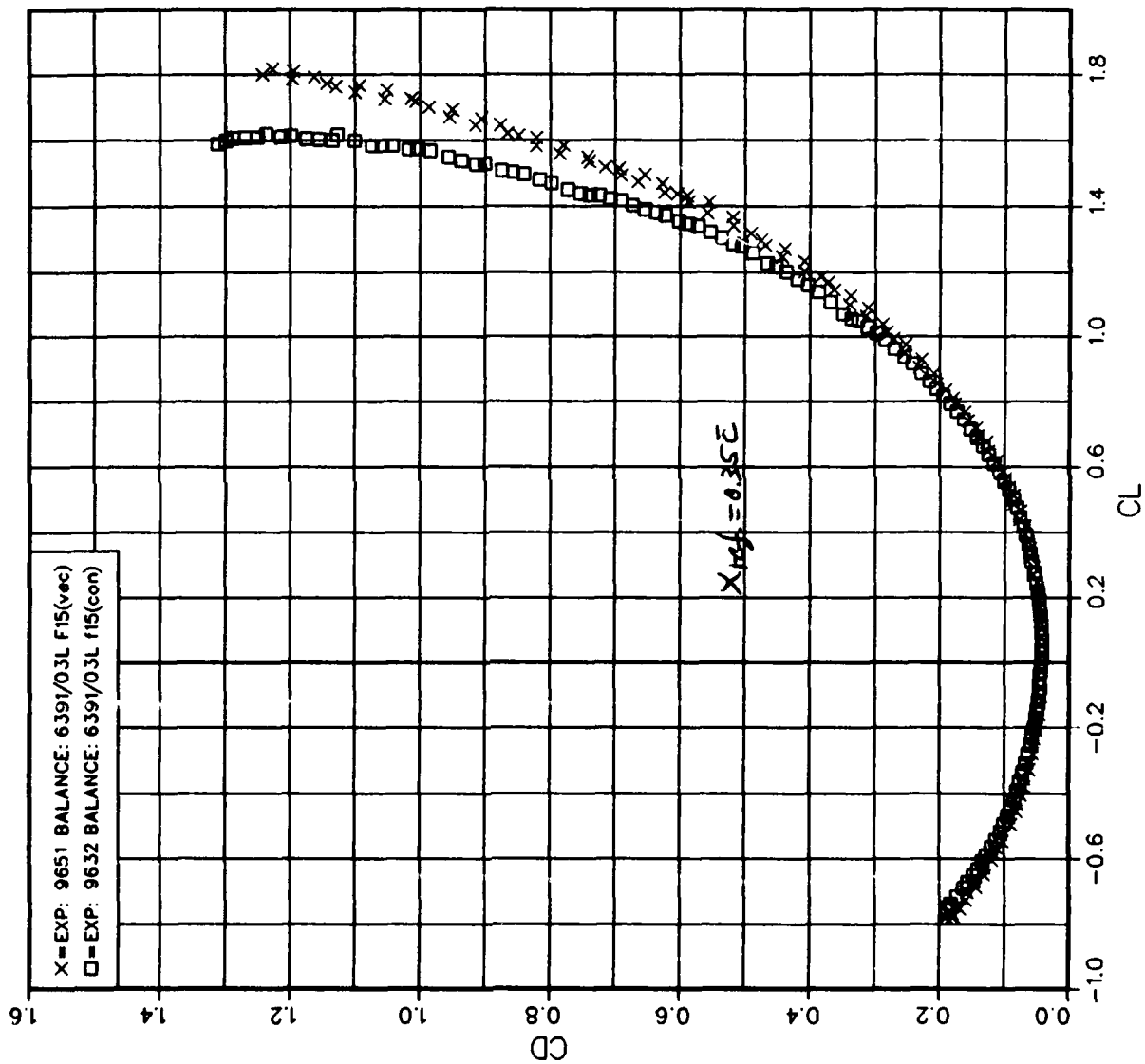


Technion, Wind Tunnel Laboratory

$x_{ref} = 35\% \bar{c}$



$X_{ref} = 35\% \bar{C}$



The next figures (1a, 1b and 1c) present the typical streamlines for subsonic and supersonic inlets, assuming the reader is familiar with the fundamentals of flow in inlets. The figures are shown mainly as a matter of establishing the terminology to be used later during this research project.

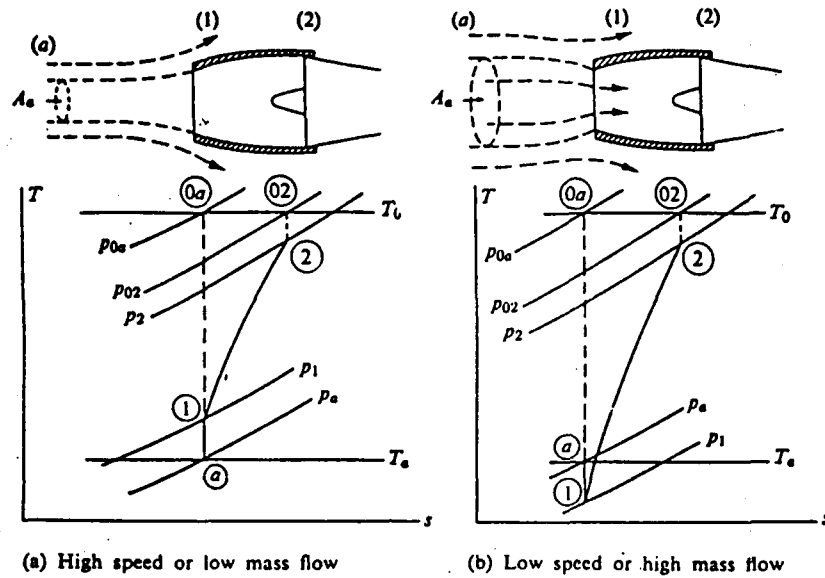


Fig. 1a - Typical streamline patterns for subsonic inlets.

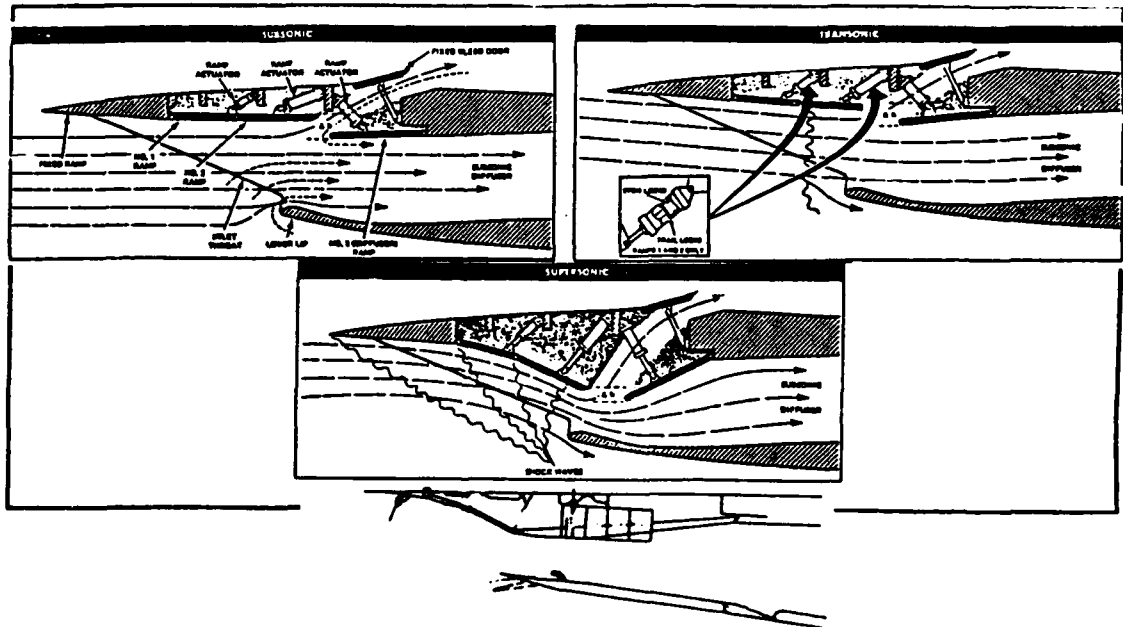
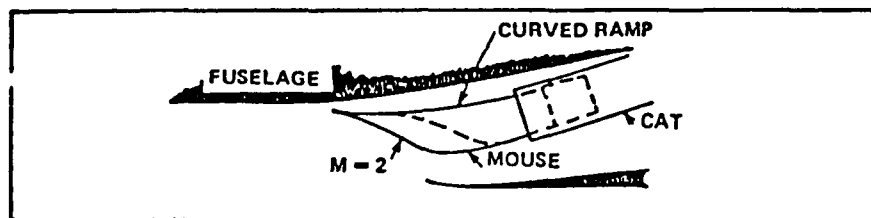
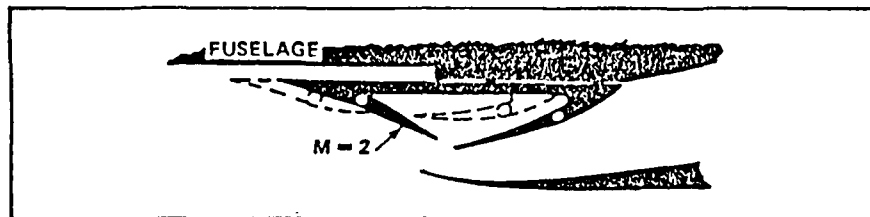


Fig. 1b

An example of conventional technology, variable-geometry inlets. Such inlets must be modified and redesigned for PSI. (Depicted are the F-14 and the B-1 engine inlets). Note the rotatable vanes at the lower wall of the B-1 inlet, and at inlet lips.

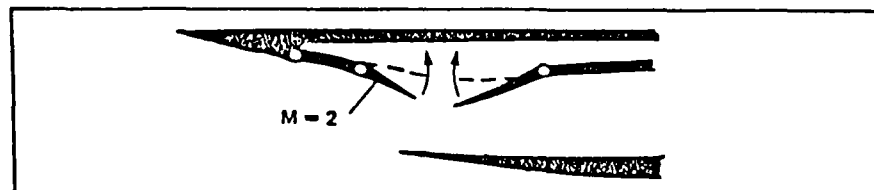


1/2 AXISYMMETRIC (MIRAGE)

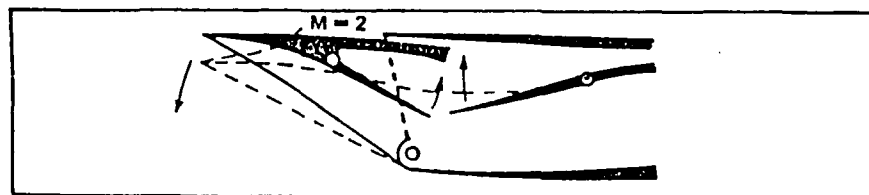


1/4 AXISYMMETRIC (F111)

- Variable geometry examples. Axisymmetric type.



FIXED FIRST WEDGE



ROTATING FORWARD INTAKE

Fig. 1c

The definitions of inlet states are given below by eq. 1, where η_{TA} is the isentropic efficiency and the subscript 0 refers to stagnation conditions, P_r to pressure recovery, M_r by eq. 1 and Fig. 2.

$$\eta_{TA} = \left(\frac{P_{02}}{P_a} \right)^{\frac{(\gamma-1)/\gamma}{(\gamma-1)/2} M^2}$$

Eq. 1

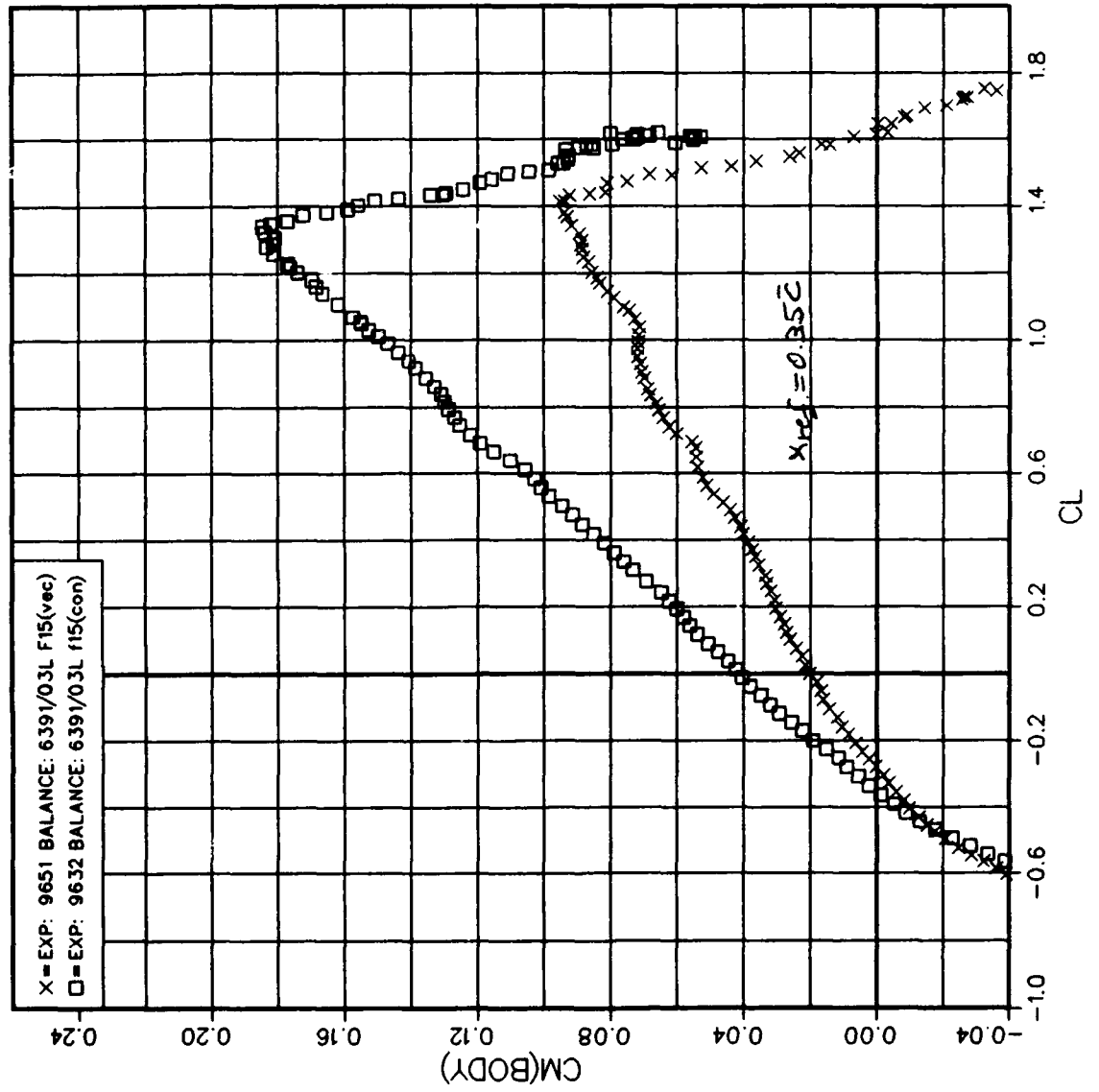
$$M_r = A_0/A_e$$

Eq. 2

Fig. 3 shows P_r as a function of M_r .

Technion, Wind Tunnel Laboratory

$x_{ref} = 35\% \bar{c}$



APPENDIX 8 Part 1 :

INTRODUCTION TO HIGH ANGLE-OF-ATTACK INLETS

INTRODUCTION

The aim of this introduction is to present the general background on high AoA inlets, their internal structure, and the problems they present to the designer of thrust-vectorred, post stall fighters.

The first figure presents the problems encountered with inlet/engine integration.

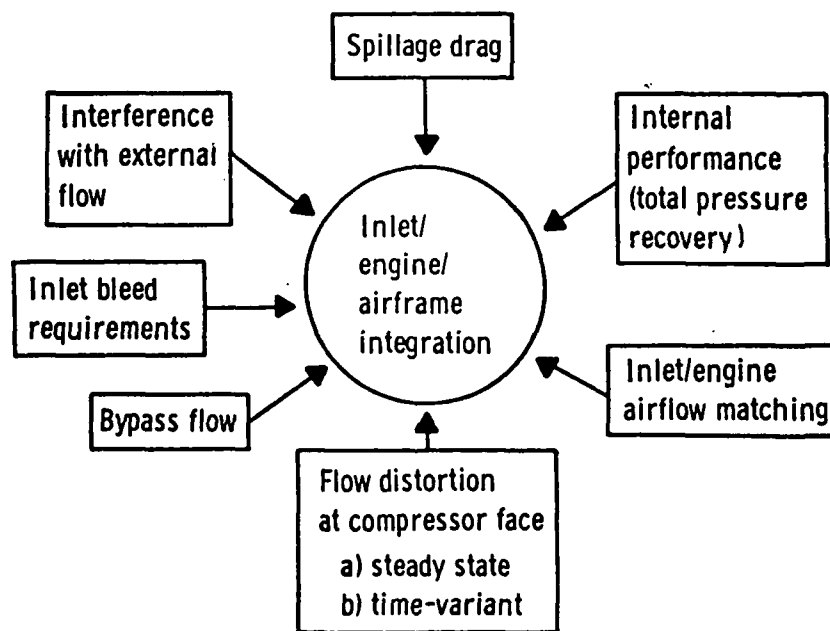


Fig. 1 - Problems encountered with inlet/ engine integration

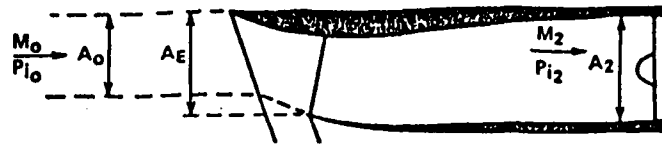


Fig. 2

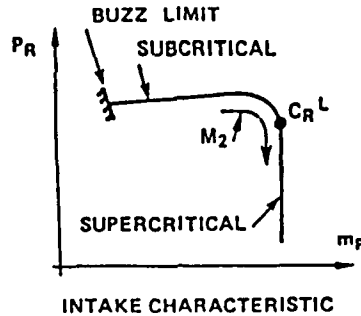


Fig. 3

DISTORTION COEFFICIENT

This is one of the most important parameters to be evaluated in these studies. It has a number of definitions; eq. 3 (British mainly), where the number refers to the sector degrees in station 2.

P_{i2min} is the minimal value of the pressure at station 2, while P_{i2avr} is the average value of the pressure over the entire cross section of the inlet in station 2. q_{2avr} is the value of the dynamic pressure in that station.

Typical values of DC60 are shown in Fig. 4

The measurement of all distortion coefficients is being done by a standard device as shown in Fig. 5.

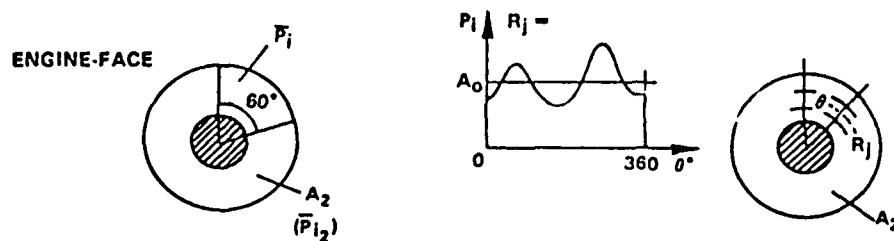


Fig. 4

Engine face flow distortion index.

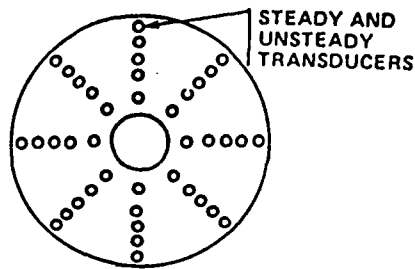


Fig. 5

$$DC60 = ((P_{i2min})_{60^\circ} - P_{i2avr}) / q_{2avr} \quad \text{Eq. 3}$$

RADIAL DISTORTION COEFFICIENT

This is defined by eq. 4.

$$K_{ra} = (\sum (P_{i2avr} - P_j) * 1/R_j) / (q_{2avr} * \sum 1/R_j) \quad \text{Eq. 4}$$

OTHER DEFINITIONS OF THE GENERAL DISTORTION COEFFICIENT

Eqs. 5 and 6 are alternative definitions where A_j is the distortion coefficient in a ring of radius R_j .

Eq. 7 provides another alternative where SA is a coefficient related to a specific engine.

$$K_{\theta} = (\sum A_j * W_j / R_j) / (q_{2avr} * \sum W_j / R_j) \quad \text{Eq. 5}$$

$$K_a = K_{\theta} + K_{ra} \quad \text{Eq. 6}$$

$$IDC_j = (P_{ijavr} - (p_{imin})_j) / P_{t2avr} * SA \quad \text{Eq. 7}$$

THE DISTORTION COEFFICIENT EMPLOYED IN THESE STUDIES

This coefficient is defined by eq. 8, where

P_{t2max} is the maximum pressure for the entire cross-sectional area in station 2.

P_{t2min} is the minimal pressure for the entire cross-sectional area in station 2.

P_{t2avr} is the average pressure in the same cross-sectional area.

$$DC = K_d = (P_{tmax} - P_{tmin}) / P_{tavr} \quad \text{Eq. 8}$$

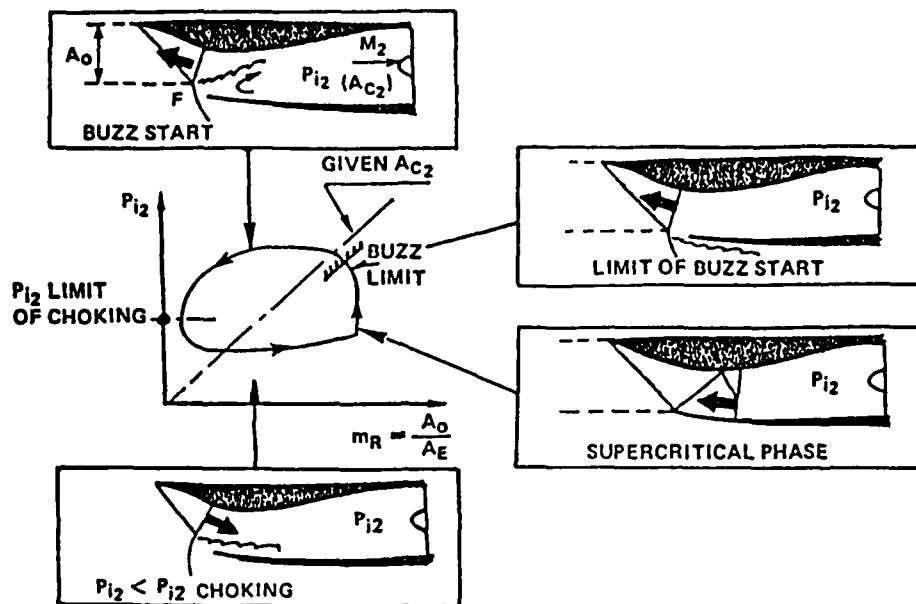


Fig. 6 - Buzz cycle

INLET PRESSURE RECOVERY - Pr

This parameter (the ratio between the total average pressure at inlet *upstream*, to the average total pressure at compressor inlet [station 2]), is the 2nd most important variable for these studies.

Fig. 7 shows the influence of inlet shape on Pr .

Fig. 8 shows Buzz limit vs. inlet airflow.

Fig. 9 shows the variations of Pr for the F-111E aircraft also as a function of the Mach number.

Fig. 10 is another interesting example which demonstrates the effects of blunt or sharp leading edges.

The length of the inlet is also important, the longer it is the better is the disturbance dumping.

However, other overall design limitations of the aircraft dictate an optimal length.

IDEAL PRESSURE RECOVERY (FRICTIONLESS)

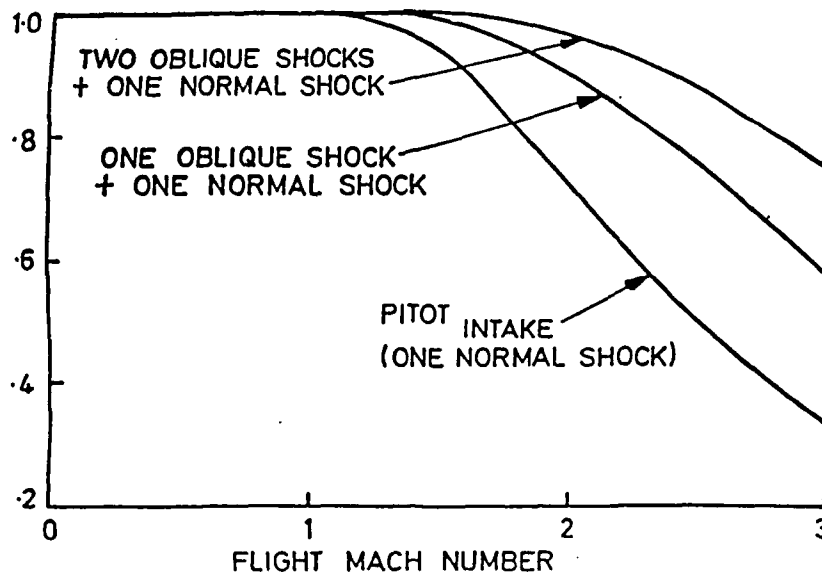


Fig. 7

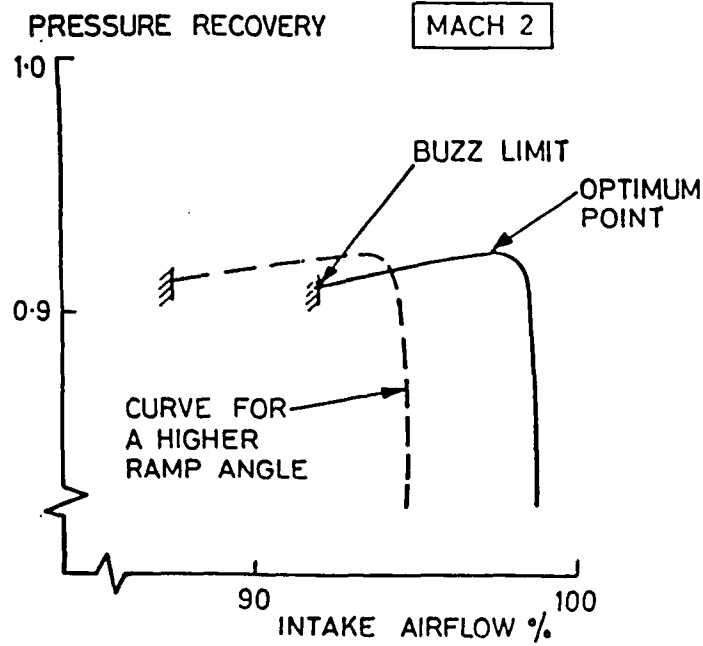


Fig. 8

Performance of a ramp-type supersonic intake

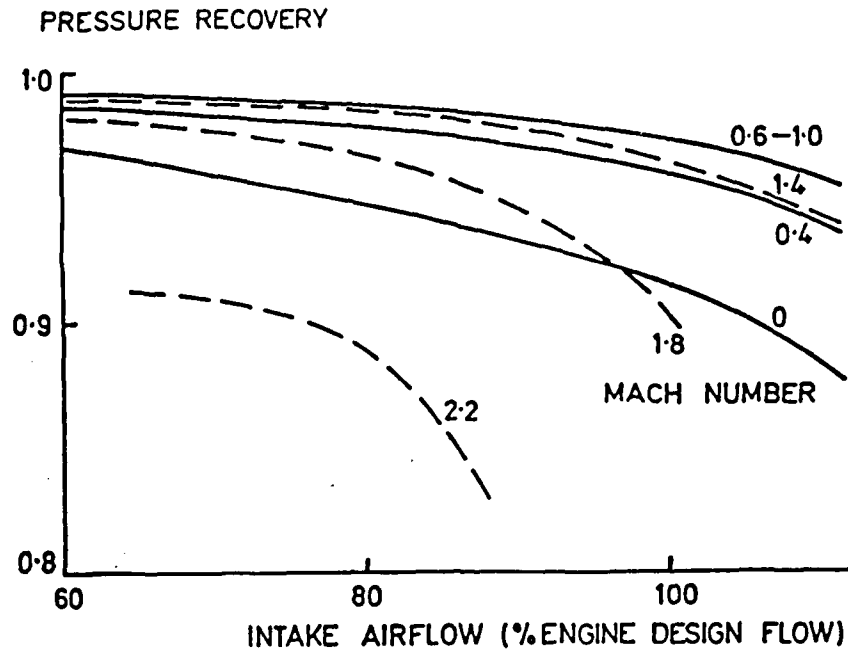


Fig. 9

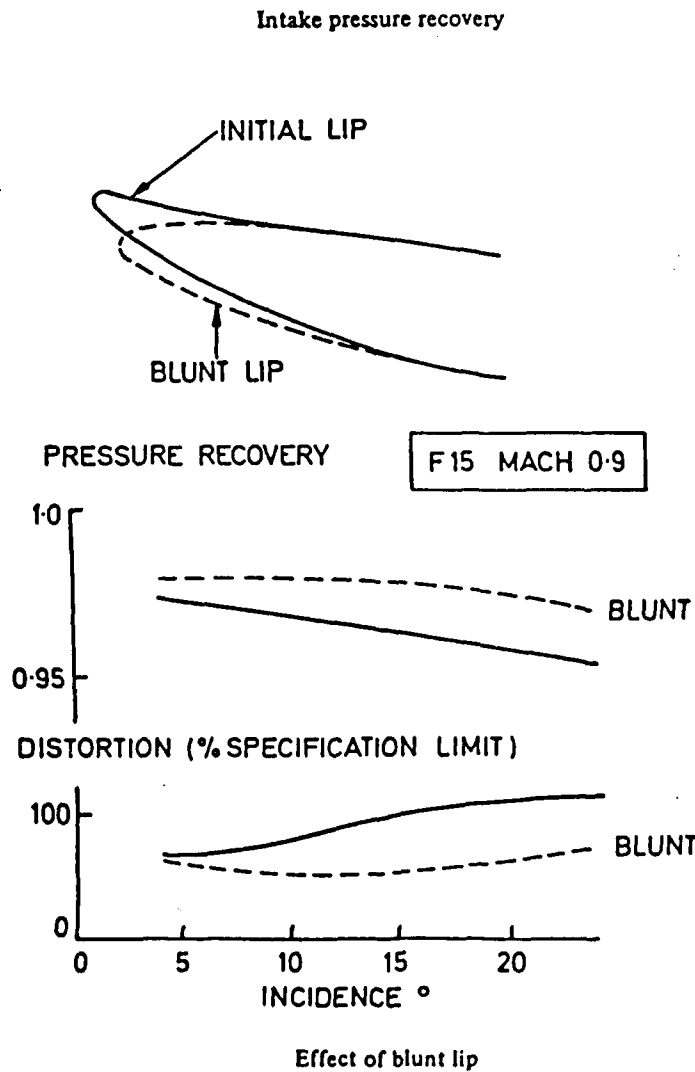


Fig. 10

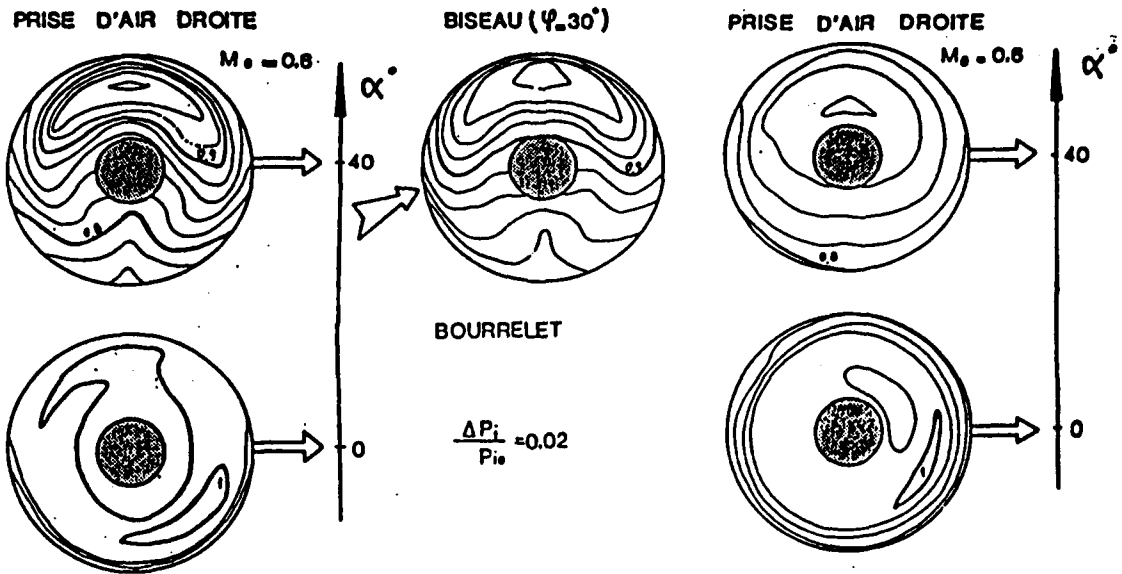
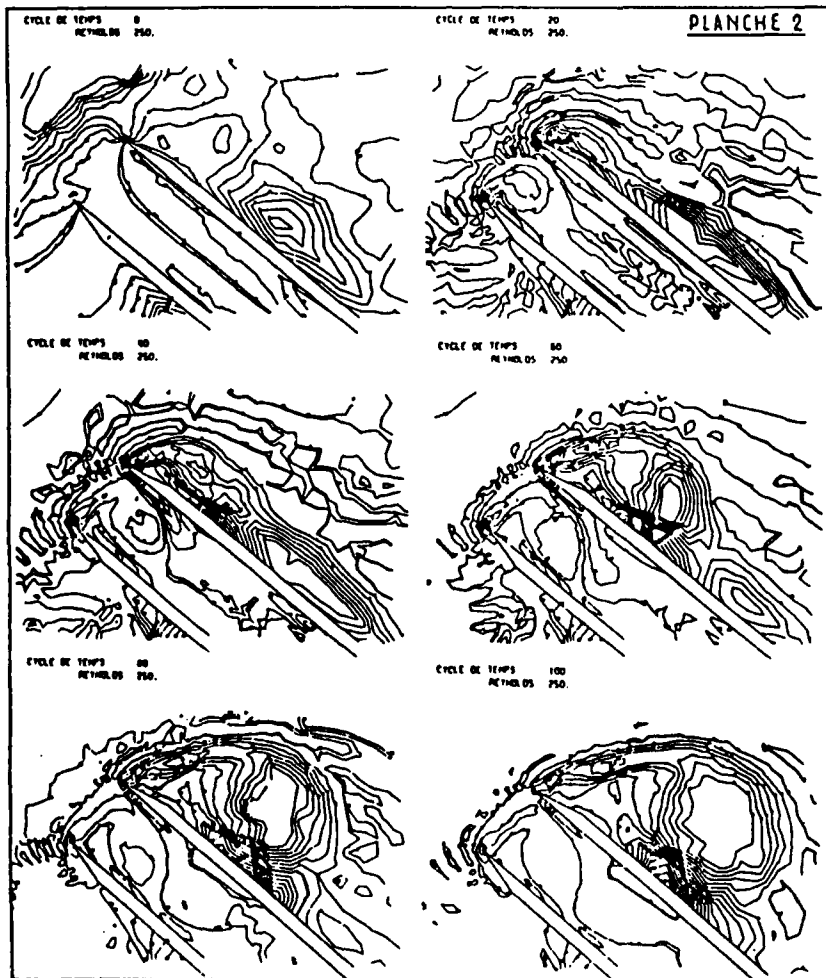
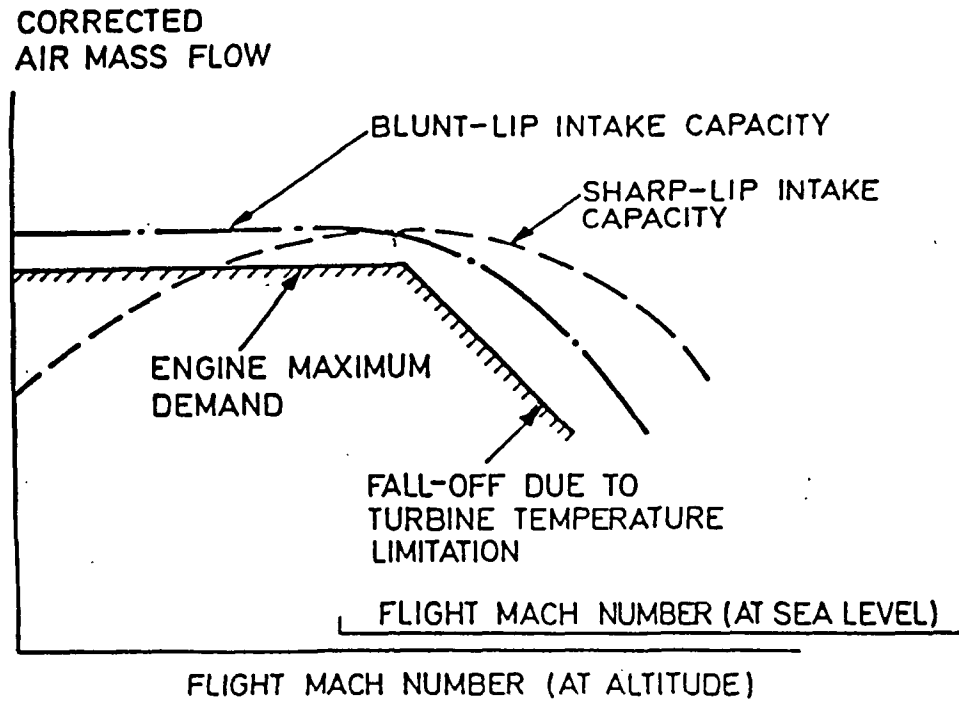


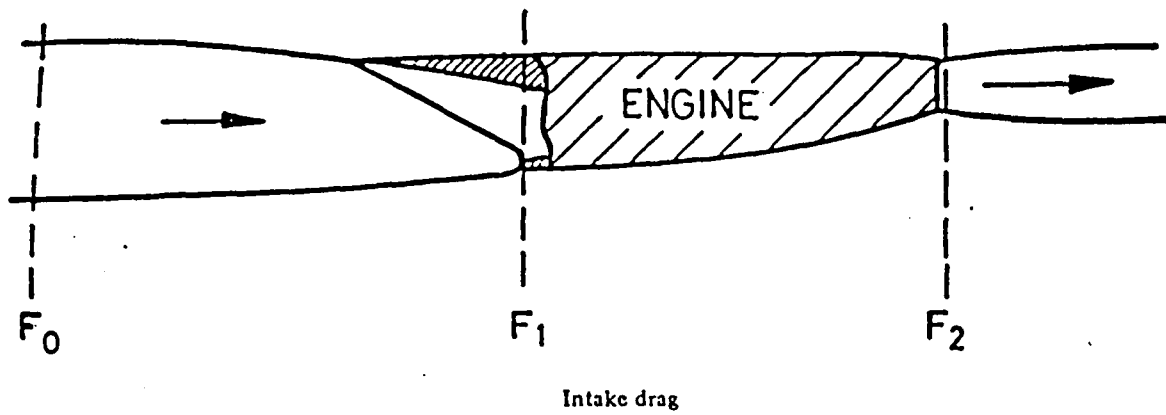
Fig. 9 - Pressions d'arrêt moyennes.
 $M_0 \approx 0.6$ $X/D = 4$

Fig. 10 - Pressions d'arrêt moyennes.
 $M_0 \approx 0.6$ $X/D = 8$

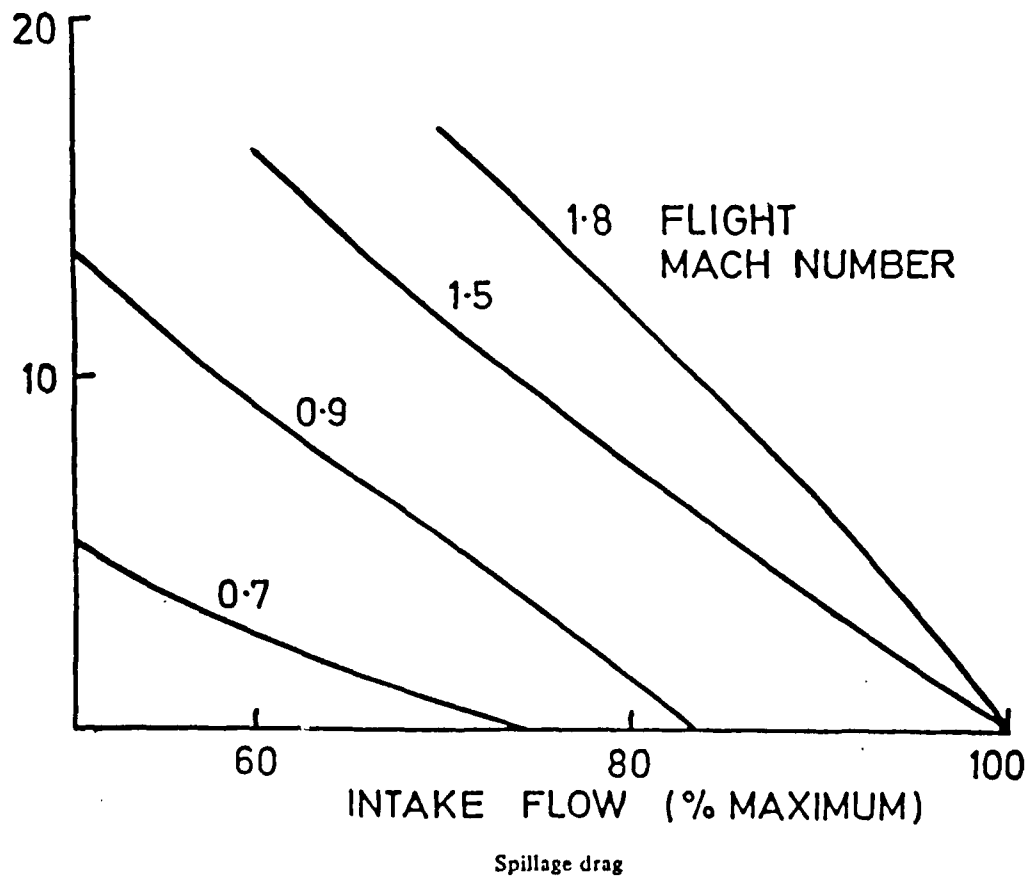


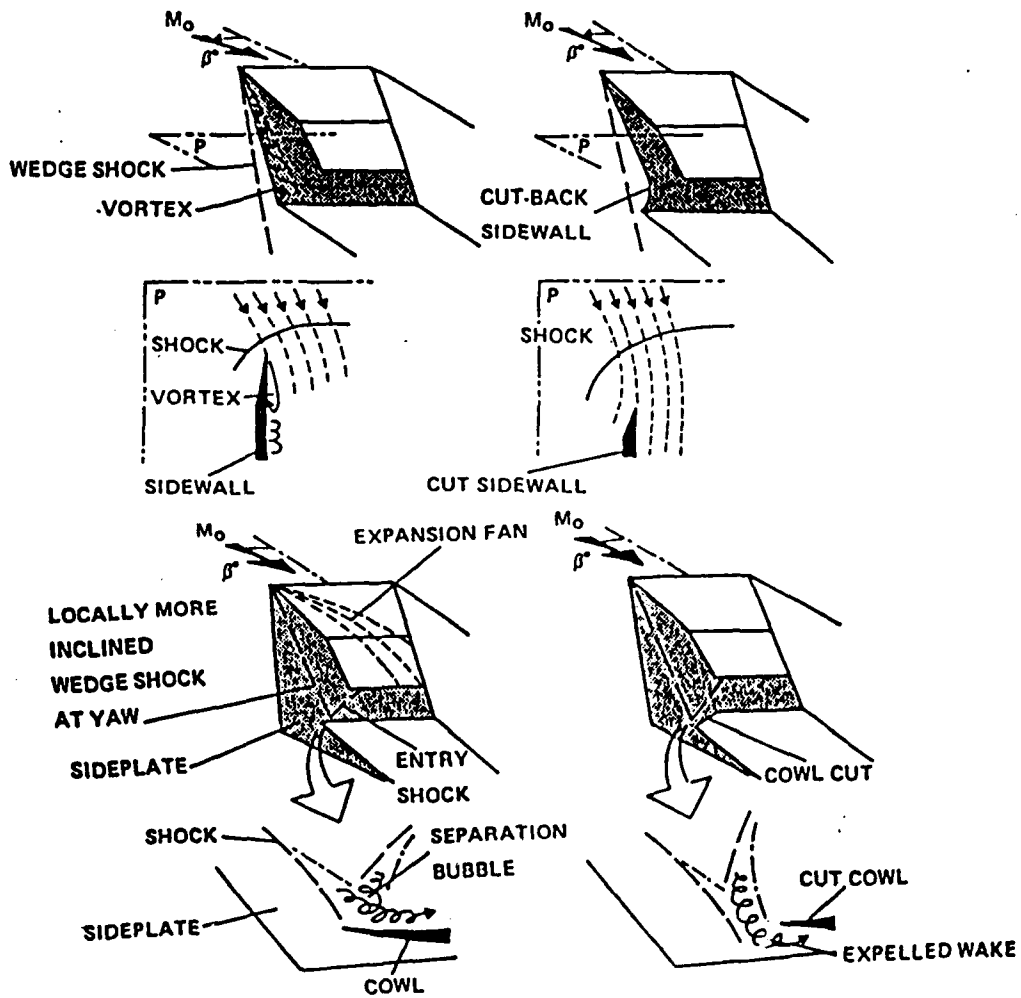


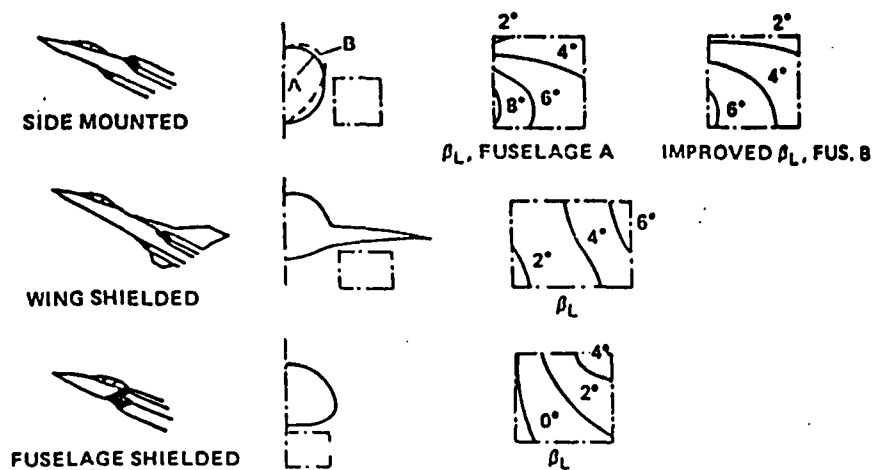
Airflow matching diagram



$\frac{\text{SPILLAGE DRAG}}{\text{TOTAL ZERO-LIFT DRAG}} \%$

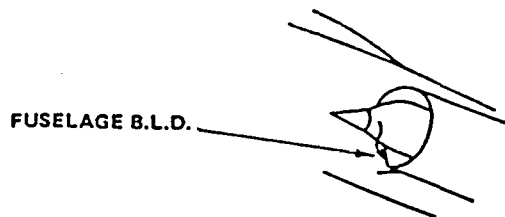






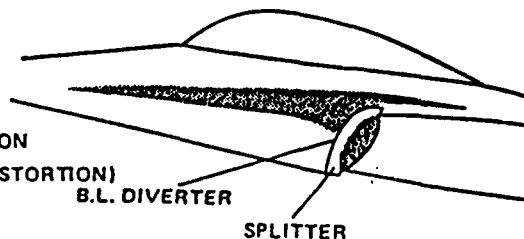
Air intake/airframe integration. [Richay, Surber, Laughrey], Angle of sideslip map at $\alpha = 15^\circ$, $\beta = 0^\circ$, $M_0 = 2.2$

MIRAGE

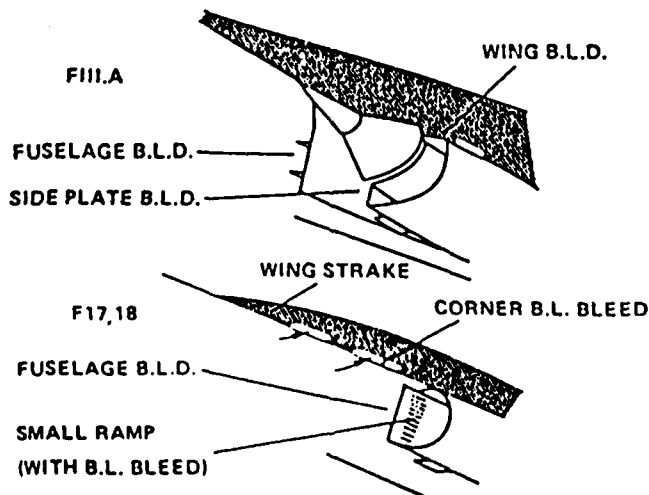


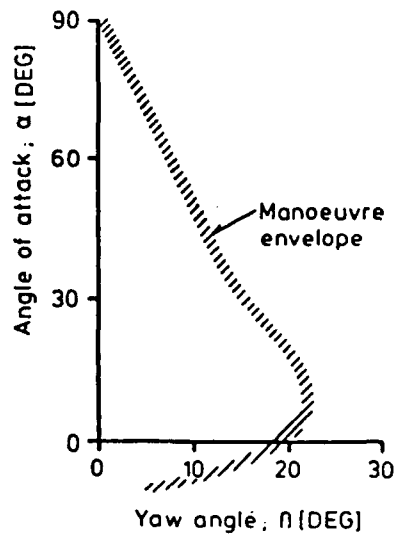
RAFALE

- α AND β PROTECTION
- 2 ENGINE EFFICIENT SEPARATION
- LONG DIFFUSOR (= REDUCED DISTORTION)

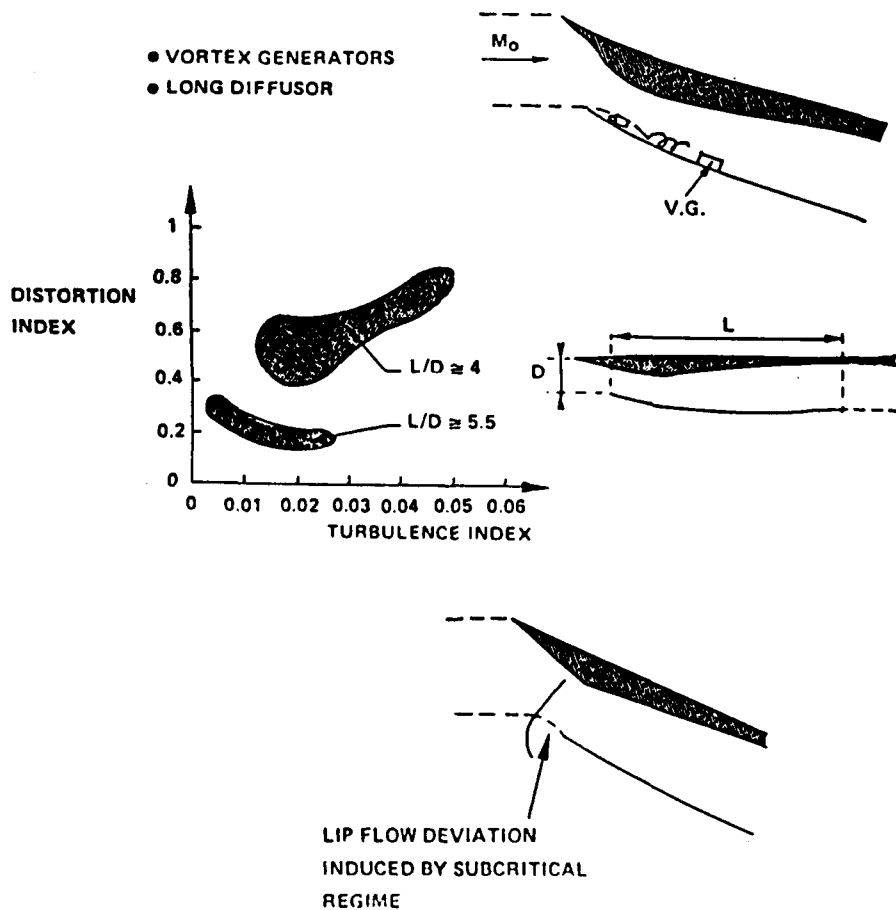


Fuselage boundary layer diverter. Mirage. Rafale.





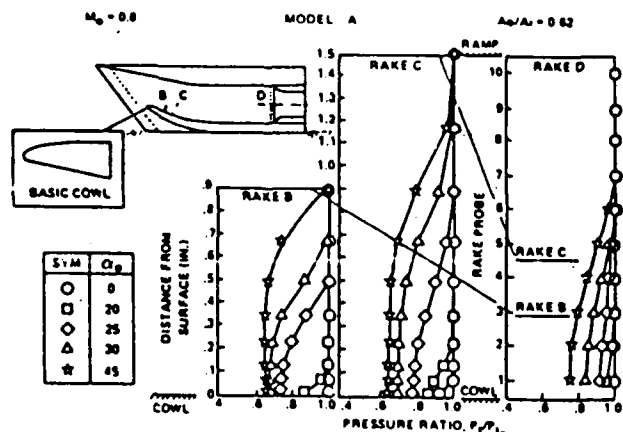
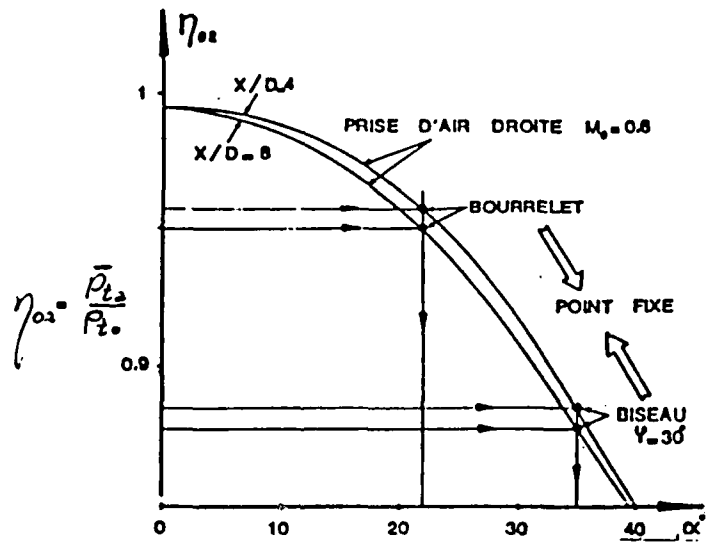
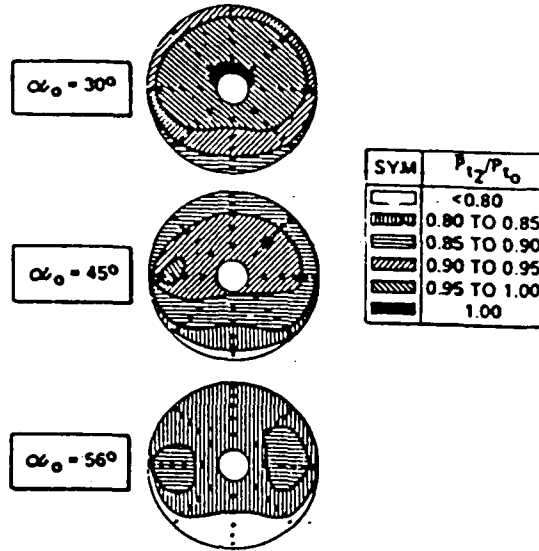
Aircraft attitude envelope at low speed for future fighters



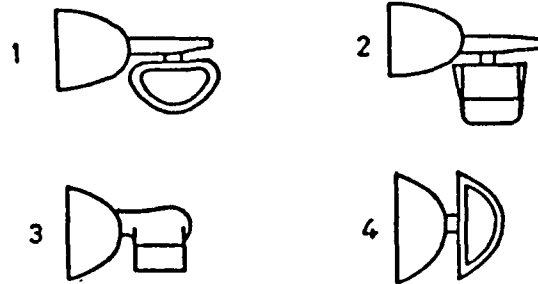
Angle of attack sensitivity improvement by subcritical regime.

$M_0 = 0.9$

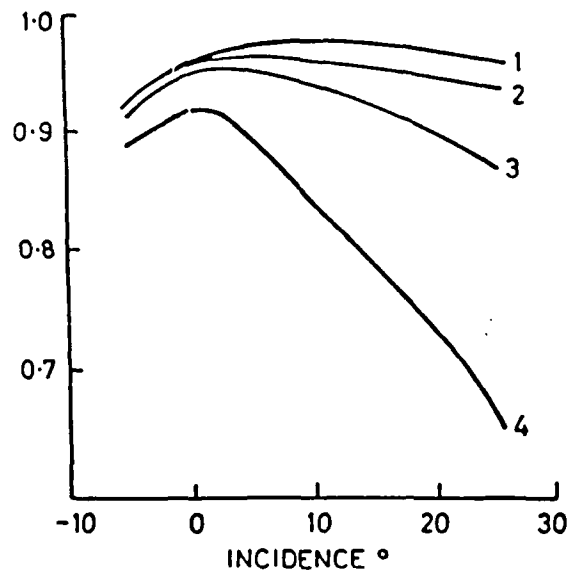
BASIC COWL



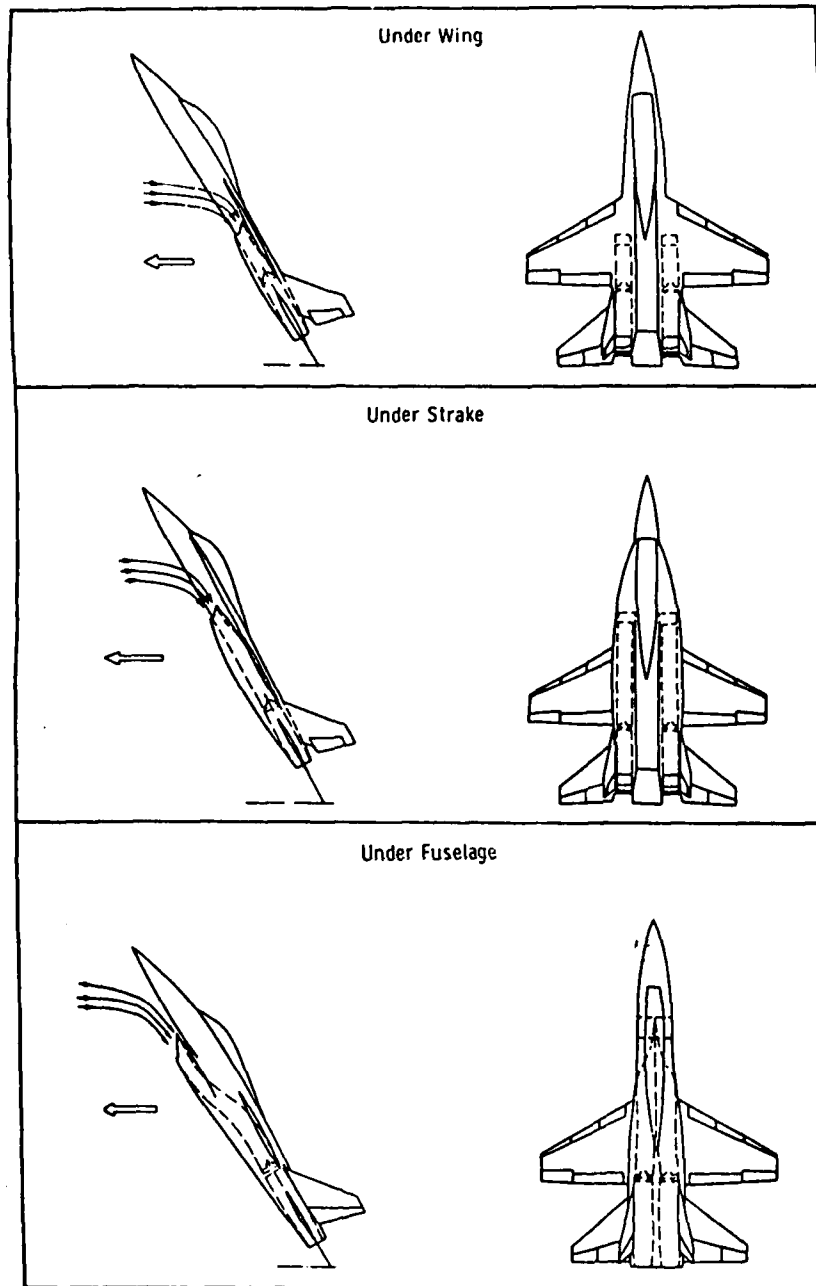
Effect of Angle of Attack on Duct Total-Pressure Profiles - Model A, Basic Cowl



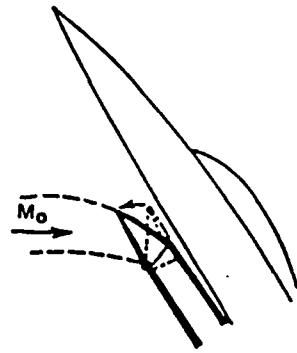
PRESSURE RECOVERY



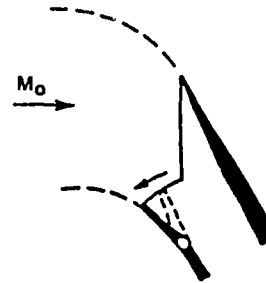
Effect of intake shielding



Shielded intake location



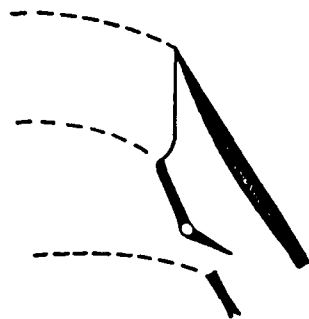
ROTATING FORWARD INTAKE (F 15)



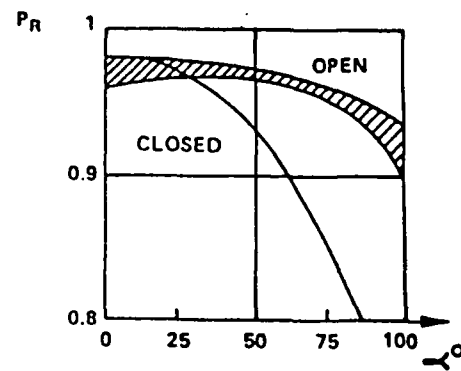
ROTATING COWL LIP

High angle of attack special devices.

HIGH INCIDENCE DEVICES



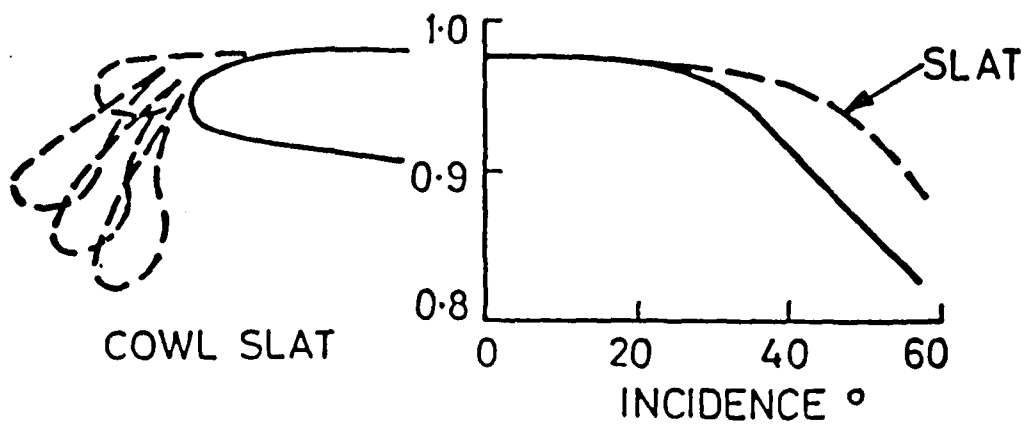
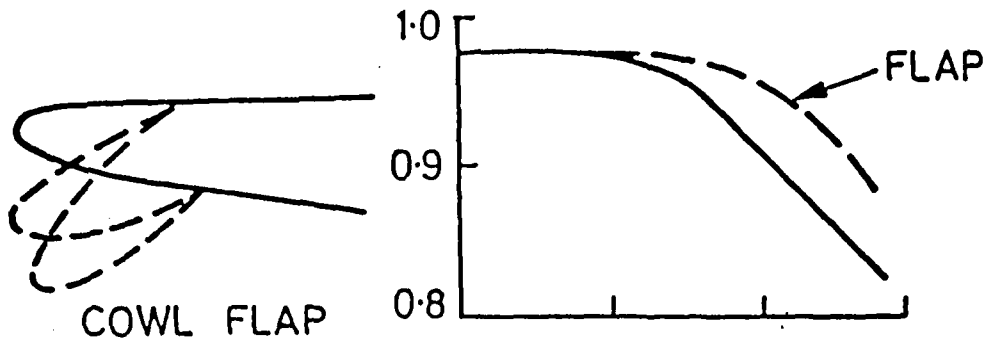
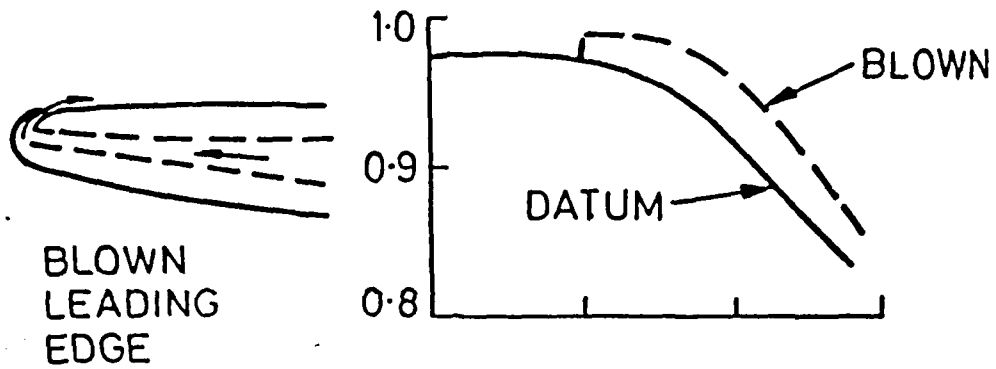
AUXILIARY DOOR



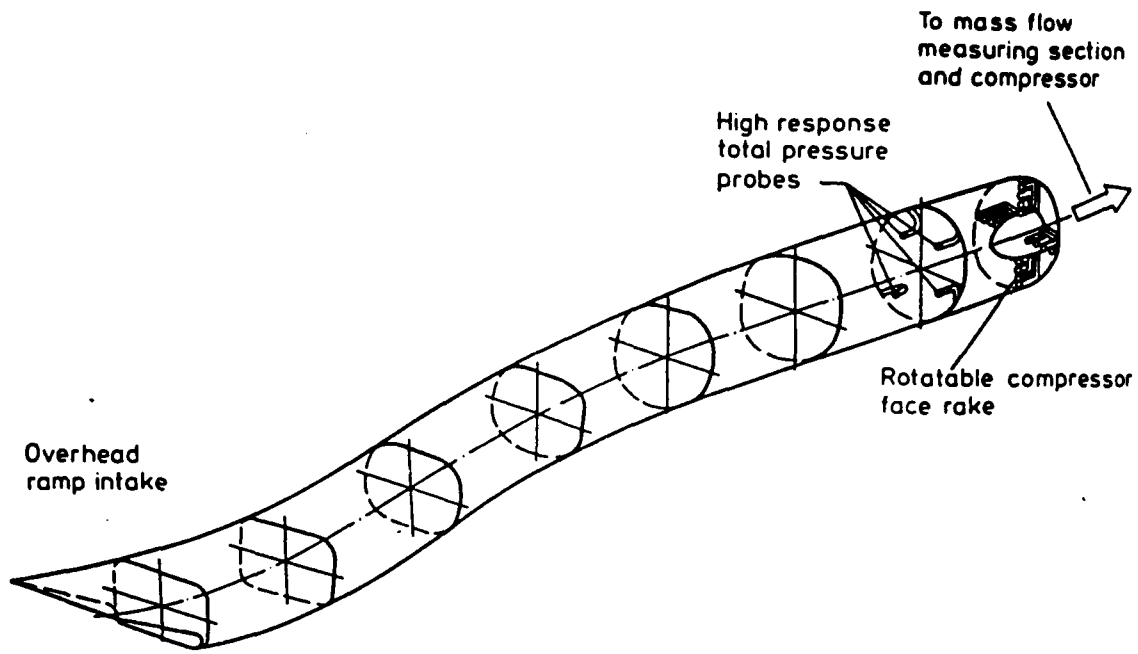
MBB Auxiliary door at high angle of attack [Lotter, Malefakis, 78]

MACH 0.9

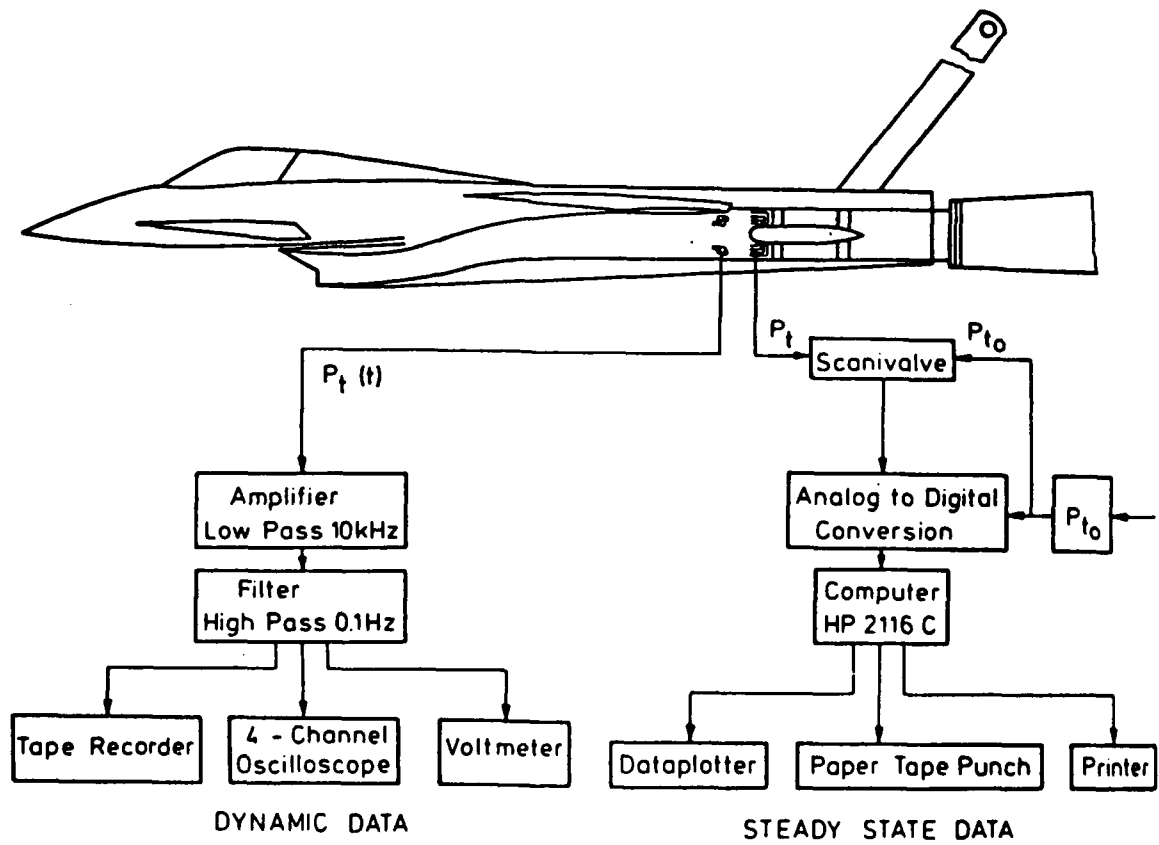
PRESSURE RECOVERY



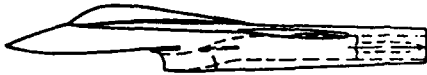

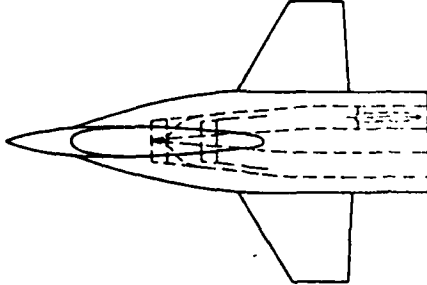




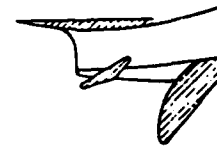




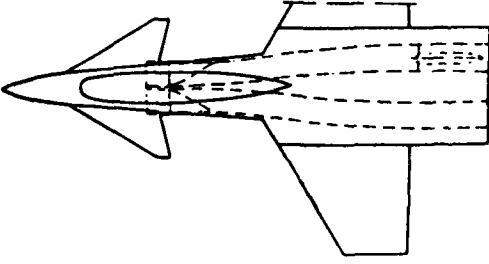

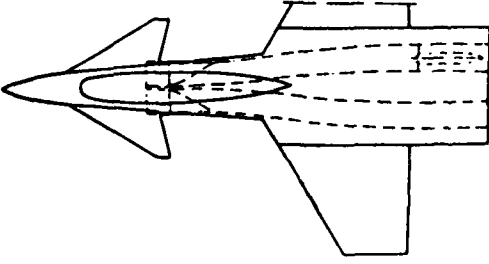

High incidence cowl lips



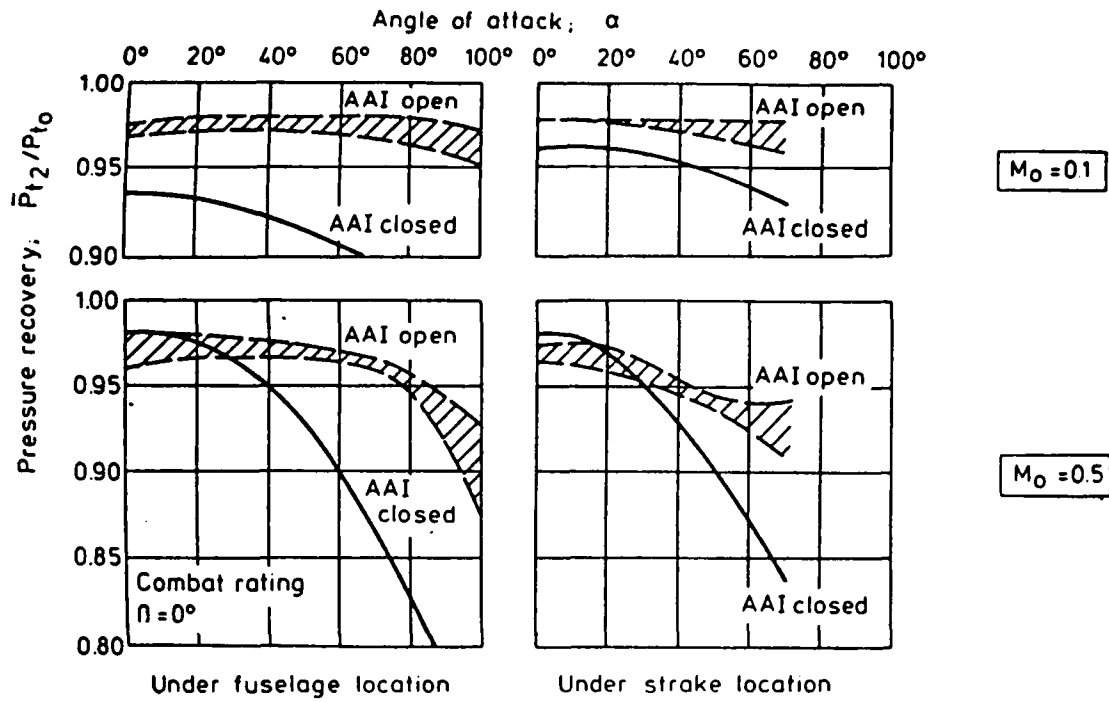
M88 Model instrumentation



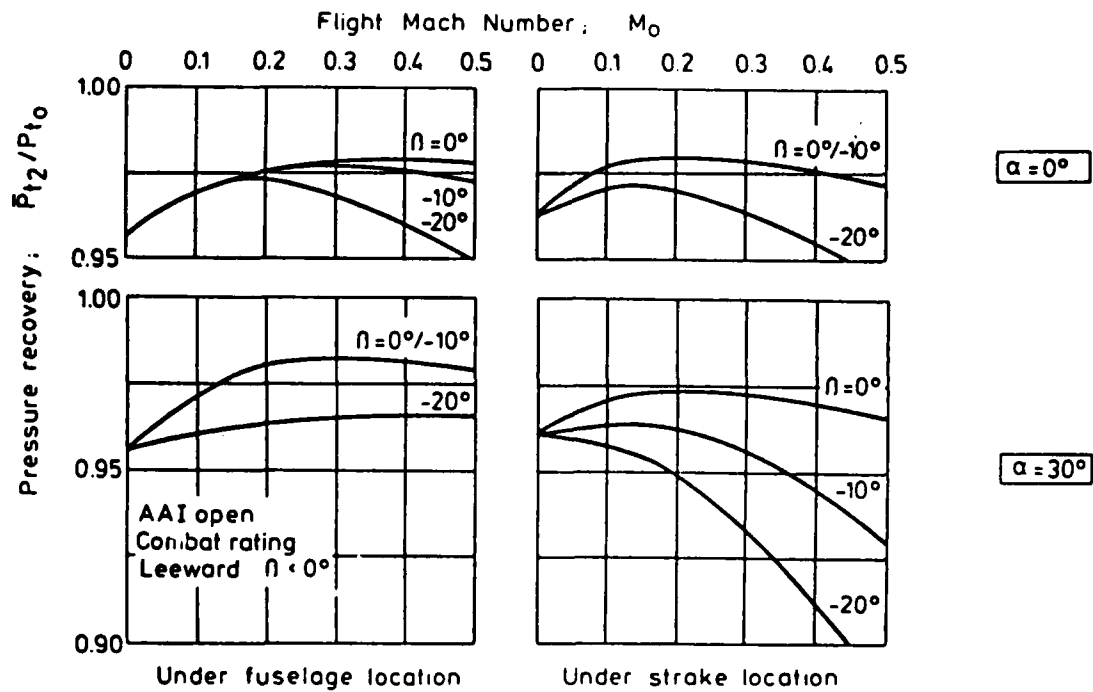
Data acquisition(M88 Test Rig).

	MBB Model Configuration	MBB Auxiliary Intake Variation
1 st Test Phase (Strake Configuration)	Intake under Fuselage	
		
		
		
2 nd Test Phase (Delta-Canard Configuration)	Intake under Strake	
		
		
		
2 nd Test Phase (Delta-Canard Configuration)	Intake under Fuselage	
		
		
		

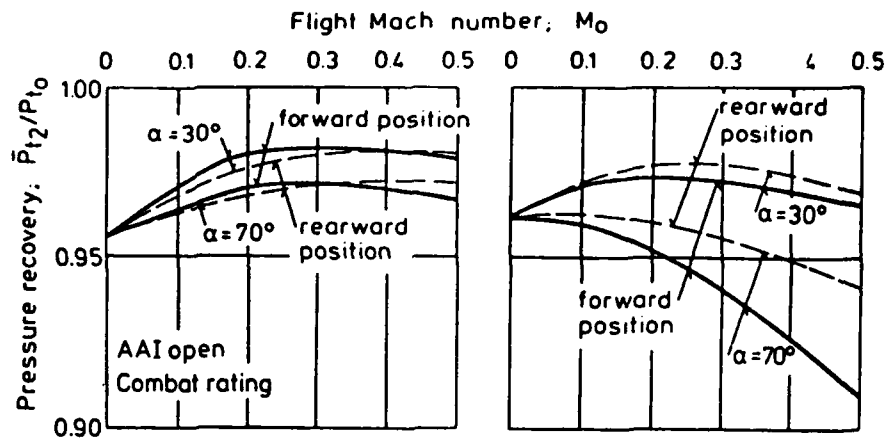
MBB Model configurations



Effect of angle of attack on pressure recovery (M88)



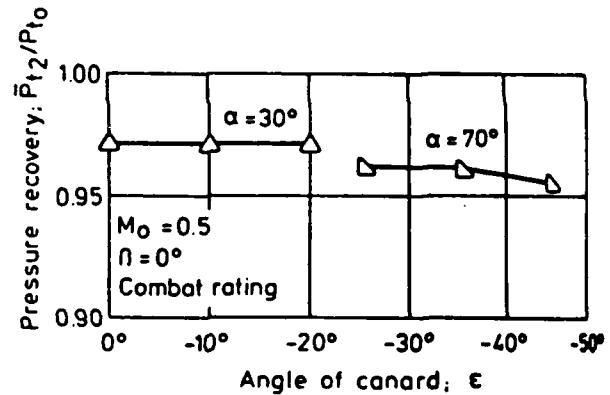
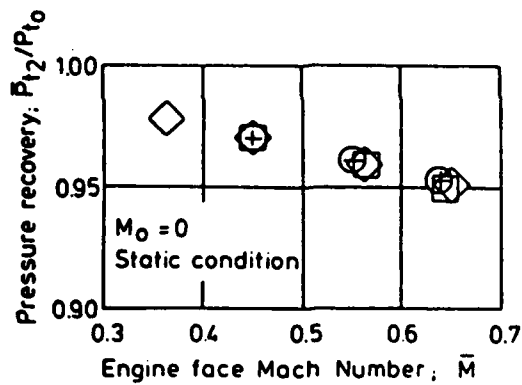
Effect of yaw angle on pressure recovery (M88)



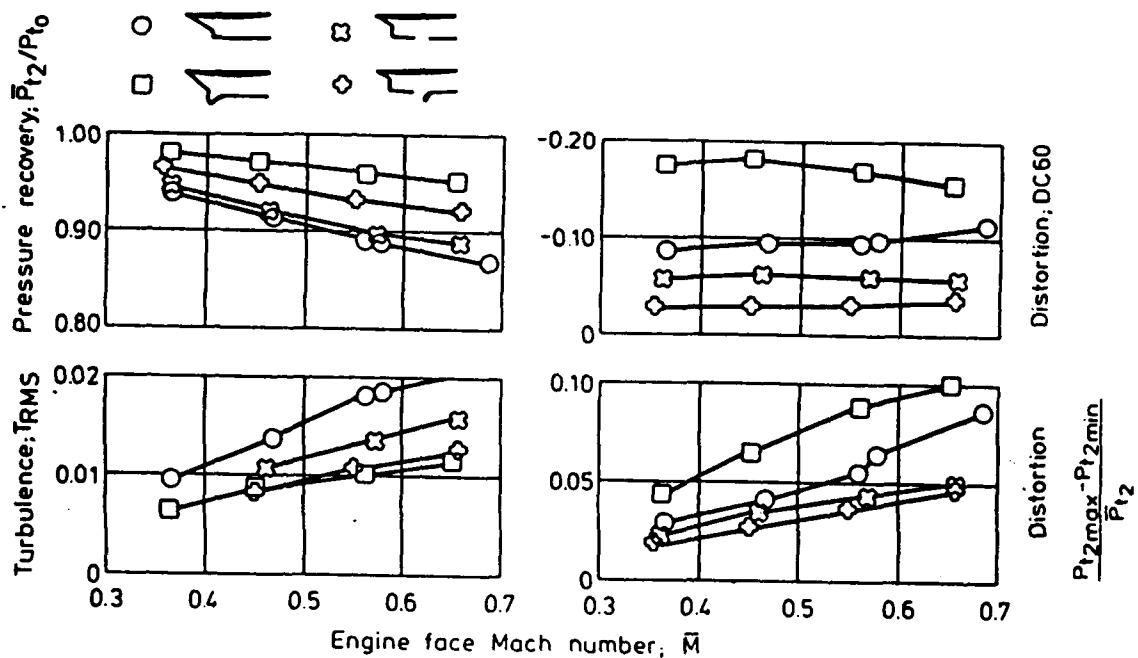
Under fuselage location

Under strake location

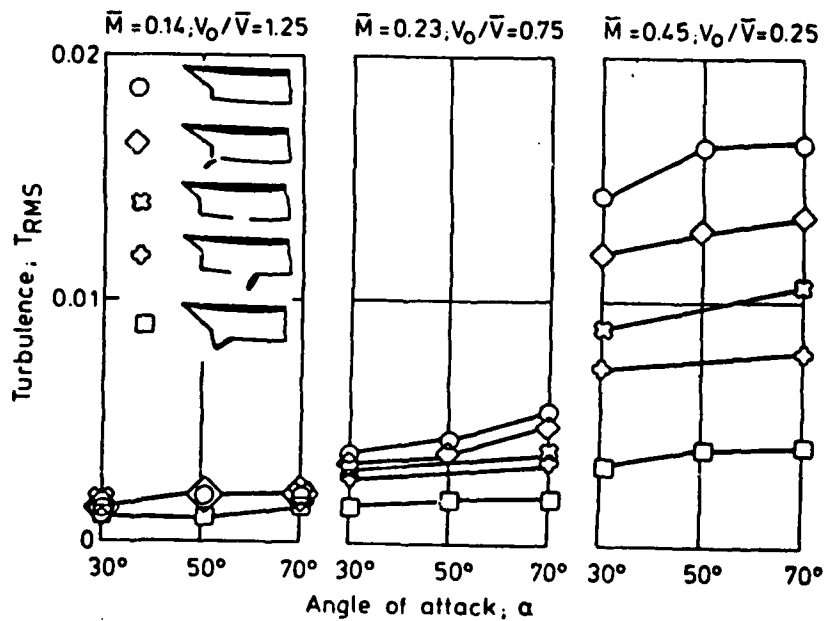
Effect of axial inlet position on pressure recovery (M88)



Effect of canard on pressure recovery (M88)



Static intake performance



Engine face turbulence

Concluding Remarks Extracted From
Previously Published PST-Inlet Works

The most important conclusions are deduced from the recent MBB studies (especially from the figures shown in p.99 to 103). These conclusions have been employed in the design of the EFA.

The conclusions are:

- 1) - The inlet-under-fuselage is the best choice for PST inlets (p.100-103)
- 2) - Inlets-under-strakes provide longer ducts with good pressure recovery values (p.101).
- 3) - With the help of an Auxiliary Air Intake Variations (AAI) shown on p. 100, a reasonable Pr can be maintained up to 100 degrees AoA (with under-fuselage-location) and up to about 70 AoA with under-strake-location (the last design option was not tested beyond 70 deg. AoA).
- 4) - 20 degrees yaw-flight angles can be maintained at $M=0.0$ to 0.5 with AAI. Under fuselage-location provides better performance than the under-strake location.
- 5) - The effects of canards on Pr are shown in p.102.
- 6) - The best inlet performance is obtainable with rotatable inlet lips (p.103).
- 7) - Engine-face-turbulence increases considerably with internal Mach number, but only slightly with AoA (p.103).
- 8) - Using these conclusions one must design new test rigs for upgrading existing (side-mounted), F-15 inlets to become effective PST-Inlets.

Such preliminary efforts are described in p.20 to 21b, and below (Appendix B - Parts 2 to 7).

Bibliography

- [1] AGARD-R-740 /SPECIAL COURSE ON FUNDAMENTALS OF FIGHTER AIRCRAFT DESIGN.
- [2] COMMENTS ON PROPULSION/AIRFRAME INTEGRATION FOR IMPROVING COMBAT AIRCRAFT OPERATIONAL CAPABILITIES/BY PH. POISSON-QUINTON
- [3] AGARD-CP-241/FIGHTER AIRCRAFT DESIGN
- [4] AIAA/SAE 14TH JOINT PROPULSION CONFERENCE/ADVANCED ENGINE INLET MATCHING FOR A V/STOL B-FIGHTER/R. TINDELL
- [5] AIAA 76-701/DESIGN AND PRELIMINARY EVALUATION OF INLET CONCEPTS SELECTED FOR MANEUVER IMPROVEMENT/J.A CAWTHON
- [6] NASA AIAA 77-878 /USE OF EXPERIMENTAL SEPERATION LIMITS IN THE THEORETICAL DESIGN OF V/STOL INLETS /M.A BOLES
- [7] AIAA 77-802 /FAN INLETS FOR A V/STOL AIRPLANE/J. KONSCEK
- [8] SUBSONIC DIFFUSER DESIGN AND PERMORMANCE FOR ADVANCED FIGHTER AIRCRAFT /AIAA 85-3073
- [9] BOUNDARY LAYER TRANSITION EFFECTS ON FLOW SEPERATION AROUND V/STOL ENGINE INLETS AT HIGH INCIDENCE/AIAA 84-0432
- [10] INTAKE /AIRFRAME INTERGRATION FOR A POST-STOL FIGHTER AIRCRAFT CONCEPT /K.W LOTTER
- [11] "MECHANICS AND THERMODYNAMICS OF PROPULSION" /HILL AND PETERSON

APPENDIX B ; PART 2

By Ido and Roni

F-15 Inlet Test Rigs For PST Simulations

Model A F-15 Inlet

⑤(Fig.1) A

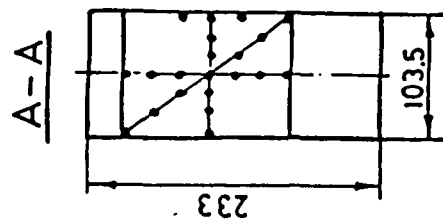
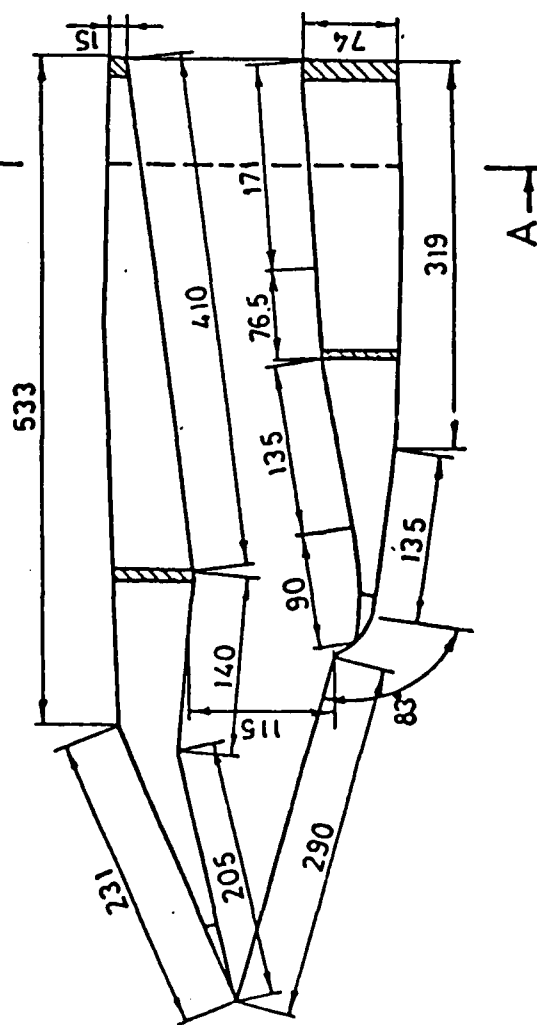


Fig. B-2.1 : Subscale F-15 Inlet dimensions.

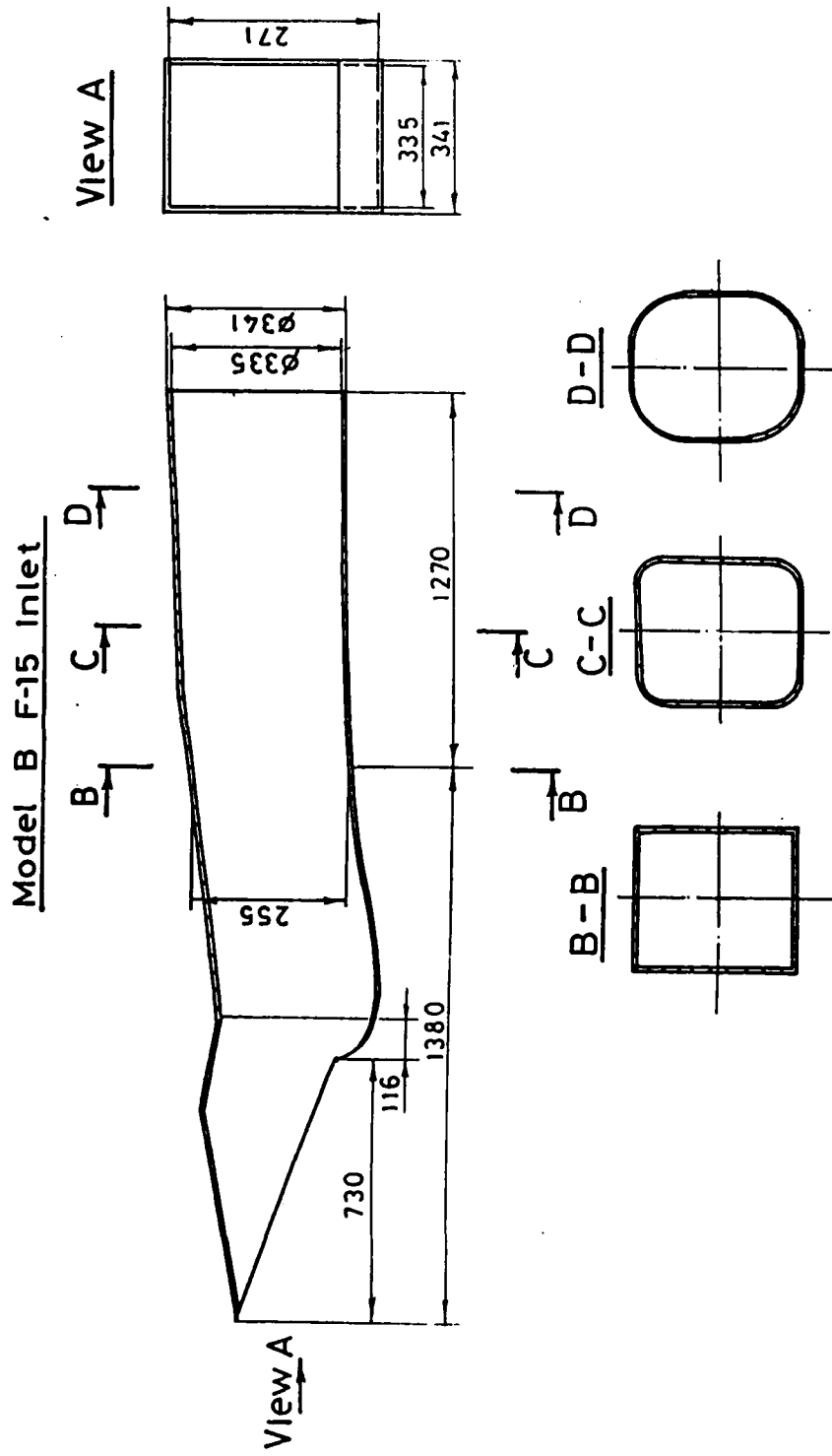


Fig. B-2.2 : -"Fullscale" F-15 Inlet dimensions.

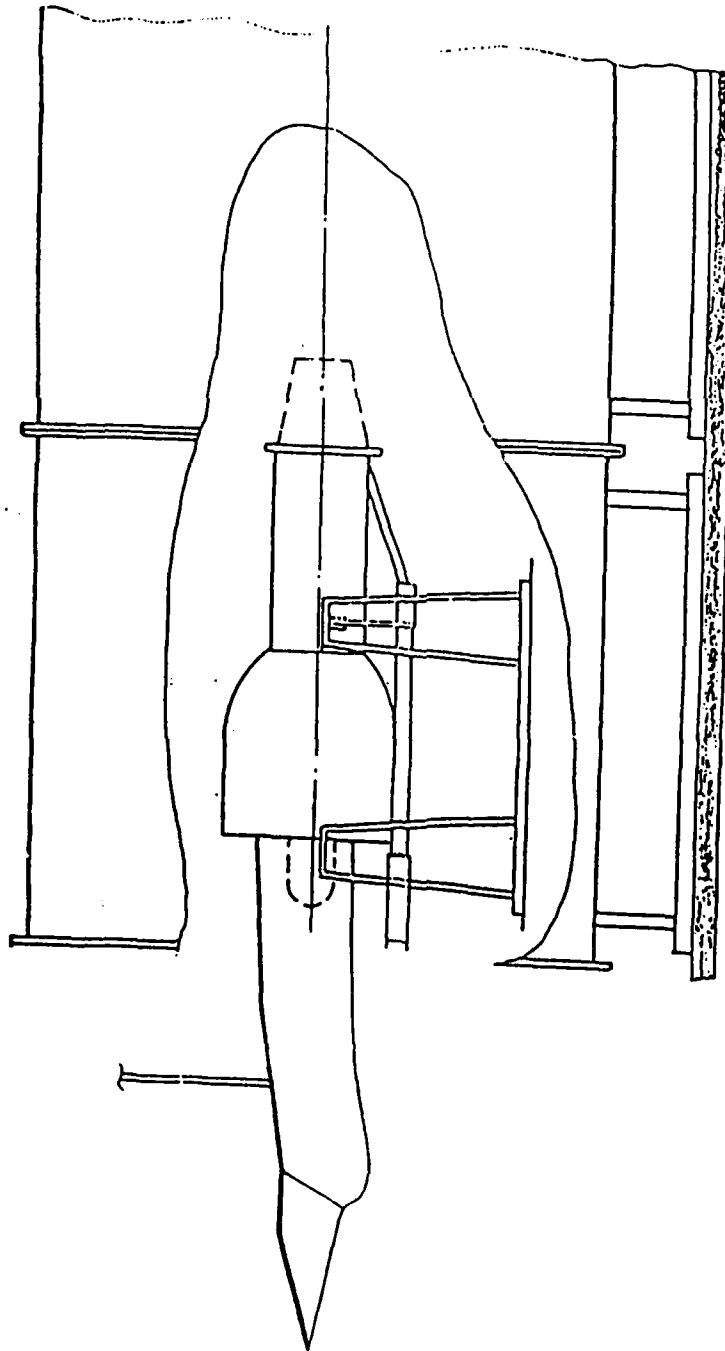


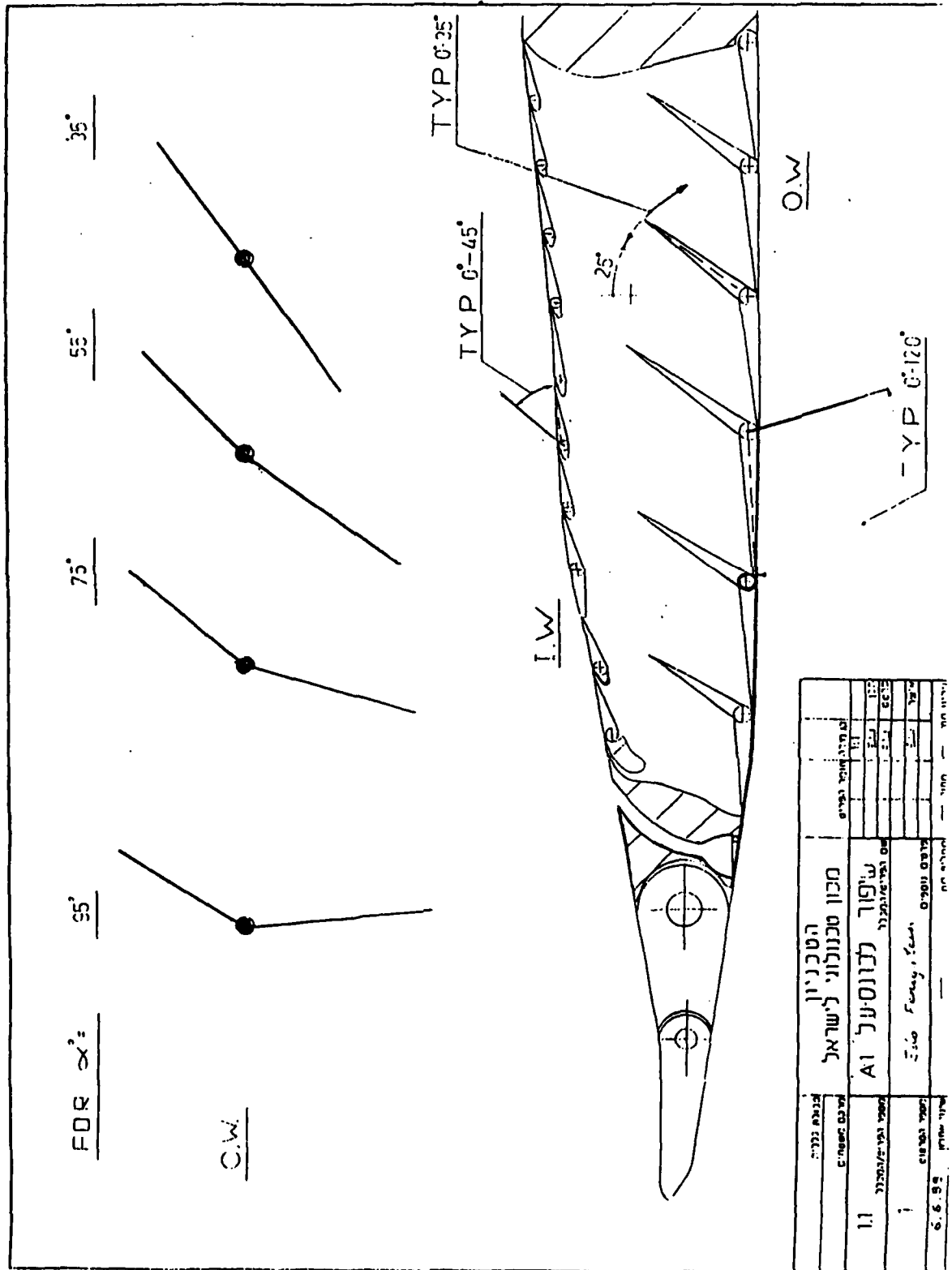
Fig. B-2.3: The "Fullscale" F-15 inlet installed on Marbore Jet Engine. It will be tested with axisymmetric and 2D-CD vectoring nozzles

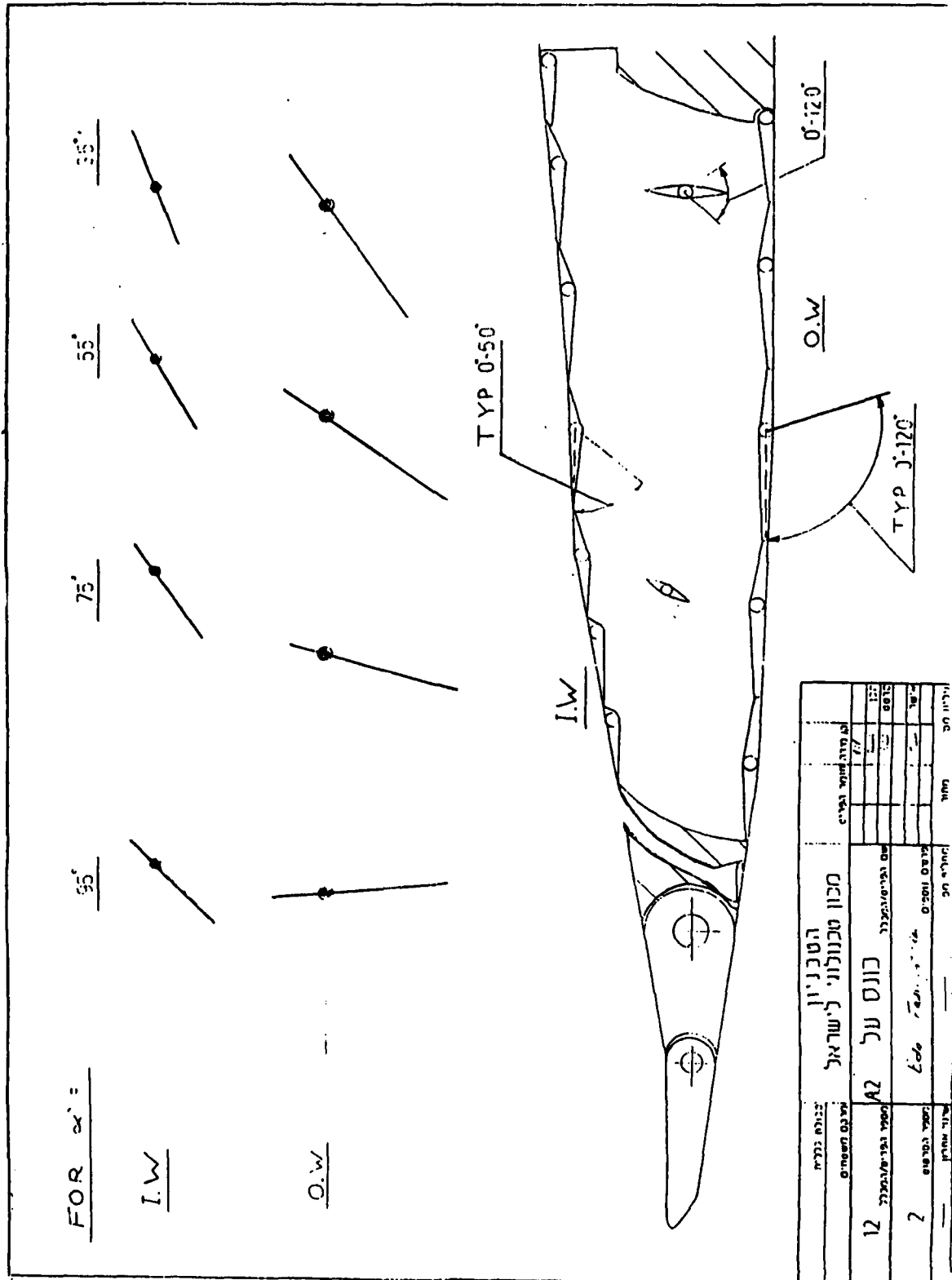
APPENDIX B - PART 3

A Number of Conceptual Configurations
For "Vectorable" PST F-15 Inlets

These configurations may be compared with the ones shown in pages 100 to 103.

The first configuration to be tested during the next stage of this research is the variable lip configuration. A primitive fixed lip (called "shelf") was installed during the preliminary calibration tests depicted on pages 118 to 150. However, the tests should be resumed with the suction blower operating at various AoA and inlet Mach numbers.





APPENDIX B - PART 4

Subscale Calibration and Preliminary Test Results

For Current "Unvectorable" F-15 Inlet
at Zero and High Incidence Angles
(Conducted by Ido Fenygstein and
Roni Sade)

The limitations of the subscale experimental evaluations are discussed in pages 21 to 21a. Due to these limitations we shall rely mainly on the full-scale test results and employ the following subscale test results only as rough indicators. *For the new test standards see p.174.*

For the definition of KD see eq.8, p.84.

Pr is the inlet pressure recovery defined in p.85.

Examples of Pr variations with % of engine design flow are shown in p.87

In the following diagrams "Comp". means the level of blowing-fan-mass-flowrate, as calibrated in the laboratory, i.e., increasing numbers from 1 to 3 increase the flow rate. cf. P. 156.

("Shelf" means a primitive inlet lip whose angle with respect to the free flow varies between 0,75 and 100 degrees.

Aircraft AoA-Yaw envelope at low speed is shown in page 93. It has also been discussed in Appendix F of our book.(1).

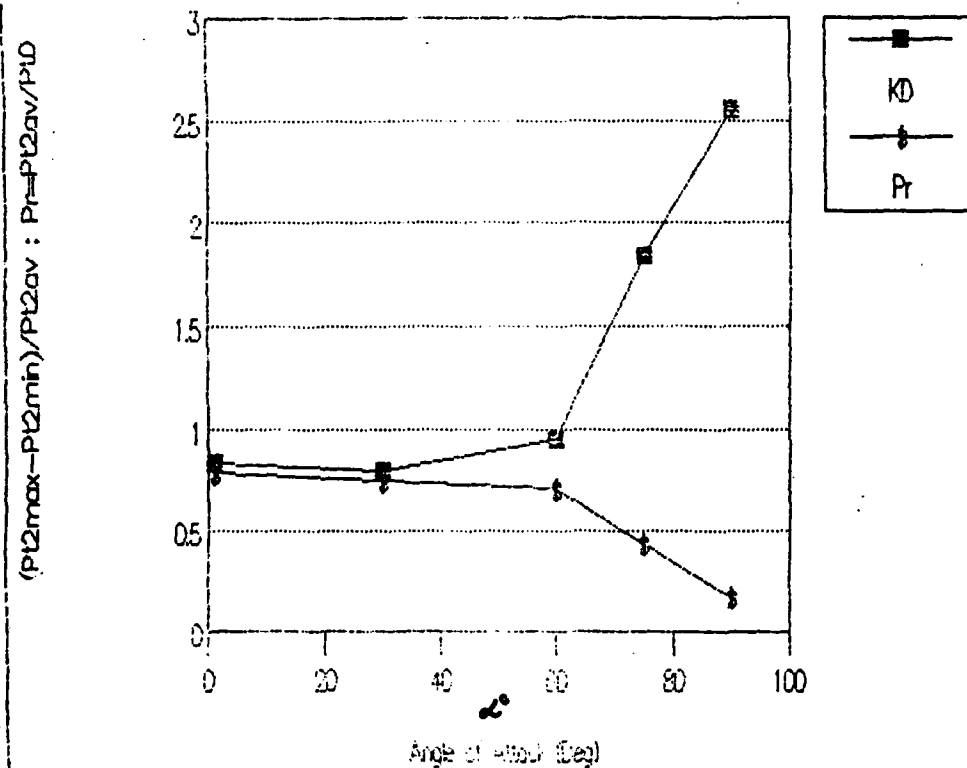
Effects of incidence angles (from -10 to +30 degrees) for various inlet configurations is shown in p.95. Streamlines for high-alpha intakes are shown in pages 96 to 97.

Examples of variable lips/vanes investigated at MBB for the EFA are shown in pages 100 to 103.

Turbulence [T_{RMS}] is a third parameter to be investigated during the next year of this investigation.

Distorsion prm. Vs. Alfa ; No "Shelf".

Pres. Recovery Vs. Alfa ; comp. 1.



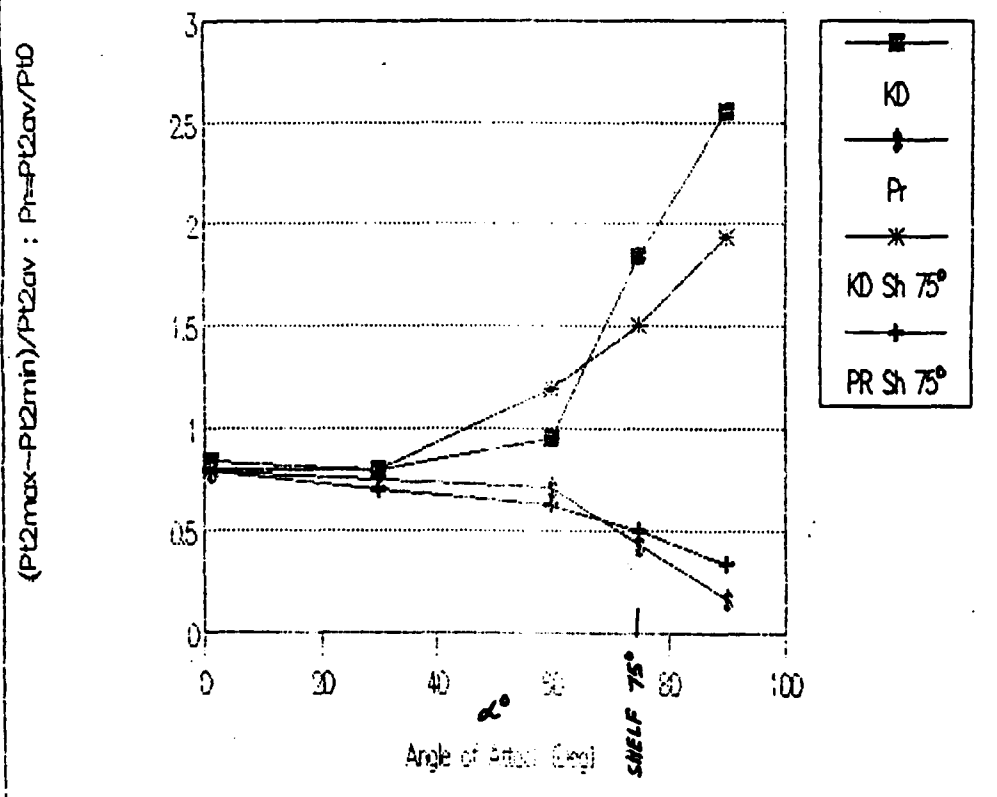
Graph 1

Tentative Concluding Remarks (see also p.20-21a)

- The distortion parameter K_d increases significantly beyond 60 degrees AoA (alpha). See eq.8, p. 84
- The pressure recovery decreases significantly beyond 60 degrees AoA(alpha).

Distorsion prm. Vs. Alfa. "Sh" = 0;75°.

Pres. Recovery Vs. Alfa ; comp. 1.



Graph 2

Tentative Concluding Remarks (see also Graph 1):

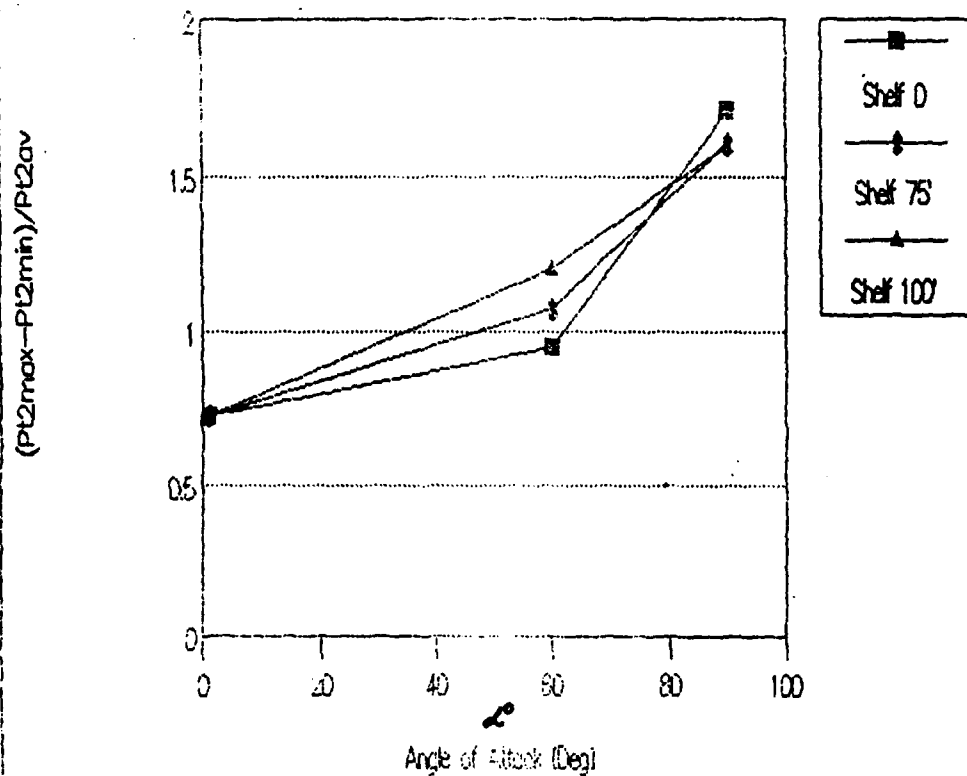
Beyond AoA 60 degrees both the distortion parameter K_d and the pressure recovery Pr begin to deteriorate the F-15 inlet performance.

A primitive inlet lip ("shelf") tentatively appears to improve inlet performance.

However, these are only preliminary calibration tests with the suction blower closed.

Distorsion prm. Vs. Alfa.

"Angle-of-Shelf" 0,75,100, comp. 2

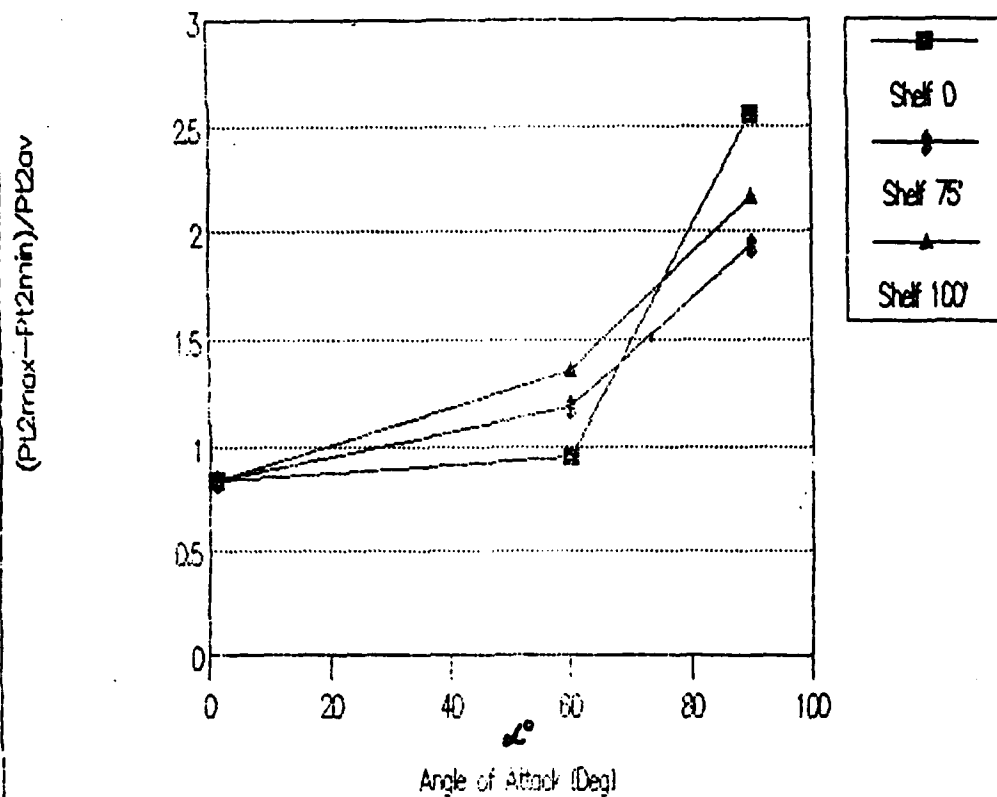


Graph 3

See the Notes On Graphs 1 and 2 (p. 117)

Distorsion prm. Vs. Alfa.

"Angle-of-Shelf" 0,75,100, comp. 1

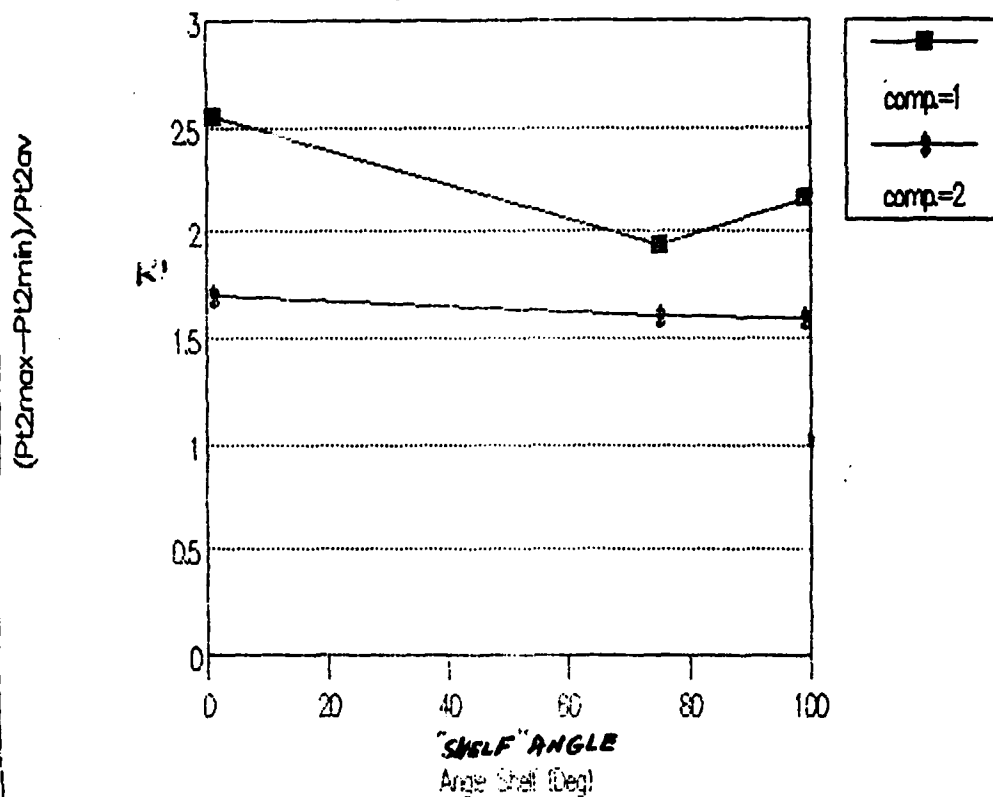


Graph 4

See the Notes On Graphs 1 and 2 (p. 117)

Distorsion prm. Vs. "Shelf angle".

comp.=1;2, Alfa=90 deg.



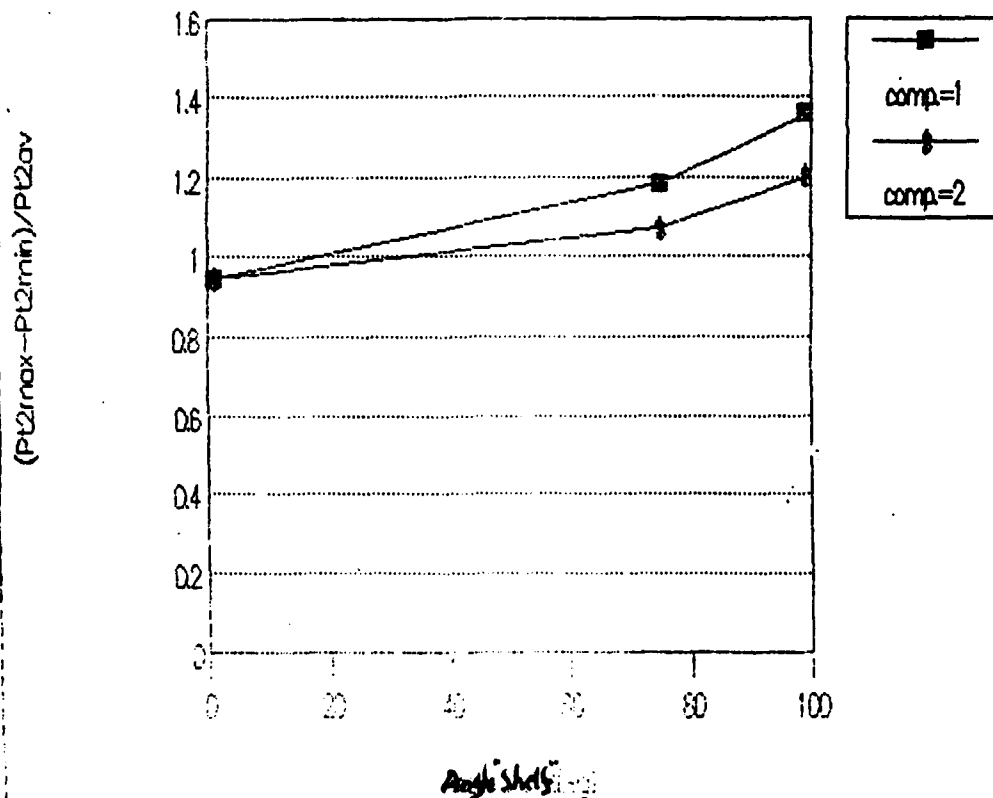
Graph 5

See the Notes on Graphs 1 and 2 (p. 117)

Distorsion prm.

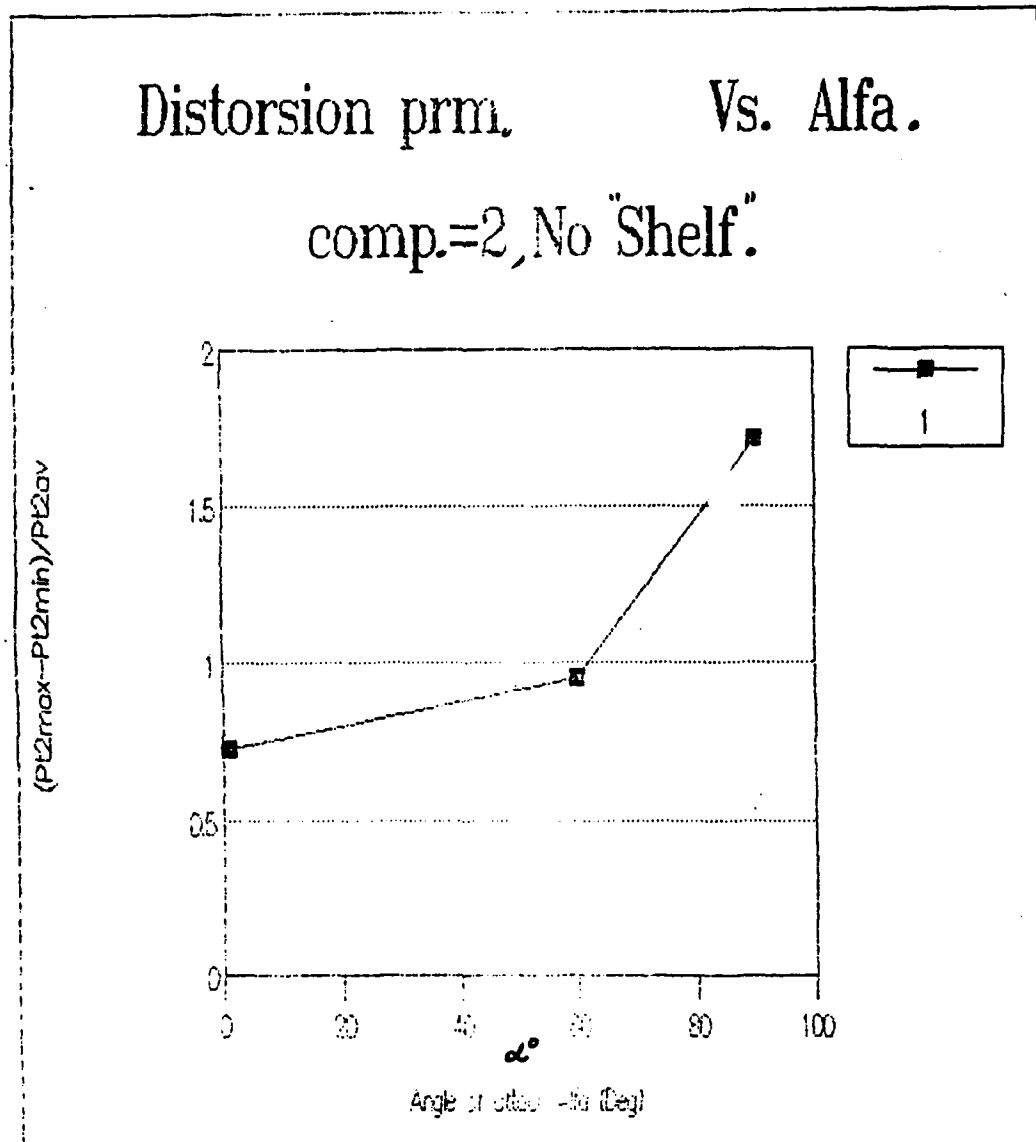
Vs. 'Shelf angle'.

comp.=1;2 Alfa=60 deg.



Graph 6

See the Notes On Graphs 1 and 2 (p. 117)

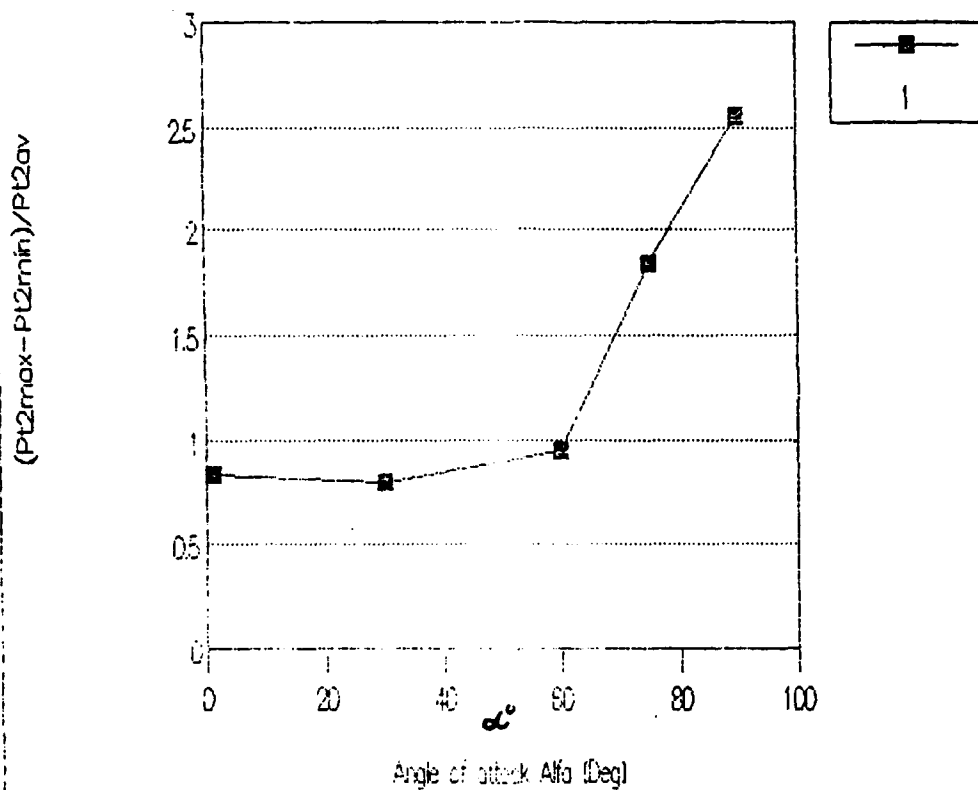


Graph 7

See The Notes On Graph 1 and 2 (p. 117)

Distorsion prm. Vs. Alfa.

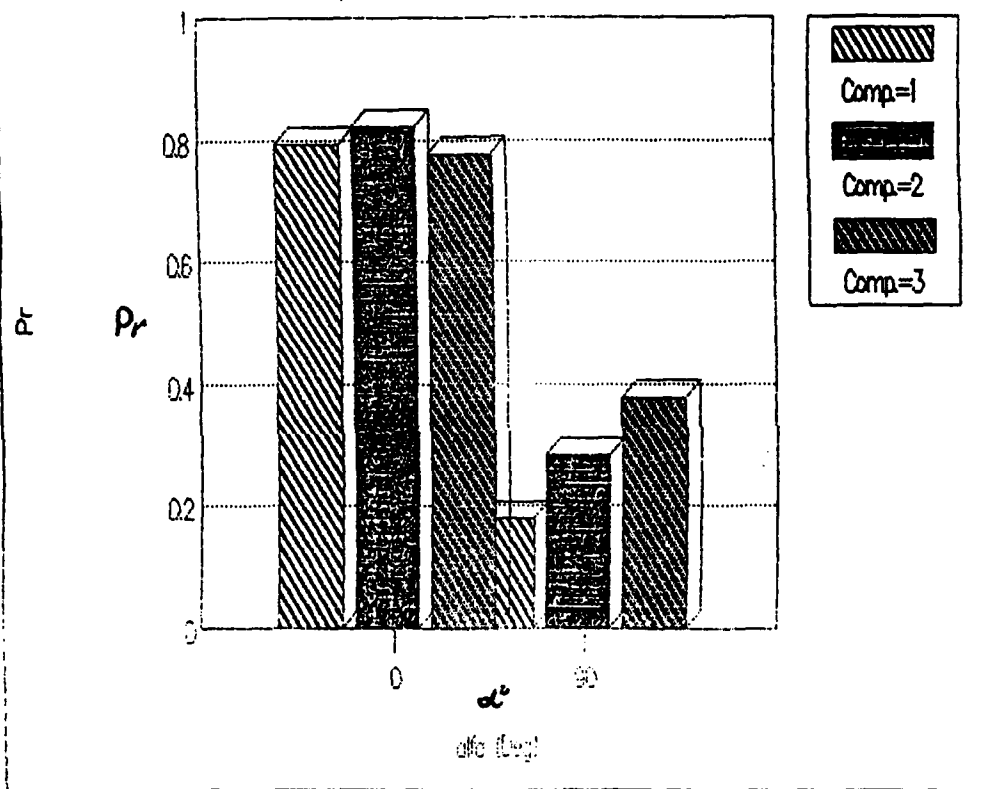
comp.=1, No "Shelf".



Graph 8

See The Notes On Graph 1 and 2 (p. 117).

Pres. Recovery change
for Comp=1,2,3 ; Alfa=0;90 deg.



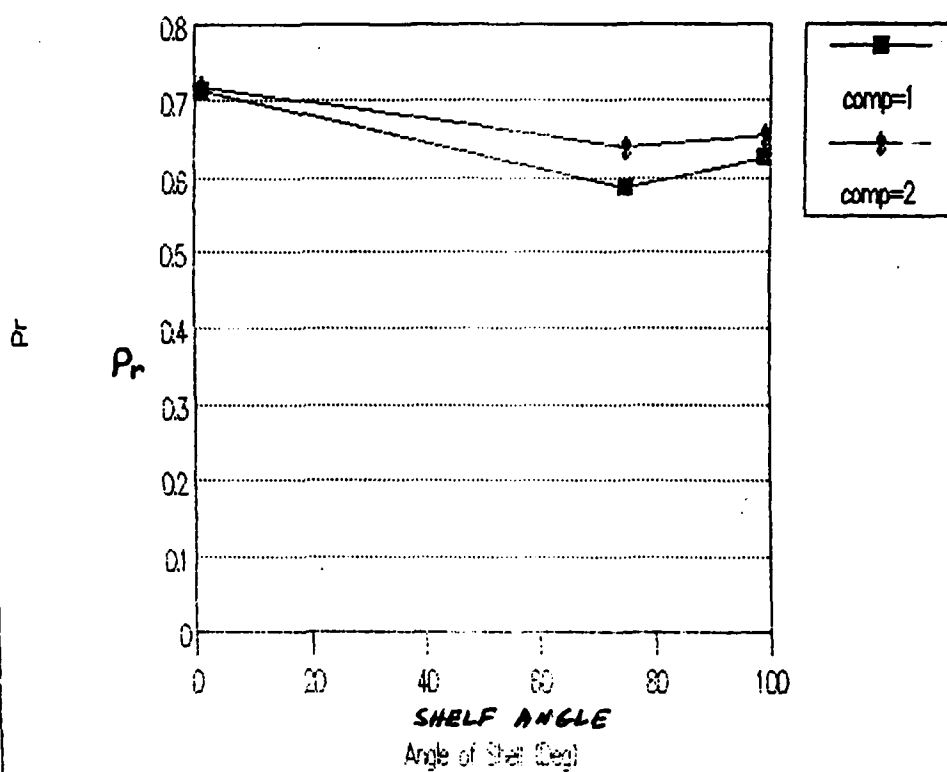
Graph 9

Preliminary Calibration Tests For the Expected Range of Pr for
AoA = 0 and AoA = 90 degrees.

These preliminary data support the tentative conclusions resulted
from the previous graphs regarding the drastic deterioration of F-15
inlet performance beyond 60 degrees AoA.

Pres. Recovery Vs. Shelf Angle.

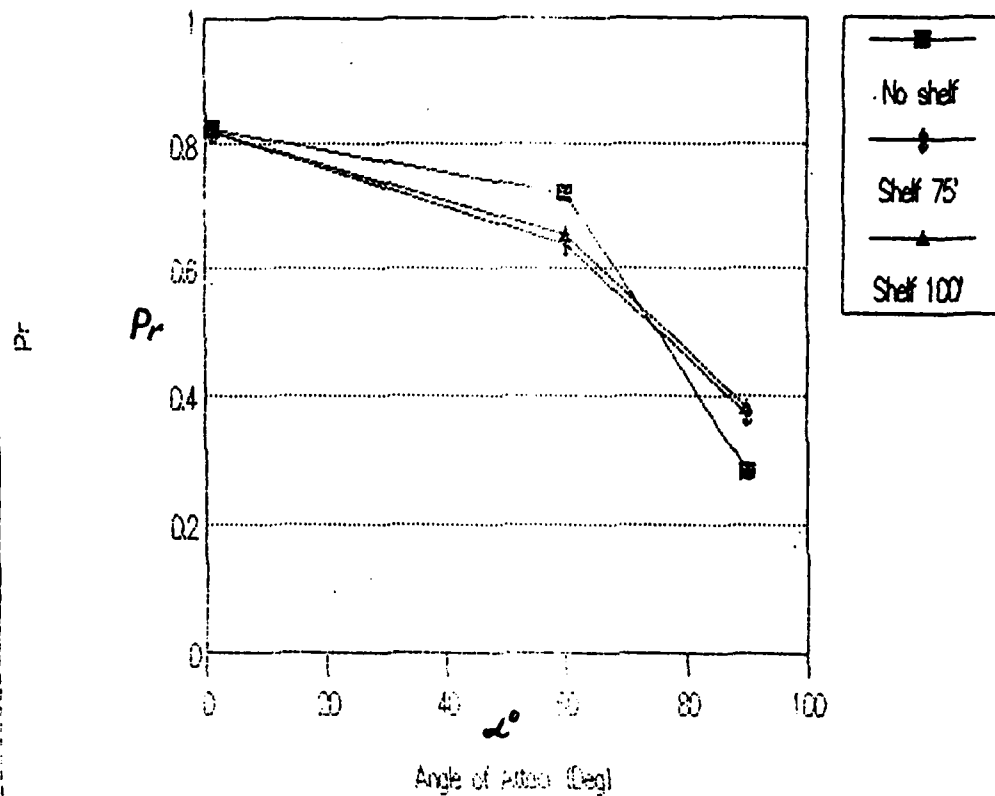
Angle-of-Attack=60 Deg.



Graph 11

See Notes on Map 1 (p.133)

Pres. Recovery Vs. Angle of Attack.
Effect of "Shelf", Comp=2.

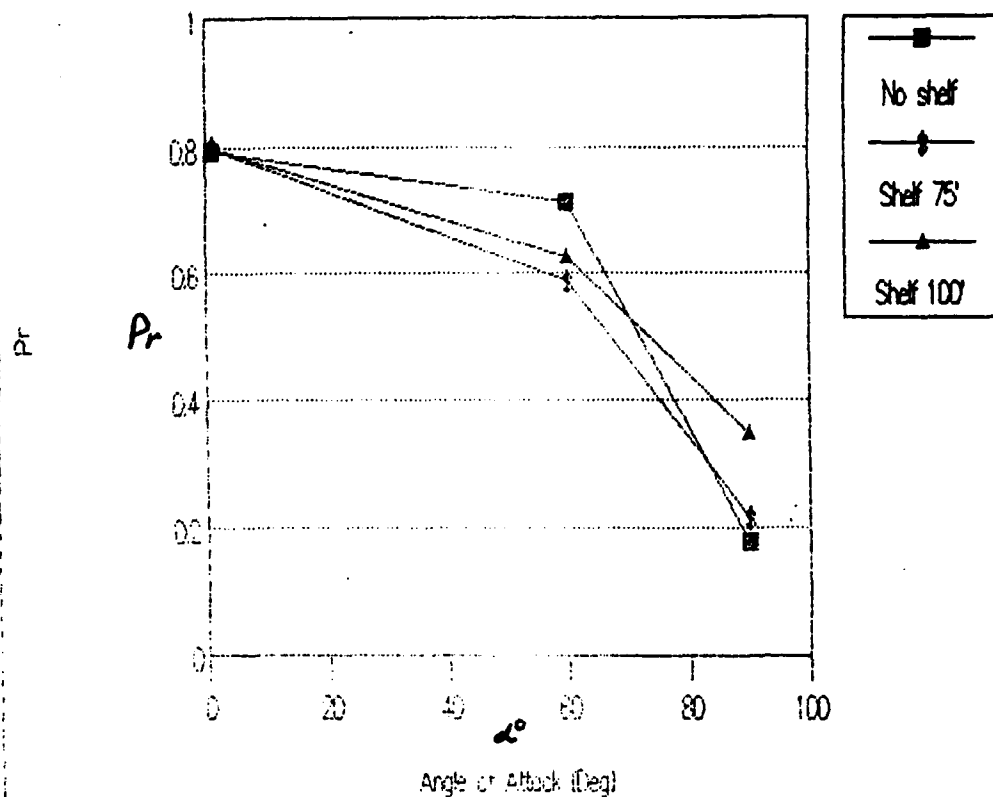


Graph 12

See Notes on Map 1 (p 133)

Pres. Recovery Vs. Angle of Attack.

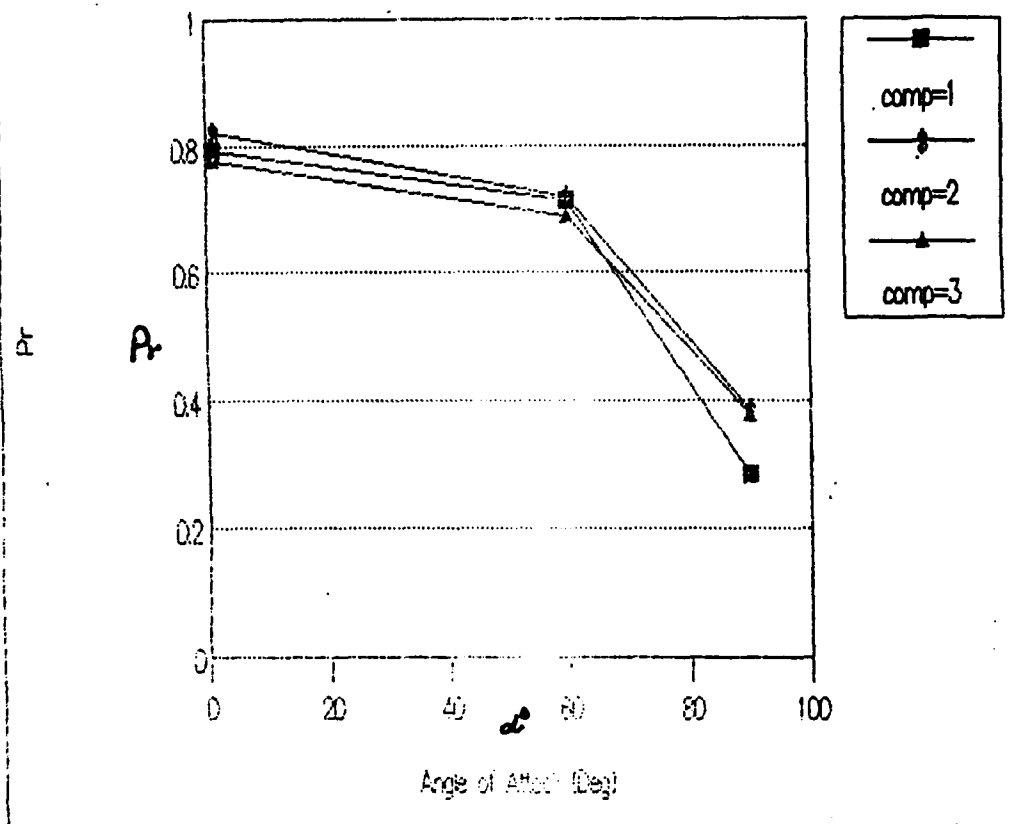
Effect of Shelf; Comp=1.



Graph 13

See Notes on Map 1 (p. 133)

Pres. Recovery Vs. Angle of Attack.
Effect of Comp. on Pr.

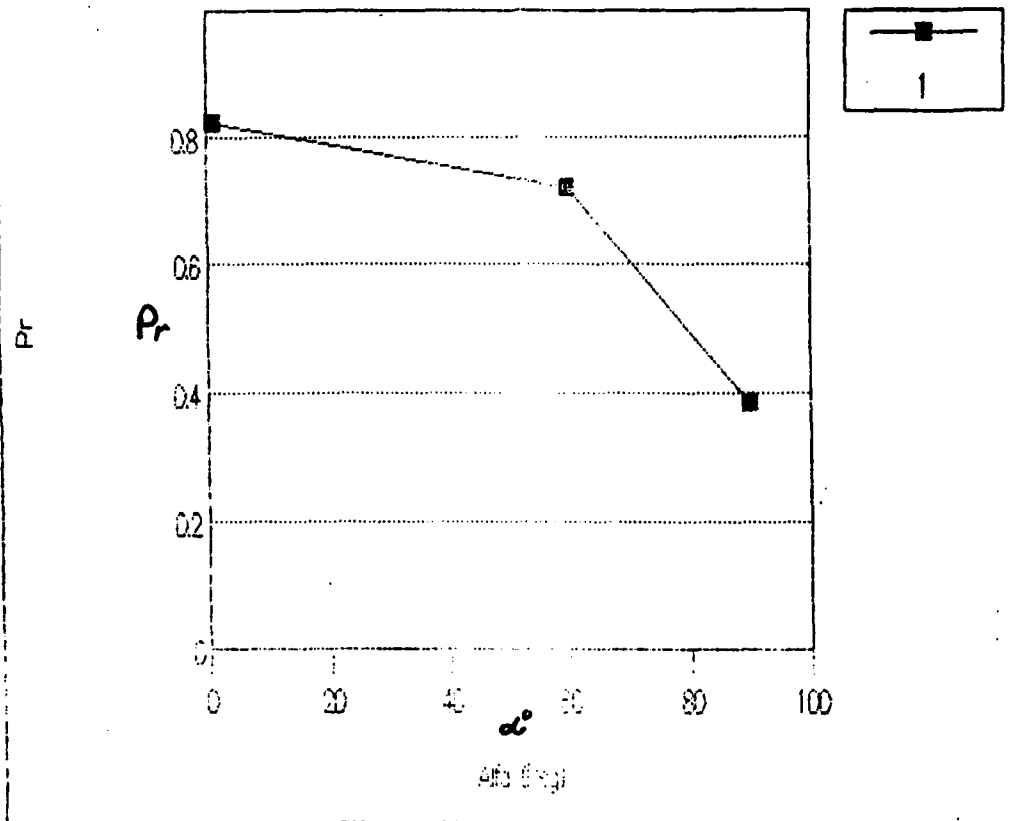


Graph 14

See Notes on Map 1 (p. 133)

Pres. Recovery Vs. Angle of Attack.

Comp=2.No "Shelf".

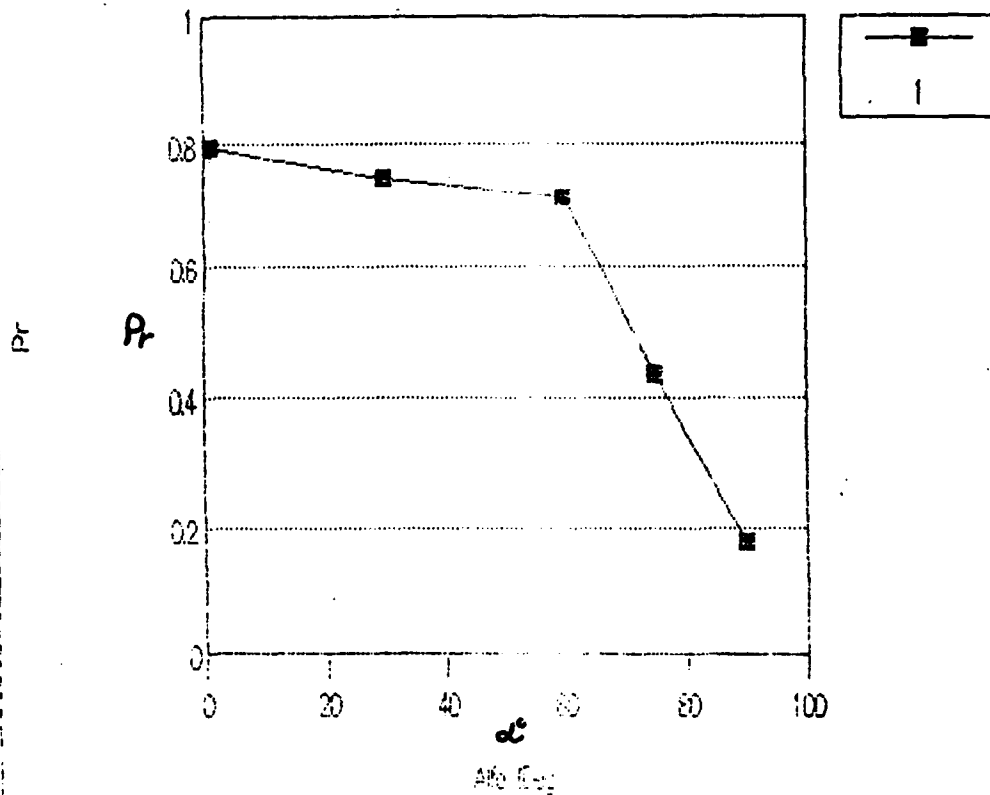


Graph 15

See Notes On Map 1 (P.133)

Pres: Recovery Vs. Angle-of-Attack.

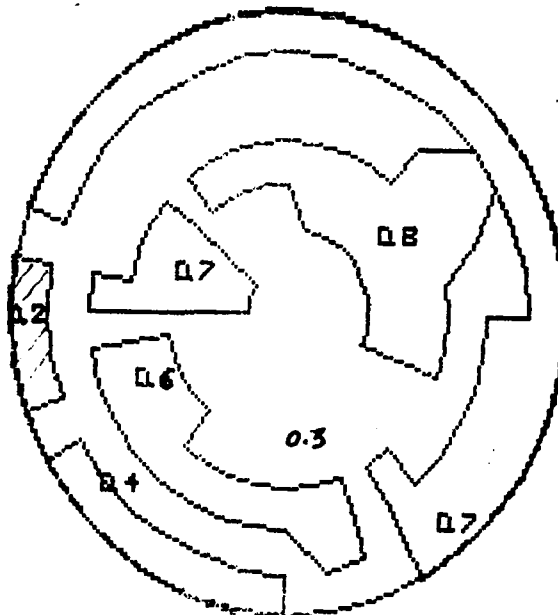
Comp=1.No "Shelf".



Graph 16

See Notes on Map 1 (p.133)

ANGLE-OF-ATTACK=0 [deg]
COMPRESSION=1* , 'SHELF'=0 [deg]



Map 1 Preliminary Probes Tests/Calibrations

For our new "Map standard" see p. 174. For
general Notes and Remarks see also p.20-21a.

For definitions see p.83. For test limitations see p.20-21a.

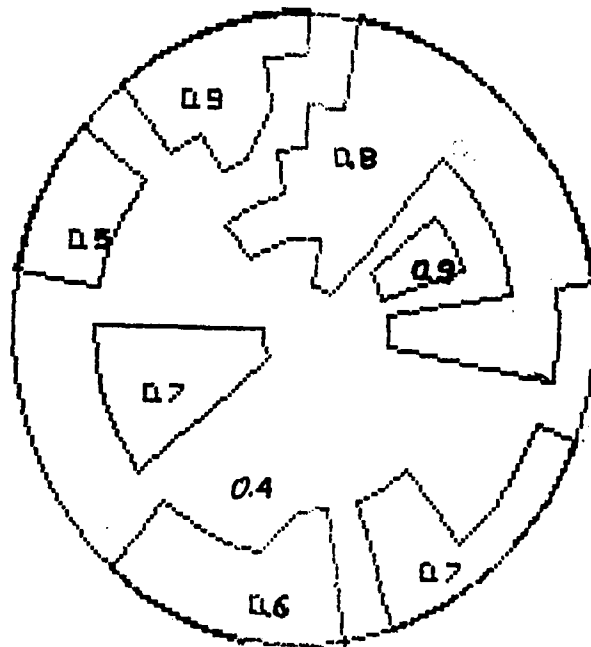
"Shelf" means a primitive inlet lip whose angle varies with respect
to the free flow.*"Comp." see blowing position in p.156.

All the test results reported in Maps 1 to 18 are preliminary
calibration tests. They would be repeated with and without the
suction blower (cf. p.156, p.174, p.158-172).

The cross-sectional areas with maximum distortion levels are
made darker for comparisons with the other maps. However, all the
results shown below are highly tentative and need statistical/
operational verification (cf. p.156-172, p.174).

The next tests will be conducted with various
engine throttle simulations (cf. p.156 and p.174.)

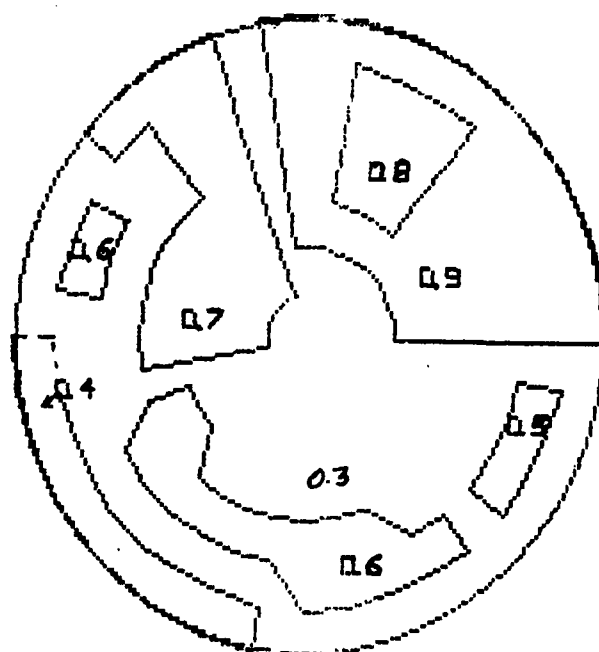
ANGLE-OF-ATTACK=0 [deg]
COMPRESSION=2 , "SHELF"=0 [deg]



Map 2

See Notes on Map 1.

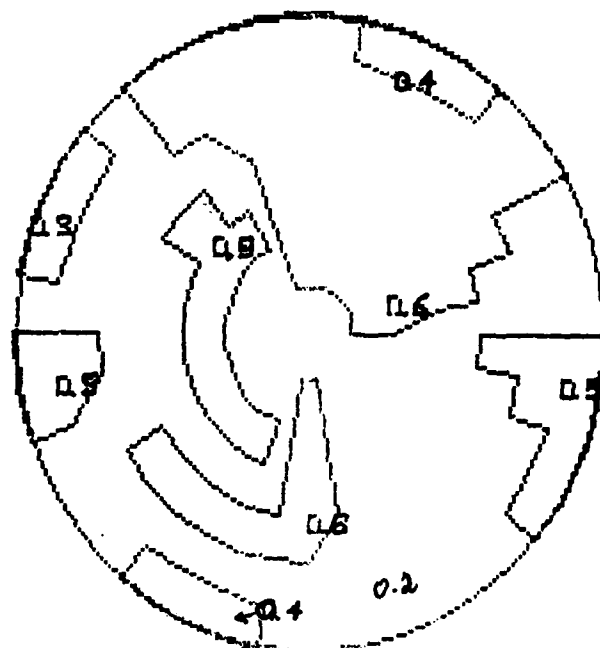
ANGLE-OF-ATTACK=0 [deg]
COMPRESSION=3 , "SHELF"=0 [deg]



Map 3

See Notes on Map 1.

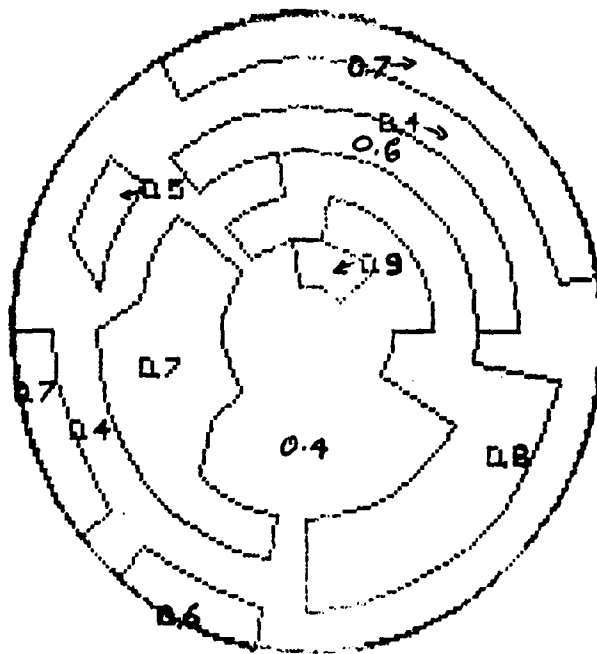
ANGLE-OF-ATTACK=30 [deg]
COMPRESSION=1 , "SHELF"=0 [deg]



Map 4

See notes on Map 1

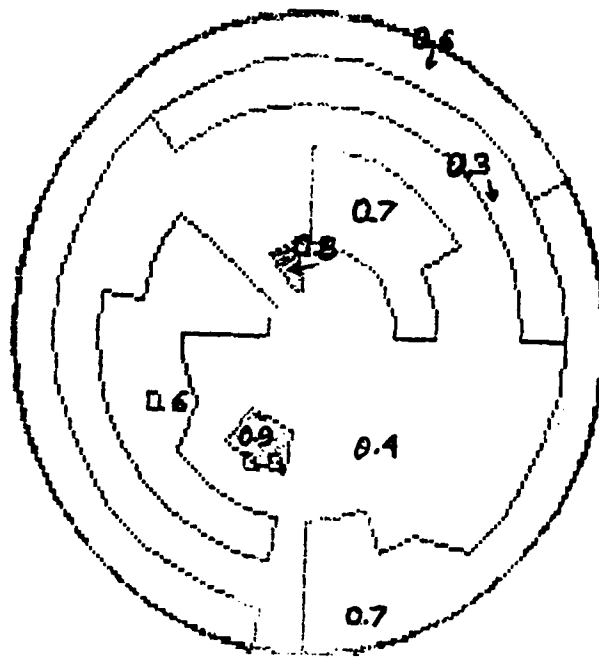
ANGLE-OF-ATTACK=60 [deg]
COMPRESSION=1 , "SHELF"=0 [deg]



Map 5

See Notes on Map 1

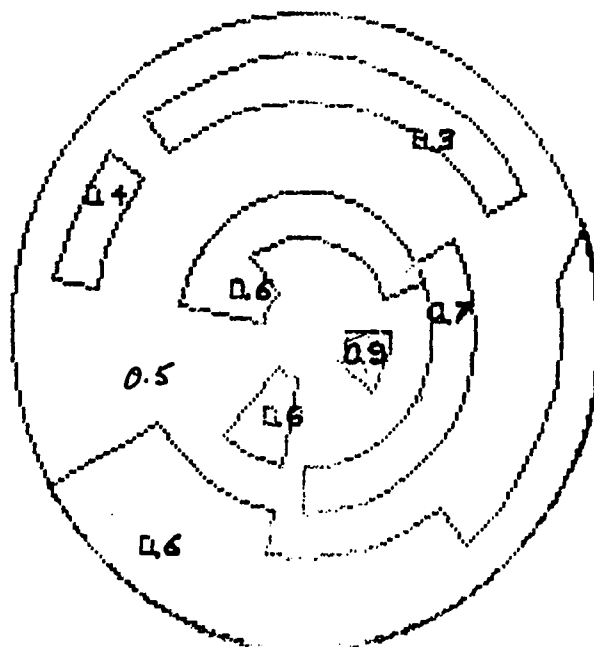
ANGLE-OF-ATTACK=60 [deg]
COMPRESSION=2 , "SHELF"=0 [deg]



Map 6

See Notes on Map 1.

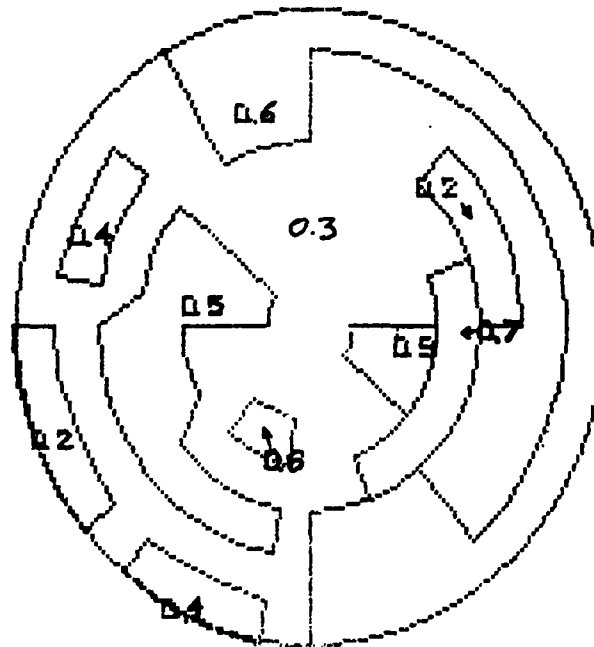
ANGLE-OF-ATTACK=60 [deg]
COMPRESSION=1 , 'SHELF'=100 [deg]



Map 7

See notes on Map 1.

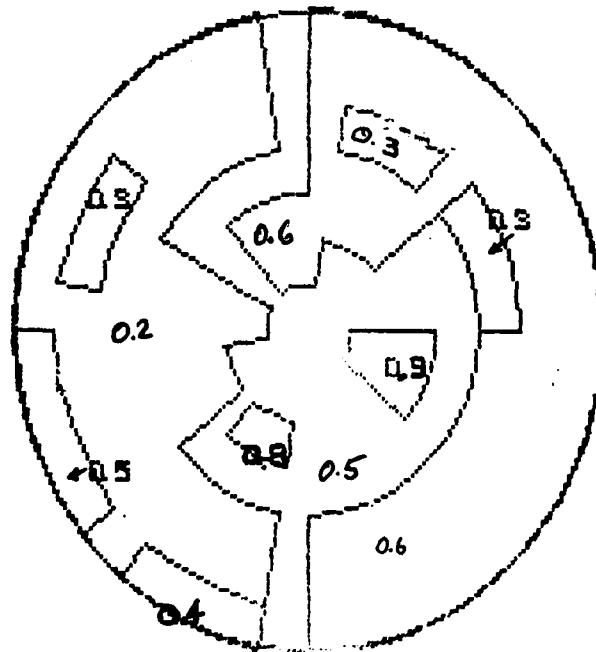
ANGLE-OF-ATTACK=60 [deg]
COMPRESSION=2 , "SHELF'=100 [deg]



Map 8

See Notes On Map 1.

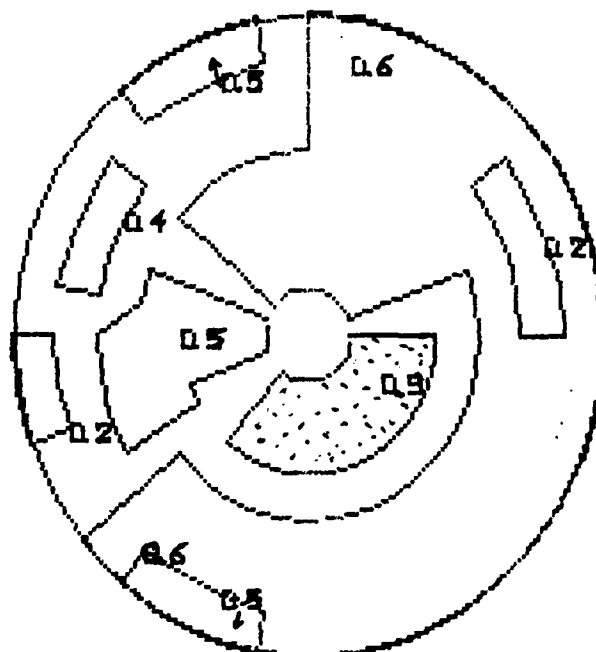
ANGLE-OF-ATTACK=60 [deg]
COMPRESSION=1 , "SHELF"=75 [deg]



Map 9

See Notes On Map 1

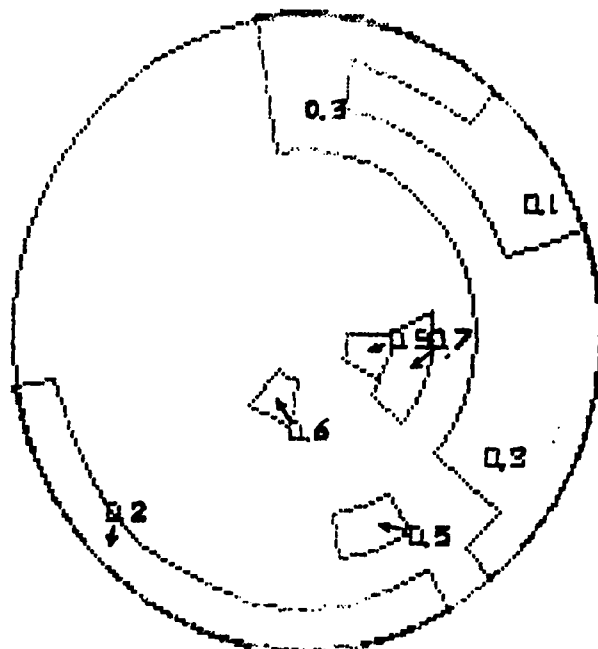
ANGLE-OF-ATTACK=60 [deg]
COMPRESSION=2 , "SHELF"=75 [deg]



Map 10

See Notes On Map 1

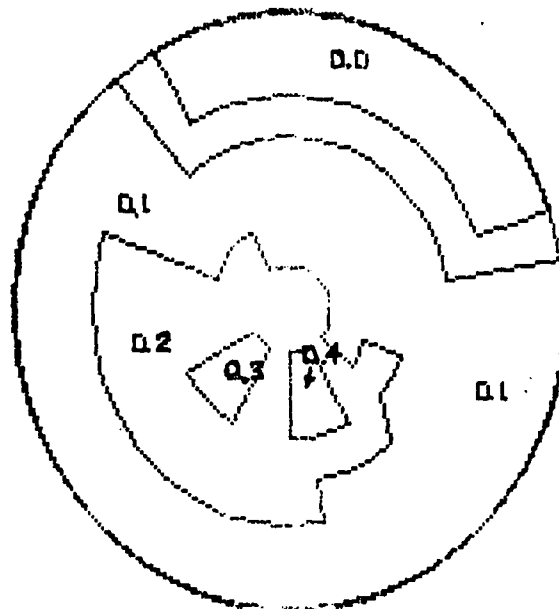
ANGLE-OF-ATTACK=75 [deg]
COMPRESSION=1 'SHELF'=0 [deg]



Map 11

See Notes On Map 1

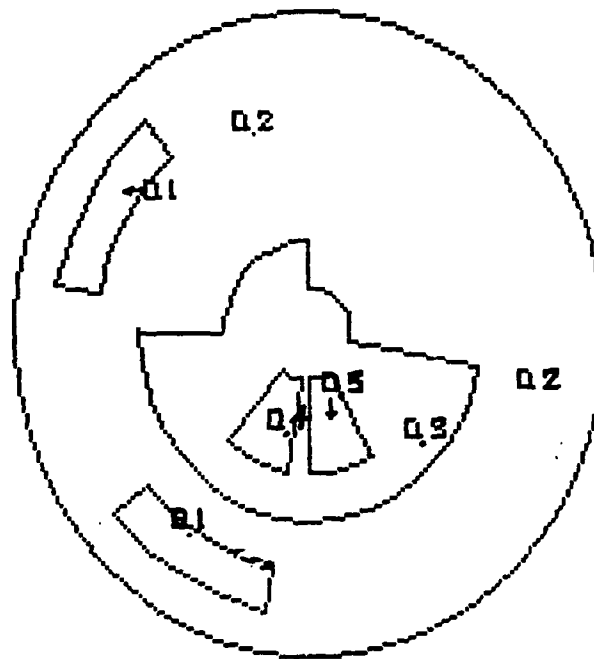
ANGLE-OF-ATTACK=90 [deg].
COMPRESSION=1. 'SHELF'=0 [deg].



Map 12

See Notes On Map 1.

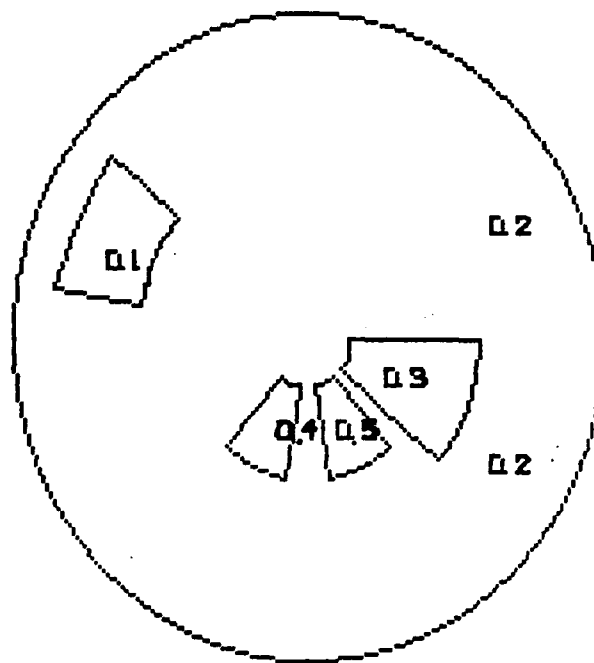
ANGLE-OF-ATTACK=90 [deg]
COMPRESSION=2 , "SHELF"=0 [deg]



Map 13

See Notes On Map 1.

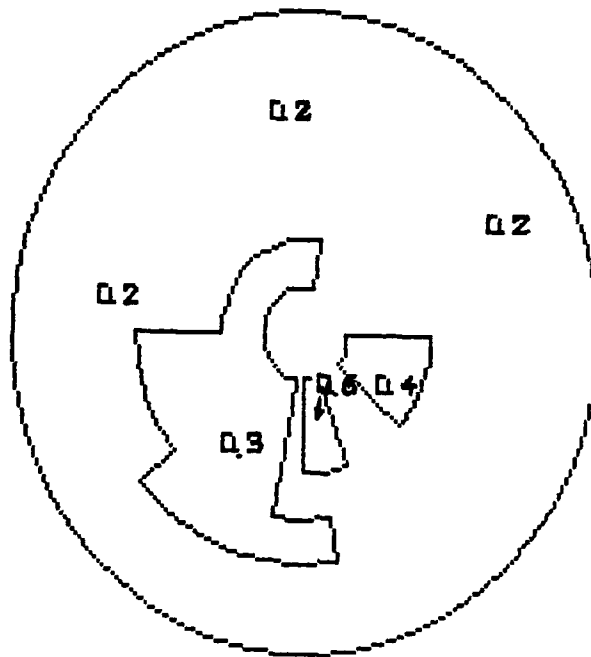
ANGLE-OF-ATTACK=90 [deg]
COMPRESSION=3 "SHELF"=0 [deg]



Map 14

See Notes on Map 1.

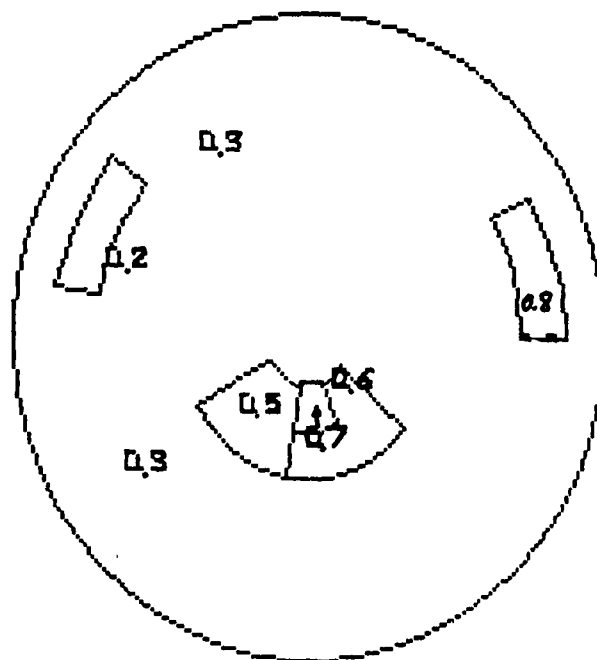
ANGLE-OF-ATTACK=90 [deg]
COMPRESSION=1 , "SHELF"=100 [deg]



Map 15

See Notes on Map 1.

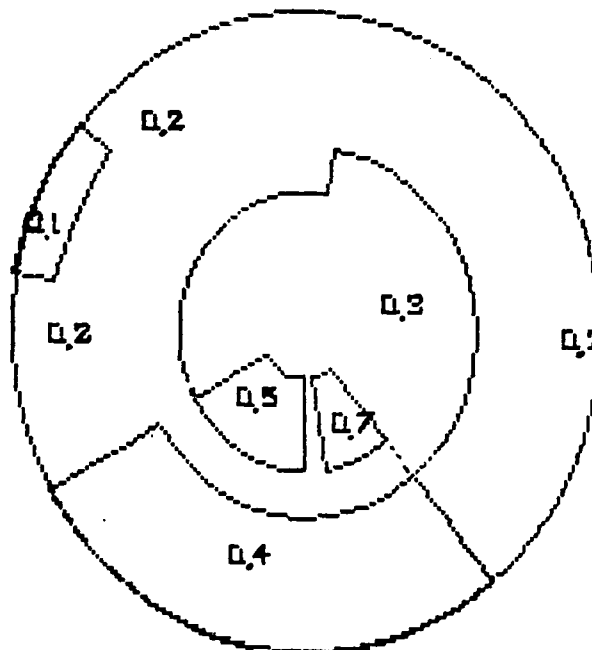
ANGLE-OF-ATTACK=90 [deg]
COMPRESSION=2 , 'SHELF'=100 [deg]



Map 16

See Notes on Map 1.

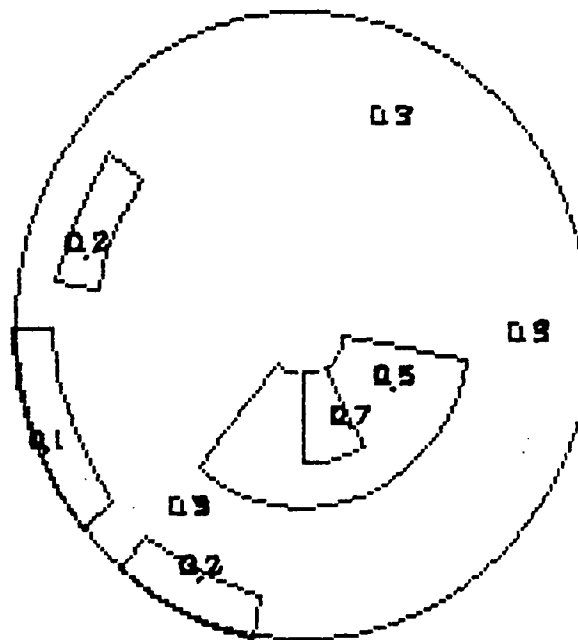
ANGLE-OF-ATTACK=90 [deg]
COMPRESSION=1 , "SHELF"=75 [deg]



Map 17

See Notes on Map 1

ANGLE-OF-ATTACK=90 [deg]
COMPRESSION=2 , "SHELF"=75 [deg]



Map 18

See Notes on Map 1

APPENDIX - B - PART 5

INFLIGHT MANEUVERING BENEFITS

Aircraft Pitch Control

Currently, to benefit maneuvering performance and agility, advanced tactical aircraft are designed for fairly large static instability margins. Unfortunately, when operating at high angles-of-attack, where aerodynamic control surfaces offer little if any nose-down pitching moment, such advanced aircraft designs are especially prone to deep stall, spin, and departure. A solution to this operational dilemma appears to be offered by the multifunction advanced exhaust nozzle configuration.

By employing thrust vectoring control power, the high angle-of-attack maneuvering effectiveness of the advanced aircraft can be preserved and post stall control of the aircraft becomes possible. For illustration Fig. 1 shows the effect of angle-of-attack on the pitching moment characteristics of a baseline aircraft configuration operating at Mach 0.4 and 20,000 ft altitude. As shown, with the use of canard power only, nearly all nose-down pitching moment capability is lost in the 30° to 60° angle-of-attack range due to canard stall. This clearly represents a critical deep stall regime for the aircraft. Effective operation in this regime appears possible, however, when thrust vectoring is employed. As shown, a 30° effective nozzle deflection at maximum afterburning power setting produces a nose-down pitching moment equal to that produced aerodynamically at very low angles-of-attack. More than emphasizing the important potential role of thrust vectoring in pitch initiation and aircraft control, it is implicit in the illustration that thrust vectoring can permit aircraft designs having margins of static instability consistent with superior sustained maneuver performance.

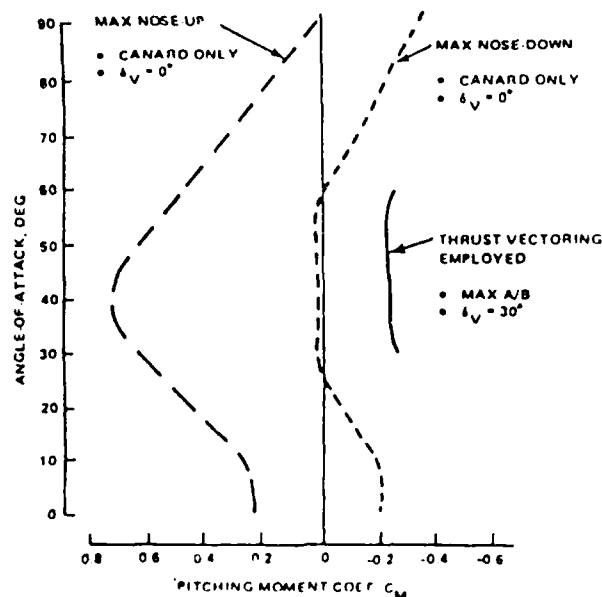


Fig. 1 Role of thrust vectoring for aircraft pitch control in air combat maneuvering

To examine the dynamic stability characteristics involved in using thrust vectoring for deep stall avoidance, a digital simulation methodology was employed by Grumman, resulting in the time history data shown in Fig. 2. In the simulation the aircraft was subjected to an incremental 4-g step input of 2 sec duration, causing an upright stable deep stall. The stall characteristics are displayed through the high angle-of-attack oscillation, altitude loss, and speed decay time histories shown. Superimposed on these results is the behavior experienced when thrust vectoring is implemented in conjunction with an ideal auto-throttle. The nozzle deflection was programmed to vary linearly from 0° to a maximum of 33.5° as angle-of-attack increased from 18° to 28° , and the auto-throttle was programmed to advance power as required to maintain constant airspeed.

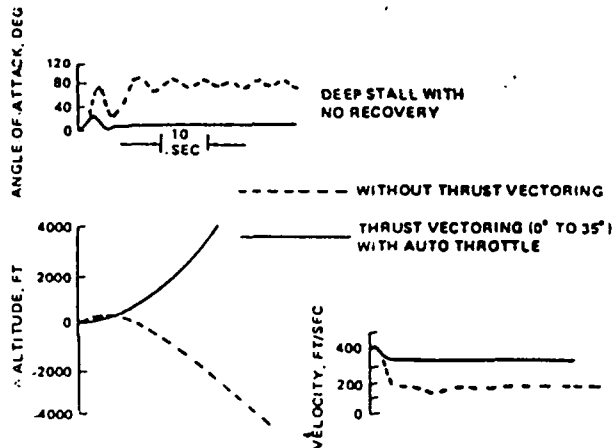


Fig. 2 Role of thrust vectoring in deep-stall avoidance.

The results of this simulation dramatically demonstrate the longitudinal control advantage available through thrust vectoring with positive control maintained throughout the flight maneuver.

Direct Lift Control

For a trimmed aircraft in level flight with undeflected exhaust nozzles, significant canard power for pitch control is normally available. By exploiting the excess canard power, while simultaneously employing exhaust nozzle thrust vectoring to maintain trimmed flight, incremental load factors become available to produce aircraft flight path change without pitch plane rotation. In an air combat engagement, the resulting direct lift control can offer future tactical aircraft at least two important potential advantages:

- Initiation of flight path change without visual clue.
- Preservation of nose pointing during flight path change.

Additional direct lift control advantages which can be identified for tactical aircraft operating in the penetrator role at low altitude include:

- Fight path conformance for terrain following/avoidance.
- Weapons delivery "pop-up" maneuver.

Thrust vectoring provides the potential for supplying significant additional control power to preserve high angles-of-attack and post-stall maneuvering effectiveness.

Use of thrust vectoring in conjunction with excess canard power has the potential to provide aircraft direct lift control advantages important to air combat superiority. Such advantages include surreptitious flight path change, sustained fuselage nose pointing, terrain following/avoidance capability, and weapons delivery "pop-up" maneuvering.

Appendix B - PART 6

Sub-scale Laboratory Tests of Distortion and Pressure Recovery

Coefficients for F-15 Inlet at Various AoA

Written by Dr. Valery Sherbaum in association with Dr. Alexander Rasputnis.

For definitions see p.155. Additional definitions are provided in p. 83-85.

Objectives:

1. Design, construction and testing of sub-scale F-15 inlet test facility.
2. Design, construction and testing of full-scale F-15 inlet test facility using Marbore IIC jet engine.

Limitations on the experimental evaluations of these objectives are discussed in pages 20 - 21a.

PRELIMINARY TEST RESULTS

The following figures provide preliminary test results obtained from our subscale test rig. Table 1 summarizes the over-all results.

Further work is now in progress at increasing AoA and in modification of the rotating probe assembly so as to cover 360° , i.e., the entire cross-sectional area at inlet-end/compressor-face [station 2].

The first test results extracted by this improved method are depicted on p.174. Such maps will become our Standard Distortion Maps (SDM) during the rest of this program.

It should be stressed that Fig. 6 and 7 [p.163-164] provide the "TAKEOFF-FLOW-SIMULATION BASELINE". Deviations from this Baseline can be attributed to AoA-induced distortion, Mach-Number effects, and external-flow non-uniformities in our subscale facility (cf. p.42). A computer program that will plot these deviations, as well as SDM is now being developed.

LIST OF SYMBOLS

M	Inlet Mach Number
LDC	Local distortion coefficient $(P_{tloc} - P_{tav})/P_{tav}$
DC	Distortion coefficient $(P_{tmax} - P_{tmin})/P_{tav}$
PR	Pressure recovery P_{tav}/P_{tin}
P_{tloc}	"Engine-face" local <u>total</u> pressure, cm WG
P_{tav}	"Engine-face" average <u>total</u> pressure, cm WG
P_{tmax}	"Engine-face" maximum <u>total</u> pressure, cm WG
P_{tmin}	"Engine-face" minimum <u>total</u> pressure, cm WG
P_{tin}	Inlet <u>total</u> pressure, cm WG
q	"Engine-face" <u>dynamic</u> pressure, cm WG
Re	"Engine-face" Reynolds number
AoA	Angle-of-attack, deg
Sector 1:	0-90 ⁰ , cf. Fig.27, p.42
Sector 2:	90-180 ⁰ , cf. Fig.27, p.42
Sector 3:	180-270 ⁰ , cf. Fig.27, p.42
Sector 4:	270-360 ⁰ , cf. Fig.27, p.42

Sub-scale Inlet Tests

(For definitions see p.155)

Test No	Re	M	AoA deg	Average Test Results	Remarks
Test-1	10^5	0.15	10	Distortion Coef. = 0.001766 Pressure Recovery = 0.997433 Suction Mass Flow Rate = 0.21 Kg/s	Suction Fan Position 4 Blowing Fan Position 3
Test-2	10^5	0.09	10	Distortion Coef. = 0.001185 Pressure Recovery = 0.998678 Suction Mass Flow Rate = 0.21 Kg/s	Suction Fan Position 4 Blowing Fan Position 2
Test-3 <i>T-0</i> <i>Simulat.</i>	10^5	0		Distortion Coef. = 0.00069 Pressure Recovery = 0.996106 Suction Mass Flow Rate = 0.21 Kg/s	Suction Fan Position 4 Blowing Fan Closed
Test-4	10^5	0.15	-4	Distortion Coef. = 0.001954 Pressure Recovery = 0.996106 Suction Mass Flow Rate = 0.21 Kg/s	Suction Fan Position 4 Blowing Fan Position 3
Test-5	10^5	0.103	-4	Distortion Coef. = 0.000689 Pressure Recovery = 0.996407 Suction Mass Flow Rate = 0.21 Kg/s	Suction Fan Position 4 Blowing Fan Position 2
Test-6	10^5	0.09	18	Distortion Coef. = 0.000792 Pressure Recovery = 0.998912 Suction Mass Flow Rate = 0.21 Kg/s	Suction Fan Position 4 Blowing Fan Position 2
Test-7	10^5	0.15	18	Distortion Coef. = 0.001767 Pressure Recovery = 0.997845 Suction Mass Flow Rate = 0.21 Kg/s	Suction Fan Position 4 Blowing Fan Position 3

Test No	Re	M	AOA deg	Average Test Results	Remarks
Test-8 T-O Simulat.	4×10^5	0		Distortion Coef. = 0.024875 Pressure Recovery = 0.970035 Suction Mass Flow Rate = 0.84 Kg/s	Suction Fan Open Max. Blowing Fan Closed
Test-9	10^5	0.14	0	Distortion Coef. = 0.001568 Pressure Recovery = 0.996287 Suction Mass Flow Rate = 0.21 Kg/s	Suction Fan Position 4 Blowing Fan Position 3
Test-10	10^5	0.09	0	Distortion Coef. = 0.001484 Pressure Recovery = 0.998320 Suction Mass Flow Rate = 0.21 Kg/s	Suction Fan Position 4 Blowing Fan Position 2

Fig. 1 : Test-1 Local Distortion Coefficient
vs. Each Sector's Angle & Radius
 $M = 0.15$, $Re = 10^5$, $AoA = 10$ deg
Suction Fan: Position 4. Blowing Fan: Position 3

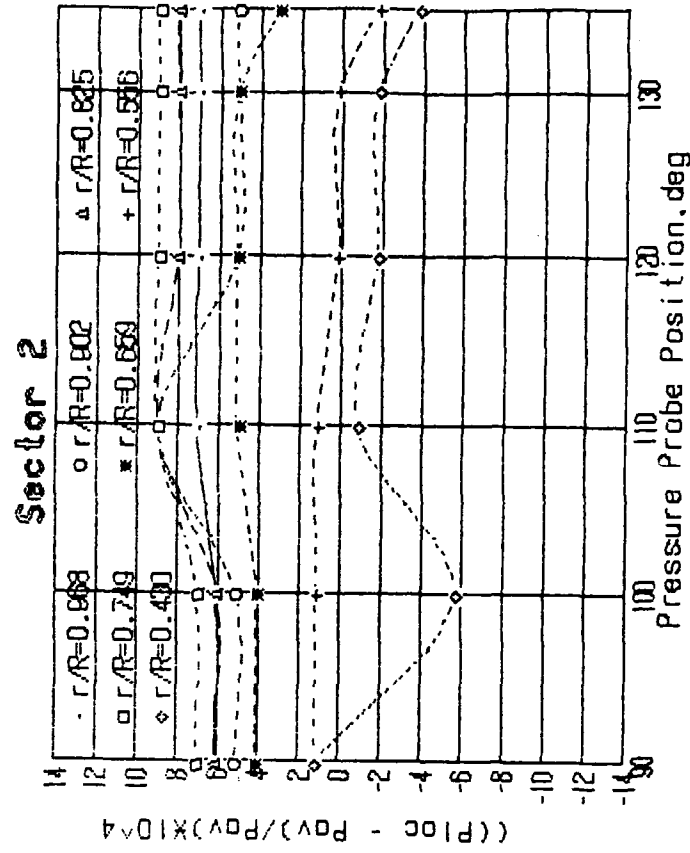
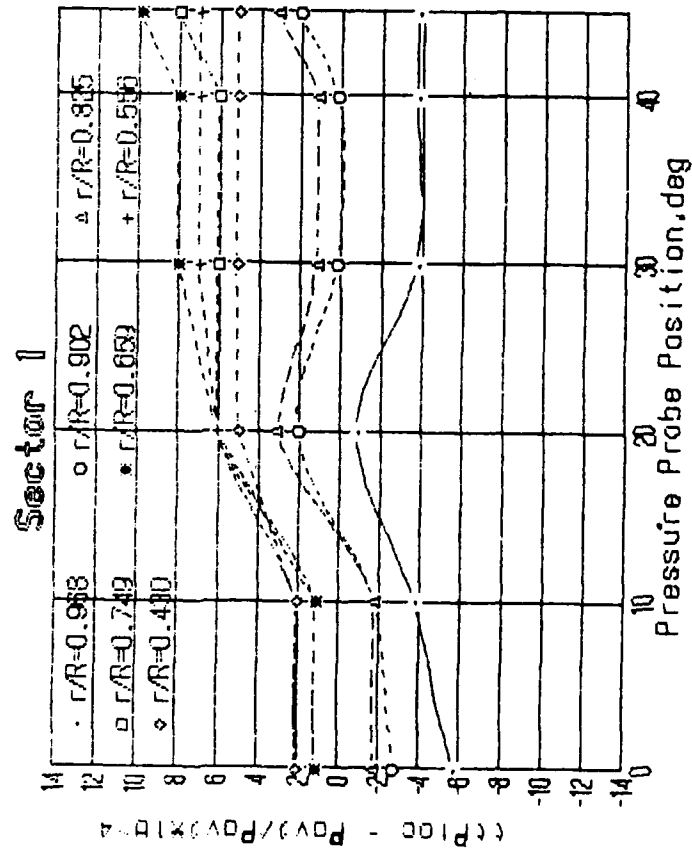
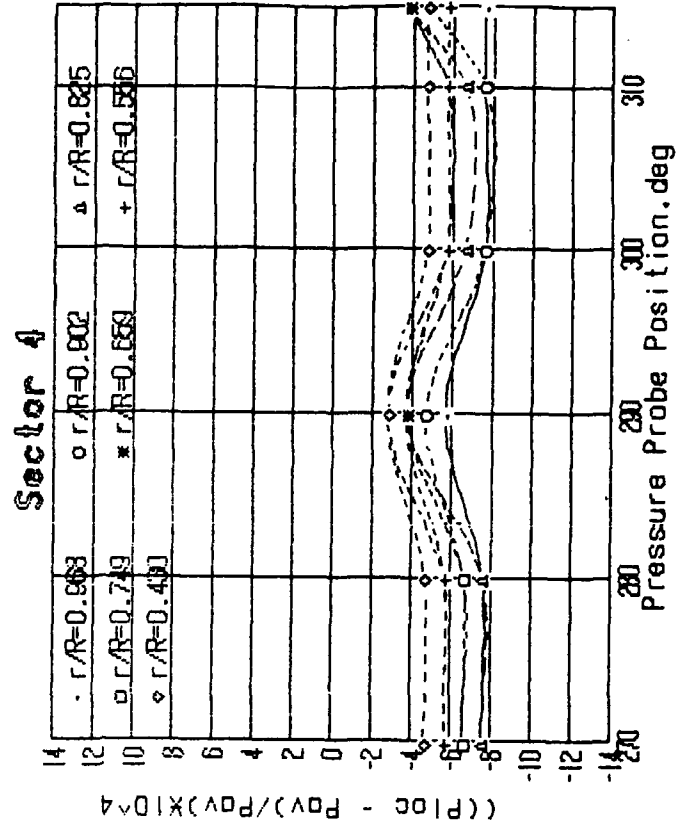
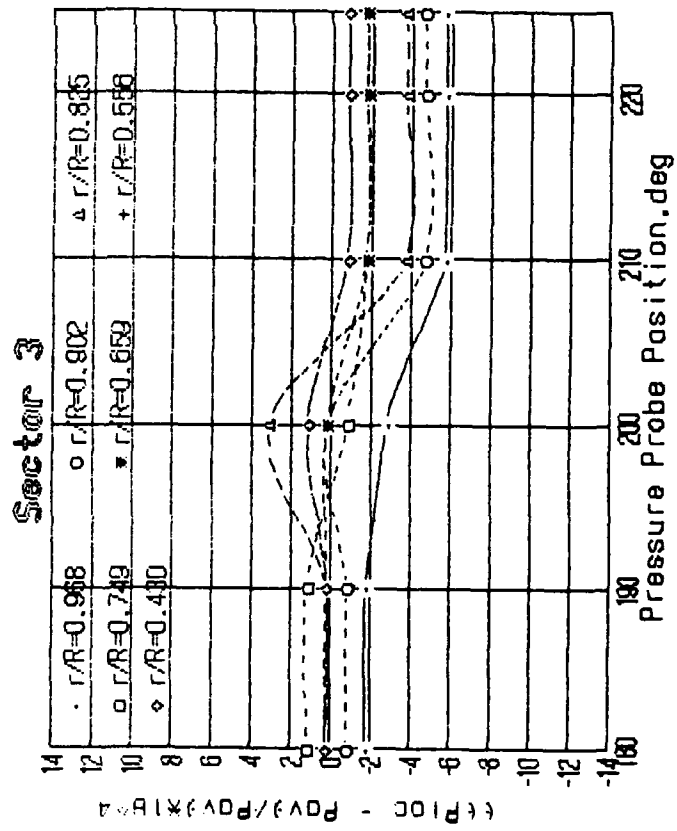


Fig. 2 : Test-1 Local Distortion Coefficient
 vs. Each Sector's Angle & Radius
 $M = 0.15$, $Re = 10^5$, $AoA = 10$ deg
 Suction Fan: Position 4. Blowing Fan: Position 3



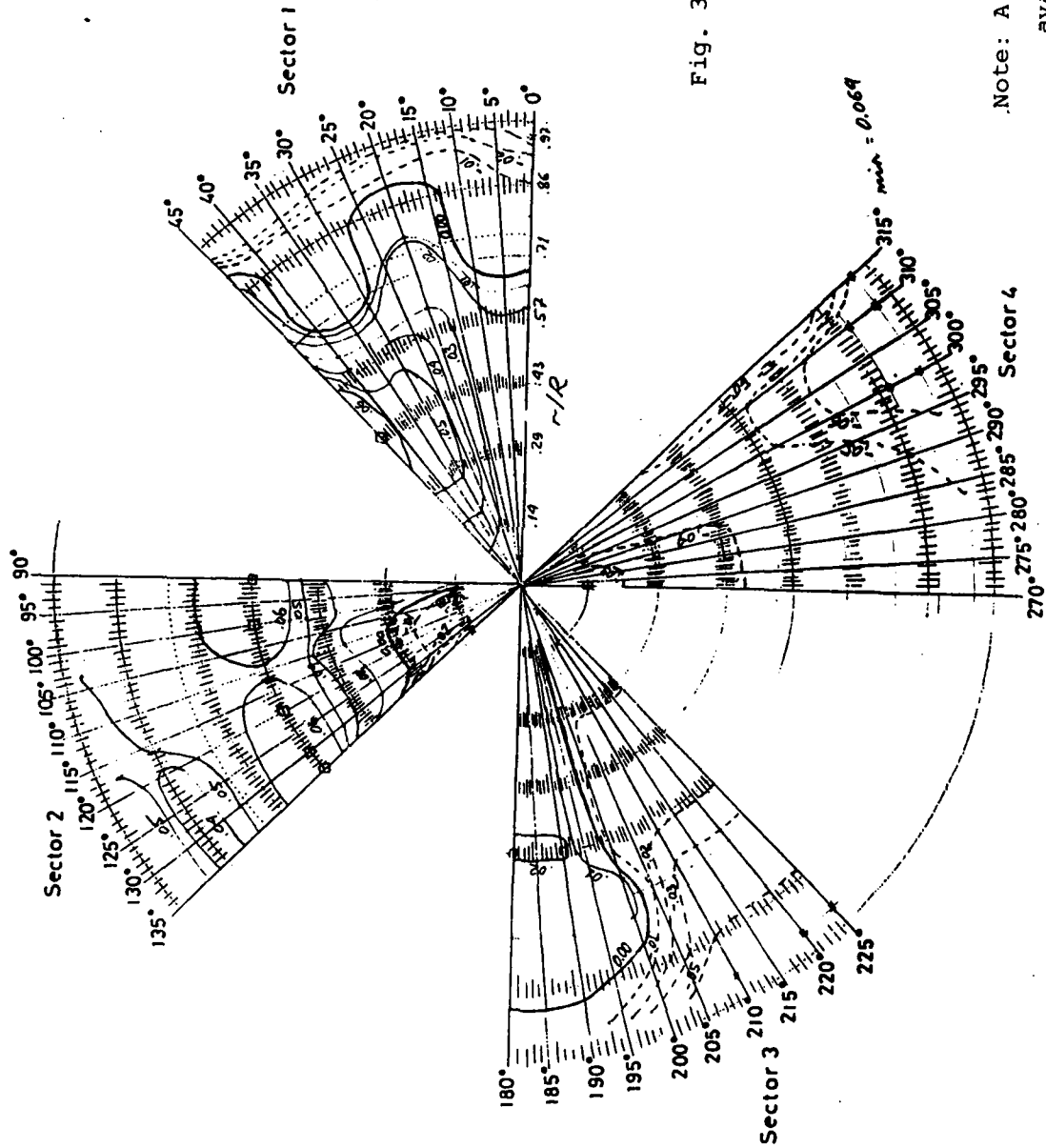


Fig. 3 : Test-1, $\text{AoA} = 10^\circ$
Inlet Mach Number $M=0.15$

Note: A new computer program is available now to plot these data and variations from the baseline (cf. p.174).

Fig. 4 : Test-2 Local Distortion Coefficient
 vs. Each Sector's Angle & Radius
 $M = 0.09$, $Re = 10^5$, $AoA = 10$ deg
 Suction Fan: Position 4. Blowing Fan: Position 2

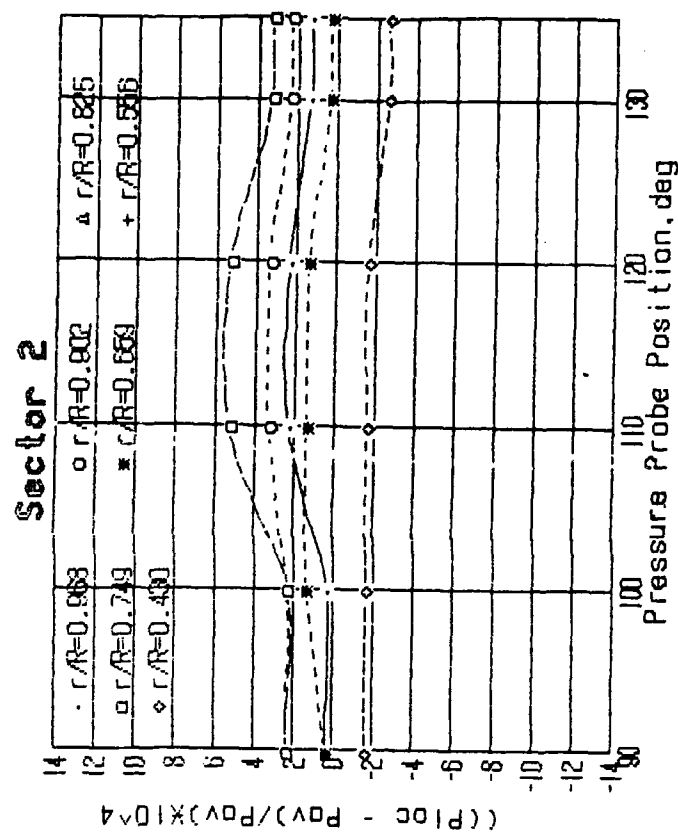
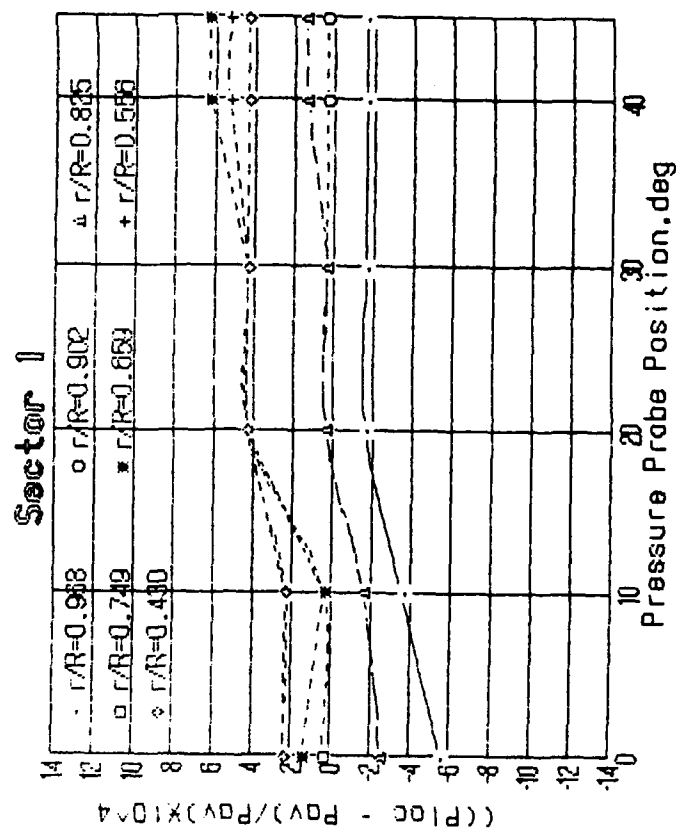


Fig. 5 :
 Test-2 Local Distortion Coefficient
 vs. Each Sector's Angle & Radius
 $M = 0.09$, $Re = 10^5$, $AoA = 10$ deg
 Suction Fan: Position 4. Blowing Fan: Position 2

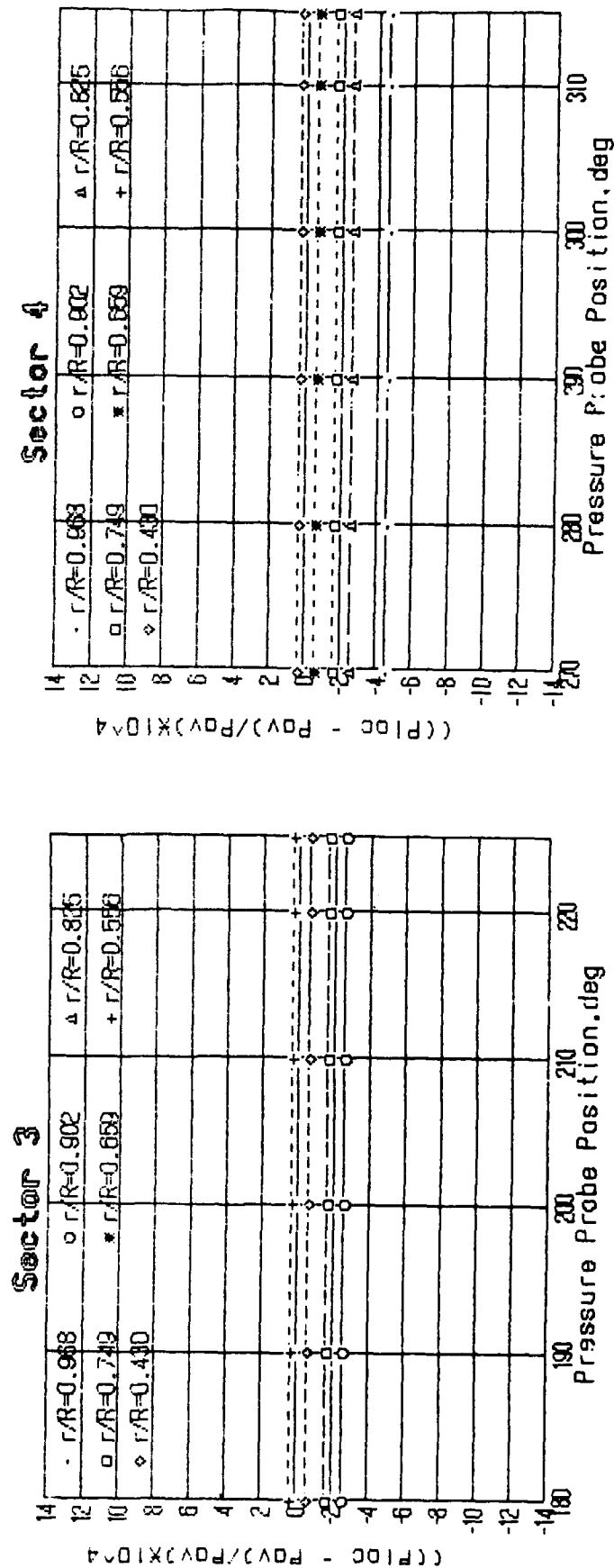


Fig. 6 : Test-3 Local Distortion Coefficient
 vs. Each Sector's Angle & Radius
 $M = 0$, $Re = 10^5$, $AoA = 0$ deg
 Suction Fan: Position 4. Blowing Fan: Closed

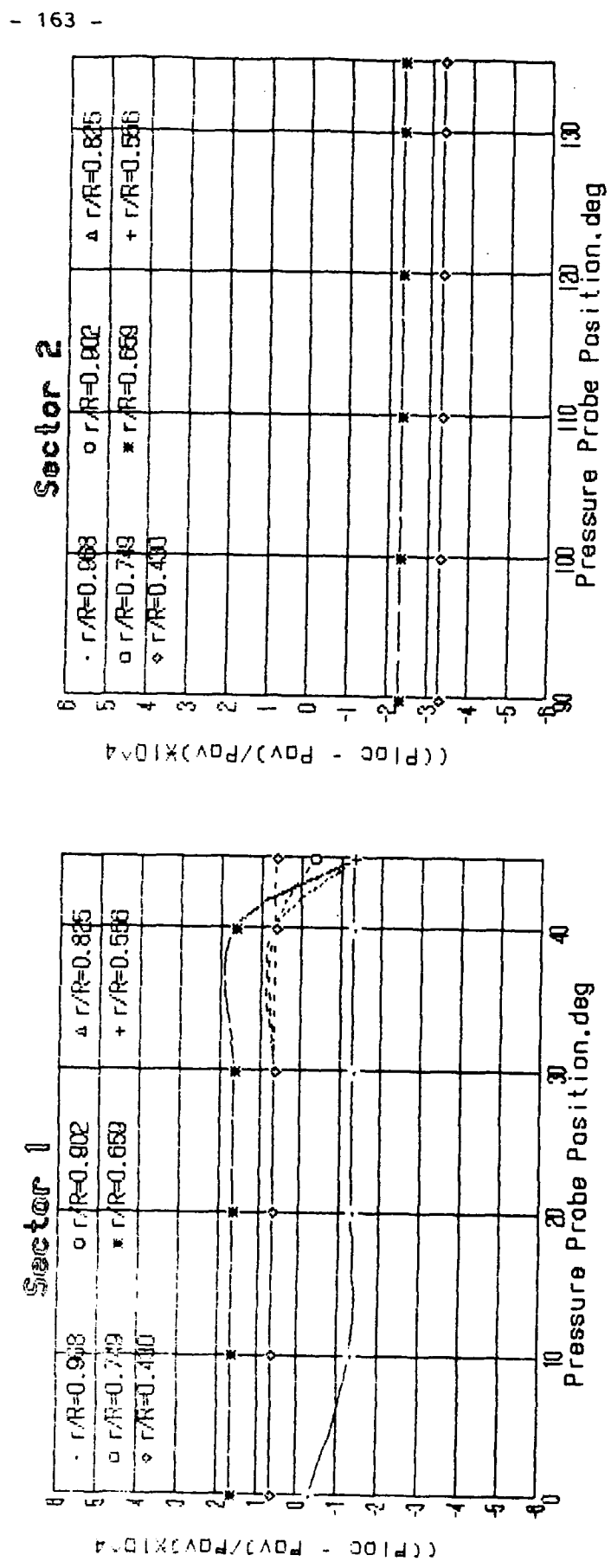


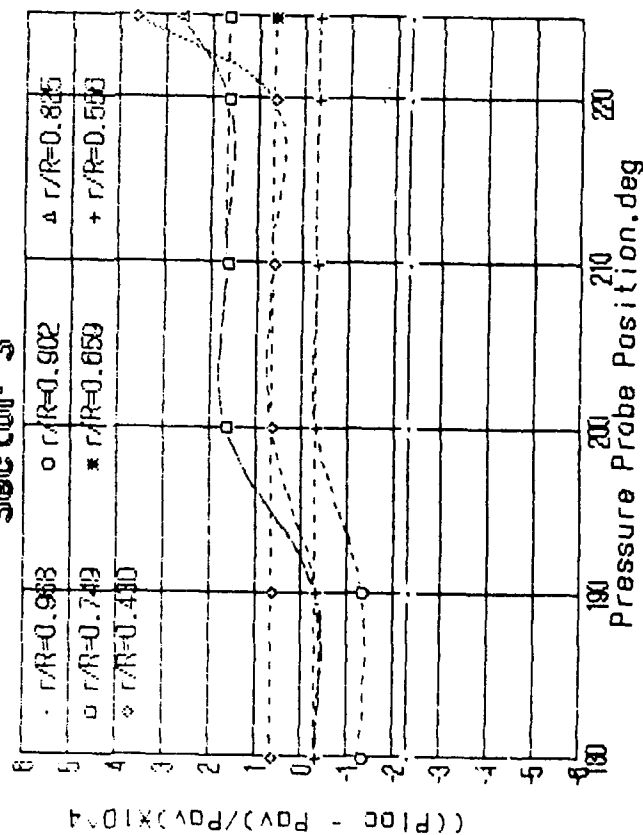
Fig. 7 :

Test-3 Local Distortion Coefficient vs. Each Sector's Angle & Radius

$M = 0$. $Re = 10^5$. $\text{AoA} = 0 \text{ deg}$

Suction Fan: Position 4. Blowing Fan: Closed

Sector 3



Sector 4

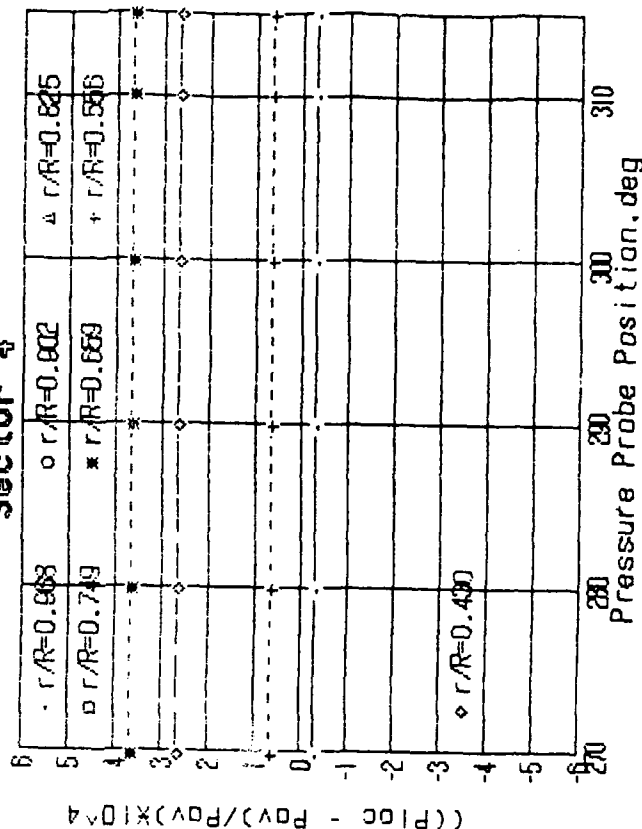


Fig. 8.: Test-4 Local Distortion Coefficient
 vs. Each Sector's Angle & Radius
 $M = 0.15$, $Re = 10^5$, $AoA = -4$ deg
 Suction Fan: Position 4. Blowing Fan: Position 3

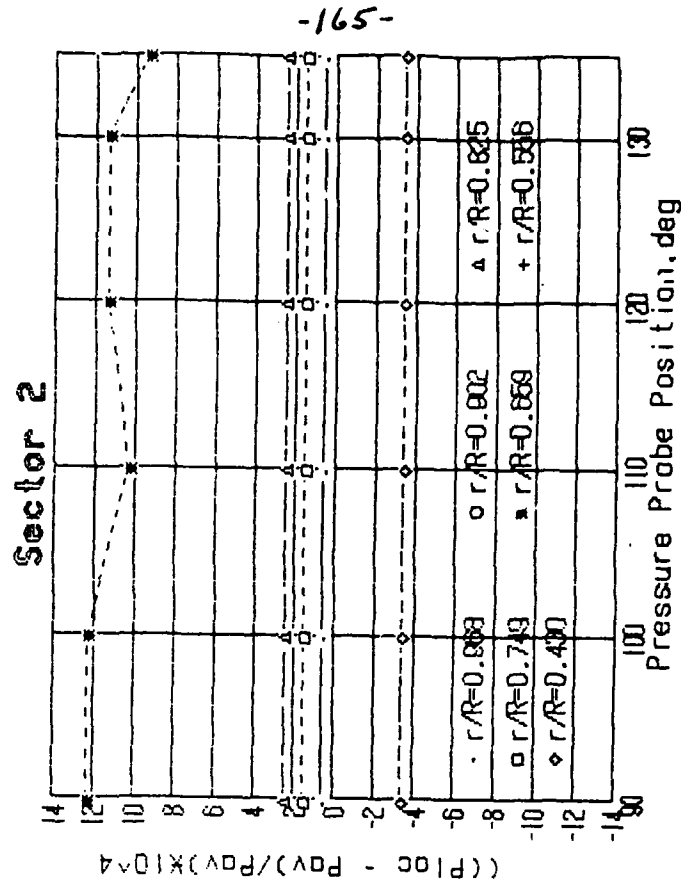
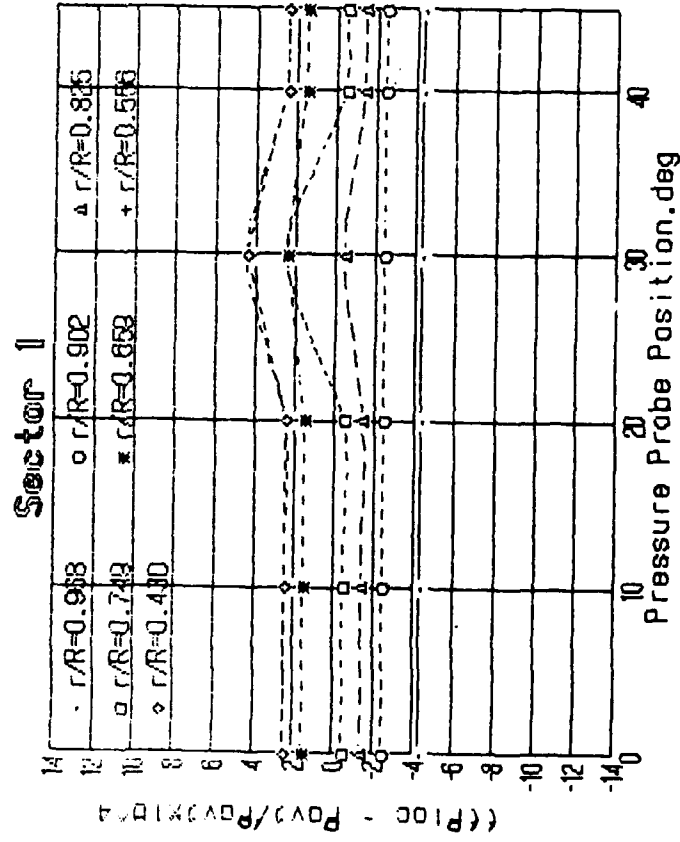


Fig. 9 : Test-4 Local Distortion Coefficient
 vs. Each Sector's Angle & Radius
 $M = 0.15$, $Re = 10^5$, $AoA = -4$ deg
 Suction Fan: Position 4. Blowing Fan: Position 3

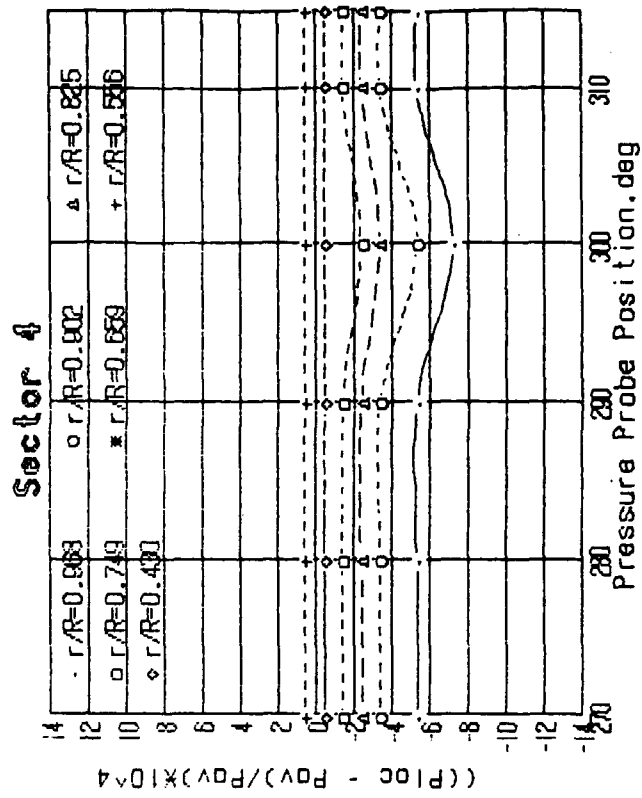
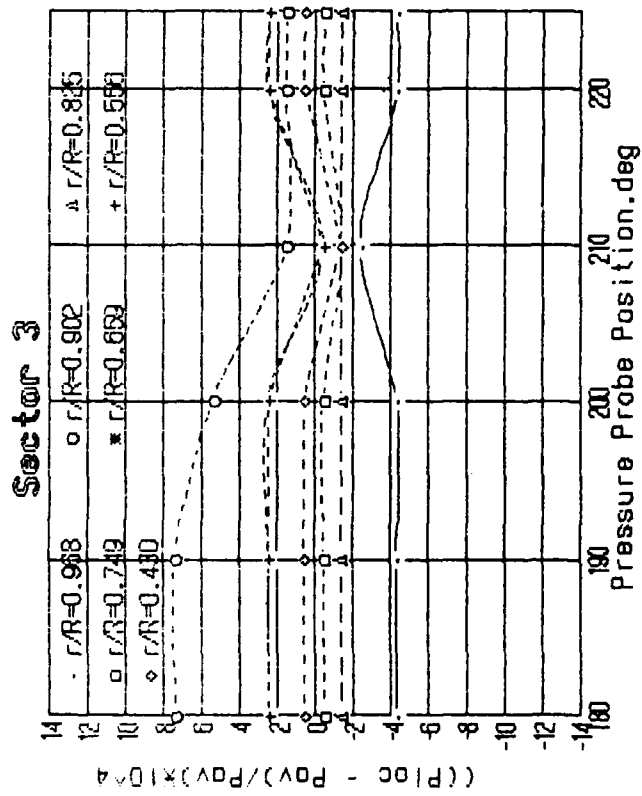


Fig. 10 : Test-5 Local Distortion Coefficient
 vs. Each Sector's Angle & Radius
 $M = 0.103$, $Re = 10^5$, $AoA = -4$ deg
 Suction Fan: Position 4. Blowing Fan: Position 2

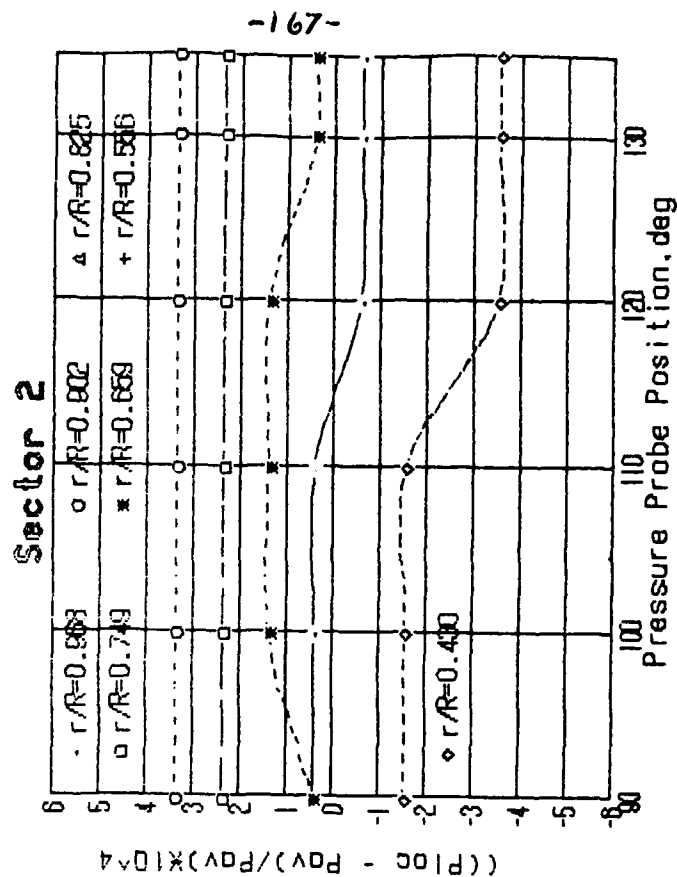
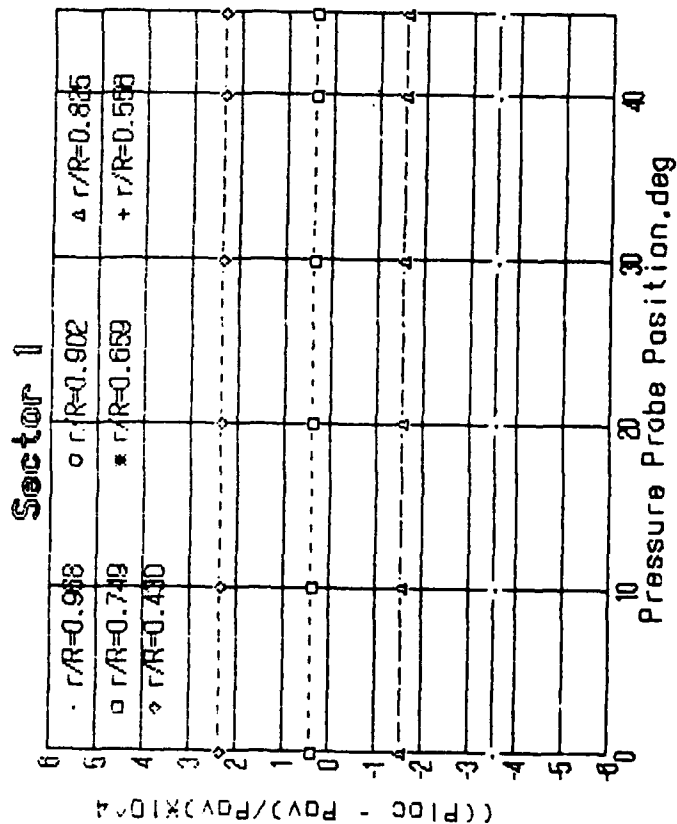


Fig. 11: Test-5 Local Distortion Coefficient
 vs. Each Sector's Angle & Radius
 $M = 0.103$, $Re = 10^5$, $AoA = -4$ deg
 Suction Fan: Position 4. Blowing Fan: Position 2

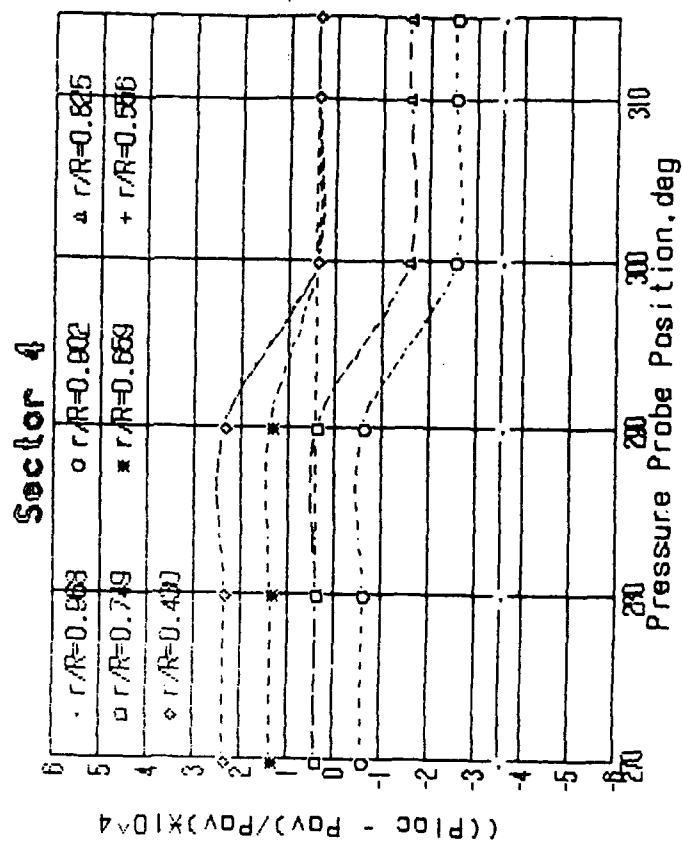
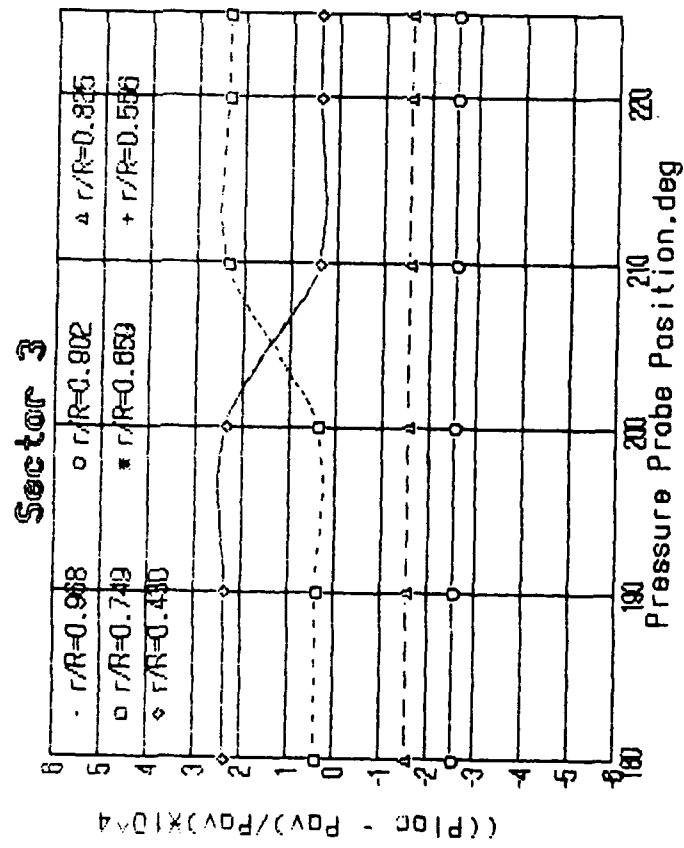


Fig. 12: Test-6 Local Distortion Coefficient
 vs. Each Sector's Angle & Radius
 $M = 0.09$, $Re = 10^5$, $AoA = 18$ deg
 Suction Fan: Position 4. Blowing Fan: Position 2

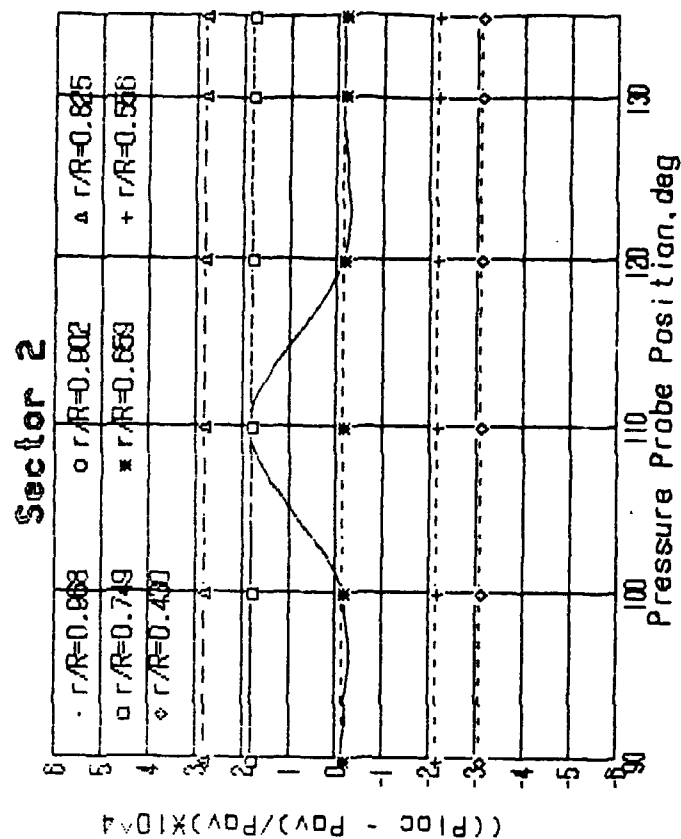
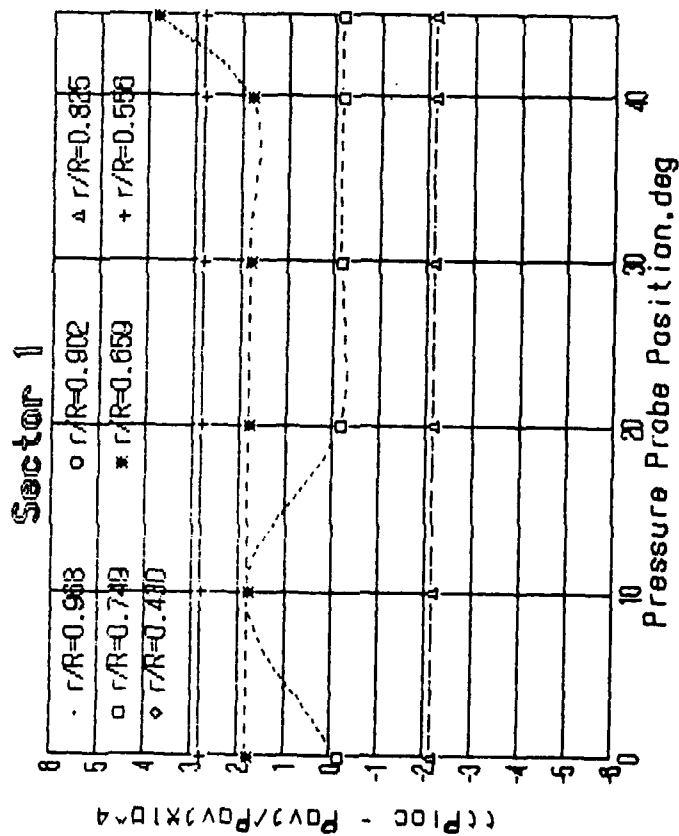


Fig. 13: Test-6 Local Distortion Coefficient
 vs. Each Sector's Angle & Radius
 $M = 0.09$, $Re = 10^5$, $AoA = 18 \text{ deg}$
 Suction Fan: Position 4. Blowing Fan: Position 2

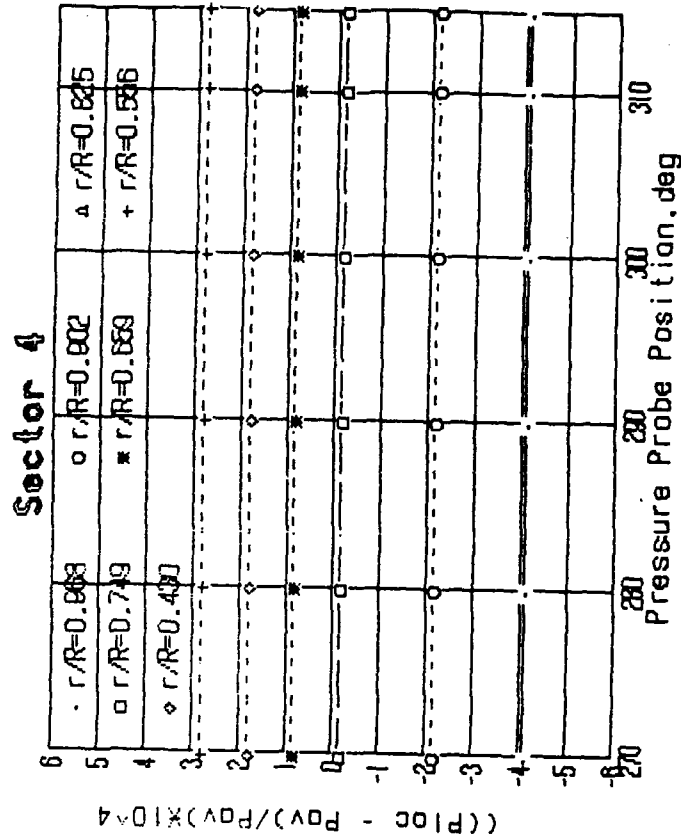
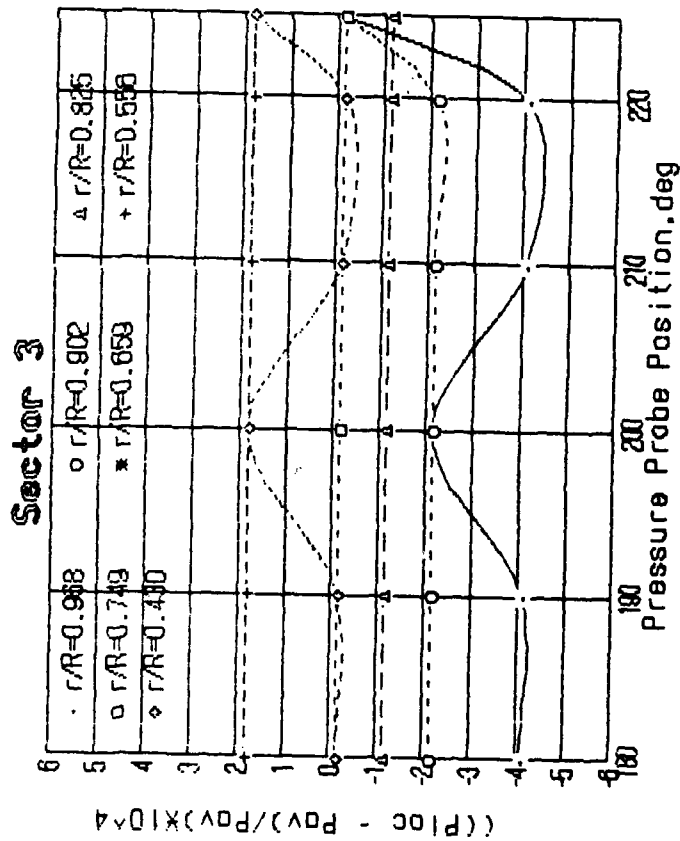


Fig 4: Test-7 Local Distortion Coefficient
vs. Each Sector's Angle & Radius
 $M = 0.15$, $Re = 10^5$, $AoA = 18$ deg
Suction Fan: Position 4. Blowing Fan: Position 3

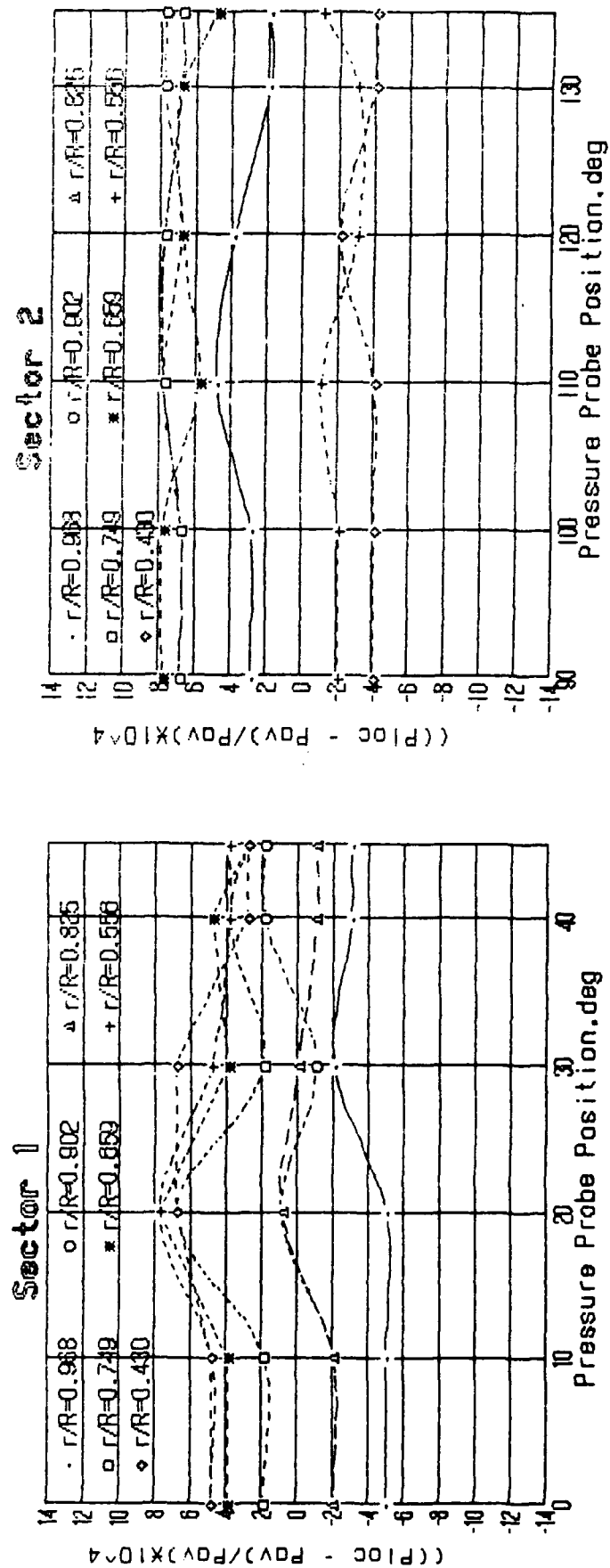
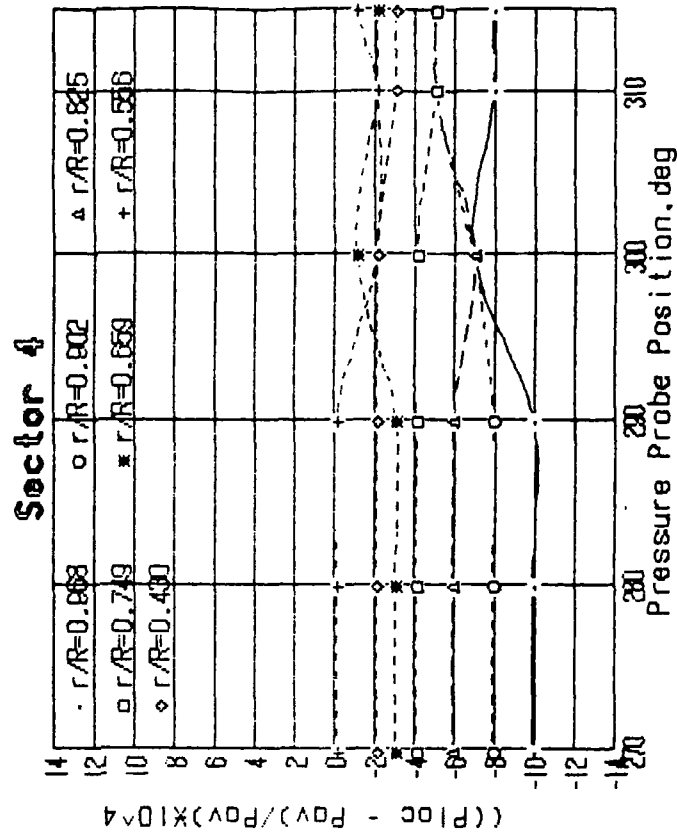
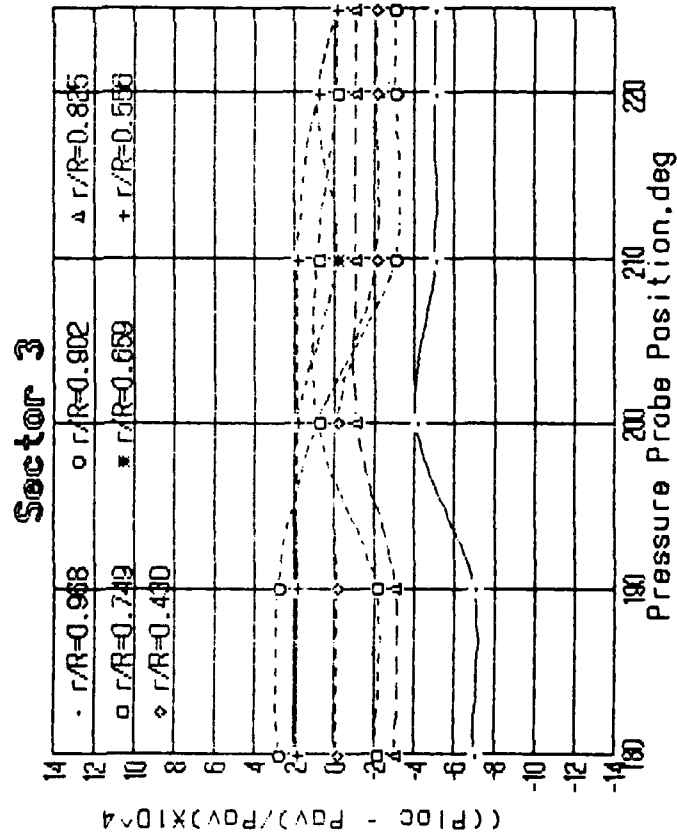


Fig 15: Test-7 Local Distortion Coefficient
 vs. Each Sector's Angle & Radius
 $M = 0.15$, $Re = 10^5$, $AoA = 18$ deg
 Suction Fan: Position 4. Blowing Fan: Position 3



APPENDIX B - PART 7 :

The New Inlet-Test-Data-Plotting Standard

(Recent work conducted by Dr. V. Sherbaum and Dr. A. Rasputnis)

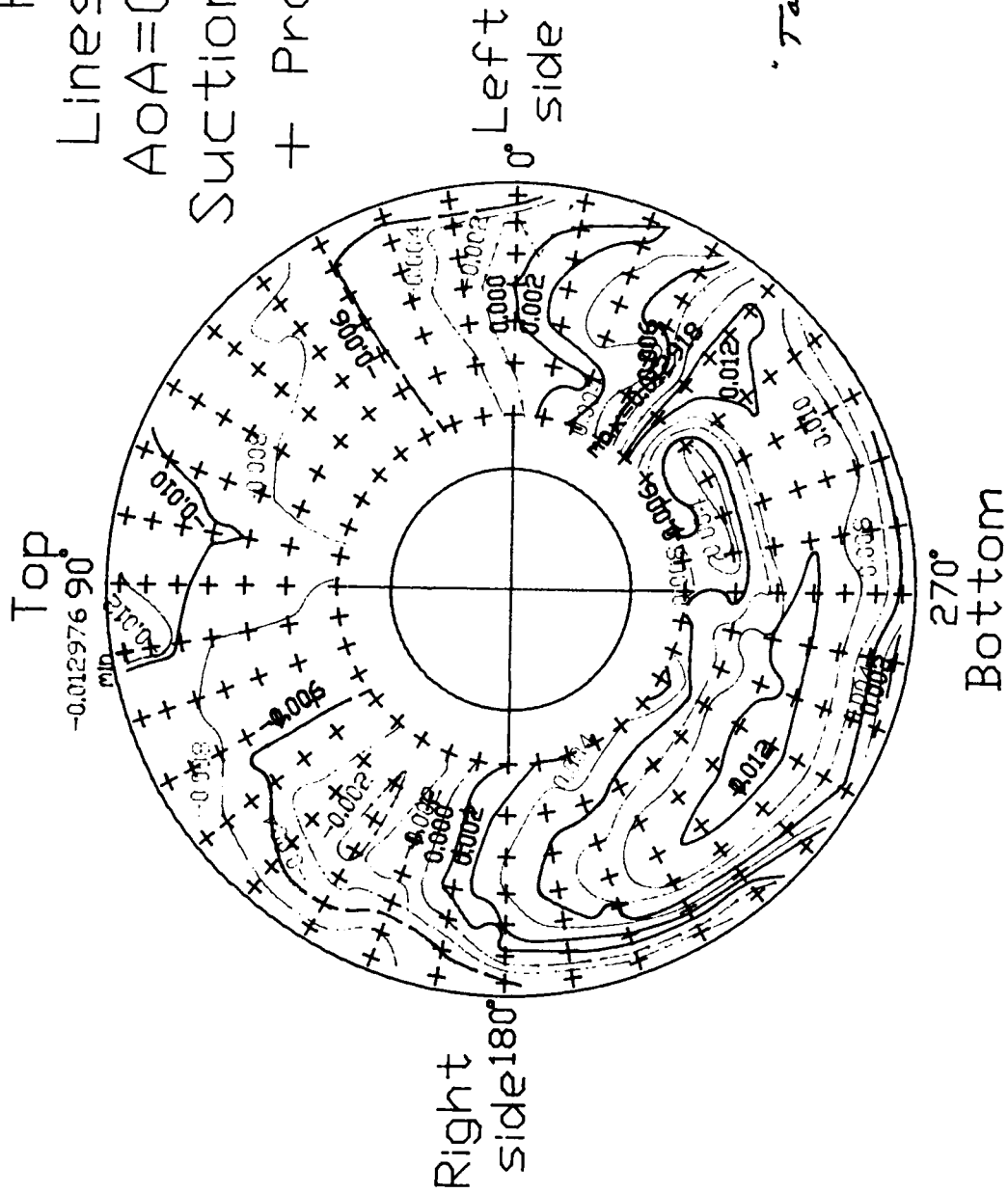
An example of the recently obtained test data from the improved 360° - degrees-sweep subscale F-15 inlet test rig, is enclosed.

It represents our new STANDARD for plotting DC and Pr maps and also maps which show the calculated "variations-from-a-Baseline". The new additions to our program are based on a new computer program, which has been advanced by Dr. A. Rasputnis.

The test results were obtained by Dr. Valery Sherbaum. Additional remarks are available in p.20-21b.

Further test results will be submitted to the USAF Project Manager within the framework of our monthly progress reports and interim Progress Reports. They would gradually include test data from our full-scale test rig.

Fig.1 Test-8 *cf. p.18*
 Lines of LDC=Const.
 $AoA=0$, $M=0$, $Re=4*10^5$
 Suction fan opened max.
 + Probe locations



"Takeoff-Simulation-Baseline"

Fig.2 Test-8 *cf. p.156*
 Lines of $LDC=Const.$,
 $AoA=0$, $M=0$, $Re=4*10^5$
 Suction fan opened max.

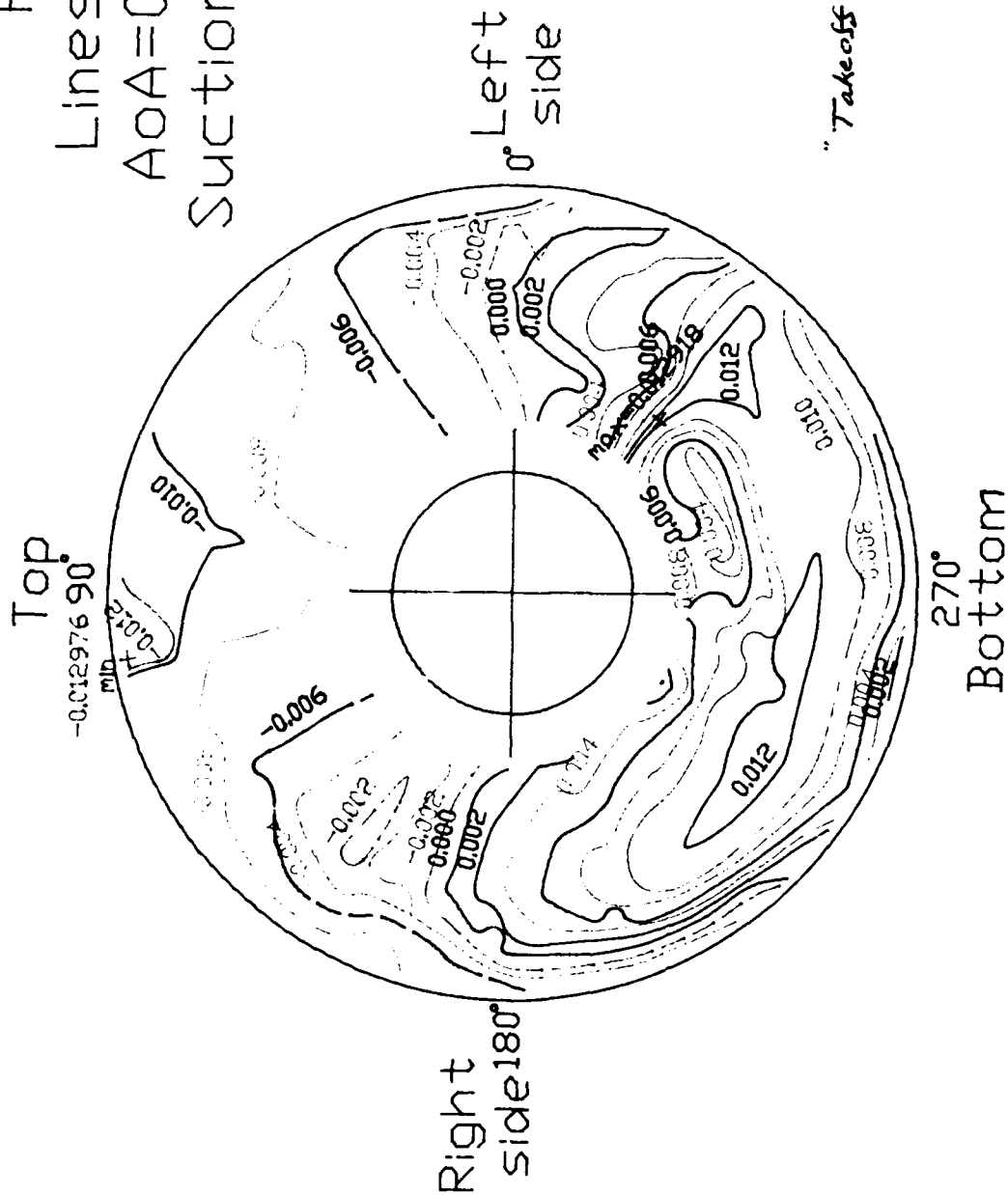
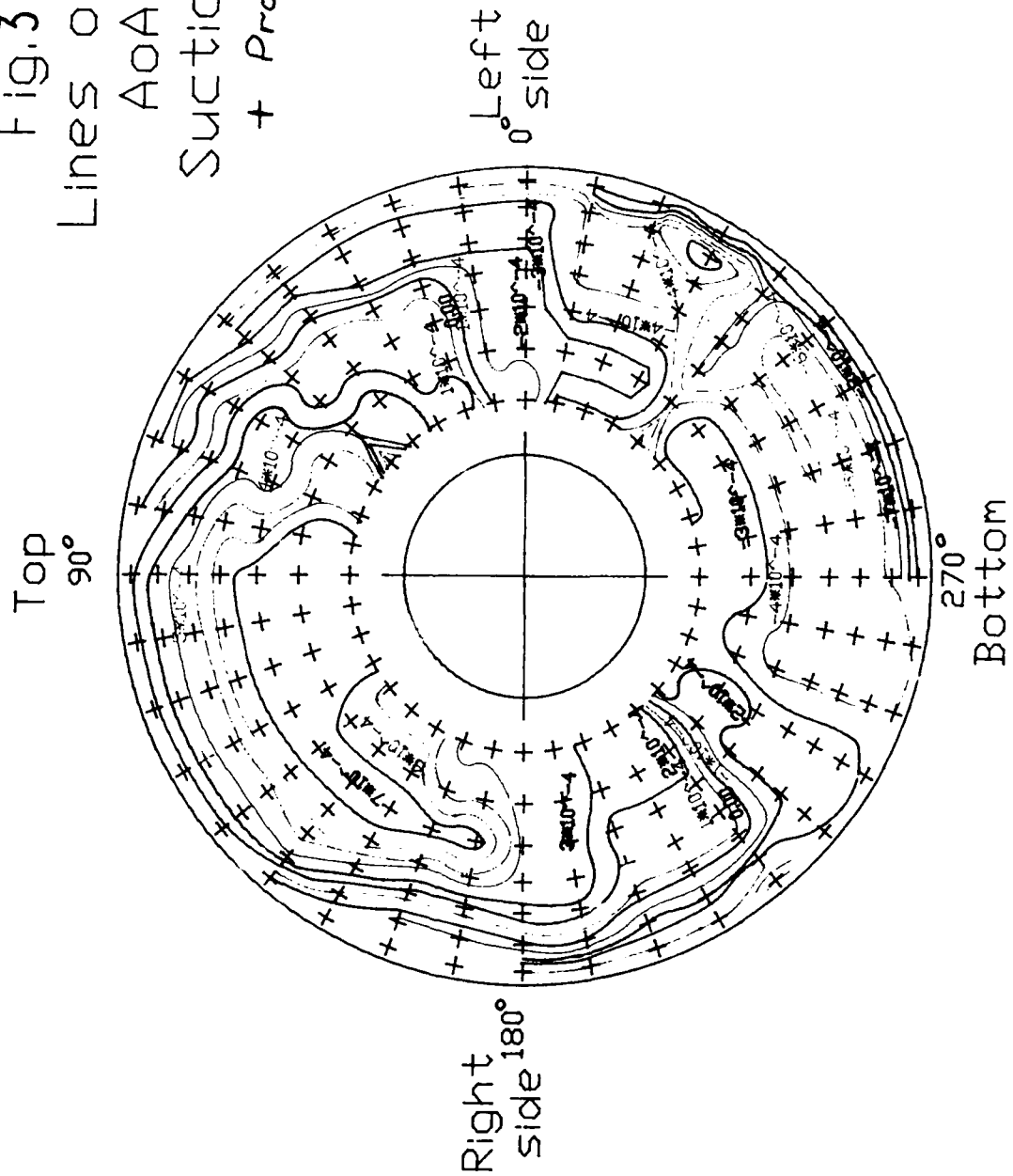


Fig.3 Test-9 *cf. p.156*
Lines of LDC=Const.,
AoA=0, $M=0.14$
Suction blower=4
+ Probe locations



Appendix C

How to measure the 3 moments of inertia

I_{xx} , I_{yy} , I_{zz} , about the three main axes of the "9-feet" F-15 RPV

By: Ostrovsky G. and Voldman E.

Submitted to Prof. B. Gal-Or

Introduction:

Our project is to design, construct, test and validate the method for direct measurements of the moments of Inertia of F-15 RPV about the 3 main axes which pass through the center of gravity of the RPV.

A Simplified Mathematical model (cf. Fig. 1)

We first consider a linear-vibrations model. When the system is in torsion vibration it may be described by the linear differential equation

$$(1) I\ddot{\theta} + K\theta = 0,$$

$$\text{when } \ddot{\theta} = \frac{d^2\theta}{dt^2}$$

θ - angle of turn (rad.)

I - moment of inertia about axis x [kg.m^2]

K - torsion-spring constant [$\frac{\text{N.m}}{\text{rad}}$]

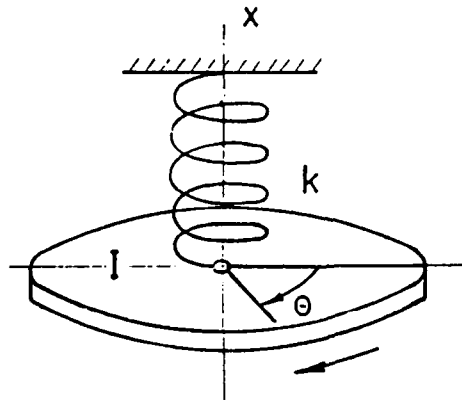


Fig. 1.

The general solution of equation (1) is

$$(2) \theta(t) = A \sin\left(\sqrt{\frac{k}{I}} t\right) + B \cos\left(\sqrt{\frac{k}{I}} t\right)$$

Here

$$\omega_n = \sqrt{\frac{k}{I}} \quad \hat{=} \quad \text{natural frequency of the system [rad/sec]}$$

$$T = \frac{2\pi}{\sqrt{k/I}} \quad (\text{sec}) - \text{the period of vibration.}$$

When the spring-constant is known one may determine the moment of inertia:

$$(3) \quad I = \frac{KT^2}{4\pi^2}$$

Spring - constant determination

1) Definitions of Spirial Coiled-Springs of Rectangular Cross Sections

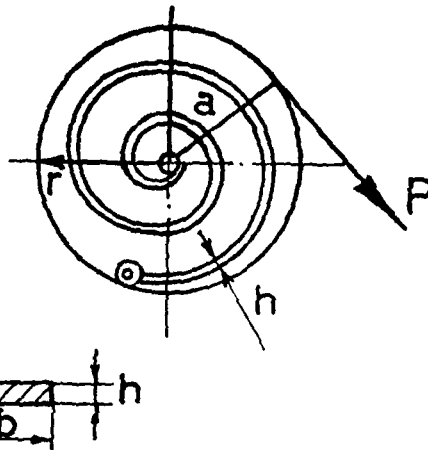


Fig. 2

$$f=ra = \frac{Plr^2}{EIk} = \frac{12Plr^2}{Ebh^3k} = \frac{2rlS}{hEk}$$

$$k = (3c-1)(3c-3) ; C=2R/h$$

$$I = \frac{bh^3}{12}$$

$R \approx$ minimum radius of curvature at the center of the spirial

$K = \frac{EIk}{1}$	- <u>the spring constant</u>
---------------------	------------------------------

2. Cylindrical Helical Spring of Circular Cross Section

$$f = \frac{Plr^2}{EI k} = 64 Plr^2 / \pi E d^4 k = \frac{2rlSs}{dEk} = \Delta a$$

$$I = \pi d^4 / 64$$

For (heavy) closely-coiled springs :

$$k = (4c-1)/(4c-4) ; C = 2r/d$$

$$K = \frac{EI k}{l}$$

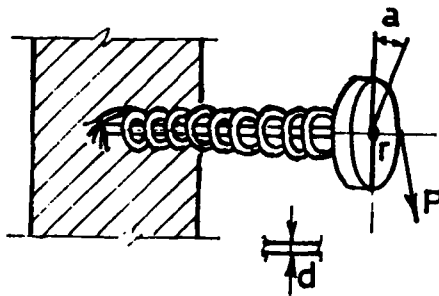


Fig. 3

3. Cylindrical Helical Spring of Rectangular Cross Section

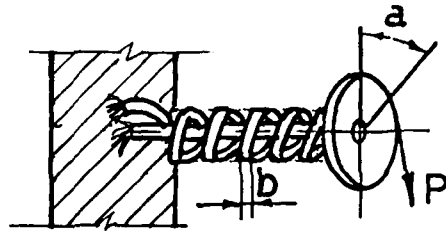


Fig. 4

$$f = ra = Plr^2 / EIk = 12Plr^2 / Ebh^3 \quad k = 2rlSs / hEk$$

$$I = bh^3 / 12$$

$$k = (3c - 1) / (3c - 3) ; \quad C = 2r / h$$

$$K = \frac{EIk}{l}$$

Notation: P=safe load, lb.

f=deflection for a given load P, in.

l=Length of spring, in.

Ss=Safe stress (due to bending)

Reference : Mechanical Engineers Handbook

Lionel S. Marks

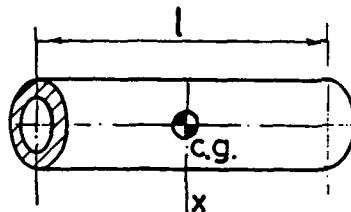
Fifth Edition

Evaluation of the Test Method

To check our method by simulation on a small model, we take a hollow cylindrical body whose moment of inertia can be computed as

$$I_{xx} = m \left[\frac{r^2}{2} + \frac{l^2}{12} \right]$$

where



r - mean radius

m - mass of body

l - length

Fig. 5

Body data

$$r = 0.009375 \text{ (m)}$$

$$l = 0.398 \text{ (m)}$$

$$m = 0.458 \text{ (kg)}$$

$$\text{Computed moment of Inertia } I_{\text{comp}} = 6,06587 \cdot 10^{-3} \text{ (kg.m}^2\text{)}$$

Spring data

$$\text{Young modulus (typical)} \quad E = 29 \cdot 10^3 \text{ KPSI} = 1.9353 \cdot 10^{11} \left(\frac{\text{N}}{\text{m}^2} \right)$$

$$\text{wire diameter} \quad d = 0,0014 \text{ (m)}$$

$$\text{spring diameter} \quad D = 0,015 \text{ (m)}$$

$$\text{number of loops} \quad N = 5$$

$$\text{spring constant is } K = \frac{Ed^4}{ND} = 0,155 \left(\frac{\text{N.m}}{\text{rad}} \right)$$

The period was measured as

$$T = 1.26 \text{ (sec)}$$

Hence according to (3)

$$\text{measured } I_{xx} = 6,233.10^{-3} \text{ (kg.m}^2\text{)}$$

$$\text{computed } I_{xx} = 6,06587.10^{-3} \text{ (kg.m}^2\text{)}$$

The test precision is 2,76%

The tests are to be completed by the end of July 1990.